universität wien

DISSERTATION

Titel der Dissertation

Development of Dermal O/W Emulsions with Natural Surfactants and Cyclodextrins and Optimisation of the Tape Stripping Method

Verfasserin

Mag.pharm. Victoria Klang

angestrebter akademischer Grad

Doktorin der Naturwissenschaften (Dr.rer.nat.)

Wien, Januar 2012

Studienkennzahl lt. Studienblatt:	A 091 449
Dissertationsgebiet lt. Studienblatt:	Pharmazie
Betreuerin / Betreuer:	Ao.Univ.-Prof. Mag. Dr. Claudia Valenta

> The proper scientific response to any new discovery or theory, especially your own, is to look for ways to disprove it. That is, to try to find a different story that explains the same things [...] 'I don't know' is one of the great, though admittedly under-utilised, scientific principles.

T. Pratchett, I. Stewart, J. Cohen: The Science of Discworld II – The Globe

Acknowledgements

My gratitude goes to all the people who have contributed to this work, scientifically or otherwise. I would like to thank all members or former members of the Department of Pharmaceutical Technology and Biopharmaceutics who have made the past years an enjoyable experience. Special thanks go to Prof. Claudia Valenta for her continuous scientific and personal support and for granting me the opportunity to realise all my ideas. At this point, special thanks also go to my colleague Mag. Julia Schwarz for always having an open ear to discuss those ideas and joining me putting them into action.

I would further like to thank Dr. Nadejda Matsko of the FELMI-ZFE Graz for her enthusiasm and for devoting time to our mutual projects. Likewise, cordial thanks go to MSc. Elham Rezvani of the University of Natural Resources and Life Sciences Vienna, Prof. Jürgen Lademann and colleagues at the Charité Berlin, Dr. Perry Xiao of the London Southbank University, Prof. Bob Imhof and Dr. Lori Ciortea of Biox Systems Ltd. and Rainer Vögeli of DSM Switzerland for sharing their experience and their valuable time for discussions.

Speaking of time, special thanks also go to the people who have successfully distracted me from work to gain new energy. In particular, I would like to thank my brother David, my long-term climbing partner Veronika, my favourite scientist Dr. Jooofi, the pub quizzers and the usual suspects. Last but not least, my gratitude goes to my parents for their support all those years and to my companion Arvid for his constructive criticism and for sharing his expertise in the realms of mathematics, statistics and information technology.

Contents

Contents **5**

1 Introduction and Aim of this Work **7**
1.1 Introduction and Objectives 7
1.2 Einleitung und Zielsetzung 10

2 Theoretical Background **13**
2.1 Skin Morphology and Dermal Drug Delivery 13
2.2 Emulsion Systems for Dermal Application 17
2.3 Cyclodextrins in Dermal Formulations 24
2.4 The Tape Stripping Technique 26
2.5 Skin Integrity Testing in Vitro 27

3 Publications **33**
3.1 Lecithin-based Nanoemulsions 35
3.2 Sucrose Stearate-based Nanoemulsions 45
3.3 Facilitating in Vitro Tape Stripping 55
3.4 Semi-solid Sucrose Stearate Emulsions 69
3.5 In Vivo/in Vitro - Correlation 101
3.6 Effect of γ-Cyclodextrin 113
3.7 Skin Integrity Testing 121
3.8 Optimisation of Sucrose Stearate Emulsions 137

4 Conclusions **155**

5 References **157**

6 Abstracts **167**
6.1 Abstract 167
6.2 Zusammenfassung 169

7 Scientific Contributions within this Work **171**

8 Scientific Contributions beyond this Work **175**

9 Curriculum Vitae **177**

List of Acronyms

CD	cyclodextrin
TEM	transmission electron microscopy
NIR	near infrared
TEWL	transepidermal water loss
SC	stratum corneum
HLB	hydrophilic-lipophilic balance
DLS	dynamic light scattering
LD	laser diffraction

CHAPTER 1

Introduction and Aim of this Work

1.1 Introduction and Objectives

In recent years, methodological advances have led to the development of numerous colloidal carrier systems for an optimised delivery of active substances into the skin. As a result of the increased consumer interest in environmental aspects and health issues such as allergies, the focus of attention during formulation development has steadily shifted towards the use of safe, biodegradable and skin-friendly raw materials such as lecithin or sucrose ester mixtures. The growing number of vehicles has instigated the need for reliable methods to characterise the skin penetration potential of novel formulations. Accordingly, the main objectives of this work can be divided into two interrelated fields: the development of topical formulations and the optimisation of methods to characterise the skin penetration of these formulations.

The first objective of this work was the development of optimised dermal formulations for application of lipophilic drugs. Lecithin-based nanoemulsions should be optimised to avoid the commonly used polyethoxylated co-surfactants that are usually employed to obtain stable systems. To this end, sucrose ester surfactants and natural cyclodextrins (CDs) were tested for their potential as additional co-stabilising agents. Their influence on the long-term stability of lecithin-based nanoemulsions, the interaction of the systems with model skin in vitro and on the skin permeation of lipophilic model drugs was determined. These aspects were investigated for both negatively and positively charged nanoemulsions.

Since lecithin itself exhibits certain drawbacks as an emulsifier, the next step of this work was to develop nanoemulsions based on the investigated sucrose stearate

mixture alone. A comparative study revealing the advantages and drawbacks of lecithin and sucrose stearate emulsifier mixtures regarding formulation stability, formulation morphology and skin permeation was conducted. Again, the effect of additional CD in combination with these emulsifiers was evaluated to confirm the previous results. Cryo transmission electron microscopy (cryo TEM) should be employed for an exact characterisation of the different systems.

In the context of these studies, a peculiar rheological behaviour was observed for certain sucrose stearate mixtures with intermediate hydrophilic-lipophilic balance. It was possible to create semi-solid oil-in-water emulsions stabilised solely by sucrose stearate. Interestingly, these creamy systems were created merely by modification of the production process and exhibited the exact same composition as the corresponding nanoemulsions. Thus, comparative studies were performed with these simple systems to investigate the potential of the novel emulsions as dermal drug carriers. The obtained nanoemulsions and emulsions which differed only in their mean droplet size and viscosity were characterised by dynamic light scattering and laser diffraction measurements, respectively, as well as optical light microscopy and cryo TEM. The long-term stability and morphology of both formulation types was investigated and the influence of the different physical properties of the otherwise identical systems on their skin permeation behaviour was investigated in vitro using diffusion cell setups. In further studies, the influence of the exact sucrose stearate blend composition, the nature of the employed oil phase and the exact processing conditions were investigated using thermoanalytical and rheological techniques as well as fluorescence microscopy.

As a second major objective of this work, the tape stripping technique was optimised for laboratory use using excised porcine ears to gain more accurate data on the skin penetration behaviour of the novel vehicles. The tape stripping technique is a well-established method to determine the skin penetration of active substances in vivo. However, such in vivo studies require a lot of organisatorial and legislative effort and cannot be performed in every lab. Thus, we decided to validate in vitro tape stripping on excised porcine ears in combination with the novel technique of near infrared (NIR) densitometry for the determination of the skin penetration profiles of different model drugs. In this context, the assessment of the transepidermal water loss (TEWL) by means of a closed condenser-chamber system as well as skin hydration mapping with a capacitance-based sensor should be adapted for skin integrity testing and monitoring of the changes in skin barrier function during tape stripping.

Having established these experimental techniques for in vitro tape stripping experiments, the skin penetration of different model drugs from the developed sucrose stearate-based formulations should be investigated in comparative studies. Likewise, the experimental setup should be employed to test the potential permeation enhancement effect of CDs under a finite dose in vitro setup. Finally,

comparative tape stripping experiments with model formulations should be conducted both in vivo on human forearm skin and in vitro on porcine ear skin to confirm the validity of the porcine ear model for in vitro tape stripping.

1.2 Einleitung und Zielsetzung

Die Entwicklung kolloidaler Arzneistoffabgabesysteme zur dermalen Applikation wurde durch technologische Fortschritte während der letzten Jahrzehnte stark begünstigt. Aufgrund des verstärkten Interesses der Konsumenten an Umwelt- und Gesundheitsaspekten liegt der Schwerpunkt bei der Entwicklung neuer Dermatika heute auf der Verwendung von hautfreundlichen und bioabbaubaren Rohstoffen wie beispielsweise natürlichen Lezithin- oder Saccharoseester-Mischungen. Die wachsende Anzahl an dermalen Arzneiformen bedingt eine stetige Entwicklung verlässlicher Methoden zur Charakterisierung des Penetrationsvermögens neuer Formulierungen. Dementsprechend bestanden die Ziele dieser Arbeit aus zwei miteinander verknüpften Teilgebieten: einerseits aus der Entwicklung neuer kolloidaler Vehikel, andererseits aus der Optimierung von Methoden zur Charakterisierung der Hautpenetration dieser Formulierungen.

Das erste Ziel dieser Arbeit bestand in der Entwicklung von dermalen Formulierungen zur Verabreichung von lipophilen Arzneistoffen. Lezithin-basierte Nanoemulsionen, die zumeist mittels polyethoxylierter Co-Tenside stabilisiert werden, sollten mit Hilfe natürlicher Co-Stabilisatoren in Bezug auf Langzeit-Stabilität und Hautpermeation optimiert werden. Daher sollte der Effekt von Saccharoseester-Tensiden und natürlichen Cyclodextrinen auf die physikalische Stabilität der Lezithin-basierten Nanoemulsionen, auf deren Wechselwirkung mit Modellhaut in vitro sowie auf die Hautpermeation lipophiler Modellarzneistoffe festgestellt werden. Diese Aspekte wurden sowohl für positiv als auch für negativ geladene Nanoemulsionen untersucht.

Da Lezithin bei alleiniger Verwendung als Tensid gewisse Nachteile aufweist, wurde als nächster Schritt die Eignung der untersuchten Saccharoseester-Mischung zur alleinigen Stabilisation von Nanoemulsionen untersucht. Eine Studie zum Vergleich der Lezithin- und Saacharoseester-basierten Nanoemulsionen bezüglich physikalischer Stabilität, Morphologie sowie Hautpermeation sollte in diesem Rahmen durchgeführt werden. Zudem wurde erneut der Effekt von zusätzlichem γ-Cyclodextrin in Kombination mit diesen Tensiden untersucht, um die bisherigen Ergebnisse zu bestätigen. Kryo-Transmissions-Elektronenmikroskopie wurde zur exakten Charakterisierung der verschiedenen Systeme herangezogen.

Im Zuge dieser Studien legte die verwendete Saccharosestearat-Mischung mit mittlerem Hydrophilie-Lipophilie-Wert ein ungewöhnliches rheologisches Verhalten an den Tag. Es konnten halbfeste Öl-in-Wasser-Emulsionen hergestellt werden, die lediglich mittels der Saccharoseester-Mischung stabilisiert wurden. Die Herstellung dieser cremigen Formulierungen wurde interessanterweise durch geringfügige Modifikationen der Herstellungsbedingungen bewerkstelligt, während die Zusammensetzung exakt jener der entsprechenden Saccharosestearat-basierten Nanoemulsionen entsprach. Diese einfachen Systeme wurden in vergleichenden

Studien in Hinsicht auf ihr Potential als dermale Arzneistoff-Carrier untersucht. Die hergestellten Nano- und Makroemulsionen, die sich lediglich durch ihre Tröpfchengröße und Viskosität unterschieden, wurden mittels Dynamischer bzw. Statischer Laser-Lichtstreuungsmessung sowie Kryo-Transmissions-Elektronenmikroskopie bzw. Lichtmikroskopie charakterisiert.

Die Langzeitstabilität und Morphologie beider Systeme wurde untersucht und der Einfluss der unterschiedlichen physikalischen Eigenschaften der ansonsten identisch zusammengesetzten Systeme auf die in vitro - Hautpermeation wurde mittels Franz-Diffusionszellen analysiert. In weiterführenden Studien wurde der Einfluss der genauen Zusammensetzung von Saccharosestearat-Mischungen, der verwendeten Ölphase und der genauen Herstellungsbedingungen mittels thermoanalytischer sowie rheologischer Methoden und Fluoreszenz-Mikroskopie untersucht.

Als zweites Hauptziel dieser Arbeit sollte die Technik des Tape Stripping für den Laborgebrauch an exzidierten porzinen Ohren optimiert werden, um exaktere Daten über das Hautpenetrationsverhalten der neuen Vehikel zu erhalten. Die Tape Stripping - Methode ist eine etablierte Technik, um die Hautpenetration verschiedener aktiver Substanzen in vivo zu bestimmen. In vivo - Studien an Probanden erfordern jedoch einen erheblichen organisatorischen Aufwand und können nicht in jedem Labor durchgeführt werden. Daher war es das Ziel dieser Arbeit, die Technik des in vitro - Tape Stripping an exzidierten porzinen Ohren in Kombination mit der neuen Technik der Nah-Infrarot-Densitometrie zur Bestimmung der Hautpenetration verschiedener Modellarzneistoffe zu validieren. In diesem Zusammenhang wurden der transepidermale Wasserverlust mittels Kondensor-Kammer sowie die Hauthydratation mit Hilfe eines kapazitanzbasierten Sensors bestimmt. Diese Methoden sollten für die Überprüfung der Hautintaktheit sowie zur Überwachung von Änderungen der Hautbarrierefunktion während des Tape Strippings adaptiert werden.

Nach erfolgreicher Etablierung der in vitro Tape Stripping - Technik am porzinen Ohr sollte diese Methode zur Untersuchung der entwickelten Saccharosestearat-basierten Formulierungen herangezogen werden. Darüber hinaus wurde diese Technik zur Überprüfung des potentiell permeationsfördernden Effektes von γ-Cyclodextrin in Nanoemulsionen unter finite dose - Bedingungen eingesetzt. Schließlich sollten vergleichende Tape Stripping - Experimente an Humanhaut in vivo sowie porziner Ohrenhaut in vitro anhand von Modellformulierungen durchgeführt werden, um die praktische Anwendbarkeit des porzinen Ohrenmodells für in vitro - Tape Stripping zu überprüfen.

CHAPTER 2

Theoretical Background

2.1 Skin Morphology and Dermal Drug Delivery

Structure and Function of the Skin

The human skin as our largest organ separates our organism from the external environment. It protects us against chemical, physical or mechanical damages and prevents the intrusion of microorganisms. It prevents dehydration, but allows for a physiological evaporation of water from the skin surface. Apart from thermoregulation and mediating sensory impressions, it plays a role in immunological processes [1-4].

The skin can largely be divided into the epidermis and the dermis (Figure 1). The outermost skin layer is the epidermis, a comparatively thin epithelium that is followed by the thicker dermis and the underlying subcutaneous fatty tissue. Both hair follicles and eccrine glands are situated within the subcutis. The hair shafts and eccrine gland ducts lead through the dermis and epidermis to the skin surface. The subcutaneous vasculature and the finer dermal vasculature account for the blood perfusion of the viable tissue [1, 3].

The epidermis itself is a dynamic tissue that consists of different cell layers (Figure 2). The basement membrane, which represents the interface between the epidermis and the underlying dermis, is followed by the stratum basale or germinativum. Within this single basal layer of keratinocytes, new epidermal cells are being produced by mitosis. Upon leaving this layer, the cells start to differentiate and migrate in direction of the skin surface. The cells proceed through the stratum spinosum (prickle cell layer) which exhibits large numbers of desmosomes and

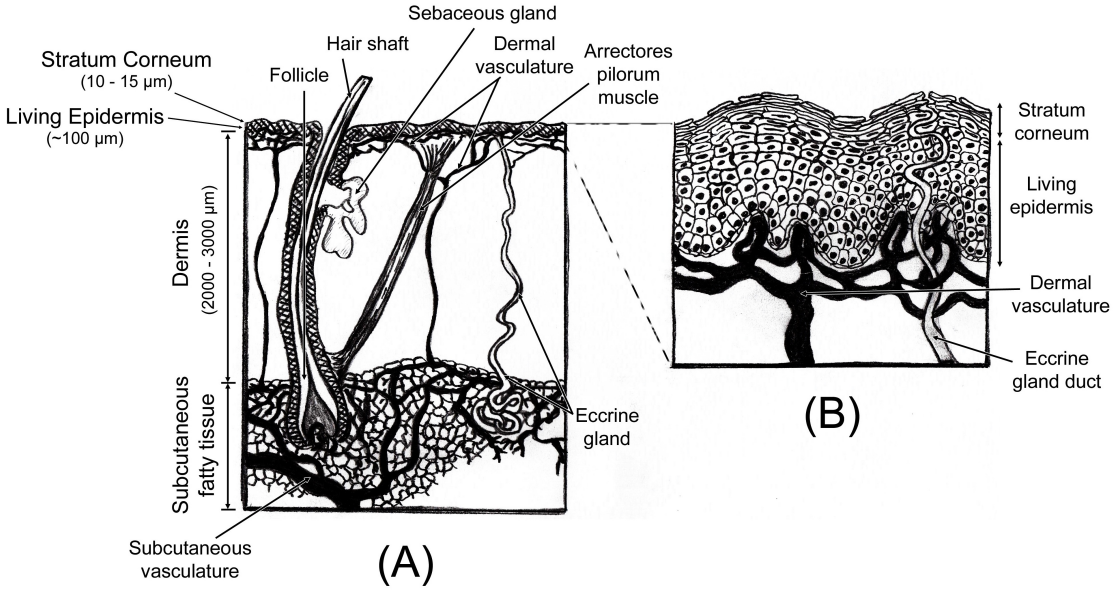

Figure 1: Schematic cross-sectional image of human skin after [1, 5]. (A) Full-thickness skin (B) Expansion of the outermost 200 μm of the epidermis.

the stratum granulosum (granular layer). A thin intermittent layer, the stratum lucidum (glossy layer), is most prominent within the palms of the hands and soles of the feet. The cells are becoming wider and flatter as they move towards the skin surface. The final differentiation at the interface to the outermost layer of the epidermis, the stratum corneum (SC), transforms the viable cells into extremely flattened dead cells filled with keratin. These non-viable cornified cells of the SC are named corneocytes and are surrounded by an envelope of cross-liked proteins as well as a lipid envelope [1, 3, 6].

The main barrier function of the skin, which prevents the loss of water and the intrusion of xenobiotic substances, is attributed to the approximate 10 to 15 μm of the SC. The overlapping corneocytes are held together by corneodesmosomes and are embedded in lipid lamellae which are orientated parallel to the cell surface. This intercellular lipid matrix consists primarily of ceramides, cholesterol, cholesteryl esters, fatty acids and cholesterol sulphate. Unlike other biological membranes, the skin does not contain any phospholipids. The outermost corneocytes are eventually peeled off of the skin surface since the SC renews itself every 14 days; the average turnover time from the formation of new cells in the basal layer to their shedding at the skin surface is approximately 28 days [6, 8-10]. The arrangement of the corneocytes within the intercellular lipid matrix of the SC has been described by means of the *bricks and mortar* model [11] (Figure 3).

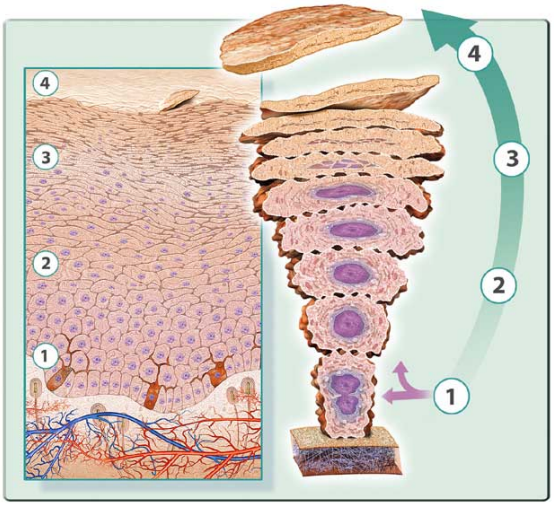

Figure 2: Life cycle of an epidermal cell and schematic cross-section through the individual layers of the epidermis: stratum basale (1), stratum spinosum (2), stratum granulosum (3), stratum corneum (4). Image reproduced with permission from [7].

Mechanisms of Dermal Drug Delivery

The complex structural organisation of the SC constitutes the main rate-limiting step against the penetration of active substances into the skin. The lipid bilayers contain alternating hydrophilic and hydrophobic areas. To deliver therapeutically relevant doses of an active agent into the skin (dermal drug delivery) or to achieve permeation of a drug through the skin for a systemic effect (transdermal drug delivery), this barrier has to be overcome. The penetration of active substances across the SC may occur along different pathways (Figure 3): the transcellular route, the intercellular route and the appendageal route, i.e. along skin appendages such as eccrine gland ducts and hair follicles.

The precise mechanism of transport has not been unequivocally determined despite years of discussion [12]. It was assumed earlier that lipophilic substances permeate mostly via the intercellular pathway and hydrophilic drugs permeate via the transcellular pathway [13]. The appendageal route was considered irrelevant since hair follicles cover only about 0.1% of the skin surface [14]. More recent studies have indicated that the intercellular pathway plays in fact an important role for most substances [3, 12] and that the hair follicles may represent an important long-term reservoir for topically applied substances [14-16].

The solubility of an applied drug is of major importance for its skin permeation behaviour. Since areas of different polarity need to be overcome, the highest

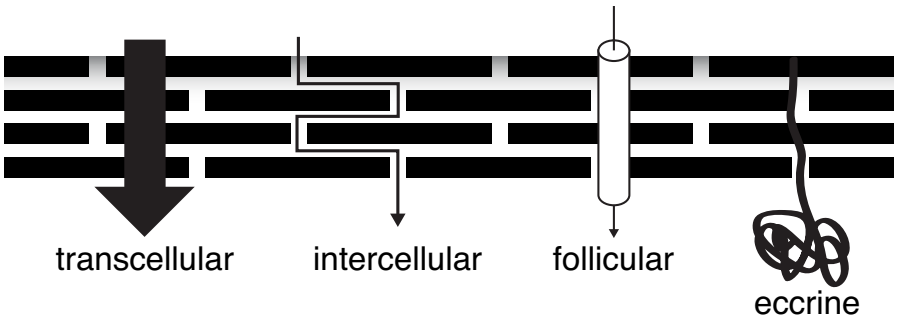

Figure 3: Penetration pathways through the skin after [9]

skin permeation can be anticipated for drugs of intermediate polarity that possess both a certain lipophilicity and hydrophilicity. Apart from the physicochemical properties of the applied drug such as molecular mass and polarity, its permeation is influenced by the applied concentration of drug, the partition coefficient of the drug between the vehicle and the skin and the diffusion coefficient of the drug within the SC [4].

The transport of substances across the skin can be regarded as a passive diffusion process that can be approximated by Fick's first law of diffusion:

$$J = \frac{DK\Delta c}{h}$$

J represents the steady-state flux of a permeant through the skin per unit area. It is directly related to the diffusion coefficient D of the permeant within the skin, the skin - vehicle partition coefficient K of the permeant and the concentration difference Δc across the skin. The flux is inversely correlated to the diffusional pathlenght h. This simplified equation can be employed to describe or predict drug diffusion across the skin [4, 9].

Penetration Enhancement Strategies

The penetration of active substances into the skin or their permeation across the skin can be improved by different strategies. Drugs or pro-drugs with optimised properties can be designed or their chemical potential can be enhanced by supersaturation within the vehicle. Alternatively, the active substances can be driven into the SC by physical penetration enhancement methods. In this context, electrical penetration enhancement methods such as iontophoresis, electroporation or ultrasound have been tested. In addition, micro needles can be employed to bypass the SC. The most frequently employed penetration enhancement strategy, however, involves modification of the SC by chemical enhancers. Chemical enhancers are

substances which temporarily reduce the skin barrier function and thus improve the flux of active substances into the skin. Extensive literature data exist on this topic and numerous chemicals have been tested. Importantly, an enhancer itself should be non-toxic to the skin, pharmacologically inactive and easily available [17, 18].

Since hydration of the SC increases the penetration of most substances by opening up the compact SC structure, water is among the safest and most effective penetration enhancers. Occlusive films, hydrophobic ointments and patches all enhance drug bioavailability in the skin due to enhanced skin hydration. Likewise, vehicles containing moisturising factors or large amounts of water can temporarily increase SC hydration [17, 19].

Among the most frequently investigated chemical penetration enhancers are surfactants, alcohols, fatty acids, essential oils and terpens [18, 20]. The mechanisms of action of penetration enhancers are often complex and difficult to elucidate. Chemical penetration enhancers have been described to affect the intracellular keratin within the corneocytes, to act on the desmosomes that maintain corneocyte cohesion, to modify the intercellular lipid domains and disrupt the intercellular lipid bilayers, e.g. by lipid extraction, or to increase the partitioning of applied drugs, co-solvents or co-enhancers into the SC [20]. The use of most chemical penetration enhancers thus involves an inherent skin irritation potential. Since dermal toxicity is a limitation for practical application and consumer compliance, there is increased interest in skin-friendly, safe and ideally bio-degradable penetration enhancers. Thus, so-called *green surfactants* based on natural raw materials are currently being investigated for the development of dermal drug delivery systems with optimised skin penetration properties. Among those, alkyl polyglucoside surfactants [21-24] and sucrose ester surfactants [25-27] are receiving increased attention.

2.2 Emulsion Systems for Dermal Application

Definition of Emulsions and Nanoemulsions

An emulsion is a multiphase system consisting of at least two immiscible liquid phases such as oil and water. One of the phases is dispersed within the other phase by means of energy input, e.g. by mechanical shearing. Different types of emulsions can be produced according to their composition, the chemical structures of oil and surfactants as well as the processing conditions. An emulsion of oil droplets surrounded by an aqueous bulk phase is termed oil-in-water emulsion (o/w emulsion) while water droplets surrounded by an oily bulk phase represent a water-in-oil system (w/o emulsion) [28]. Emulsions are metastable systems that

are kinetically stabilised with the help of surfactants, polymers or other stabilising agents that help to lower the interfacial tension between the phases. The inherent thermodynamic instability of the systems will however eventually lead to physical destabilisation [29, 30]. The considerate selection and combination of surfactants is essential to minimise destabilisation phenomena such as aggregation, flocculation, creaming, sedimentation or irreversible coalescence [31, 32]. Studies have shown that mixed interfacial films composed of different surfactants usually result in superior stability, presumably due to tighter molecular packing at the oil/water interface [28].

The term nanoemulsion is generally employed to describe emulsions with droplet sizes in the lower submicron range. The main difference to emulsions with droplets in the micrometer range lies in the superior physical stability of nanoemulsions and their usually fluid nature. According to their particle size, nanoemulsions can be transparent, translucent or milky white (Figure 4).

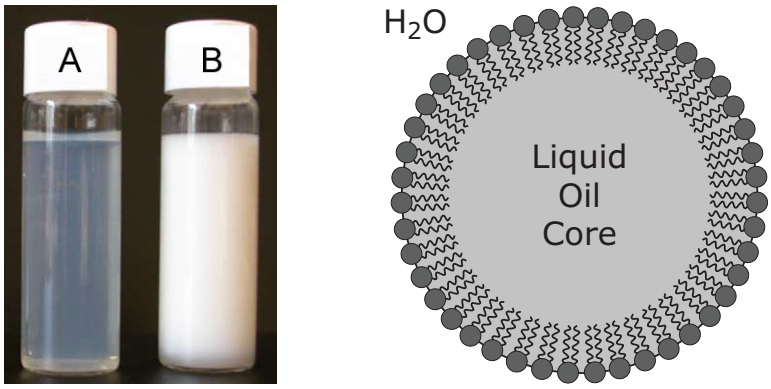

Figure 4: Optical appearance of a nanoemulsion (A, droplet diameters around 35 nm) and a conventional emulsion (B, droplet diameters around 1 μm). Image reprinted from [33] with permission from Elsevier. The structure of a nano-sized oil droplet is given on the right (modified after [34]).

The small oil droplets of o/w nanoemulsions can be kept suspended in the aqueous bulk phase for prolonged periods of time since Brownian motion largely prevents gravitationally driven sedimentation or creaming. If the oil phase possesses a certain solubility within the aqueous phase, *Ostwald ripening* may affect the physical stability of the system. Due to solubility differences between large and small emulsion droplets, the smaller droplets are incorporated into the larger ones, thus further increasing their size. This process may be an issue for nano-sized emulsions, but can be avoided by selecting appropriate excipients during formulation development. If designed correctly, nanoemulsions exhibit excellent physical stability [29].

Strictly speaking, the definition *nano* applies only to systems with droplet sizes below 100 nm, which is rarely achieved by conventional high-energy emulsification methods. Alternatively, such systems have been termed submicron emulsions, mini-emulsions, ultrafine emulsions or translucent emulsions [29, 35]. Irrespective of the inconsistent terminology throughout literature, the overall properties of nanoemulsions are accurately described by the term *emulsion*. Most importantly, nanoemulsions should not be confused with microemulsions, which are thermodynamically stable equilibrium systems that form spontaneously due to molecular self-assembly. Microemulsions generally contain large amounts of surfactants and co-surfactants or solvents and exhibit remarkable shelf lives. It should be kept in mind that they bear no similarities to actual emulsions [29].

Emulsions are classical vehicles for the loctal treatment of skin disorders. Both drug-loaded and drug-free systems can be designed for dermo-pharmaceutical or cosmetic purposes. The usually semi-solid appearance of emulsions is advantageous for practical application on skin and thus for patient compliance. Unlike microscale emulsions, nanoemulsions are usually of a fluid nature that may require the use of aerosol devices to facilitate application.

The present work was concerned with the development of both fluid nanoemulsions and semi-solid emulsions. Separate investigations as well as comparative studies were conducted to investigate the effect of the droplet size on the skin penetration of incorporated drugs. Important physical parameters that were evaluated in this context were the mean droplet size and polydispersity of the emulsions as well as the droplet surface charge and pH value of the systems. The rheological properties of dermal vehicles are of great importance for industrial processes, practical application and stability and were therefore also investigated.

Lecithin-based Nanoemulsions

The first focus of this work was the optimisation of lecithin-based nanoemulsions (see section 3.1). Lecithins are natural amphiphilic molecules that occur in cell membranes of plants and animals. They are mixtures of phospholipids and have important functions in the growth and functioning of cells. From a chemical viewpoint, the term *lecithin* specifically refers to phosphatidylcholine, which is by far the most abundant phospholipid. Thus, the name *lecithin* is commonly employed for mixtures of phosphatidylcholine with related phospholipids [36].

Lecithins are among the most widely used natural emulsifying agents in pharmaceutics, cosmetics and the food industry due to their excellent biocompatibility. The polar structure of phospholipid molecules renders them useful non-ionic emulsifying agents (Figure 5).

However, phosphatidylcholine molecules alone are not ideally suited for the formation of the curved surfaces of emulsion droplets due to their packing geometry

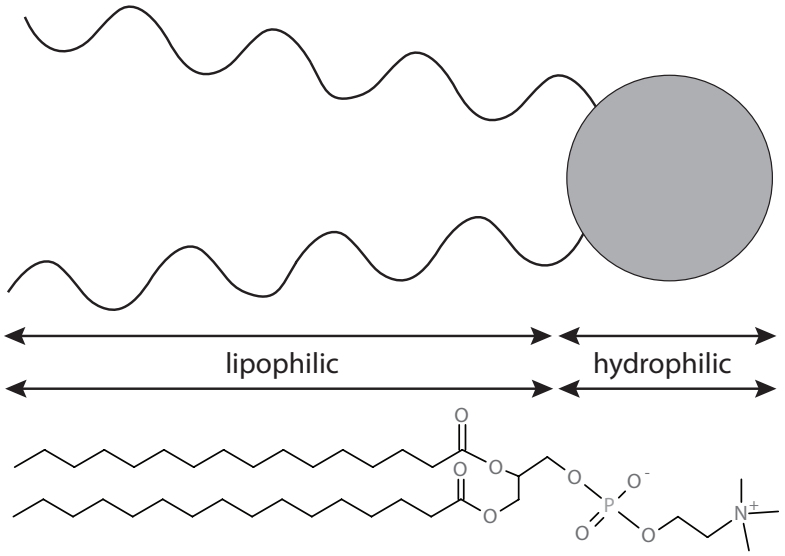

Figure 5: Schematic structure of a phospholipid after [35]

at the interface. In addition, they lack electrical charges that are required for the electrostatic stabilisation of colloidal systems. Substances that confer an electrical charge to the surface of emulsion droplets contribute beneficially to the long-term stability of the system by preventing aggregation and subsequent coalescence. In case of the highly fluid nanoemulsions, physical destabilisation through Ostwald ripening can likewise be prevented or decelerated [30, 37].

Thus, different strategies were followed for the development of nanoemulsions with optimised stability. Firstly, lecithin mixtures were employed as emulsifiers instead of the pure phosphatidylcholine. Natural lecithin mixtures contain different phospholipids such as phosphatidic acid, phosphatidylserine, phosphatidylinositol and small amounts of free fatty acids, all of which are able to confer a negative electrical charge to the droplet surface of nanoemulsions and lead to improved molecular packing at the interface [30, 37]. In addition, the physiological base phytosphingosine was employed to develop positively charged nanoemulsions for comparison. We likewise tested natural sucrose stearate mixtures and natural CDs as additives to promote the formation of mixed interfacial films for improved droplet stabilisation. Since sucrose stearate mixtures of intermediate hydrophilic-lipophilic balance (HLB) were found highly suitable for emulsion formation, they were investigated separately in extensive follow-up studies (see section 3.2 and 3.4). The conclusions derived from these studies as well as from an extensive literature research were summarised in a review article supplemental to this work [35] (see chapter 8).

Sucrose Stearate-based Nanoemulsions and Emulsions

Sucrose fatty acid esters are natural non-ionic surfactants that are increasingly employed in nutrition, cosmetics and pharmaceutics. These amphiphilic surface-active molecules consist of a sucrose molecule as hydrophilic group and different fatty acids as lipophilic groups. Since sucrose possesses 8 hydroxy groups, it may form esters with up to 8 fatty acid moities (Figure 6). The nature and the number of fatty acid residues may be varied and thus a wide range of surfactant mixtures with different HLB values can be obtained. Due to their biocompatible and skin-friendly nature, sucrose ester mixtures are approved as food additives in many countries and are raw materials for dermal applications such as personal care products, cosmetics and pharmaceutical products [38, 39].

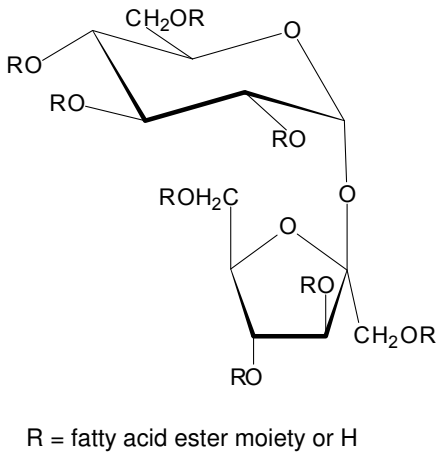

Figure 6: Chemical structure of sucrose esters after [39]

In terms of emulsion development, sucrose esters of different HLB values have been investigated for their potential to form o/w nanoemulsions [26, 40] and to influence the skin permeation of drugs [41, 42].

Since sucrose stearate mixtures were found to be highly suitable emulsifiers for nanoemulsion development, comparative studies on lecithin-based nanoemulsions and sucrose stearate-based nanoemulsions were performed (see section 3.2). The results revealed that the latter systems exhibited smaller droplet sizes, a highly homogeneous morphology, better electrochemical stabilisation and overall improved physical and chemical stability.

In addition, novel semi-solid sucrose stearate-based emulsions were developed thanks to serendipity findings during the development of the different nanoemulsions. The peculiar rheological behaviour of sucrose stearate mixtures with intermediate HLB values allowed for the production of fluid nanoemulsions and semi-solid emulsions of identical composition. In a first study (section 3.4), we focused on

the influence of the physical properties of these systems on the in vitro skin permeation and penetration of different incorporated model drugs. Interestingly, the skin penetration potential of the incorporated drugs in vitro was the same for both vehicle types. This was confirmed in subsequent in vivo tape stripping experiments (see section 3.5). In a follow-up study (section 3.8), the focus was placed on the influence of the sucrose ester blend composition, the employed oil type and the production conditions on the properties of the semi-solid emulsions.

Although the novel semi-solid emulsions exhibited complex physical properties and very exact processing conditions were required to obtain reproducible results, it should again be emphasised that an appealing semi-solid appearance was obtained without the use of additional gelling agents or stabilisers. Since these emulsions only contained 5% w/w of surfactant, high skin-friendliness may be anticipated. Thus, further research in this field might be of interest.

Characterisation of Nanoemulsions and Emulsions

The physical and chemical stability of dermal emulsions is, besides an inherent skin-friendliness, among the primary interests in formulation development. Different techniques can be employed for the initial characterisation of emulsions and the subsequent stability monitoring. When regarding the physical stability of emulsions, the mean droplet size and droplet size distribution are among the most interesting parameters. In case of nanoemulsions, these parameters can be determined by dynamic light scattering (DLS, photon correlation spectroscopy) measurements. This technique analyses the intensity fluctuations of light that is scattered by the particles in a sample. The droplets of nanoemulsions are subjected to Brownian motion. If they are illuminated with a laser, the droplets scatter the light according to their size. Smaller droplets move more rapidly and thus cause different fluctuations in light intensity than large droplets. By employing the Stokes-Einstein equation, the hydrodynamic diameters of the droplets can be calculated once the velocity of the Brownian motion has been deduced from the intensity fluctuations [43]. This technique is recommended for droplet diameters between approximately 3 nm and 10 μm depending on the manufacturer specifications of the respectively employed device. The most accurate results, however, are certainly obtained for monodisperse samples with droplet sizes in the submicron range. For conventional emulsions with droplet sizes in the higher micrometre range, laser diffraction (LD, static light scattering) is the method of choice. This technique determines droplet size distributions by comparing the scattering pattern of a sample to an appropriate optical model with the help of a mathematical inversion process. All light scattering techniques are based on certain assumptions depending on the underlying mathematical theory. Calculations employing the Mie theory are based on the assumption that the analysed particles are spherical

and homogeneous in nature [43]. Detailed information about the morphology of the analysed nanoemulsions is therefore required to verify the accuracy of DLS results. Besides, the DLS technique exhibits certain limitations regarding the characterisation of nano-sized emulsions. Small populations of large droplets, surfactant aggregates as well as lamellar or vesicular structures may remain undetected and may bias DLS calculations due to their non-spherical nature. The sample dilution that is generally required for DLS measurements may conceal reversible destabilisation phenomena such as flocculation or the appearance of aggregates [44, 45]. At the moment, electron microscopy in combination with different cryo preparation techniques represents one of the most informative approaches towards a thorough characterisation of nanoemulsion morphology [45, 46]. In the context of the present work, cryo TEM was repeatedly employed to characterise the developed nanoemulsions and to determine the effect of the different surfactants and additives on the morphology of the produced systems. The overall insights that were gathered during these studies were summarised in a recent review article supplemental to this work [45] (see chapter 8).

Apart from the droplet size distribution, the electrochemical stabilisation of the nanoemulsion droplets can be investigated. The technique of laser Doppler electrophoresis (laser Doppler anemometry) delivers information about the zeta potential (ZP), which characterises the droplet surface charge of the emulsion droplets within the aqueous bulk phase. The nanoemulsion sample is subjected to an electrical field. If the droplet surface is charged, the droplets migrate towards the electrode of the opposite charge. Their velocity is directly proportional to the magnitude of their surface charge, i.e. their ZP. When a laser beam is scattered by the moving droplets, a frequency or phase shift of the laser light results and is measured as the droplet mobility. The ZP is derived from this mobility and the dispersant viscosity, e.g. by employing the Smoluchowski theory. For nanoemulsions with high absolute ZP values above 30 mV, satisfying electrochemical stabilisation can be anticipated [47]. If necessary, appropriate charge-inducing additives can be employed to confer a high absolute charge to the droplet surfaces, thus preventing their aggregation and subsequent coalescence [35].

The DLS technique in combination with laser Doppler electrophoresis is the most frequently employed approach for investigating the physical stability of nanoemulsions. The required dilution of the sample may conceal reversible aggregation phenomena, but will otherwise exert little influence on the properties of the investigated nanoemulsion. In case of semi-solid emulsions with droplet sizes in the micrometer range, LD can be employed after extensive dilution and careful homogenisation of the creamy samples. However, the obtained results may be affected by the specific steps of sample preparation before the analysis, especially if a complex internal morphology is involved. More accurate information about the physical properties of semi-solid emulsions can be obtained by rheological mea-

surements. The reaction of a formulation to an applied shear, i.e. its resistance to deformation, may provide valuable information about its internal structure. The flow behaviour of emulsions and their viscoelastic properties depend on different factors, such as the oil volume fraction, the mean droplet size, the droplet surface charge and colloidal interactions [48]. Both linear and oscillatory measurements can be conducted to elucidate the formulation properties. In addition, optical light microscopy may assist to visualise the emulsion morphology. Due to the dense nature of semi-solid emulsions, additional techniques of sample preparation might be necessary to clarify the nature of the observed formulation structures. In the present studies, fluorescence marking of the respective oil or water phase and subsequent fluorescence microscopic analysis served to clarify previous uncertainties (see section 3.8).

The chemical stability of emulsions can be compromised during storage due to degradation processes that may not immediately affect the physical stability of the entire system. However, the progressive chemical degradation of emulsion compounds such as surfactants, incorporated drugs or natural oils will eventually affect the entire system due to an increasing drop in pH value. Accordingly, the pH value represents a useful indicator for monitoring the chemical stability of an emulsion. In the context of the present studies, lecithin-based systems generally appeared to be more prone to oxidative and hydrolytical degradation than sucrose stearate-based systems (see section 3.2).

2.3 Cyclodextrins in Dermal Formulations

Definition, Properties and Application of Cyclodextrins

CDs are cyclic oligosaccharides consisting of several α-D-glucopyranose units joined through an α-1,4 bond. These dextrose units form a torus-shaped molecule with a hydrophilic outer surface and a lipophilic central cavity. CDs with six, seven or eight dextrose units have been named α-, β- and γ-CD [43] (Figure 7).

Apart from these natural CDs, a large number of CD derivatives with improved aqueous solubility or other properties of interest have been developed for various applications. CDs are well-established pharmaceutical compounds due to their ability to form non-covalent inclusion complexes with suitable lipophilic molecules or molecule structures. These inclusion complexes may exhibit completely different physical, chemical and biological properties than either the parent drug or the CD and can be employed for various beneficial purposes. The main applications of CDs in pharmaceutical technology are the stabilisation or solubilisation of active molecules of poor aqueous solubility. Complexation with CDs can thus be employed to increase the solubility and the dissolution of drugs, to protect volatile

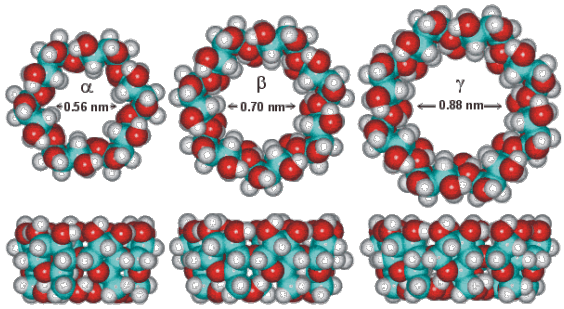

Figure 7: Molecular structure of the natural cyclodextrins α, β and γ (reprinted with courtesy of M. Chaplin, London Southbank University)

or unstable compounds, to alter drug release rates or to minimise local irritation. In addition, CDs can affect the skin permeation of drugs [49-51].

Cyclodextrins in Dermal Formulations

CDs can be incorporated in dermal drug delivery systems to improve the solubility and dispersion of drugs. In addition, they can influence the skin permeation rates of drugs. When applied as additives in dermal formulations, CDs may act as permeation enhancers by keeping lipophilic drugs in solution and consequently delivering them to the skin surface. However, this effect strongly depends on the complexation affinity between drug and CD and may lead to decreased skin permeation rates as well [49, 50]. In addition, the emulsifying potential of natural CDs has been recently discussed and employed for formulation development [52-55]. CDs can act as emulsifying agents in emulsions by forming inclusion complexes with fatty acid residues of the oil phase. If appropriate excipients are employed, these molecule complexes exhibit surface active properties and can lower the interfacial tension of the resulting systems. These amphiphilic *supermolecules* can thus contribute to the stabilisation of emulsions [55]. Due to their large molecular weight, CDs cannot permeate the skin themselves and can thus be considered as comparably eudermic stabilising agents [56]. Although the concept of using CDs as emulsifying agents in multiphase systems was introduced some time ago [57, 58], it has only been investigated to a limited extent in simple or multiple emulsions [59-61]. Thus, the practical applicability of CDs as co-stabilising agents in complex nanoemulsion systems should be investigated within the present work (see section 3.1 and 3.2). At the same time, the effect of the natural CDs on the skin permeation of incorporated model drugs was analysed. Repeated diffusion cell studies revealed a particularly pronounced enhancement effect for steroidal drugs when combined with γ-CD. Thus, an additional methodological study was

performed to elucidate the underlying mechanisms (see section 3.6).

2.4 The Tape Stripping Technique

In Vivo vs. in Vitro Tape Stripping

Different in vitro setups have been developed to investigate the permeation or penetration of active substances into the skin, such as different diffusion cell setups [62], the bovine udder skin model [63] and the Saarbruecken penetration model [64, 65]. The tape stripping technique is a classical in vivo technique to investigate the skin penetration of applied substances [66, 67], but has likewise been adapted for in vitro experiments using excised human skin [68]. During the tape stripping process, a defined amount of drug-loaded formulation is applied to a marked skin area, usually by means of a saturated glove finger. After a specific interval of residence time, the outermost corneocyte layers of the SC as well as the penetrated formulation are successively removed with the help of adhesive tapes. Each tape is pressed firmly onto the skin surface for a short interval of time and is subsequently pulled off in a single rapid movement. Preferably, the pressure application is performed with a rolling movement to minimise the influence of wrinkles. Each individual adhesive tape is then analysed for the removed corneocyte mass and the amount of penetrated drug to obtain the skin penetration profile of the active substance [69, 70]. This technique is most frequently performed on human forearm skin in vivo (Figure 8).

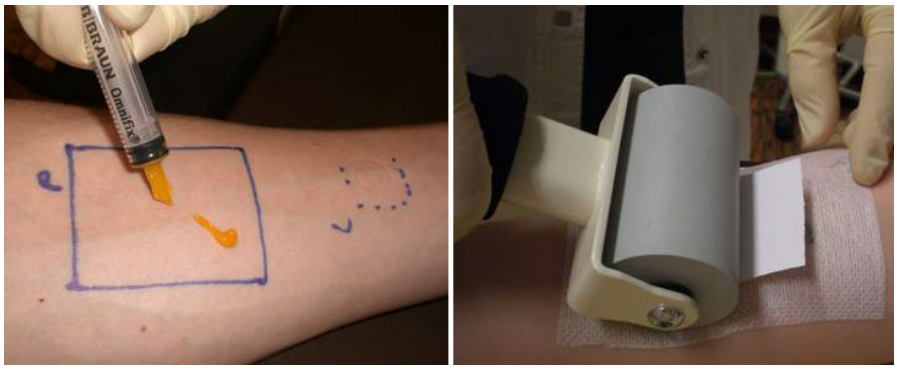

Figure 8: Preparations for the tape stripping technique on human forearm skin in vivo

Although tape stripping can be performed using excised human skin or even heat-separated human epidermis, these model skins are not entirely representative for the in vivo situation. In particular, the follicular penetration pathway

within the excised human skin is largely blocked due to the contraction of elastic fibres of the excised skin tissue. In this respect, it was suggested that porcine ear skin might represent a superior in vitro model for mimicking the skin penetration of drugs into human skin. The porcine ear skin remains on the cartilage of the excised ear. Thus, non-physiological contraction of the tissue is avoided [14]. Despite the larger size of the porcine hair follicles, this in vitro model represents a promising approach to investigate the skin penetration of novel formulations with different model drugs. We therefore decided to optimise this technique to obtain reproducible and accurate in vitro skin penetration data. In particular, the quantification of the removed corneocytes should be facilitated by adapting the technique of NIR-densitometry for this task (see section 3.3).

Methods of Corneocyte Quantification

The accuracy of the skin penetration profiles obtained by the tape stripping technique depends strongly on the accuracy of the employed methods of corneocyte quantification. Different methods have been proposed for this task, such as colorimetric protein assays [68, 71, 72], differential weighing [66, 73, 74] and optical light microscopy [75]. More recently, optical approaches of corneoycte quantification have been introduced for the analysis of human SC cells both in vivo and in vitro, such as UV/Vis spectroscopy [66, 76, 77] and NIR-densitometry [68, 78]. These methods rely on the determination of the optical pseudo-absorption of the removed adhesive tapes. Since NIR-densitometry had not yet been validated for the quantification of porcine corneocytes, this objective was included in the present work for optimisation of the tape stripping technique on excised porcine ear skin. The employed device was the NIR-densitometer SquameScan® 850A (Heiland Electronic GmbH, Wetzlar, Germany) as shown in Figure 9.

2.5 Skin Integrity Testing in Vitro

Apart from a standardised working procedure and reliable methods of corneocyte quantification, constant high quality of the employed porcine ear skin is essential to obtain reproducible results during in vitro tape stripping. Porcine ear skin may be of variable nature depending on the breed and upbringing of the sacrificed animal. The preferred area for tape stripping experiments is the central part of the dorsal ear side [79, 80], which may be damaged due to tags or injuries. Skin diseases or small lesions may remain unnoticed to the naked eye. Thus, additional techniques for quality control of the employed skin are required. In the context of the present work, the assessment of the TEWL and skin hydration imaging

Figure 9: The SquameScan® 850A near infrared-densitometer

with a capacitance-based fingerprint sensor were investigated and tested for the characterisation of porcine ear skin in vitro (see section 3.7).

Transepidermal Water Loss

An important homeostatic function of the skin is to regulate the loss of water to the external environment. For both human and porcine skin, this task is fulfilled by the outermost 10 to 20 μ of the epidermis, the SC, which allows for a certain physiological water loss by passive diffusion and from sweat glands [81]. The magnitude of the physiological TEWL of healthy human skin depends strongly on the respective skin area. Typical basal values for different skin regions have been determined [82-84]; for instance, the typical TEWL of human forearm skin may range from 9 to 16 g m^{-2} h^{-1}. If the skin barrier function is compromised by physical or chemical damages or by skin disorders, the TEWL is increased. Thus, the determination of the TEWL represents an effective method to characterise the state of the skin barrier function in vivo and is an established tool for skin integrity testing during in vivo tape stripping experiments [81]. Areas of increased TEWL can be identified and excluded from tape stripping experiments.

The TEWL can be determined by measuring the water vapour flux density. Both open- and closed-chamber devices based on different measurement principles have been developed [85-88]. Open-chamber devices require an exact climatisation and still ambient air; the results may be influenced by external factors. Closed-chamber instruments are easier to handle and result in smaller experimental scattering of the obtained data [89].

In the context of this work, the closed-chamber device Aquaflux® (Biox® Systems Ltd., London, UK) was employed since it prevents environmental factors

from directly influencing the measurement results. The measurement principle is the condenser-chamber method (Figure 10) [90].

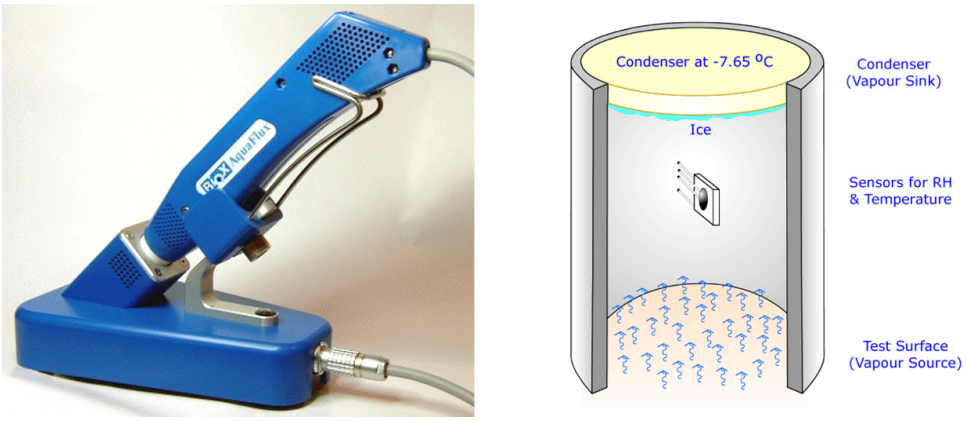

Figure 10: The Aquaflux® closed-chamber device and its measurement principle (courtesy of B. Imhof, Biox® Ltd.)

The measurement head is placed onto the skin, thereby creating a closed environment between the skin surface and the aluminium condenser at the top of the chamber that is maintained below the freezing temperature of water. At the skin surface, the water vapour emerging from the skin creates an area of high humidity while the condenser converts water vapour to ice and thus acts as humidity sink. Due to this humidity gradient, the water vapour migrates from the skin to the condenser by passive diffusion and the water vapour flux in g m^{-2} h^{-1} is calculated from the measured humidity gradient [87, 90, 91].

For in vitro studies, determination of the TEWL does of course not offer the same applicability as for in vivo experiments since excised porcine ears lack an active circulation. The skin and the underlying tissue may dehydrate during prolonged experiment times and the TEWL thus largely depends on the state of the ear. Nevertheless, determination of the TEWL in vitro can be employed to characterise the state of fresh porcine ears, to assess the skin barrier function and to monitor the defrosting process if frozen porcine ears are employed. The hydration of porcine ears within a set of experiments can be determined with satisfying accuracy and diseased skin areas or lesions with increased TEWL values can be identified and excluded [92, 93].

Capacitance-based Fingerprint Sensor Imaging

A capacitance-based sensor was tested for its suitability to characterise the skin surface properties of porcine ear skin in vitro. Skin capacitance is an electrical property of the skin that can be measured at the level of the SC. The obtained values are related to the moisture content of the tissue. Thus, skin hydration mapping can be employed to visualise and quantify the water content of the skin [94].

Skin capacitance imaging is a non-optical and non-invasive method that can distinguish different levels of SC hydration. This capacitive pixel-sensing technology is based on a silicone image sensor technology that was initially developed for fingerprint assessment in biometric security procedures. The technique allows to record capacitance images of the skin surface in relation to the skin surface hydration at 50 µm intervals. Changes in the SC structure may be related to its water holding capacity and alterations of the barrier function that affect the electrical properties of the skin can thus be detected. Sites of dermal inflammation and subclinical irritation, lesions or sweat gland disturbances can be identified in vivo [95-97].

In addition, capacitance mapping of the skin was found highly useful to investigate the skin relief or surface topography in vivo due to its simplicity and speed of data acquisition [98, 99]. Capacitive skin images give a representation of the skin topography in terms of wrinkles and cells. In dermatology and cosmetics, the characterisation of the skin surface topography can serve to investigate the effect of dermatological or cosmetic formulations or to evaluate the ageing process of the skin. Primary and secondary lines and wrinkles as well as skin pores can be visualised [94, 100-102].

The capacitance-based sensor employed for skin hydration imaging and surface analysis during this work is a novel, hand-held probe that uses fingerprint array sensors (MBF 200, Fujistu Ltd.) [103] (Figure 11). Advantages of this technique are its non-invasive nature and its rapid and simple use. The device is briefly applied onto the skin to assess the current skin hydration properties. Specifically designed algorithms calculate skin hydration maps, skin micro relief images and even 3D surface profiles of the skin. The skin surface pattern of hydration and topography is viewed as high-resolution real-time non-optical images. Skin hydration maps of 256 x 300 pixels with a spatial resolution of 50 x 50 µm are automatically generated. Each pixel is represented by an 8-bit greyscale value on a scale from 0 to 255. High greyscale values, i.e. dark pixels, represent hydrated areas of high capacitance while low greyscale values, i.e. bright pixels, represent dry spots or depressions and lines in the micro relief which impede the contact between the probe and the SC. Areas where skin moisture is lost via the SC via sweat glands or damaged skin areas can be detected [95, 96, 103].

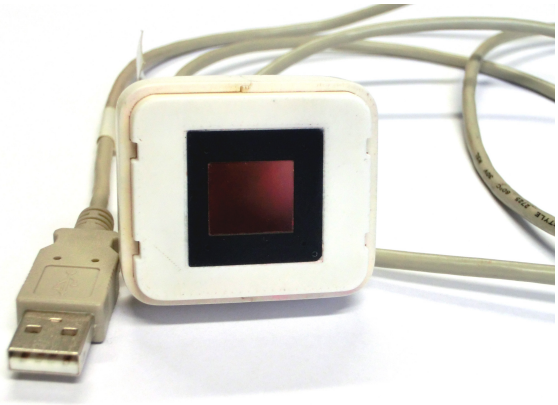

Figure 11: Capacitance-based fingerprint sensor (MBF 200, Fujistu Ltd.)

Since this technique had not been employed for skin integrity testing in context with tape stripping experiments on either human or porcine skin, we decided to investigate the applicability of capacitance-based imaging for quality control of porcine ear skin and monitoring of the changes in skin barrier function during tape stripping. Comparison of the obtained data with corresponding TEWL values should reveal whether the two techniques deliver comparable results and are equally suitable for the initial control of porcine ear skin and a subsequent in-process control during in vitro tape stripping.

CHAPTER 3

Publications

The fundamental concepts of this work are presented in the following publications:

- Lecithin-based Nanoemulsions: 'Enhancement of stability and skin permeation by sucrose stearate and cyclodextrins in progesterone nanoemulsions', *Int. J. Pharm. 393 (2010), 152–160*
- Sucrose Stearate-based Nanoemulsions: 'Development of sucrose stearate-based nanoemulsions and optimisation through γ-cyclodextrin', *Eur. J. Pharm. Biopharm. 79 (2011), 58–67*
- Facilitating in Vitro Tape Stripping: 'Facilitating in vitro tape stripping: application of infrared densitometry for quantification of porcine stratum corneum proteins', *Skin Pharmacol. Physiol. 24 (2011), 256–268*
- Semi-solid Sucrose Stearate Emulsions: 'Semi-solid Sucrose Stearate-Based Emulsions as Dermal Drug Delivery Systems', *Pharmaceutics 3 (2011), 275-306*
- In Vivo/in Vitro - Correlation: 'In Vitro vs in Vivo Tape Stripping: Validation of the Porcine Ear Model and Penetration Assessment of Novel Sucrose Stearate Emulsions', *Eur. J. Pharm. Biopharm., in press*

The remaining publications augment previous findings and allow a more detailed insight into specific aspects of the established results.

- Effect of γ-Cyclodextrin: 'Effect of γ-cyclodextrin on the in vitro skin permeation of a steroidal drug from nanoemulsions: Impact of experimental setup', *Int. J. Pharm., in press*

- Skin Integrity Testing: 'Skin integrity testing and monitoring of in vitro tape stripping by capacitance-based sensor imaging', *Skin Res. Technol., submitted Nov 18th 2011 - under review*
- Optimisation of Sucrose Stearate Emulsions: 'Semi-solid O/W emulsions based on sucrose stearates: influence of oil and surfactant type on morphology and rheological properties', *J. Disp. Sci. Technol., accepted for publication*

International Journal of Pharmaceutics 393 (2010) 152–160

Contents lists available at ScienceDirect

International Journal of Pharmaceutics

journal homepage: www.elsevier.com/locate/ijpharm

Enhancement of stability and skin permeation by sucrose stearate and cyclodextrins in progesterone nanoemulsions

Victoria Klang[a], Nadejda Matsko[b], Anna-Maria Zimmermann[a], Emina Vojnikovic[a], Claudia Valenta[a,*]

[a] University of Vienna, Department of Pharmaceutical Technology and Biopharmaceutics, Faculty of Life Sciences, Althanstraße 14, 1090 Vienna, Austria
[b] Graz University of Technology and Centre for Electron Microscopy Graz, Institute for Electron Microscopy and Fine Structure Research, 8010 Graz, Austria

ARTICLE INFO

Article history:
Received 14 January 2010
Received in revised form 20 April 2010
Accepted 21 April 2010
Available online 29 April 2010

Keywords:
Nanoemulsion
Submicron emulsion
Cyclodextrin
Progesterone
Sucrose stearate

ABSTRACT

Lecithin-based nanoemulsions are colloidal drug delivery systems which offer fundamental advantages in topical therapy, such as excellent skin permeation of lipophilic drugs; however, their physicochemical long-term stability is usually rather poor without the use of additional synthetic surfactants such as polysorbates. In a novel approach negatively and positively charged formulations were developed without the use of conventional synthetic surfactants. Natural substances such as sucrose esters and different cyclodextrins were additionally used as stabilising agents. Emphasis was laid on optimisation of the homogenisation process and formulation properties. The optimised formulations were tested for their potential as drug delivery systems for progesterone. Furthermore, crucial formulation parameters such as particle size and zeta potential were monitored for more than a year. In this context, the effect of the natural excipients sucrose stearate and cyclodextrins α, β and γ on in vitro skin permeation was investigated; the influence of the positive particle surface charge induced by incorporation of the cationic phytosphingosine was evaluated as well. The results showed that in particular the cyclodextrins seemed to induce fundamental changes in formulation microstructure as confirmed by cryo TEM, thus leading to remarkably increased skin permeation rates of progesterone compared to the control.

© 2010 Elsevier B.V. All rights reserved.

1. Introduction

Multicomponent systems with particle sizes in the submicron range play an important role as drug delivery systems today. In topical drug delivery, colloidal multiphase systems such as nanoemulsions offer fundamental advantages in terms of permeation enhancement for lipophilic drugs and skin-compatibility (Tadros et al., 2004). However, their widespread use is limited by their comparatively poor long-term stability when compared to thermodynamically stable systems such as microemulsions (Tadros et al., 2004).

Nanoemulsions are metastable systems characterised by a mean droplet diameter below 100 nm (Sonneville-Aubrun et al., 2004). However, the term is widely used to describe formulations with particle sizes in the submicron range below 500 nm (Porras et al., 2004). Hence for the sake of simplicity, the submicron-sized formulations developed in this study will be referred to as nanoemulsions.

A major amount of research has been devoted to the development of lecithin-based nanoemulsions with acceptable physicochemical stability (Yilmaz and Borchert, 2005; Hoeller et al., 2009). The small content of mostly eudermic surfactants in these formulations renders them highly suitable for dermal application.

Both negatively and positively charged nanoemulsions have been developed in order to overcome the barrier posed by the stratum corneum of the skin (Piemi et al., 1999; Yilmaz and Borchert, 2005; Hoeller et al., 2009). Literature suggests that formulations with positive droplet surface charge yield higher permeation rates for drugs because of better interaction with negatively charged residues of skin proteins (Piemi et al., 1999; Hoeller et al., 2009) or lipids (Michniak-Kohn et al., 2005). The cationic base phytosphingosine (PS) has already been incorporated into nanoemulsions successfully (Yilmaz and Borchert, 2005; Hoeller et al., 2009) and was therefore selected as additional compound to induce a positive particle surface charge.

So far, however, additional synthetic surfactants such as polysorbates (Tweens) were generally necessary to stabilise such nanoemulsions for a longer period of time (Yilmaz and Borchert, 2005; Hoeller et al., 2009). Polysorbates are ethoxylated tensides which supposedly cause skin irritation and contact dermatitis (Bergh et al., 1998a,b). They might therefore impair the skin-friendliness of the developed nanoemulsion systems.

In this context, natural emulsifiers offer an appropriate alternative to conventional synthetic surfactants. Apart from lecithin mixtures, various carbohydrates have been shown to possess interesting properties in terms of stabilising multiphase systems. In recent years, the so-called "sugar surfactants" have enjoyed increased attention in formulation development. This term not only refers to alkylpolyglucosides, but also to the less frequently investi-

* Corresponding author. Tel.: +43 1 4277 55 410; fax: +43 1 4277 9554.
E-mail address: Claudia.valenta@univie.ac.at (C. Valenta).

0378-5173/$ – see front matter © 2010 Elsevier B.V. All rights reserved.
doi:10.1016/j.ijpharm.2010.04.029

gated sucrose esters such as sucrose stearate (SS). These non-ionic surfactants are fatty acid esters of sucrose which exhibit different HLB values according to the type and number of their fatty acid residues (Csoka et al., 2007). Certain sucrose esters have been shown to increase skin permeation of drugs (Ayala-Bravo et al., 2003; Cazares-Delgadillo et al., 2005; Calderilla-Fajardo et al., 2006; Csoka et al., 2007). Therefore, these natural surfactants were chosen as co-emulsifying agents to be tested for their suitability in formulation development and their effect on skin.

Another class of carbohydrates which has recently (Duchene et al., 2003; Bochot et al., 2007; Inoue et al., 2008; Rother, 2009) been investigated in terms of emulsifying properties are the cyclic oligosaccharides called cyclodextrins (CDs). These well-known pharmaceutical compounds are able to form non-covalent inclusion complexes with suitable lipophilic molecule structures. They are therefore frequently used to stabilise or solubilise lipophilic drugs (Challa et al., 2005). Their rather poor water-solubility has led to the development of a large number of chemically modified derivatives with improved physicochemical properties. The present study, however, focuses on the use of the common natural CDs α, β and γ.

In drug delivery systems used on skin, CDs have been reported to improve the dispersion of drugs and influence their skin permeation rates (Loftsson et al., 2007). In addition, they can be used to stabilise emulsion systems by complexation of fatty acid residues of the oil phase. Thus, new surface active molecule complexes are formed which lower interfacial tension and stabilise the systems (Duchene et al., 2003; Inoue et al., 2008). These newly formed amphiphilic "supermolecules" (Rother, 2009) represent highly eudermic emulsifying agents as the CDs themselves cannot permeate the skin due to their large molecular weight (Loftsson and Masson, 2001).

The concept of using CDs as emulsifying agents in multiphase systems was first introduced by Shimada et al. (1991, 1992). However, it has only been investigated to a limited extent in simple emulsion or multiple emulsion systems (Yu et al., 2003; Hashizaki et al., 2007; Inoue et al., 2008). To date few approaches have been made to test the feasibility of using CDs as additional stabilising agents in complex multicomponent systems such as lecithin-based nanoemulsions. Hence, the natural CDs α, β and γ were chosen as respective co-stabilising excipients in order to investigate their effect on formulation properties and skin permeation of the model drug progesterone.

In conclusion, the primary aim of the present study was the development of stable nanoemulsions as delivery systems for progesterone without the use of possibly skin-irritating synthetic surfactants such as polysorbates. To this end, lecithin-based nanoemulsions with negative or positive particle surface charge were developed and optimised with the help of additional stabilising agents such as sucrose esters and CDs. The second objective of this study was the investigation of the effect of aforementioned excipients, in particular the CDs, on formulation properties and microstructure as well as skin permeation of the model drug progesterone *in vitro*. In this context, the hypothesis of superior skin permeation from positively charged formulations containing phytosphingosine in comparison to their negatively charged counterparts was evaluated as well.

2. Materials and methods

2.1. Materials

Cyclodextrin α (Cavamax® W6 Pharma) and γ (Cavamax® W8 Pharma) were obtained from Wacker Chemie AG (Munich, Germany); cyclodextrin β (Kleptose) was kindly donated by Roquette frères (Lestrem, France). Progesterone (CAS: 57-83-0) was purchased from Sigma–Aldrich (St. Louis, USA). Phytosphingosine was kindly provided by Degussa (Cosmoferm BV, NL). Lipoid E-80 was donated by Lipoid GmbH (Ludwigshafen, Germany), containing 81.8% phosphatidylcholine, 8.2% phosphatidylethanolamine and 2.0% lysophosphatidylcholine according to manufacturers' specifications. Sucrose stearate (Ryoto Sugar Ester® S-970) and sucrose laureate (Ryoto Sugar Esters® L-595 and L-1695) were supplied by Mitsubishi-Kasei Food Corporation (Tokyo, Japan). Propylene glycol (1,2-propanediol) and the antioxidant α-tocopherol were purchased from Pauli GmbH & Co. KG (Vienna, Austria). The preserving agent potassium sorbate was obtained from Herba Chemosan Apotheker-AG (Vienna, Austria). PCL-liquid (cetearyl ethylhexanoate, isopropyl myristate) was provided by Symrise GmbH & Co. KG (Holzminden, Germany). All other chemicals used were of analytical reagent grade and used as received without further purification.

2.2. Preliminary tests and solubility studies

2.2.1. Optimisation of formulation composition

Different sugar esters S-970, L-595 and L-1695 were tested as co-emulsifiers; to this end, they were incorporated (1%, w/w) into the basic formulations. Furthermore, different concentrations of CDs were incorporated into the basic mixtures both alone and in combination with sucrose esters; the most suitable concentration of CDs in terms of formulation properties was selected for further studies.

2.2.2. Solubility of progesterone

An important aspect of skin permeation studies *in vitro* is the choice of the receptor fluid. Progesterone is almost insoluble in water (3.79×10^{-5} M at 25 °C) (Zoppetti et al., 2007); since a wholly aqueous receptor medium like phosphate buffer is unsuitable for drugs with a water solubility lower than 10 μg/ml (Brain et al., 1998), propylene glycol/water (40 + 60, w/w) was chosen as receptor phase. The solubility of progesterone in this acceptor medium has already been established and has been found to be suitable for *in vitro* skin diffusion studies (Valenta et al., 2001; Biruss and Valenta, 2006).

2.3. Formulations

Nanoemulsions were prepared as previously described (Hoeller et al., 2009); process parameters were optimised. The aqueous and oily phases were prepared separately. The aqueous phase, consisting of freshly distilled water and potassium sorbate, was stirred at 50 °C. In the respective formulations, sucrose ester and CD α, β or γ were incorporated into the aqueous phase. The oil phase consisted of PCL-liquid, Lipoid E-80, propylene glycol and α-tocopherol; phytosphingosine and progesterone were dissolved in the oil phase as well in the respective formulations. The two phases were mixed and pre-homogenised for 4 min with an ultra-turrax (Omni 500) at 2500 rpm. Afterwards, the mixture was stirred and heated to 50 °C before it was further homogenised with a high-pressure homogeniser (EmulsiFlex C3, Avestin) for 16 homogenisation cycles at 750 bar. Table 1 shows the different formulations as well as their composition and abbreviations.

2.4. Nanoemulsion characterisation

2.4.1. Particle size

All formulations were analysed for their particle size and particle size distribution by photon correlation spectroscopy using a Zetasizer Nano ZS (Malvern, UK) at 25 °C. Samples were diluted with freshly distilled water 1:100 (v/v) to diminish opalescence.

Table 1
Composition of optimised nanoemulsion formulations with negative particle surface charge and abbreviations. The corresponding positively charged formulations were created by addition of the cationic phytosphingosine (PS, 0.1%, w/w) and marked with "+". Drug-loaded formulations were created by incorporation of progesterone (1%, w/w) and marked with "prog".

Excipients	Nanoemulsion composition (% w/w)							
	α	β	γ	Control	α-SS	β-SS	γ-SS	Control-SS
Lipid phase								
PCL-liquid	20	20	20	20	20	20	20	20
Lipoid E80	4	4	4	4	4	4	4	4
Propylene glycol (PG)	3	3	3	3	3	3	3	3
α-Tocopherol	1	1	1	1	1	1	1	1
Aqueous phase								
Sucrose stearate S-970 (SS)	–	–	–	–	1	1	1	1
Cyclodextrin α (α-CD)	0.5	–	–	–	0.5	–	–	–
Cyclodextrin β (β-CD)	–	0.5	–	–	–	0.5	–	–
Cyclodextrin γ (γ-CD)	–	–	0.5	–	–	–	0.5	–
Potassium sorbate	0.1	0.1	0.1	0.1	0.1	0.1	0.1	0.1
Distilled water to	100	100	100	100	100	100	100	100

The obtained polydispersity index (PDI) values represent the particle size distribution within the formulations. PDI values below 0.2 indicate a narrow size distribution; this indicates good long-term stability due to reduction of degradation processes like Ostwald ripening (Yilmaz and Borchert, 2005). The parameters of interest were measured immediately after preparation of the formulations; the obtained nanoemulsions were stored at 4 °C and measurements were performed every fortnight over a period of more than 12 months. Thus, information about the long-term stability of the formulations was gained.

2.4.2. Particle surface charge (zeta potential)

The particle surface charge of the formulations was determined by laser Doppler electrophoresis using a Zetasizer Nano ZS (Malvern, UK). Zeta potential (ZP) values of the formulations were determined at 25 °C. Samples were diluted with distilled water (1:100, v/v) containing sodium chloride (0.01 mmol) in order to ensure constant conductivity below 0.05 mS/cm. As distilled water alone might lead to fluctuating conductivity as solvent, addition of electrolytes ensures reproducible measurement conditions (Mueller, 1996; Yilmaz and Borchert, 2005). The ZP roughly characterises the surface charge of the emulsion particles. High absolute values lead to repulsive forces between particles which might improve the stability of multiphase systems. Absolute values higher than 30 mV generally indicate good long-term stability (Mueller, 1996). Zeta potential values were measured immediately after preparation of the formulations and were continuously analysed every fortnight over the observation period of more than 12 months.

2.4.3. Cryo transmission electron microscopy (Cryo TEM)

Standard nanoemulsion samples containing β-CD were compared to a control nanoemulsion without CD in order to establish differences in particle formation and microstructure of the formulations. The samples were dissolved (1:10, v/v) in distilled water (pH 6.7); then a 4 μm drop of each solution was placed on a TEM copper grid covered with a perforated carbon film (Pelco International) and blotted with a filter paper to form a thin liquid film of the sample (thickness of 100–250 nm). The thinned sample was plunged into liquid ethane at its freezing temperature (−183 °C) to form a vitrified specimen, and then transferred to liquid nitrogen (−196 °C) for storage until examination. Vitrified specimens were examined in a Philips T12 transmission electron microscope (Philips) operating at an accelerating voltage of 120 kV using an Oxford CT3500 (Oxford Instruments) cryo holder that maintained the vitrified specimens at −160 °C during sample observation. Images were recorded digitally on a cooled Gatan BioScan CCD camera (Gatan) using the DigitalMicrograph 3.4 software (Gatan) in low-dose imaging mode to minimise beam exposure and electron beam radiation damage.

2.5. Chemical stability

In order to investigate a possible influence of the CDs on stability and distribution of progesterone, stability studies were performed for all drug-loaded formulations. The drug content was analysed immediately after preparation and set as 100%. The nanoemulsions were stored at 4 °C. Samples were taken every fortnight for 6 months. Briefly, 10 mg of nanoemulsion were dissolved in 1 ml of methanol, centrifuged for 6 min at 12,000 rpm (Hermle Z323K, MIDSCI, USA) and analysed by HPLC. Samples were taken at least in triplicate ($n \geq 3$).

2.6. Skin permeation experiments

In vitro skin permeation studies were performed using standard Franz-type diffusion cells (Permegear, USA). Porcine abdominal skin was chosen as model membrane because of its morphology and permeability, which are similar to those of human skin (Cazares-Delgadillo et al., 2005; Michniak-Kohn et al., 2005). The porcine abdominal skin was freed from hair and treated with a dermatome (GB 228R, Aesculap) set at 1.2 mm. The obtained skin was stored at −20 °C until use. The samples were defrosted 2 h prior to the experiment.

Appropriate skin patches were clamped between the donor and the receptor chamber of the diffusion cells having a permeation area of 1.13 cm^2. The receptor compartment was filled with 2 ml of propylene glycol/water (40 + 60, w/w) to provide sink conditions for progesterone, as previously reported (Valenta and Wedenig, 1997; Biruss and Valenta, 2006).

The diffusion cells were kept at skin surface temperature (32 °C) and stirred with magnetic bars for 48 h. The formulation (0.6 g) was placed on the excised skin in the donor chamber. Samples of 200 μl were removed at defined time intervals for analysis and replaced by fresh receptor medium. At least five parallel experiments were performed for each formulation ($n \geq 5$). The samples were analysed for their drug content by HPLC. Permeation profiles of progesterone were constructed by plotting time (hours) against the cumulative amount of the drug (μg/cm^2) measured in the receptor solution. In addition, the steady state flux (J, μg cm^{-2} h^{-1}) was calculated by linear regression after 8 h of lag-time.

2.7. HPLC analysis of progesterone

Samples were analysed for their drug content by HPLC (PerkinElmer, USA), consisting of an auto sampler (ISS-200), a

Table 2
Physicochemical properties of different nanoemulsions: comparison of blank versus drug-loaded formulations containing β-CD. Values are means ± SD of at least three formulations ($n \geq 3$). Measurements were performed in triplicate on a Zetasizer Nano ZS (Malvern, UK) at 25 °C. Samples were diluted with distilled water (1:100, v/v) containing sodium chloride (0.01 mmol) before the experiments to ensure constant conductivity around 0.025 mS/cm. Parameters shown are mean particle size (MPS), polydispersity index (PDI) and zeta potential (ZP).

	MPS (nm)	PDI	ZP (mV)	Conductivity (mS/cm)
β	149.58 ± 10.05	0.07 ± 0.01	−23.54 ± 3.38	0.023 ± 0.002
β prog	194.62 ± 13.18	0.07 ± 0.01	−20.82 ± 4.47	0.025 ± 0.003
β-SS	140.35 ± 6.40	0.08 ± 0.01	−41.96 ± 2.67	0.025 ± 0.002
β-SS prog	174.33 ± 13.86	0.08 ± 0.01	−37.51 ± 4.57	0.024 ± 0.003
β+	258.80 ± 56.56	0.19 ± 0.06	55.20 ± 3.238	0.028 ± 0.005
β + prog	316.59 ± 20.42	0.24 ± 0.04	52.90 ± 3.64	0.023 ± 0.005
β-SS+	175.37 ± 12.43	0.11 ± 0.02	46.33 ± 3.46	0.031 ± 0.006
β-SS + prog	266.67 ± 22.65	0.20 ± 0.03	44.75 ± 3.61	0.023 ± 0.002

pump (lc pump, ISS-200) and an UV-diode array detector (235C). A previously reported method was used with slight adaptations (Biruss and Valenta, 2006), using a Nucleosil 100-5 C18 column (250 mm × 4 mm, Macherey-Nagel, USA) plus pre-column (SS 8/4). The mobile phase consisted of methanol/water (70 + 30, w/w). The detection wavelength was set at 255 nm and the retention time was approximately 7 min at a flow rate of 1.0 ml/min. A calibration curve was calculated based on peak area measurements of diluted standard solutions ranging from 0.79 to 101.30 μg/ml. The obtained correlation coefficient was 0.9999.

2.8. Differential scanning calorimetry (DSC)

Skin samples were analysed with a differential scanning calorimeter (PerkinElmer DSC-7) according to an established method in order to investigate the thermal transitions of the porcine skin used for the experiments (Valenta et al., 2001; Hoeller et al., 2009). In short, about 25 mg of porcine skin were impregnated with 3 ml of nanoemulsion for 24 h. Control samples were treated with 3 ml of distilled water in the same fashion. The skin samples were then blotted dry, sealed within an aluminium holder and heated from 30 to 120 °C at a heating rate of 5 °C/min. The obtained DSC curves were compared to the control samples in terms of linear onset and transition temperature (peak maximum) of the obtained endothermic peak. Gravimetric analysis of the samples prior to DSC experiments showed an average water content of 55.61 ± 1.82% (w/w).

2.9. Statistical data analysis

Statistical data analysis was performed with the software program GraphPadPrism using the Student's *t*-test with $P < 0.05$ as minimum level of significance. Results are expressed as means of at least three experiments ± SD.

3. Results

3.1. Formulations

Based on previous studies, basic lecithin-based nanoemulsions were optimised in terms of composition and production conditions. Blank and drug-loaded nanoemulsions were created using an established method (Hoeller et al., 2009). Table 2 shows the physicochemical properties of the different formulations. It was also possible to introduce a positive surface charge by addition of PS; a concentration of 0.1% (w/w) proved to be most suitable.

Preliminary studies with different concentrations of CDs showed an amount of 0.5% (w/w) to be appropriate for creating stable nanoemulsions with acceptable solubilising capacity for other compounds.

Three saccharose esters were tested as co-surfactants. Sucrose laureate L-595 led to systems with high lipophilicity, thus rendering incorporation of lipophilic drugs impossible. Sucrose laureate L-1695 led to unstable formulations with quick increase in particle size and fluctuating zeta potential. Sucrose stearate S-970 (SS) led to satisfying results; it was therefore chosen as most suitable co-surfactant for all further studies.

3.2. Nanoemulsion characterisation

Visual inspection revealed whitish, homogenous formulations of low viscosity in all cases. As the droplet size is above 100 nm, the formulations appear white due to significant multiple scattering of light (Mason et al., 2006).

3.2.1. Particle size, polydispersity index and zeta potential

All formulations were analysed directly after production. Critical parameters such as particle size, PDI and zeta potential were determined. Since properties of corresponding formulations were similar irrespective of the type of CD used, nanoemulsion properties are demonstrated only on formulations containing β-CD as representative example. Table 2 demonstrates their physicochemical properties after 16 homogenisation cycles.

Negatively charged blank nanoemulsions showed particle sizes between 140 and 195 nm while particle sizes of drug-loaded formulations were slightly increased. Formulations containing additional SS exhibited lower particle sizes. As Table 2 clearly shows, PDI values of all negatively charged formulations were far below 0.2 which indicates high homogeneity within the formulations. Addition of PS led to positively charged nanoemulsions with increased particle sizes of at least 170 nm up to over 300 nm. As expected, the PDI was slightly deteriorated, thus affecting storage stability of the formulations. The additional incorporation of SS again decreased particle sizes in most cases. In contrast, the addition of progesterone led to strongly increased particle sizes.

The particle surface charge (zeta potential, ZP) values were determined for all formulations. Conductivity was kept constantly below 0.05 mS/cm, thus ensuring reproducible measurement conditions. Average conductivity of the diluted samples was around 0.025–0.030 mS/cm for all measurements. Negatively charged nanoemulsions showed average ZP values around −20 mV. Addition of SS led to an increase in absolute ZP values from around −20 to −40 mV, thereby increasing electrochemical stability. Addition of PS led to formulations with positive ZP values between +44 up to +55 mV. In these positively charged nanoemulsions, incorporation of SS only induced minor changes in surface charge; ZP values were not influenced or even decreased in some cases. Incorporation of progesterone generally led to a slight decrease of absolute ZP values.

The physicochemical long-term stability of the formulations was monitored over 12 months and investigations are still ongo-

Table 3
Influence of cyclodextrins on long-term stability: effect of β-cyclodextrin on positively charged drug-loaded formulations with (a) or without (b) sucrose stearate (SS). Parameters shown are mean particle size (MPS) in nm, polydispersity index (PDI) and zeta potential (ZP) in mV. Measurements were performed at least in triplicate ($n \geq 3$; Zetasizer Nano) every 2 weeks for 12 months or until phase separation occurred (*). Numbers are means ± SD.

(a)

Time (weeks)	β + prog			Control + prog		
	MPS ± SD	PDI ± SD	ZP ± SD	MPS ± SD	PDI ± SD	ZP ± SD
0	316.59 ± 20.42	0.24 ± 0.04	52.90 ± 3.64	465.47 ± 70.66	0.35 ± 0.04	54,45 ± 4.60
2	320.89 ± 41.49	0.25 ± 0.02	53.39 ± 2.16	472.32 ± 50.50	0.32 ± 0.04	50,02 ± 1.55
4	314.20 ± 28.87	0.24 ± 0.05	50.37 ± 4.70	524.64 ± 95.74	0.37 ± 0.05	44.78 ± 5.02
6	307.57 ± 13.54	0.21 ± 0.03	49.33 ± 3.42	*	*	*
8	325.35 ± 34.64	0.21 ± 0.01	49.65 ± 1.58	*	*	*
10	312.77 ± 7.78	0.24 ± 0.03	50.41 ± 2.51	*	*	*
12	334.74 ± 25.82	0.23 ± 0.09	46.60 ± 3.82	*	*	*
14	350.15 ± 52.30	0.22 ± 0.07	41.11 ± 1.80	*	*	*
16	362.41 ± 48.32	0.26 ± 0.08	40.72 ± 6.06	*	*	*
18	336.06 ± 17.83	0.26 ± 0.04	48.52 ± 1.80	*	*	*
20	352.01 ± 36.34	0.28 ± 0.06	38.08 ± 2.78	*	*	*
22	375.77 ± 55.26	0.23 ± 0.07	37.93 ± 4.74	*	*	*
24	326.45 ± 10.36	0.23 ± 0.05	33.97 ± 9.36	*	*	*
52	465.41 ± 56.76	0.34 ± 0.06	34.24 ± 6.79	*	*	*

(b)

Time (weeks)	β-SS + prog			Control-SS + prog		
	MPS ± SD	PDI ± SD	ZP ± SD	MPS ± SD	PDI ± SD	ZP ± SD
0	266.67 ± 22.65	0.20 ± 0.03	44.75 ± 3.61	504.36 ± 81.79	0.32 ± 0.04	56.54 ± 3.93
2	274.04 ± 21.78	0.18 ± 0.04	45.46 ± 1.75	487.41 ± 136.26	0.34 ± 0.12	46.80 ± 2.96
4	287.23 ± 49.09	0.162 ± 0.07	40.65 ± 1.33	511.18 ± 85.54	0.34 ± 0.02	46.79 ± 1.50
6	326.66 ± 57.14	0.21 ± 0.03	40.18 ± 1.21	*	*	*
8	353.21 ± 74.78	0.21 ± 0.05	38.15 ± 6.71	*	*	*
10	381.09 ± 102.43	0.19 ± 0.01	34.92 ± 3.83	*	*	*
12	474.67 ± 188.08	0.24 ± 0.01	35.35 ± 4.73	*	*	*
14	516.09 ± 199.21	0.25 ± 0.02	29.54 ± 8.13	*	*	*
16	630.00 ± 307.00	0.24 ± 0.03	31.63 ± 10.20	*	*	*
18	*	*	*	*	*	*

ing. For negatively charged nanoemulsions, particle sizes and ZP values remained almost constant for both blank and drug-loaded formulations. Fig. 1 clearly illustrates that incorporation of progesterone hardly influenced formulation properties of negatively charged formulations. However, its effect on the corresponding positively charged formulations was more pronounced. The droplet sizes of positively charged nanoemulsions showed a more rapid increase and ZP values generally showed a stronger decrease, indicating a more rapid destabilisation process (data not shown). These effects were aggravated in the presence of progesterone (Table 3). However, the degree of destabilisation caused by incorporation of progesterone was dependent on the CD incorporated. In this context, formulations containing α- or β-CD showed acceptable particle sizes between 250 and 350 nm, followed by γ-CD. Control formulations without any CD, however, were completely unstable with particle sizes soon deteriorating far beyond 500 nm. In addition, the respective PDI values were increased. Table 3a and b distinctly show the physical destabilisation of the control formulations caused by agglomeration of particles. As can be seen in Table 3b, no positive influence of the additional SS was noticeable here. This indicates that it is the presence of CD alone that contributes to the enhanced physical stability of the respective formulations.

3.2.2. Cryo TEM

As illustrated in Fig. 2, the nanoemulsion droplets appeared mostly spherical, if slightly deformed; this observation is in accordance with previous studies (Mason et al., 2006; Shakeel et al., 2007). The observed droplet size is in good correspondence with the results achieved by photon correlation spectroscopy measurements. However, the incorporated CD apparently leads to the formation of additional multilamellar structures, as can be seen

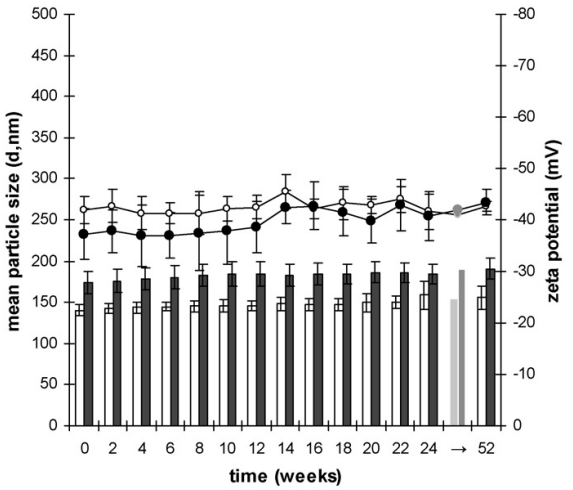

Fig. 1. Influence of progesterone incorporation on long-term stability of nanoemulsions: development of mean particle size (bars) and zeta potential (lines) over an observation period of 12 months as observed on negatively charged formulations, shown on systems containing β-cyclodextrin. Measurements were performed at least in triplicate ($n \geq 3$) every 2 weeks for over a year, again using a Zetasizer Nano. For reasons of clarity, the time frame is shortened in these graphs. Indicated values are means ± SD. β-SS (white bars (□) and white dots (○), respectively); β-SS prog (black bars (■) and black dots (●), respectively).

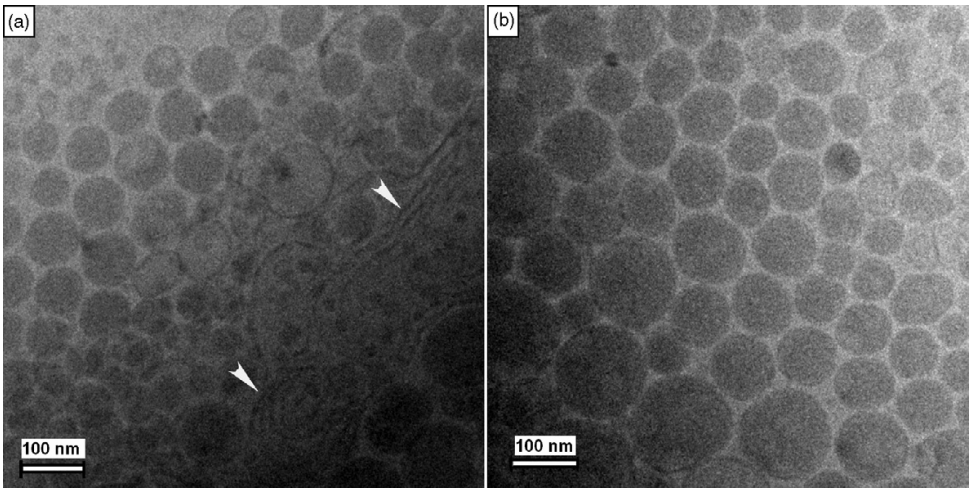

Fig. 2. Cryo TEM photographs of the microstructure of nanoemulsions (a) with β-cyclodextrin and (b) without cyclodextrin. The white arrows indicate the multilamellar structures detected in formulations containing cyclodextrin. The magnification is illustrated by the scale bars.

in Fig. 2a. None of these structures were observed in the control formulation without CD (Fig. 2b).

3.3. Chemical stability

The chemical stability of all drug-loaded formulations was analysed by HPLC every fortnight during 6 months or until decomposition. The average content of progesterone remained around 80% for most nanoemulsions during the observation period (data not shown). Variations in drug content were rather due to problems in analysis than to instability of the steroid hormone, as literature suggests (Kunze, 2006). No degradation products could be detected by HPLC. The incorporation of CDs apparently did not influence the recovered drug content.

3.4. Skin permeation experiments

Permeation profiles of progesterone from different nanoemulsions are shown in Fig. 3. Comparison of the cumulative amounts permeated after 48 h revealed a significant influence of the CDs on skin diffusion rates of progesterone compared to the control ($P < 0.05$). In negatively charged formulations, all CDs led to an increase in skin permeation of progesterone despite the different sizes of their lipophilic cavities. The highest permeation rates were achieved with γ-CD, which was up to 5-fold compared to the control (Table 4) in terms of the cumulative amount of progesterone. These permeation rates were followed by formulations containing β-CD and α-CD. Interestingly, the same ranking of permeation enhancement was observed both in presence or absence of SS, namely γ-CD > β-CD > α-CD > control. An additional effect of SS as permeation enhancer was noticed in all formulations irrespective of the type of CD used (Table 4). The sugar surfactant led to increased skin permeation from negatively charged formulations, acting in synergy with the CDs used. Furthermore, Table 4 clearly indicates that the drug fluxes obtained by linear regression are in good accordance with the conclusions derived from analysis of the cumulative amounts permeated. A comparison of the mean drug fluxes shows a significant if slightly smaller effect of the different CDs with a 3.5-fold increase for formulations with γ-CD and SS.

In positively charged formulations, similar tendencies were observed. The addition of PS led to a further increase of skin permeation, especially in formulations containing γ-CD (Fig. 3). In formulations containing β- and α-CD the effect was not as pronounced in all cases. Further studies are being conducted to achieve consistent results.

3.5. Differential scanning calorimetry (DSC)

DSC studies were performed using a single piece of porcine skin, which showed one endothermic peak at around 78 °C. This peak corresponds to intracellular lipid layers and is in good accordance with literature (Golden et al., 1987). All negatively charged formulations led to a significant change in peak maximum and linear onset of the peak compared to the control samples which were pre-impregnated with water ($P < 0.05$) (Table 5). Both of these parameters were shifted to lower values. This indicates changes

Table 4
Influence of cyclodextrin α, β and γ on cumulative amounts permeated and mean drug flux J of progesterone; indicated values are means ($n \geq 5$) ± SD. The calculated enhancement factor highlights the effect of the cyclodextrins alone or in synergy with sucrose stearate (SS) compared to the control formulation.

Formulation	Cumulative amount ± SD ($\mu g/cm^2$, after 48h)	Enhancement factor versus control	Mean drug flux ± SD (J, $\mu g\,cm^{-2}\,h^{-1}$)
Control prog	9.57 ± 3.56	1.00	0.35 ± 0.08
α prog	18.06 ± 2.22	1.89	0.58 ± 0.14
β prog	25.05 ± 2.29	2.62	0.63 ± 0.06
γ prog	41.86 ± 4.46	4.37	1.04 ± 0.10
α-SS prog	24.53 ± 5.37	2.56	0.72 ± 0.08
β-SS prog	34.16 ± 5.00	3.57	0.86 ± 0.12
γ-SS prog	48.63 ± 5.08	5.08	1.21 ± 0.11

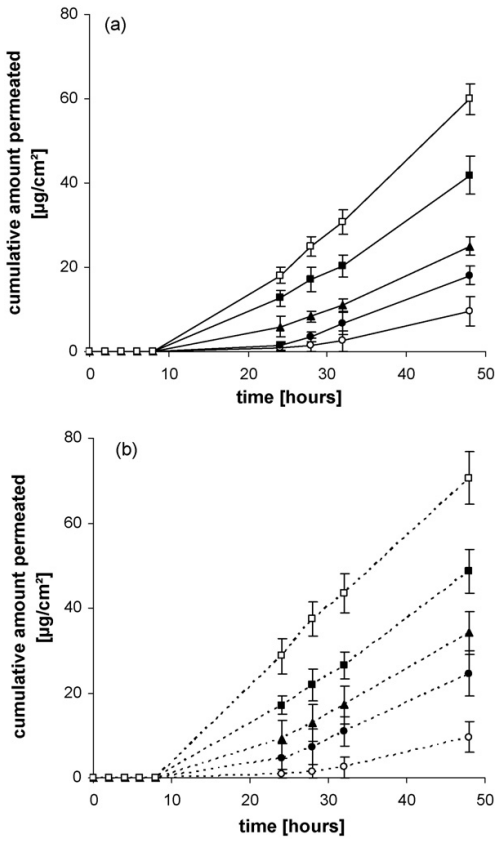

Fig. 3. Effect of cyclodextrin α, β and γ alone (a) and in combination with sucrose stearate (SS) (b) on in vitro skin permeation rates of progesterone from negatively and positively charged nanoemulsions; positively charged formulations are marked with "+". Drug permeation through porcine skin was determined by HPLC. At least five experiments were performed for each formulation ($n \geq 5$) using Franz-type diffusion cells. Indicated values are means ± SD. *Abbreviations*: (a) α prog (●); β prog (▲); γ prog (■); γ + prog (□); control prog (○). (b) α-SS prog (●); β-SS prog (▲); γ-SS prog (■); γ-SS + prog (□); control prog (○).

in thermal transition of the skin lipids, as previously observed in similar investigations (Hoeller et al., 2009). In addition, negatively charged formulations containing α-, β- or γ-CD showed a slightly stronger influence on skin lipids than the control nanoemulsion. However, only minor differences between the effects of the individual CDs were detected. For more distinguished analysis of the different formulations a more sensitive method should be employed.

In positively charged formulations, the changes in terms of peak maximum and linear onset were smaller, if significant in most cases (Table 5) when compared to the water-impregnated control. This is in accordance with previous data (Hoeller et al., 2009); it can therefore be assumed that the positive effect of PS on skin permeation is caused by other interactions than those with skin lipids. However, a slightly stronger effect on skin lipids could be achieved than with previously developed formulations containing PS (Hoeller et al., 2009).

4. Discussion

The primary objective of this study was the development of stable formulations without the use of conventional synthetic surfactants like polysorbates. Emphasis was laid on the use of natural products; hence, the applicability of different sucrose esters as well as CDs was tested extensively. The positive effects induced by incorporation of CDs clearly show that not all possible benefits of CDs as compounds in topical drug delivery systems have been thoroughly investigated yet. The effect of CDs on formulation microstructure might offer applications apart from drug solubilisation or stabilisation. However, it should be brought to mind that the effect of CDs on a complex multiphase system cannot be generally predicted, but has to be investigated separately for every novel formulation. It is of utmost importance to perform CD formulation studies in media that closely resemble the final drug-loaded formulation (Jansook and Loftsson, 2009). The present study is the first evaluation of the effect of CDs on complex nanoemulsion systems on a long-term basis.

First off, we succeeded in developing basic negatively charged formulations stabilised by lecithin only. Corresponding nanoemulsions with positive particle surface charge were created with the help of the cationic phytosphingosine. However, incorporation of progesterone led to destabilisation and skin permeation rates were rather poor. Therefore, CDs and sucrose esters were tested as additional stabilising agents. This strategy proved to be successful. In particular, a stabilising effect of the incorporated CDs was noticeable in positively charged formulations containing progesterone. The addition of CD α, β or γ led to increased physicochemical stability compared to the control nanoemulsion, which was unstable soon after production. This stabilising effect, however, was not as pronounced in negatively charged formulations during the observation period; it was possibly obscured by the effects of the other surfactants. All of the negatively charged formulations were stable for over 1.5 years and stability evaluations are still ongoing.

In order to visualise the differences in formulation properties caused by incorporation of CDs, the nanoemulsion microstructure was analysed by cryo TEM. Indeed, additional multilamellar structures were found in nanoemulsions containing β-CD while none of these were detected in the control formulation without CD. Furthermore, formulations with CD seemed to exhibit stronger surface tension and their freezing behaviour was completely different from the behaviour of formulations without CD. These two phenomena are most certainly related as carbohydrate containing solutes possess higher cohesion and a certain cryoprotective ability.

Table 5
Thermal transition changes of porcine skin induced by pre-impregnation with positively and negatively charged nanoemulsions containing progesterone (1%, w/w) for 24 h. Porcine skin pre-impregnated with water served as a control. Experiments were performed at least in quadruplicate ($n \geq 4$). Indicated values are means ± SD. T_m indicates the temperature of the transition's maximum. Gravimetric analysis of the samples prior to DSC measurements showed average water content of about 55% (w/w).

Treatment ($n \geq 4$)	DSC T_m (°C)	Linear onset (°C)
Skin treated with water (control)	79.64 ± 0.75	65.83 ± 0.28
Formulations		
Control prog	75.99 ± 0.48	63.06 ± 0.66
α prog	73.63 ± 0.58	62.53 ± 0.44
β prog	74.39 ± 0.94	62.83 ± 0.48
γ prog	75.22 ± 0.66	62.53 ± 0.74
α-SS prog	74.53 ± 0.29	62.97 ± 0.33
β-SS prog	74.49 ± 0.71	62.64 ± 0.06
γ-SS prog	75.13 ± 0.38	62.74 ± 0.55
α + prog	79.51 ± 0.53	64.48 ± 0.73
β + prog	78.85 ± 0.45	64.40 ± 0.55
γ + prog	77.04 ± 0.72	63.74 ± 0.52
α-SS + prog	77.74 ± 0.91	63.89 ± 1.15
β-SS + prog	77.32 ± 0.64	63.65 ± 0.28
γ-SS + prog	76.07 ± 0.68	63.12 ± 0.62

Therefore, vitrification of larger volumes of formulations stabilised by carbohydrates, such as the additional cyclodextrins, is possible. In contrast, crystallisation of water almost always occurred in the control nanoemulsions before the cryofixation was completed. The stronger surface tension of the CD containing formulation also might be related to the presence of the additional multilamellar structures. A possible explanation for these formations could be the tendency of lecithin to self-aggregate and form multilamellar structures or other structural units (Shchipunov, 1997; Meier and Schreiber, 2005). These multilamellar layers formed by lecithin molecules can be regarded as an effective structural-mechanical barrier (Shchipunov, 1997). After all, an important issue in terms of destabilisation of lecithin-based emulsions is the separation into an aqueous layer and a concentrated emulsion phase (Shchipunov, 1997). During the present study, this phenomenon was only observed in positively charged nanoemulsions and could be delayed by addition of CDs. In negatively charged formulations, sufficient stability was apparently achieved irrespective of the additional CDs. In this case only extended studies might reveal a more distinctive stabilising effect of the CDs in the long term.

Why the observed multilamellar structures were only formed in the presence of CDs remains to be investigated. Possibly, occupation of interfacial regions by CDs leads to an excess of free lecithin molecules which consequently form said vesicles. It is a well-known fact that amphiphilic molecules like lecithin tend to form higher structural units when dispersed in water at high concentrations; the formation of multiple bilayer membranes can lead to flat lamellar phases or vesicles (Shchipunov, 1997; Meier and Schreiber, 2005). It might be assumed that larger CDs displace more lecithin molecules and therefore lead to increased formation of additional multilamellar structures. The sugar ester present in the investigated formulations might contribute to the formation of these multilamellar or perhaps even micelle-like structures. Literature reports that similar phenomena have been observed in formulations containing elastic vesicles based on a sucrose ester (Bouwstra et al., 2003).

As a second aim of this study, the influence of CDs as well as sucrose stearate on skin permeation of progesterone was evaluated. Indeed, these compounds led to enhanced skin permeation rates of the drug. The enhancement effect of a positive particle surface charge induced by phytosphingosine was not consistent throughout the studies and will be further investigated. Overall, the achieved skin permeation rates from both positively and negatively charged formulations were satisfying. The permeation rates of progesterone from nanoemulsions with γ-CD exceeded those of previously developed formulations such as liposomes when tested under similar conditions (Biruss and Valenta, 2006).

The sucrose ester S-970, namely sucrose stearate, was found to enhance skin permeation from all formulations. In consideration of its HLB value, even stronger permeation enhancement effects might have been achieved with sucrose esters of higher HLB values, such as sucrose laureate L-1695, if they had led to stable formulations in the first place. Previous studies show a satisfying enhancement effect of sucrose stearate S-970 for the release of metoprolol from transdermal therapeutic systems. However, sucrose esters with higher HLB values of around 15–16 which are esterified with short chain fatty acids performed even better in this respect (Csoka et al., 2007). Within the scope of the present study, the use of sucrose stearate S-970 seemed to constitute the best compromise to achieve satisfying results both in terms of formulation stability and skin permeation.

In this context it has to be recollected that the HLB value of lecithin is comparable to that of sucrose stearate S-970. It can therefore be concluded that the addition of sucrose stearate S-970 did not alter the HLB value of approximately 9 of the emulsifying agents within the system. Consequently, the observed enhancement of skin permeation can rather be ascribed to the additional presence of sucrose stearate than to a change in overall HLB value of the emulsifier system used.

Interestingly, the observed skin permeation enhancement was correlated to the cavity size of the incorporated CDs. The mechanism of permeation enhancement through CDs is normally ascribed to the complexation and thus better dispersion of drug molecules within the formulation (Loftsson and Bodor, 1995). In the present formulations, however, it is rather unlikely that the permeation enhancement is caused only by solubilisation of progesterone as the molar amount of CD is very low when compared to the molarity of the drug. It might therefore be assumed that the CDs do not mainly solubilise the drug, but rather contribute to the stabilisation of the interfacial regions between oil droplets and water. According to recent studies, insertion of CD-oil complexes as additional surfactants in this interfacial film can lead to increased release of drugs (Rother, 2009). The amphiphilic molecule complexes supposedly lead to areas of decreased thickness within the interfacial film through which drug molecules can permeate more rapidly. Furthermore, the additional multilamellar structures might promote interactions between skin and formulation in general and could thus exert a positive influence on skin permeation.

5. Conclusion

The results of the present study show that it is possible to develop eudermic nanoemulsions with optimised long-term stability without the use of conventional synthetic tensides. In this respect, emulsifying additives such as sucrose esters are highly recommendable both in terms of stabilisation and skin permeation. Furthermore, the natural CDs α, β and γ proved to be of great interest as additional compounds. The CDs seemed to induce fundamental changes in formulation structure as confirmed by cryo TEM, thus leading to increased skin permeation rates of progesterone. In addition, a positive effect of CD incorporation on formulation stability was noticed for certain formulations.

References

Ayala-Bravo, H.A., Quintanar-Guerrero, D., Naik, A., Kalia, Y.N., Cornejo-Bravo, J.M., Ganem-Quintanar, A., 2003. Effects of sucrose oleate and sucrose laureate on in vivo human stratum corneum permeability. Pharm. Res. 20, 1267–1273.

Bergh, M., Magnusson, K., Nilsson, J.L., Karlberg, A.T., 1998a. Formation of formaldehyde and peroxides by air oxidation of high purity polyoxyethylene surfactants. Contact Dermatitis 39, 14–20.

Bergh, M., Shao, L.P., Hagelthorn, G., Gafvert, E., Nilsson, J.L., Karlberg, A.T., 1998b. Contact allergens from surfactants. Atmospheric oxidation of polyoxyethylene alcohols, formation of ethoxylated aldehydes, and their allergenic activity. J. Pharm. Sci. 87, 276–282.

Biruss, B., Valenta, C., 2006. Skin permeation of different steroid hormones from polymeric coated liposomal formulations. Eur. J. Pharm. Biopharm. 62, 210–219.

Bochot, A., Trichard, L., Le Bas, G., Alphandary, H., Grossiord, J.L., Duchene, D., Fattal, E., 2007. alpha-Cyclodextrin/oil beads: an innovative self-assembling system. Int. J. Pharm. 339, 121–129.

Bouwstra, J.A., Honeywell-Nguyen, P.L., Gooris, G.S., Ponec, M., 2003. Structure of the skin barrier and its modulation by vesicular formulations. Prog. Lipid Res. 42, 1–36.

Brain, K.R., Walters, K.A., Watkinson, A.C., 1998. Investigation of skin permeation in vitro. In: Roberts, M.S., Walters, K.A. (Eds.), Dermal Absorption and Toxicity Assessment. Marcel Dekker, New York, pp. 161–187.

Calderilla-Fajardo, S.B., Cazares-Delgadillo, J., Villalobos-Garcia, R., Quintanar-Guerrero, D., Ganem-Quintanar, A., Robles, R., 2006. Influence of sucrose esters on the in vivo percutaneous penetration of octyl methoxycinnamate formulated in nanocapsules, nanoemulsion, and emulsion. Drug Dev. Ind. Pharm. 32, 107–113.

Cazares-Delgadillo, J., Naik, A., Kalia, Y.N., Quintanar-Guerrero, D., Ganem-Quintanar, A., 2005. Skin permeation enhancement by sucrose esters: a pH-dependent phenomenon. Int. J. Pharm. 297, 204–212.

Challa, R., Ahuja, A., Ali, J., Khar, R.K., 2005. Cyclodextrins in drug delivery: an updated review. AAPS PharmSciTech 6, E329–E357.

Csoka, G., Marton, S., Zelko, R., Otomo, N., Antal, I., 2007. Application of sucrose fatty acid esters in transdermal therapeutic systems. Eur. J. Pharm. Biopharm. 65, 233–237.

Duchene, D., Bochot, A., Yu, S.C., Pepin, C., Seiller, M., 2003. Cyclodextrins and emulsions. Int. J. Pharm. 266, 85–90.
Golden, M.G., Guzek, D.B., Kennedy, A.H., McKie, J.E., Potts, R.O., 1987. Stratum corneum lipid phase transitions and water barrier properties. Biochemistry 26, 2382–2388.
Hashizaki, K., Kageyama, T., Inoue, M., Taguchi, H., Ueda, H., Saito, Y., 2007. Study on preparation and formation mechanism of n-alkanol/water emulsion using alpha-cyclodextrin. Chem. Pharm. Bull. (Tokyo) 55, 1620–1625.
Hoeller, S., Sperger, A., Valenta, C., 2009. Lecithin based nanoemulsions: a comparative study of the influence of non-ionic surfactants and the cationic phytosphingosine on physicochemical behaviour and skin permeation. Int. J. Pharm. 370, 181–186.
Inoue, M., Hashizaki, K., Taguchi, H., Saito, Y., 2008. Emulsion preparation using beta-cyclodextrin and its derivatives acting as an emulsifier. Chem. Pharm. Bull. (Tokyo) 56, 1335–1337.
Jansook, P., Loftsson, T., 2009. CDs as solubilizers: effects of excipients and competing drugs. Int. J. Pharm. 379, 32–40.
Kunze, J., 2006. Development and application of a content determination method for 17-beta-estradiol and progesterone in an innovative hormone emulsion. Ph.D. Thesis, Faculty of Medicine, University of Ulm, Germany.
Loftsson, T., Bodor, N., 1995. Effect of cyclodextrins on percutaneous transport of drugs. In: Smith, E.W., Maibach, H.I. (Eds.), Percutaneous Penetration Enhancers. CRC Press, Boca Raton, FL, pp. 335–342.
Loftsson, T., Masson, M., 2001. Cyclodextrins in topical drug formulations: theory and practice. Int. J. Pharm. 225, 15–30.
Loftsson, T., Vogensen, S.B., Brewster, M.E., Konradsdottir, F., 2007. Effects of cyclodextrins on drug delivery through biological membranes. J. Pharm. Sci. 96, 2532–2546.
Mason, T.G., Wilking, J.N., Meleson, K., Chang, C.B., Graves, S.M., 2006. Nanoemulsions: formation, structure, and physikal properties. J. Phys.: Condens. Matter 18, R635–R666.
Meier, W., Schreiber, J., 2005. Intelligent polymers and self organizing liposome gel delivery systems. In: Rosen, M.R. (Ed.), Delivery System Handbook for Personal Care and Cosmetic Products. William Andrew, Inc., New York, pp. 587–602.
Michniak-Kohn, B.B., Wertz, P.W., Al-Khalili, M., Meidan, V.M., 2005. Skin: physiology and penetration pathways. In: Rosen, M.R. (Ed.), Delivery System Handbook for Personal Care and Cosmetic Products. William Andrew, Inc., New York, pp. 77–100.
Mueller, R.H., 1996. Zetapotential und Partikelladung in der Laborpraxis. Wissenschaftliche Verlagsgesellschaft mbH Stuttgart, Germany.
Piemi, M.P., Korner, D., Benita, S., Marty, Jp, 1999. Positively and negatively charged submicron emulsions for enhanced topical delivery of antifungal drugs. J. Control Release 58, 177–187.
Porras, M., Solans, C., González, C., Martinez, A., Guinart, A., Gutiérrez, J.M., 2004. Studies of formation of W/O nano-emulsions. Colloids Surf. A: Physicochem. Eng. Aspects 249, 115–118.
Rother, P., 2009. Influence of cyclodextrins on oil-in-water emulsions containing hypromellose (HPMC) as a polymeric emulsifier. Ph.D. Thesis, Faculty of Chemistry and Pharmacy, Eberhard-Karls-Universität Tübingen, Germany.
Shakeel, F., Baboota, S., Ahuja, A., Ali, J., Aqil, M., Shafiq, S., 2007. Nanoemulsions as vehicles for transdermal delivery of aceclofenac. AAPS PharmSciTech 8, E104.
Shchipunov, Y.A., 1997. Self-organising structures of lecithin. Russ. Chem. Rev. 66, 301–322.
Shimada, K., Kawano, K., Ishii, J., Nakamura, T., 1992. Structure of inclusion complexes of cyclodextrins with triglyceride at vegetable oil/water interface. J. Food Sci. 57, 655–656.
Shimada, K., Ohe, Y., Ohguni, T., Kawano, K., Ishii, J., Nakamura, T., 1991. Emulsifying properties of α-, β- and γ-cyclodextrins. Nippon Shokuhin Kogyo Gakkaishi 38, 16–20.
Sonneville-Aubrun, O., Simonnet, J.T., L'Alloret, F., 2004. Nanoemulsions: a new vehicle for skincare products. Adv. Colloid Interface Sci. 108–109, 145–149.
Tadros, T., Izquierdo, P., Esquena, J., Solans, C., 2004. Formation and stability of nanoemulsions. Adv. Colloid Interface Sci. 108–109, 303–318.
Valenta, C., Nowak, M., Hadgraft, J., 2001. Influence of phloretin and 6-ketocholestanol on the permeation of progesterone through porcine skin. Int. J. Pharm. 217, 79–86.
Valenta, C., Wedenig, S., 1997. Effects of penetration enhancers on the in-vitro percutaneous absorption of progesterone. J. Pharm. Pharmacol. 49, 955–959.
Yilmaz, E., Borchert, H.H., 2005. Design of a phytosphingosine-containing, positively-charged nanoemulsion as a colloidal carrier system for dermal application of ceramides. Eur. J. Pharm. Biopharm. 60, 91–98.
Yu, S.C., Bochot, A., Bas, G.L., Cheron, M., Mahuteau, J., Grossiord, J.L., Seiller, M., Duchene, D., 2003. Effect of camphor/cyclodextrin complexation on the stability of O/W/O multiple emulsions. Int. J. Pharm. 261, 1–8.
Zoppetti, G., Puppini, N., Ospitali, F., Fini, A., 2007. Solid state characterization of progesterone in a freeze dried 1:2 progesterone/HPBCD mixture. J. Pharm. Sci. 96, 1729–1736.

European Journal of Pharmaceutics and Biopharmaceutics 79 (2011) 58–67

Contents lists available at ScienceDirect

European Journal of Pharmaceutics and Biopharmaceutics

journal homepage: www.elsevier.com/locate/ejpb

Research paper

Development of sucrose stearate-based nanoemulsions and optimisation through γ-cyclodextrin

Victoria Klang [a], Nadejda Matsko [b], Karoline Raupach [a], Nivine El-Hagin [a], Claudia Valenta [a,*]

[a] University of Vienna, Department of Pharmaceutical Technology and Biopharmaceutics, Vienna, Austria
[b] Graz University of Technology and Centre for Electron Microscopy Graz, Institute for Electron Microscopy and Fine Structure Research, Graz, Austria

ARTICLE INFO

Article history:
Received 7 December 2010
Accepted in revised form 13 January 2011
Available online 26 January 2011

Keywords:
Lecithin
Sucrose stearate
Nanoemulsion
Cryo TEM
γ-Cyclodextrin
Fludrocortisone acetate

ABSTRACT

Nanoemulsions aimed at dermal drug delivery are usually stabilised by natural lecithins. However, lecithin has a high tendency towards self-aggregation and is prone to chemical degradation. Therefore, the aim of this study was to develop nanoemulsions with improved structure and long-term stability by employing a natural sucrose ester mixture as sole surfactant. A thorough comparison between the novel sucrose stearate-based nanoemulsions and corresponding lecithin-based nanoemulsions revealed that the sucrose ester is superior in terms of emulsifying efficiency, droplet formation as well as physical and chemical stability. The novel formulations exhibited a remarkably homogeneous structure in cryo TEM investigations, as opposed to the variable structure observed for lecithin-based systems. The in vitro skin permeation rates of lipophilic drugs from sucrose stearate nanoemulsions were comparable to those obtained with their lecithin-based counterparts. Furthermore, it was observed that addition of γ-cyclodextrin led to enhanced skin permeation of the steroidal drug fludrocortisone acetate from 9.99 ± 0.46 to 55.10 ± 3.67 μg cm^{-2} after 24 h in the case of sucrose stearate-based systems and from 9.98 ± 0.64 to 98.62 ± 24.89 μg cm^{-2} after 24 h in the case of lecithin-based systems. This enhancement effect was significantly stronger in formulations based on lecithin ($P < 0.05$), which indicates that synergistic mechanisms between the surfactant and the cyclodextrin are involved. Cryo TEM images suggest that the cyclodextrin is incorporated into the interfacial film, which might alter drug release rates and improve the droplet microstructure.

© 2011 Elsevier B.V. All rights reserved.

1. Introduction

Classical O/W nanoemulsions can be produced by high-pressure homogenisation using small amounts of natural lecithin as emulsifier, which accounts for their high skin friendliness [1–3]. Although particle sizes below 100 nm are hardly reached with lecithin-type emulsifiers, the term nanoemulsion is commonly used for such systems with droplet sizes in the lower submicron range. Since phospholipid mixtures possess superior emulsifying properties compared to purified phosphatidylcholine, they are preferred for nanoemulsion production [4,5]. However, these classical nanoemulsion surfactants pose certain problems in formulation development. On the one hand, phospholipids are prone to oxidative and hydrolytical degradation [6], which results in an unfavourable visual and olfactory appearance after a certain storage time. On the other hand, lecithin mixtures have a high potential for self-aggregation phenomena, which leads to the formation of vesicular or multilamellar structures during the production of nanoemulsions [4]. Although numerous studies report the presence of liposomal vesicles in lecithin-based O/W nanoemulsions [7–11], few propositions have been made on how to avoid such by-products of high-pressure homogenisation. Despite decades of research in this field, it is still unclear whether these structures can be entirely avoided [6]. Moreover, it has not been fully clarified whether the presence of such structures has a negative effect on the formulations' long-term stability. Micelle-mediated transport of oil and the occurrence of liposomes have been reported to impair nanoemulsion stability due to increased Ostwald ripening [12–15]. Technological issues aside, the occurrence of liposomes in parenteral nanoemulsion systems is held responsible for dyslipidemias and embolisms [6,16]. The development of homogeneous, vesicle-free O/W nanoemulsions might therefore be desirable to achieve reproducible properties and storage stability.

Although many aspects of lecithin behaviour are hard to predict, few studies discuss the issue of nanoemulsion homogeneity. Common particle size measurement techniques such as dynamic

Abbreviations: CD, cyclodextrin; DLS, dynamic light scattering; PDI, polydispersity index; ZP, zeta potential.

* Corresponding author. University of Vienna, Department of Pharmaceutical Technology and Biopharmaceutics, Faculty of Life Sciences, Althanstraße 14, 1090 Vienna, Austria. Tel.: +43 1 4277 55 410; fax: +43 1 4277 9554.

E-mail addresses: victoria.klang@univie.ac.at (V. Klang), nadejda.matsko@felmi-zfe.at (N. Matsko), raupach@gmx.at (K. Raupach), nivine.el-hagin@chello.at (N. El-Hagin), claudia.valenta@univie.ac.at (C. Valenta).

0939-6411/$ - see front matter © 2011 Elsevier B.V. All rights reserved.
doi:10.1016/j.ejpb.2011.01.010

light scattering fail to distinguish between oil droplets and other nano-sized structures. In addition, information on how to avoid the formation of unwanted surfactant aggregates is scarce. While lecithin molecules have a pronounced tendency towards self-aggregation, other natural and eudermic emulsifiers might be more suitable to form reproducible O/W droplets. Hardly any information on the disposition of different emulsifier types to form these by-products of high-pressure homogenisation can be found. The present investigation addresses this shortcoming by a thorough comparison of a commonly used lecithin mixture and a sucrose ester mixture. It has been shown recently that sucrose esters can successfully be employed as co-surfactants in nanoemulsions [17–19]. However, the use of these natural emulsifier mixtures as main surfactants for classical nanoemulsion systems has not been thoroughly investigated yet. Especially, sucrose stearate S-970 has been shown to exert positive effects on stability and skin permeation of lecithin-based nanoemulsions [20]. Its HLB value of around 9 is comparable to that of lecithin; therefore, it should be determined whether the previously employed natural lecithin mixture lecithin E-80 could be replaced as sole emulsifier. To this end, a thorough characterisation of blank and drug-loaded nanoemulsions in terms of physicochemical formulation parameters, microscopic appearance and long-term stability was conducted.

As a second major focus of this study, the in vitro skin permeation of four model drugs from the novel sucrose stearate-based nanoemulsions was investigated and compared to the permeation from lecithin-based systems. Although O/W nanoemulsions are generally more suitable for the delivery of lipophilic drugs, hydrophilic drugs were also included for reasons of comparison. Moreover, the effect of additional γ-cyclodextrin (CD) was investigated to confirm a previously reported enhancement effect on the skin permeation of a lipophilic steroidal drug [20]. Thus, further insights into the suitability of natural CDs as additives in nanoemulsions are gained.

2. Materials and methods

2.1. Materials

Egg lecithin Lipoid E-80 was donated by Lipoid GmbH (Ludwigshafen, Germany). Sucrose stearate (Ryoto Sugar Ester® S-970) was supplied by Mitsubishi-Kagaku Food Corporation (Tokyo, Japan). Cyclodextrin γ (Cavamax® W8 Pharma) and cyclodextrin α (Cavamax® W6 Pharma) were obtained from Wacker Chemie AG (Munich, Germany). Cyclodextrin β (Kleptose®) was donated by Roquette frères (Lestrem, France). Fludrocortisone acetate (CAS: 514-36-3, Batch No. 075K1029) was purchased from Sigma Aldrich (St. Louis, USA). Fluconazole (CAS: 86386-73-4, Batch No. 050418), and flufenamic acid (CAS: 530-78-9, Batch No. 1619) was obtained from Kemprotec Limited (Middlesbrough, UK). Minoxidil (CAS: 38304-91-5, Batch No. 81835129) was purchased from Caesar & Loretz GmbH (Hilden, Germany). The preserving agent potassium sorbate was obtained from Herba Chemosan Apotheker-AG (Vienna, Austria). PCL-liquid (cetearyl ethylhexanoate, isopropyl myristate) was purchased from Dr. Temt Laboratories (Vienna, Austria). All other chemicals used were of analytical reagent grade and used without further purification.

2.2. Preliminary investigations and solubility studies

2.2.1. Optimisation of formulation composition

Preliminary studies were conducted to optimise formulation composition and processing parameters. Different surfactant concentrations between 1% and 5% (w/w) were tested. Likewise, the most suitable oil volume fraction for particle size reduction was determined. Oil concentrations of 10%, 15% and 20% (w/w) were investigated. Finally, the natural CDs α, β and γ were incorporated (1% w/w) in order to investigate their influence on formulation properties.

2.2.2. Solubility of model drugs: choice of the receptor medium

The suitability of the chosen phosphate buffer (pH 7.4, 0.012 M) as acceptor medium for in vitro skin diffusion studies has already been established for all employed model drugs in previous work by our group; details on solubility studies can be found in the literature [17,21,22]. The use of propylene glycol or ethanol as additives to enhance the solubility of the lipophilic drugs in the aqueous buffer was avoided to prevent solvent effects. For reasons of comparison both within this study and with previous results, the same phosphate buffer was employed for all investigated drugs even if the permeation of the lipophilic drugs might be comparatively lower than under actual in vivo conditions due to their low solubility.

2.3. Formulations

Nanoemulsions were prepared as previously described [17,20]. The aqueous phase, consisting of freshly distilled water and potassium sorbate, was stirred at 50 °C. Sucrose stearate S-970 was incorporated into the aqueous phase, while lecithin E-80 was dissolved in the oil-phase PCL-liquid of the respective formulations. Additional γ-CD was incorporated into the aqueous phase where appropriate. The lipophilic drugs fludrocortisone acetate and flufenamic acid were dissolved in the oil phase, while the hydrophilic drugs fluconazole and minoxidil were dissolved in the aqueous phase. The two phases were mixed and pre-homogenised for 4 min with an ultra-turrax (Omni 500) at 2500 rpm. Afterwards, the mixture was stirred and heated to 50 °C before further homogenisation with a high-pressure homogeniser (EmulsiFlex C3, Avestin) for 20 homogenisation cycles at 750 bars. Longer homogenisation times led to an increase in particle size due to overprocessing. Table 1 shows the optimised formulations as well as their composition and abbreviations.

2.4. Nanoemulsion characterisation

2.4.1. Particle size

All formulations were analysed for their particle size and particle size distribution by dynamic light scattering (DLS, photon correlation spectroscopy) using a Zetasizer Nano ZS (Malvern, UK) at 25 °C. Samples were diluted with freshly distilled water 1:100 (v/v) to diminish opalescence. The obtained polydispersity index (PDI) values represent the particle size distribution within the formulations. PDI values below 0.2 indicate a narrow size distribution

Table 1
Composition of basic optimised nanoemulsion formulations and abbreviations. Drug-loaded formulations were created by incorporation of 1% w/w of fludrocortisone acetate (flud), flufenamic acid (fluf), fluconazole (fluc) and minoxidil (min). *Abbreviations*: LN, lecithin-based nanoemulsion; SN, sucrose stearate-based nanoemulsion; γ-LN, lecithin-based nanoemulsion with γ-CD; γ-SN, sucrose stearate-based nanoemulsion with γ-CD.

Excipients	Nanoemulsion composition (% w/w)			
	LN	SN	γ-LN	γ-SN
PCL-liquid	20	20	20	20
Lipoid E-80	2.5	–	2.5	–
Sucrose stearate S-970	–	2.5	–	2.5
Potassium sorbate	0.1	0.1	0.1	0.1
γ-Cyclodextrin	–	–	1.0	1.0
Model drug	1.0	1.0	1.0	1.0
Distilled water to	100	100	100	100

and thus good long-term stability due to reduction in degradation processes like Ostwald ripening [23]. The formulation parameters of interest were measured immediately after preparation. The obtained nanoemulsions were stored at 4 °C, and consecutive measurements were performed in regular intervals over a period of 6 months.

2.4.2. Particle surface charge (zeta potential)

The particle surface charge of the formulations was determined by laser Doppler electrophoresis using a Zetasizer Nano ZS (Malvern, UK). Zeta potential (ZP) values of the formulations were determined at 25 °C. Samples were diluted with distilled water (1:100 v/v) containing sodium chloride (0.01 mmol) in order to ensure constant conductivity below 0.05 mS/cm. As distilled water alone might lead to fluctuating conductivity, addition of electrolytes ensures reproducible measurement conditions [23,24]. The ZP roughly characterises the surface charge of the emulsion particles. High absolute values lead to repulsive forces between particles, which may improve the physical stability of multiphase systems. Absolute values higher than 30 mV generally indicate good stability, while values above 60 mV indicate excellent long-term stability [24]. Zeta potential values were determined after production and in regular intervals over 6 months.

2.4.3. Cryo transmission electron microscopy (cryo TEM)

Standard nanoemulsion samples containing either 2.5% of lecithin or 2.5% of sucrose stearate were compared in order to establish differences in particle formation and microstructure of the formulations. Corresponding nanoemulsions containing additional γ-CD (1% w/w) were investigated as well to investigate the effect of the CD on the nanoemulsion structure. The samples were dissolved (1:10 as well as 1:5 v/v, respectively) in distilled water (pH 6.7); then, a 4-μm drop of each solution was placed on a TEM copper grid covered with a perforated carbon film (Pelco International) and blotted with a filter paper to form a thin liquid film of the sample (thickness of 100–250 nm). The thinned sample was plunged into liquid ethane at its freezing temperature (−183 °C) to form a vitrified specimen and then transferred to liquid nitrogen (−196 °C) for storage until examination. Vitrified specimens were examined in a Philips T12 transmission electron microscope (Philips) operating at an accelerating voltage of 120 kV using an Oxford CT3500 (Oxford Instruments) cryo holder that maintained the vitrified specimens at −160 °C during sample observation. Images were recorded digitally on a cooled Gatan BioScan CCD camera (Gatan) using the DigitalMicrograph 3.4 software (Gatan) in low-dose imaging mode to minimise beam exposure and electron beam radiation damage.

2.5. Chemical stability

2.5.1. Chemical stability of incorporated drugs

Both the drug content and the chemical stability of all drug-loaded formulations were investigated. Potential differences between the emulsifiers in terms of drug solubilisation and of the long-term stability of the incorporated drugs should be revealed in this fashion. The results should, however, rather be regarded as an overview than as a comprehensive stability study since the latter would require far more sophisticated methods of analysis which are validated for the detection of anticipated degradation products. The drug content was analysed immediately after preparation and set as 100%. The nanoemulsions were stored at 4 °C. Samples were taken in regular intervals over 6 months. Briefly, 10 mg of nanoemulsion was dissolved in 1 ml of methanol, centrifuged for 6 min at 12,000 rpm (Hermle Z323K, MIDSCI, USA) and analysed by HPLC. Samples were taken at least in triplicate ($n \geqslant 3$).

2.5.2. Chemical stability of the formulations

Oil components as well as surfactants may be affected by chemical degradation through hydrolysis or oxidation. Since such phenomena result in a decrease in pH [6], pH values of all nanoemulsions were determined in regular intervals over 6 months. At least three formulations ($n \geqslant 3$) were investigated at room temperature (25 °C) with a pH meter (Orion 420A, Bartelt, Austria).

2.6. Skin permeation experiments

In vitro skin permeation studies were performed using standard Franz-type diffusion cells (Permegear, USA). Porcine abdominal skin was chosen as model membrane because of its morphology and permeability, which are similar to those of human skin [25,26]. The porcine abdominal skin was freed from hair and treated with a dermatome (GB 228R, Aesculap) set at 1.2 mm. The skin was stored at −20 °C until use and thawed prior to the experiments. Appropriate skin patches were clamped between the donor and the receptor chamber of the diffusion cells having a permeation area of 1.13 cm^2. The receptor compartment was filled with 2 ml of phosphate buffer (pH 7.4). The diffusion cells were kept at skin surface temperature (32 °C) and stirred with magnetic bars for 24 h. The formulation (0.6 g) was placed on the excised skin in the donor chamber. Samples of 200 μl were removed at defined time intervals for analysis and were replaced by fresh receptor medium. In the case of minoxidil, the whole acceptor fluid of 2 ml was removed and replaced in order to ensure sink conditions. At least five parallel experiments were performed for each formulation ($n \geqslant 5$). The samples were analysed for their drug content by HPLC. Permeation profiles of the drugs were constructed by plotting time (hours) against the cumulative amount of the drug (μg/cm^2) as measured in the receptor solution. In addition, the steady-state flux (J, μg cm^{-2} h^{-1}) was calculated by linear regression after the respective lag times.

2.7. HPLC analysis

All samples were analysed for their drug content by HPLC (Series ISS-200, Perkin Elmer, USA), consisting of an autosampler, an lc pump and an UV-diode array detector (235C). Previously reported methods were used using a Nucleosil 100-5 C18 column (250 mm × 4 mm, Macherey–Nagel, USA) plus a Nucleosil 100-5 C18 pre-column (CC8/4, 40 mm × 4 mm, Macherey–Nagel, USA). For all analyses, the oven temperature was set at 50 °C and the injection volume was 20 μl. The analysis of the data was performed using the TotalChrom Navigator 6.2.0 software. Standard solutions of the drugs were prepared, and calibration curves were calculated by plotting the analysed drug concentrations against the obtained peak area values. The limit of quantification, set well above the limit of detection in all cases, is represented by the respective lowest point of the standard solution measurements for each drug as given below.

The quantification of fludrocortisone acetate was performed as previously described [21,27].The mobile phase consisted of acetonitrile and water (40/60 v/v). The detection wavelength was 240 nm, and the retention time was around 11 min at a flow rate of 0.8 ml/min. The concentration range of the standard solutions was between 1.84 μg/ml and 1340.0 μg/ml with a coefficient of determination of $R^2 = 0.9999$.

The quantification of flufenamic acid and minoxidil was conducted according to previously described methods with slight adaptations [21,22]. In both cases, the mobile phase consisted of methanol/water (75/25 w/w); glacial acetic acid was added until a pH value of 3.2 was reached. The flow rate was 1.0 ml/min. For flufenamic acid, the detection wavelength was set at 245 nm with a retention time of 4.5 min. A calibration curve was calculated

based on peak area measurements of diluted standard solutions ranging from 0.82 μg/ml to 104.40 μg/ml with R^2 = 0.9990. In case of minoxidil, the detection wavelength was set at 255 nm with a retention time of 4 min. The calibration curve was calculated using standard solutions from 0.6 μg/ml to 207.10 μg/ml. The obtained coefficient of determination was R^2 = 1.00.

The quantification of fluconazole was performed as reported [21]. The mobile phase consisted of freshly prepared phosphate buffer (0.012 M, pH 7.4) and methanol (55/45 v/v) with addition of 1 mmol of octanesulfonic acid. The detection wavelength was set at 260 nm with a retention time around 4.5 min and a flow rate of 1.0 ml/min. The concentration range of the standard solutions was between 17.3 μg/ml and 548.0 μg/ml with R^2 = 0.9999.

2.8. Statistical data analysis

Results are expressed as means of at least three experiments ± SD. Statistical data analyses were performed with the software program GraphPadPrism3. Parametric data were analysed using the Student's *t*-test with $P < 0.05$ as minimum level of significance, while non-parametric data were analysed using the Mann–Whitney test with $P < 0.05$.

3. Results

3.1. Formulation optimisation

The first aim of the study was to develop a stable nanoemulsion system with one or more sucrose esters as emulsifying agents. Since satisfying results could already be obtained with S-970 as sole emulsifier, no co-surfactants were necessary. Further preliminary studies were thus conducted with either sucrose stearate S-970 or lecithin E-80 as individual emulsifiers in simple nanoemulsions. Different amounts of 1%, 2.5% or 5% (w/w) of the respective surfactant were incorporated. The results are given in Table 2. The particle size measurements revealed that sucrose stearate is a superior emulsifying agent when compared to lecithin. Smaller particle sizes could be obtained especially at low concentrations. The ZP values obtained with the different emulsifiers showed that sucrose stearate is likewise superior in terms of electrochemical stability. Overall, the ZP values of sucrose stearate-based nanoemulsions were higher than those of their lecithin-based counterparts at all concentrations and increased concomitantly with increasing surfactant concentration. In contrast, the ZP of lecithin-based nanoemulsions remained at low values for 1% and 2.5% (w/w) of surfactant and only increased when higher amounts of 5% (w/w) of lecithin were added. This tendency is in good agreement with the changes in particle size at the respective surfactant concentrations.

At increasing surfactant-to-oil ratios, the emulsifying efficiency of both surfactants increased and smaller particle sizes were obtained. At 5% (w/w) of surfactant, the performance of lecithin improved notably, if not enough to compete with sucrose stearate. Since high-pressure homogenisation of nanoemulsions with 5% (w/w) of sucrose stearate proved to be hardly feasible due to its increased viscosity, the formulations with 2.5% (w/w) of surfactant were chosen for all further studies.

Different oil volume fractions were investigated as well. Although literature reports otherwise [28], no particle size reduction was achieved by reducing the oil content from 20% to 15% or 10% (w/w). Quite the contrary, a slight increase in particle sizes with a concomitant decrease of ZP values was observed. Therefore, the oil content was maintained at 20% (w/w), which is advantageous in terms of solubilising capacity for lipophilic drugs.

Finally, the influence of the natural CDs α, β and γ on formulation properties was investigated. Neither of these CDs affected formulation parameters such as particle size or ZP in a negative way when included at 1% (w/w), as can be seen in Table 3 for γ-CD. Since previous studies had shown that γ-CD had the strongest enhancement effect on the skin permeation of a steroidal drug [20], it was chosen as additive for further investigations.

3.2. Formulations

Blank and drug-loaded nanoemulsions were created using an established method [17]. Table 3 shows the physicochemical properties of the different nanoemulsions. The effect of drug incorporation was comparable for all investigated drugs. Therefore, only systems with fludrocortisone acetate and fluconazole are shown as representative examples for a lipophilic and a hydrophilic drug. The incorporation of γ-CD did not alter formulation properties notably except for systems with minoxidil, which could not be homogenised due to viscosity alterations and were therefore excluded from further investigations.

3.3. Nanoemulsion characterisation

All formulations were highly fluid and homogeneous upon visual inspection. Their optical appearance was translucent to whitish. A bluish touch was noticeable for formulations based on sucrose stearate due to Rayleigh scattering, an optical effect caused by the nano-sized emulsion droplets [29].

Table 2
Physicochemical properties of basic blank nanoemulsions investigated in preliminary studies: comparison of different surfactant concentrations. Values are means ± SD of three formulations (n = 3). Measurements were performed in triplicate on a Zetasizer Nano ZS (Malvern, UK) at 25 °C. Samples were diluted with distilled water (1:100 v/v) containing sodium chloride (0.01 mmol) before the experiments to ensure constant conductivity below 0.05 mS/cm. Parameters shown are mean particle size (MPS), polydispersity index (PDI), zeta potential (ZP) and conductivity (Cond).

Parameters	Mean particle size (nm)	PDI	Zeta potential (mV)	Conductivity (mS/cm)
Lecithin				
1.0% (w/w)	281.40 ± 02.92	0.180 ± 0.027	−25.20 ± 02.20	0.016 ± 0.007
2.5% (w/w)	231.39 ± 14.28	0.269 ± 0.012	−26.33 ± 02.43	0.030 ± 0.005
5.0% (w/w)	132.52 ± 26.03	0.118 ± 0.024	−56.43 ± 03.81	0.027 ± 0.001
Sucrose stearate				
1.0% (w/w)	193.79 ± 01.76	0.065 ± 0.003	−48.36 ± 01.19	0.014 ± 0.003
2.5% (w/w)	141.56 ± 09.02	0.075 ± 0.007	−57.28 ± 05.77	0.016 ± 0.008
5.0% (w/w)	120.39 ± 09.15	0.134 ± 0.017	−70.81 ± 13.25	0.020 ± 0.006

Table 3
Physicochemical properties of different nanoemulsions after 20 homogenisation cycles: comparison of blank versus drug-loaded formulations shown on systems containing fludrocortisone acetate or fluconazole. Values are means ± SD of at least three formulations ($n \geqslant 3$). Measurements were performed in triplicate on a Zetasizer Nano ZS (Malvern, UK) at 25 °C. Samples were diluted with distilled water (1:100 v/v) containing sodium chloride (0.01 mmol) before the experiments to ensure constant conductivity below 0.05 mS/cm. Parameters shown are mean particle size (MPS), polydispersity index (PDI), zeta potential (ZP) and conductivity (Cond).

Parameters	Mean particle size (nm)	PDI	Zeta potential (mV)	Conductivity (mS/cm)
LN blank	186.41 ± 11.06	0.13 ± 0.05	−21.72 ± 1.83	0.023 ± 0.002
LN flud	183.13 ± 05.50	0.11 ± 0.04	−26.64 ± 4.86	0.027 ± 0.002
LN fluc	156.87 ± 09.73	0.05 ± 0.01	−24.70 ± 3.41	0.029 ± 0.004
γ-LN flud	175.82 ± 00.47	0.09 ± 0.04	−30.19 ± 4.12	0.027 ± 0.003
γ-LN fluc	155.60 ± 07.96	0.07 ± 0.02	−22.50 ± 2.20	0.022 ± 0.002
SN blank	141.21 ± 08.73	0.08 ± 0.02	−57.28 ± 5.77	0.016 ± 0.008
SN flud	146.66 ± 08.53	0.13 ± 0.03	−63.38 ± 9.14	0.020 ± 0.001
SN fluc	136.79 ± 04.49	0.09 ± 0.03	−56.68 ± 0.05	0.022 ± 0.005
γ-SN flud	144.77 ± 10.61	0.11 ± 0.02	−63.77 ± 6.22	0.020 ± 0.008
γ-SN fluc	135.74 ± 04.57	0.08 ± 0.01	−65.19 ± 5.50	0.016 ± 0.007

3.3.1. Particle size, polydispersity index and zeta potential

The different nanoemulsions were analysed directly after production. Critical formulation parameters such as particle size, PDI and ZP were determined (Table 3). Blank lecithin-based nanoemulsions exhibited a mean particle size of around 180 nm, which remained unchanged or was even slightly decreased upon incorporation of the different drugs. In the case of sucrose ester-based nanoemulsions, the mean particle size was found to be very consistently around 140 nm for blank as well as for all drug-loaded formulations. The incorporation of γ-CD had no impact on the particle size of either of the nanoemulsion systems ($P > 0.05$ in all cases). The PDI values of all systems were far below 0.2. Overall, the mean particle size of sucrose stearate-based nanoemulsions was significantly smaller for all systems ($P < 0.05$).

The particle surface charge values were determined for all formulations. Nanoemulsions containing lecithin showed average ZP values around −20 to −30 mV irrespective of the nature of the incorporated drugs. In contrast, nanoemulsions stabilised by sucrose stearate exhibited significantly higher ZP values of over −50 mV up to −65 mV, which indicates an improved electrochemical stability ($P < 0.05$).

The physicochemical long-term stability of the formulations was monitored over 6 months. The particle size of blank formulations with either lecithin or sucrose stearate remained largely constant during the whole observation period. However, Fig. 1 clearly demonstrates that the mean ZP values remained only constant in the case of sucrose stearate-based nanoemulsions. The lecithin-based systems showed a noticeable increase in absolute ZP values from around −20 to −40 mV.

The incorporation of the model drugs hardly influenced the destabilisation process of either nanoemulsion system. Although drug-loaded lecithin-based nanoemulsions generally exhibited larger particle sizes and a more pronounced increase in mean particle size over the course of 6 months, none of the observed changes were statistically significant ($P > 0.05$). Table 4 shows the development of the mean particle size as well as PDI and ZP values of formulations with fludrocortisone acetate. The particle sizes of all drug-loaded systems remained largely constant, while the ZP increased in lecithin-based systems due to chemical degradation. Sucrose stearate-based nanoemulsions showed a slow decrease in absolute ZP values as commonly observed during the ageing process of nanoemulsions.

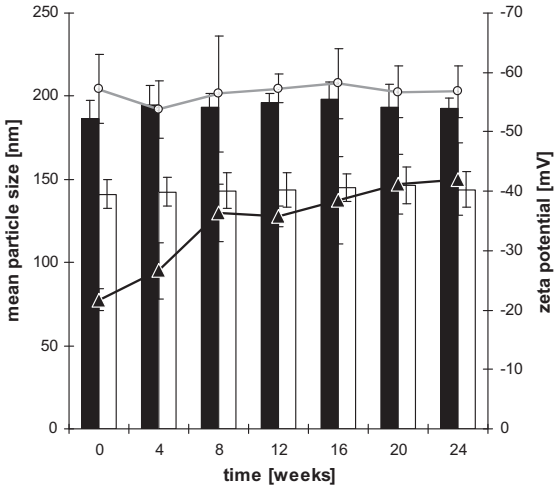

Fig. 1. Influence of surfactant on long-term stability in the case of lecithin (LN) or sucrose stearate (SN): development of mean particle size in nm and zeta potential in mV over a storage time of 6 months as observed on blank formulations with lecithin or sucrose stearate. The bars represent the particle size as indicated on the left-hand scale (black bars ■: LN, white bars □: SN). The lines show the development of the mean zeta potential (black symbol —▲—: LN, white symbol —○—: SN) as indicated on the right-hand scale of the figure. The drug-loaded formulations showed a highly similar trend. Measurements were performed at least in triplicate ($n \geqslant 3$; Zetasizer Nano) every two weeks. Numbers are given ±SD. For the sake of clarity, only monthly measurements are shown.

Table 4
Physical stability of drug-loaded nanoemulsions with either lecithin (LN) or sucrose stearate (SN) shown on systems containing fludrocortisone acetate (flud) (**3a**). The corresponding systems with additional γ-CD are shown for comparison (**3b**). Experiments were performed in triplicate ($n = 3$) in regular intervals over an observation period of 6 months. The indicated parameters are the mean particle size (MPS), polydispersity index (PDI) and zeta potential (ZP). Numbers are given as means ± SD.

(4a) Time (weeks)	MPS (nm) ± SD	PDI ± SD	ZP (mV) ± SD
LN flud			
0	183.13 ± 05.50	0,11 ± 0.04	−26.64 ± 04.86
4	184.01 ± 05.44	0.11 ± 0.06	−26.62 ± 02.18
8	188.66 ± 08.03	0.13 ± 0.08	−31.06 ± 03.03
12	185.87 ± 09.61	0.09 ± 0.04	−33.40 ± 00.58
16	186.01 ± 04.57	0.08 ± 0.02	−39.38 ± 03.91
20	197.73 ± 25.50	0.09 ± 0.04	−35.92 ± 03.70
24	189.58 ± 18.77	0.09 ± 0.04	−41.51 ± 03.70
SN flud			
0	146.66 ± 08.53	0.13 ± 0.03	−63.38 ± 09.14
4	144.10 ± 06.00	0.09 ± 0.02	−55.81 ± 05.79
8	143.26 ± 05.83	0.10 ± 0.03	−52.88 ± 01.13
12	143.24 ± 07.08	0.08 ± 0.01	−55.38 ± 06.74
16	141.89 ± 07.38	0.08 ± 0.02	−54.99 ± 02.40
20	147.08 ± 07.35	0.10 ± 0.05	−54.89 ± 08.56
24	142.88 ± 08.24	0.11 ± 0.02	−51.77 ± 12.36
(4b)			
γ-LN flud			
0	175.82 ± 00.47	0.09 ± 0.04	−30.19 ± 04.12
4	179.17 ± 08.76	0.05 ± 0.01	−30.34 ± 00.84
8	182.80 ± 13.11	0.06 ± 0.02	−35.98 ± 07.11
12	185.27 ± 16.82	0.07 ± 0.02	−34.21 ± 03.82
16	187.20 ± 21.36	0.07 ± 0.06	−37.07 ± 03.01
20	185.02 ± 17.28	0.11 ± 0.05	−36.18 ± 01.95
24	184.59 ± 14.70	0.09 ± 0.07	−34.91 ± 06.01
γ-SN flud			
0	144.77 ± 10.61	0.11 ± 0.02	−63.77 ± 06.22
4	154.44 ± 04.43	0.07 ± 0.02	−58.36 ± 02.23
8	155.86 ± 05.66	0.10 ± 0.01	−60.26 ± 03.69
12	163.24 ± 03.68	0.12 ± 0.04	−62.41 ± 13.26
16	158.72 ± 03.67	0.09 ± 0.03	−62.80 ± 04.67
20	159.20 ± 02.05	0.11 ± 0.04	−64.60 ± 01.95
24	161.93 ± 00.87	0.10 ± 0.02	−59.74 ± 06.14

3.3.2. Cryo transmission electron microscopy (cryo TEM)

Blank nanoemulsions stabilised with lecithin or sucrose stearate were investigated by cryo TEM. This technique is frequently used to visualise colloidal systems such as nanoemulsions or liposomes [7]. Fig. 2a and b illustrates the effect of the different emulsifiers on the nanoemulsion structure. It was found in several rounds of analysis that the lecithin-based formulations were far from homogeneous in their microstructure. The left-hand side of Fig. 2a shows not only irregularly shaped nanoemulsion oil droplets but also large numbers of vesicular structures such as various types of liposomes and multilamellar phospholipid layers. These images confirm that a large variety of such structures emerge during high-pressure homogenisation if lecithin E-80 is used as a surfactant. In contrast, the nanoemulsions stabilised by sucrose stearate S-970 as shown on the right-hand side of Fig. 2b had a perfectly reproducible structure. Several consecutive rounds of analysis revealed that these formulations consisted almost exclusively of perfectly spherical oil droplets.

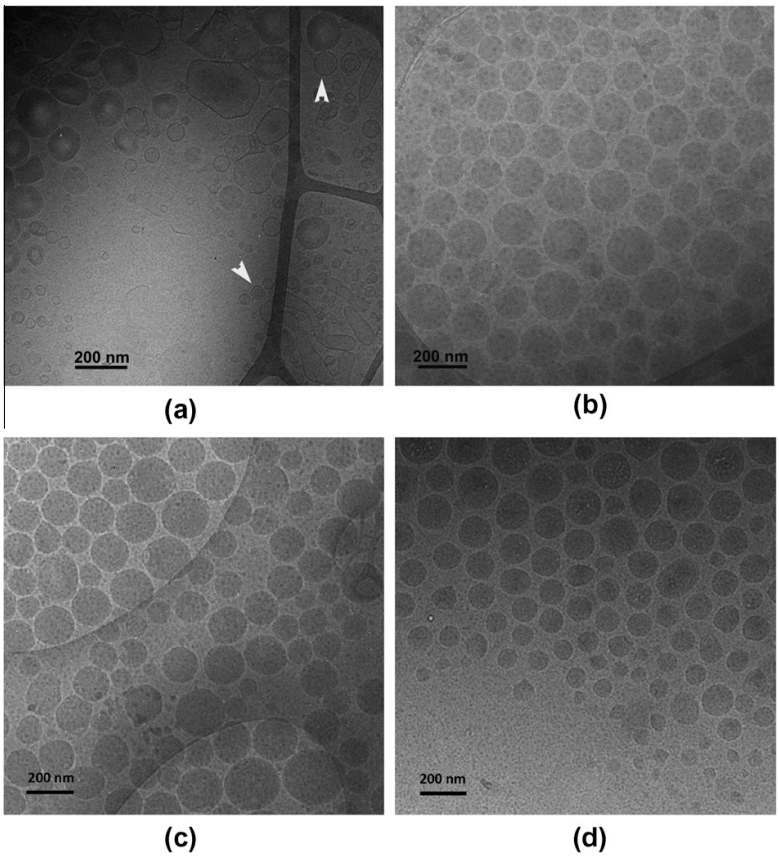

Fig. 2. Cryo TEM photographs of the microstructure of blank nanoemulsions (a) with 2.5% lecithin E-80 and (b) with 2.5% sucrose stearate S-970 as sole emulsifying agent. The corresponding formulations containing additional γ-cyclodextrin are shown below for lecithin (c) as well as for sucrose stearate (d). The magnification is illustrated by the black scale bars. Dark spheres represent nanoemulsion oil droplets. Other vesicular structures such as uni- or bilamellar liposomes (light spheres) or multilamellar structures (light lamellar layers) are indicated by white arrows. Occasional dark crystals are due to ice formation during cryo preparation of the sample.

Interestingly, the addition of γ-CD to these emulsion systems apparently had a remarkable influence on the process of emulsion formation in the case of lecithin (Fig. 2c). A much more homogeneous emulsion structure was observed than for the nanoemulsion based on lecithin alone. The sample contained remarkably less vesicular structures, and the shape of the oil droplets was more regular and spherical, if slightly rough on the surface. The images were analysed with the help of the DigitalMicrograph 3.4 software (Gatan) for their content of oil droplets and vesicular structures. In case of lecithin-based formulations without γ-CD (Fig. 2a), a total of 62.45 ± 33.12% of vesicular structures were observed per image (n = 3 analysed images, total number of structures n = 981). In case of the lecithin-based formulations with additional γ-CD (Fig. 2c), merely 13.39 ± 10.76% of vesicles were found per image (n = 5 analysed images, total number of structures n = 701). In contrast, no visual differences in the highly homogeneous structure of sucrose stearate-based nanoemulsions were noticeable after addition of γ-CD (Fig. 2d).

3.4. Chemical stability

3.4.1. Chemical stability of incorporated drugs

After the initial determination of the drug content, the chemical stability of all incorporated drugs was analysed in regular intervals over 6 months. The average content of all drugs remained between 80% and 116% of the initial value for all nanoemulsions during the observation period (data not shown). The slight fluctuations in drug content are rather due to inhomogeneous drug dispersion and methodological issues in analysis than to any actual degradation processes. Indeed, no degradation products were detected by HPLC. Neither the type of surfactant nor the presence of γ-CD exerted a noticeable influence on the recovered drug content. However, it has to be kept in mind that more sophisticated analytical methods are needed to give a full insight into the individual drugs' actual fate within the formulations over the course of time. The presented data merely serve to give an overview about the basic quality of the formulations.

3.4.2. Chemical stability of the formulations

Additional information about the physicochemical stability of the nanoemulsions was derived from the change in pH value over the course of time. A continuous decrease in pH over the course of 6 months was observed. The influence of the surfactant type on the chemical stability of the nanoemulsions was assessed on all blank and drug-loaded formulations. Although both types of nanoemulsion exhibited a significant decrease in pH value after 6 months (P < 0.05), lecithin-based nanoemulsions showed a more pronounced change from 6.98 ± 0.31 to 5.81 ± 0.36 (n = 18) when com-

pared to sucrose stearate-based systems with a drop from 6.75 ± 0.33 to 6.26 ± 0.24 (n = 19). Apparently, lecithin molecules have a stronger disposition towards chemical degradation than the sucrose ester surfactant. The formation of lyso-lecithin and free fatty acids through hydrolysis of lecithin molecules not only increases the negative ZP values but also causes a drop in pH and promotes further degradation [6].

3.5. Skin permeation experiments

Permeation profiles of all drugs from lecithin-based and sucrose stearate-based nanoemulsions were established after 24 h. A comparison of the cumulative drug amounts clearly shows that the hydrophilic drugs permeate through the model skin more rapidly and to a larger extent. The permeated amounts of lipophilic drugs were confined to percentages between 0.2% and 0.8% of the applied dose. In contrast, around 30–40% of the applied hydrophilic drug amounts were recovered from the receptor medium. Although nanoemulsions are generally recommended for the incorporation of lipophilic drugs, they may also be employed for the delivery of hydrophilic drugs. Table 5 shows the mean cumulative permeated drug amounts after 24 h as well as the corresponding mean drug fluxes for all investigated formulations. The concentrations of fludrocortisone acetate and flufenamic acid that were able to permeate through the porcine skin were comparatively small. The released amounts of both fluconazole and minoxidil are around 20–40 times higher than the corresponding amounts of the lipophilic drugs.

What can be further derived from these data is the fact that incorporation of γ-CD influenced mainly the skin permeation rate of the steroidal drug fludrocortisone acetate. The effect of γ-CD on skin permeation was investigated for fludrocortisone acetate, flufenamic acid and fluconazole. The incorporation of the additional compound γ-CD led to significantly enhanced skin permeation rates of the lipophilic fludrocortisone acetate ($P < 0.05$) (Fig. 3). Interestingly, this was not the case for the lipophilic flufenamic acid although a slight trend was noticeable. As expected, the skin permeation rate of the hydrophilic drug fluconazole was not increased by incorporation of the CD. In fact, the skin permeation was even slightly decreased for both lecithin-based and sucrose stearate-based nanoemulsions.

A comparison of the skin permeation efficiency of the different emulsifiers shows that the skin permeation of the hydrophilic drugs fluconazole and minoxidil was significantly higher from lecithin-based nanoemulsions ($P < 0.05$). The skin permeation of the lipophilic drugs fludrocortisone acetate and flufenamic acid was the same for both types of surfactant ($P > 0.05$). A statistical analysis was performed for the cumulative permeated drug amounts as well as for the corresponding drug fluxes. Both evaluations led to consistent results.

Table 5
Skin permeation rates of fludrocortisone acetate (flud), flufenamic acid (fluf), fluconazole (fluc) and minoxidil (min) from both lecithin-based nanoemulsions (LN) and sucrose stearate-based nanoemulsions (SN) expressed as cumulative permeated drug amounts (μg cm^{-2}) and mean drug fluxes (J, μg cm^{-2} h^{-1}). At least five experiments were performed for each formulation ($n \geqslant 5$); indicated values are means ± SD.

Formulation	Cumulative drug amount after 24 h ± SD (μg cm^{-2})	Mean drug flux ± SD (J, μg cm^{-2} h^{-1})
SN flud	9.99 ± 0.46	0.55 ± 0.02
LN flud	9.98 ± 0.64	0.55 ± 0.04
γ-SN flud	55.10 ± 3.67	2.56 ± 0.14
γ-LN flud	98.62 ± 24.89	4.53 ± 0.99
SN fluf	48.88 ± 18.27	1.55 ± 0.87
LN fluf	42.22 ± 20.47	1.21 ± 0.62
γ-SN fluf	56.62 ± 17.35	1.83 ± 0.87
γ-LN fluf	45.97 ± 18.63	1.42 ± 0.69
SN fluc	1993.45 ± 256.77	88.39 ± 9.40
LN fluc	2481.67 ± 297.86	109.55 ± 11.30
γ-SN fluc	1885.14 ± 132.48	81.74 ± 5.92
γ-LN fluc	2157.13 ± 108.32	93.63 ± 3.80
SN min	1957.93 ± 296.12	84.27 ± 11.99
LN min	2402.55 ± 236.00	102.56 ± 9.41

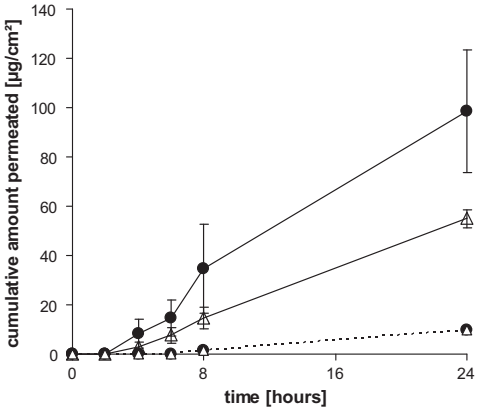

Fig. 3. Effect of γ-cyclodextrin on the in vitro skin permeation profile of fludrocortisone acetate from lecithin-based nanoemulsions (LN flud) and sucrose stearate-based nanoemulsions (SN flud). The drug permeation through porcine abdominal skin over the course of 24 h was determined by HPLC. The cumulative permeated drug amounts are plotted versus time. At least five experiments were performed for each formulation ($n \geqslant 5$) using Franz-type diffusion cells. Indicated values are means ± SD. Abbreviations: LN flud: dashed line (- -●- -); SN flud: dashed line (- -△- -); γ-LN flud: full line (—●—); γ-SN flud: full line (—△—).

4. Discussion

4.1. Comparison of emulsifying efficiency: sucrose stearate versus lecithin

Although the surfactants lecithin E-80 and sucrose stearate S-970 possess similar HLB values, the produced formulations differed in their physicochemical properties. The novel sucrose stearate-based systems exhibited smaller mean droplet sizes and a higher electrochemical stability. This tendency was observed for both blank and drug-loaded formulations. Likewise, these systems were less prone to chemical degradation, as both visual observation and monitoring of the pH indicated. The nanoemulsion production process was more reliable and controllable in the case of sucrose stearate since lecithin is more sensitive to changes in temperature. The storage of lecithin-based nanoemulsions at room temperature leads to changes in colour and odour. This destabilisation was decelerated by refrigerated storage but was nevertheless noticeable after 6 months. The chemical degradation of the emulsifier rendered the system less appealing despite the largely constant particle size. In contrast, sucrose ester nanoemulsions showed a clean white colour and no changes in odour after 6 months. The PDI of all systems remained below or around 0.2, which indicates a very homogeneous droplet size distribution and high physical stability [20].

The high negative ZP of sucrose stearate-based systems was directly correlated with the amount of sucrose ester. This might be ascribed to the presence of larger amounts of residual, non-esterified fatty acids in the sucrose ester mixture. An observed decrease in pH at increasing sucrose stearate concentrations as well as a comparison of the manufacturers' product specifications supports

this theory. While lecithin E-80 contains a maximum of 0.05% of free fatty acids, sucrose stearate S-970 may contain up to 10% of residual fatty acids, free sucrose, moisture and ash.

In terms of long-term stability, the ZP of sucrose stearate-based systems remained stable while the negative droplet surface charge of lecithin-based systems increased. This increase was most likely caused by hydrolysis of lecithin molecules. The chemical degradation of the surfactant results in increasing concentrations of lysolecithin and free fatty acids, which confer more negative charges to the droplets' surfaces [30]. This phenomenon has therefore to be considered a sign of physicochemical destabilisation.

Since the analysis of particle size distributions through DLS alone may provide incomplete information [31,32], additional cryo TEM investigations were performed. Thus, the exact nature of the measured structures and remarkable differences caused by the use of the different surfactants were visualised. Systems stabilised by sucrose stearate exhibited perfectly homogeneous nanoemulsion droplets, while systems stabilised by lecithin had a variable morphology. Sucrose stearate apparently possesses a better packing geometry at the O/W interface and is therefore more suitable for the formation of curved surfaces. In terms of droplet sizes, the images confirmed the results obtained by DLS.

Previously conducted cryo TEM analyses of lecithin-based nanoemulsions showed more regular droplet shapes, most likely due to the presence of additional emulsifiers and stabilisers [20]. The presented results confirm that the lecithin mixture alone is less efficient in nanoemulsion formation and that co-surfactants should be employed. In this context, it was shown that γ-CD might serve as a co-stabilising agent.

4.2. Effect of γ-CD on the nanoemulsion structure

Further cryo microscopic images revealed that addition of γ-CD to the lecithin-based system remarkably improved the homogeneity of the formulation. This indicates that the CD might be involved in the formation of the interfacial film which apparently became more suitable to form curved surfaces. Neither composition nor production process were altered in any other way; thus, the effect can only be ascribed to the presence of additional surface-active molecule complexes formed by CD molecules and fatty acid residues of the oil phase [33–37]. Since the rather voluminous CD molecules represent the hydrophilic region of the newly formed "surfactants", the resulting surface-active agents may have a suitable interfacial packing parameter to promote the formation of droplets. These observations are in good agreement with recent data [20]. It may be assumed that the previously detected excess of lecithin aggregates in the bulk water phase was caused by CD molecules which were inserted into the interfacial film of the O/W droplets, thus forcing surplus lecithin molecules into the aqueous phase. No such effect was observed in the present study since the overall amount of surfactant was low.

4.3. Effect of γ-CD on nanoemulsion stability

An additional aspect of the stability monitoring was the incorporation of γ-CD. The results showed that emulsion stability was not impaired by the presence of the CD. Cyclodextrins have a high potential for undesired interactions with various excipients. A high affinity of the CD towards lipophilic moieties of surfactant molecules may lead to complexation and subsequent inactivation [38]. Likewise, the decomposition of certain drugs may be accelerated by CDs [39]. It is therefore of utmost importance to investigate the specific effect of CD incorporation on every new system. Previous investigations have shown that CDs may have a stabilising effect on nanoemulsions [20]. In the present case, the addition of γ-CD seemed to stabilise ZP values of lecithin-based systems, thus conferring increased electrochemical stability to the nano-sized droplets.

4.4. Effect of the different emulsifiers and γ-CD on skin permeation

Since the skin permeation of drugs is influenced by factors such as their molecular mass and their log *P* value, the skin permeation of the investigated drugs differed considerably. The skin permeation rates of minoxidil were highest, followed by fluconazole and fludrocortisone acetate as well as flufenamic acid. Although nanoemulsions are aimed at the incorporation of lipophilic drugs, larger amounts of hydrophilic drugs could be delivered by incorporation into the aqueous phase. In the present experimental setup, this is probably related to the higher solubilities of the hydrophilic drugs in the aqueous receptor medium. In addition, the increased hydration of the skin in the experimental setting may have contributed to the enhanced permeation of the hydrophilic drugs [40]. Apart from these general aspects, the performance of sucrose stearate-based nanoemulsions in terms of skin permeation was evaluated and compared to that of lecithin-based systems. In case of both lipophilic drugs, similar skin permeation rates were achieved with lecithin- and sucrose stearate-based nanoemulsions ($P > 0.05$). Interestingly, the skin permeation of both hydrophilic drugs was higher from lecithin-based nanoemulsions than from their sucrose ester-based counterparts ($P < 0.05$), possibly due to the presence of liposomes as confirmed by cryo TEM. The hydrophilic drugs might be incorporated into the liposomal structures to a certain extent, which may enhance their skin permeation from lecithin-based systems. In addition, lecithin molecules themselves are known to interact with skin lipids and promote the skin permeation of actives [1,41,42].

In the context of the skin permeation studies, the enhancement effect of γ-CD on various drugs was investigated. A highly significant permeation enhancement was found for fludrocortisone acetate ($P < 0.05$), which confirmed previous results [20]. This indicates that γ-CD can indeed be employed to enhance the skin permeation of steroidal drugs from O/W nanoemulsions. No such effect was observed for the lipophilic flufenamic acid. Interestingly, the release of fluconazole from lecithin-based nanoemulsions was significantly decreased by the addition of γ-CD ($P < 0.05$). This might be explained by the observed strong decrease in liposomal structures through addition of γ-CD. It may thus be concluded that the superior release of hydrophilic drugs from lecithin-based systems was indeed caused by the additional liposomes.

In summary, the lack of permeation enhancement for drugs other than steroidal ones leads to certain useful conclusions. It can be assumed that the extraction of cholesterol or other skin components by the CD [43,44] can be excluded as a possible mechanism of action since such an effect would have affected the skin permeation of all drugs. Accordingly, an occlusion effect [45,46] through increased film-building capacity of the CD-containing formulations can be ruled out as well. However, it is well known that CDs can enhance the skin permeation of drugs by forming an inclusion complex and thus increasing drug solubility and dispersion within the formulation [43,47,48]. Hence, more drug is available at the skin surface to enter the stratum corneum through diffusion. However, such an effect appears unlikely if only small molar amounts of CD are incorporated, such as the presented amount of CD/drug of around 1:3.

It is particularly interesting that the permeation enhancement effect of γ-CD was linked to the nature of the employed emulsifier. The effect was significantly higher in lecithin-based nanoemulsions than in sucrose stearate-based systems ($P < 0.05$). This leads to the conclusion that some kind of underlying synergistic mechanism must be taken into account. As previously mentioned, the CD molecules can complex fatty acid residues of the oil phase, thus

forming new surface-active molecule complexes [33–37]. It is most likely that the CDs are incorporated into the interfacial film in this fashion, as the cryo TEM images suggest. The insertion of such additional emulsifiers may facilitate drug release [49]. It is commonly known that mixed interfacial films are more flexible and thus more suitable to form spherical droplets [50]. It might be deduced that this structural flexibility might also promote the release of specific drugs from the oil core, especially if they have an affinity for the CD cavities. Such a dynamic system might lead to an accelerated release of the incorporated drug, as is obviously the case for steroidal drugs in the presence of γ-CD. The complexation affinity between drug and CD may play a significant role in this context. The release of compounds from structures like solid lipid nanoparticles or nanoemulsion droplets is slower from the core than from the surface of the phospholipid layer [51]. If the CD acts as a "transporter" and enhances the affinity of the drug to leave the oil core through complexation, accelerated skin permeation may result. However, the exact mechanism behind the enhancement effect remains to be investigated. It has to be kept in mind that the involved processes are of a dynamic nature. In any case, the addition of γ-CD represents a skin-friendly way to promote the permeation of steroidal drugs without affecting the skin barrier function.

5. Conclusion

Sucrose stearate is a highly suitable emulsifier for nanoemulsion production and superior to lecithin in several aspects. Excellent skin friendliness can be expected from the novel formulations which contain only 2.5% of the mild surfactant. In addition, it was found that the formation of nano-sized droplets could be promoted by the addition of γ-CD in the case of lecithin while the number of vesicular structures was decreased. The concomitantly enhanced release of a steroidal drug from the oil core might be associated with its complexation affinity to the CD, which will be subject of further investigations.

6. Conflict of interest

The authors declare that no conflicts of interest occurred during this work and no funding sources were involved.

References

[1] Y. Baspinar, Nano- and microemulsions for topical application of poorly soluble immunosuppressives, PhD Thesis, Free University Berlin, 2009.
[2] R. Daniels, Galenic principles of modern skin care products, Skin Care Forum Online Issue 25, Society for Dermopharmacy, 2001. <http://www.scf-online.com/english/25_e/galenic_25_e.htm>.
[3] V.B. Patravale, S.D. Mandawgade, Novel cosmetic delivery systems: an application update, Int. J. Cosmet. Sci. 30 (2008) 19–33.
[4] Y.A. Shchipunov, Self-organising structures of lecithin, Russ. Chem. Rev. 66 (1997) 301–322.
[5] L. Rydhag, I. Wilton, The function of phospholipids of soybean lecithin in emulsions, J. Am. Oil Chem. Soc. 58 (1981) 830–837.
[6] C. Wabel, Influence of Lecithin on Structure and Stability of Parenteral Fat Emulsions, PhD Thesis, Friedrich-Alexander-Universität Erlangen-Nürnberg, 1998.
[7] T.P. Norden, B. Siekmann, S. Lundquist, M. Malmsten, Physicochemical characterisation of a drug-containing phospholipid-stabilised o/w emulsion for intravenous administration, Eur. J. Pharm. Sci. 13 (2001) 393–401.
[8] X. Liu, Y. Zhang, X. Tang, H. Zhang, Determination of entrapment efficiency and drug phase distribution of submicron emulsions loaded silybin, J. Microencapsul. 26 (2009) 180–186.
[9] D. Watrobska-Swietlikowska, M. Sznitowska, Partitioning of parabens between phases of submicron emulsions stabilized with egg lecithin, Int. J. Pharm. 312 (2006) 174–178.
[10] J. Han, C. Washington, Partition of antimicrobial additives in an intravenous emulsion and their effect on emulsion physical stability, Int. J. Pharm. 288 (2005) 263–271.
[11] J.J. Wang, K.C. Sung, O.Y. Hu, C.H. Yeh, J.Y. Fang, Submicron lipid emulsion as a drug delivery system for nalbuphine and its prodrugs, J. Control. Release 115 (2006) 140–149.
[12] M. Krafft, J. Rolland, J.G. Riess, Detrimental effect of excess lecithin on the stability of fluorocarbon/lecithin emulsions, J. Phys. Chem. 95 (1991) 5673–5676.
[13] T. Tadros, P. Izquierdo, J. Esquena, C. Solans, Formation and stability of nano-emulsions, Adv. Colloid Interface Sci. 108–109 (2004) 303–318.
[14] S.C. Yang, S. Benita, Enhanced absorption and drug targeting by positively charged submicron emulsions, Drug Dev. Res. 50 (2000) 476–486.
[15] J.V. Henry, P.J. Fryer, W.J. Frith, I.T. Norton, Emulsification mechanism and storage instabilities of hydrocarbon-in-water sub-micron emulsions stabilised with Tweens (20 and 80), Brij 96v and sucrose monoesters, J. Colloid Interface Sci. 338 (2009) 201–206.
[16] P.C. Calder, G.L. Jensen, B.V. Koletzko, P. Singer, G.J. Wanten, Lipid emulsions in parenteral nutrition of intensive care patients: current thinking and future directions, Intensive Care Med. 36 (2010) 735–749.
[17] S. Hoeller, A. Sperger, C. Valenta, Lecithin based nanoemulsions: a comparative study of the influence of non-ionic surfactants and the cationic phytosphingosine on physicochemical behaviour and skin permeation, Int. J. Pharm. 370 (2009) 181–186.
[18] S.B. Calderilla-Fajardo, J. Cazares-Delgadillo, R. Villalobos-Garcia, D. Quintanar-Guerrero, A. Ganem-Quintanar, R. Robles, Influence of sucrose esters on the in vivo percutaneous penetration of octyl methoxycinnamate formulated in nanocapsules, nanoemulsion, and emulsion, Drug Dev. Ind. Pharm. 32 (2006) 107–113.
[19] S. Takegami, K. Kitamura, H. Kawada, Y. Matsumoto, T. Kitade, H. Ishida, C. Nagata, Preparation and characterization of a new lipid nano-emulsion containing two cosurfactants, sodium palmitate for droplet size reduction and sucrose palmitate for stability enhancement, Chem. Pharm. Bull. (Tokyo) 56 (2008) 1097–1102.
[20] V. Klang, N. Matsko, A.M. Zimmermann, E. Vojnikovic, C. Valenta, Enhancement of stability and skin permeation by sucrose stearate and cyclodextrins in progesterone nanoemulsions, Int. J. Pharm. 393 (2010) 152–160.
[21] S. Hoeller, C. Valenta, Effect of selected fluorinated drugs in a "ringing" gel on rheological behaviour and skin permeation, Eur. J. Pharm. Biopharm. 66 (2007) 120–126.
[22] A. Hasanovic, C. Hollick, K. Fischinger, C. Valenta, Improvement in physicochemical parameters of DPPC liposomes and increase in skin permeation of aciclovir and minoxidil by the addition of cationic polymers, Eur. J. Pharm. Biopharm. 75 (2010) 148–153.
[23] E. Yilmaz, H.H. Borchert, Design of a phytosphingosine-containing, positively-charged nanoemulsion as a colloidal carrier system for dermal application of ceramides, Eur. J. Pharm. Biopharm. 60 (2005) 91–98.
[24] R.H. Mueller, Zetapotential und Partikelladung in der Laborpraxis, Band 37, Paperback APV, Wissenschaftliche Verlagsgesellschaft mbH, Stuttgart, 1996.
[25] J. Cazares-Delgadillo, A. Naik, Y.N. Kalia, D. Quintanar-Guerrero, A. Ganem-Quintanar, Skin permeation enhancement by sucrose esters: a pH-dependent phenomenon, Int. J. Pharm. 297 (2005) 204–212.
[26] B.B. Michniak-Kohn, P.W. Wertz, M. Al-Khalili, V.M. Meidan, Skin: physiology and penetration pathways, in: M.R. Rosen (Ed.), Delivery System Handbook for Personal Care and Cosmetic Products, Springer, Berlin, 2005, pp. 77–100.
[27] S. Cisternino, J. Schlatter, J.L. Saulnier, Stability of fludrocortisone acetate solutions prepared from tablets and powder, Eur. J. Pharm. Biopharm. 55 (2003) 209–213.
[28] B. Lundberg, Preparation of drug-carrier emulsions stabilized with phosphatidylcholine–surfactant mixtures, J. Pharm. Sci. 83 (1994) 72–75.
[29] T.G. Mason, J.N. Wilking, K. Meleson, C.B. Chang, S.M. Graves, Nanoemulsions: formation, structure, and physical properties, J. Phys. Condens. Matter 18 (2006) R635–R666.
[30] M.T. Baker, M. Naguib, Propofol: the challenges of formulation, Anesthesiology 103 (2005) 860–876.
[31] K. Bouchemal, S. Briancon, E. Perrier, H. Fessi, Nano-emulsion formulation using spontaneous emulsification: solvent, oil and surfactant optimisation, Int. J. Pharm. 280 (2004) 241–251.
[32] S. Benita, M.Y. Levy, Submicron emulsions as colloidal drug carriers for intravenous administration: comprehensive physicochemical characterization, J. Pharm. Sci. 82 (1993) 1069–1079.
[33] K. Shimada, Y. Ohe, T. Ohguni, K. Kawano, J. Ishii, T. Nakamura, Emulsifying properties of α-, β- and γ-cyclodextrins, Nippon Shokuhin Kogyo Gakkaishi 38 (1991) 16–20.
[34] D. Duchene, A. Bochot, S.C. Yu, C. Pepin, M. Seiller, Cyclodextrins and emulsions, Int. J. Pharm. 266 (2003) 85–90.
[35] A. Bochot, L. Trichard, G. Le Bas, H. Alphandary, J.L. Grossiord, D. Duchene, E. Fattal, α-Cyclodextrin/oil beads: an innovative self-assembling system, Int. J. Pharm. 339 (2007) 121–129.
[36] M. Inoue, K. Hashizaki, H. Taguchi, Y. Saito, Emulsion preparation using beta-cyclodextrin and its derivatives acting as an emulsifier, Chem. Pharm. Bull. (Tokyo) 56 (2008) 1335–1337.
[37] K. Hashizaki, T. Kageyama, M. Inoue, H. Taguchi, H. Ueda, Y. Saito, Study on preparation and formation mechanism of *n*-alkanol/water emulsion using alpha-cyclodextrin, Chem. Pharm. Bull. (Tokyo) 55 (2007) 1620–1625.
[38] W. Saenger, A. Mueller-Fahrnow, Cyclodextrins increase surface tension and critical micelle concentrations of detergent solutions, Angew. Chem. Int. Ed. Engl. 27 (1988) 393–394.
[39] R.H. Mueller, G.E. Hildebrand, Pharmazeutische Technologie: Moderne Arzneiformen, second ed., Wissenschaftliche Verlagsgesellschaft mbH, Stuttgart, 1998.

[40] N. Otberg, D. Grone, L. Meyer, S. Schanzer, G. Hoffmann, H. Ackermann, W. Sterry, J. Lademann, Water-filtered infrared-A (wIRA) can act as a penetration enhancer for topically applied substances, Ger. Med. Sci. 6 (2008) 1–14.
[41] M. Kirjavainen, A. Urtti, I. Jaaskelainen, T.M. Suhonen, P. Paronen, R. Valjakka-Koskela, J. Kiesvaara, J. Monkkonen, Interaction of liposomes with human skin in vitro – the influence of lipid composition and structure, Biochim. Biophys. Acta 1304 (1996) 179–189.
[42] R.H. Neubert, U. Schmalfuss, C. Huschka, W.A. Wohlrab, Recent developments in the area of dermal drug application, Pharm. Ind. 60 (1998) 149–156.
[43] T. Loftsson, S.B. Vogensen, M.E. Brewster, F. Konradsdottir, Effects of cyclodextrins on drug delivery through biological membranes, J. Pharm. Sci. 96 (2007) 2532–2546.
[44] K. Cal, K. Centkowska, Use of cyclodextrins in topical formulations: practical aspects, Eur. J. Pharm. Biopharm. 68 (2008) 467–478.
[45] R.H. Mueller, M. Radtke, S.A. Wissing, Solid lipid nanoparticles (SLN) and nanostructured lipid carriers (NLC) in cosmetic and dermatological preparations, Adv. Drug Deliv. Rev. 54 (2002) 131–155.
[46] R.H. Mueller, A. Dingler, The next generation after the liposomes: solid lipid nanoparticles (SLN, Lipopearls) as dermal carrier in cosmetics, Eurocosmetics 7–8 (1998) 19–26.
[47] T. Loftsson, N. Bodor, Effect of cyclodextrins on percutaneous transport of drugs, in: E.W. Smith, H.I. Maibach (Eds.), Percutaneous Penetration Enhancers, CRC Press, Boca Raton, FL, 1995, pp. 335–342.
[48] T. Loftsson, M. Masson, Cyclodextrins in topical drug formulations: theory and practice, Int. J. Pharm. 225 (2001) 15–30.
[49] P. Rother, Influence of cyclodextrins on oil-in-water emulsions containing hypromellose (HPMC) as a polymeric emulsifier, PhD Thesis, Faculty of Chemistry and Pharmacy, Eberhard-Karls-Universität, Tübingen, 2009.
[50] M. Trotta, F. Pattarino, T. Ignoni, Stability of drug-carrier emulsions containing phosphatidylcholine mixtures, Eur. J. Pharm. Biopharm. 53 (2002) 203–208.
[51] P. Ahlin, K. Julijana, S. Pečar, J. Štrancar, M. Šentjurc, The effect of lipophilicity of spin-labeled compounds on their distribution in solid lipid nanoparticle dispersions studied by electron paramagnetic resonance, J. Pharm. Sci. 92 (2003) 58–66.

Original Paper

Skin Pharmacology and Physiology

Skin Pharmacol Physiol 2011;24:256–268
DOI: 10.1159/000326072

Received: November 30, 2010
Accepted after revision: February 5, 2011
Published online: April 21, 2011

Facilitating in vitro Tape Stripping: Application of Infrared Densitometry for Quantification of Porcine Stratum Corneum Proteins

V. Klang[a] J.C. Schwarz[b] A. Hartl[a] C. Valenta[a, b]

[a]Department of Pharmaceutical Technology and Biopharmaceutics, Faculty of Life Sciences, and
[b]Research Platform 'Characterisation of Drug Delivery Systems on Skin and Investigation of Involved Mechanisms', University of Vienna, Vienna, Austria

Key Words
Tape stripping · In vitro · Infrared densitometry · Corneofix® · D-Squame® · Stratum corneum protein · Porcine ear skin · Micro BCA™ protein assay

Abstract
Infrared (IR) densitometry is a highly practical method recently proposed for protein analysis during in vivo tape stripping. However, this method has not yet been validated for the quantification of porcine stratum corneum (SC) proteins. Therefore, the aim of this study was to establish calibration curves for the analysis of adhesive tapes removed from porcine ear skin. To this end, the protein absorption (as determined via IR densitometry) was correlated with the protein content determined with the Micro BCA™ protein assay after extraction of the tapes. The obtained linear regressions confirm that IR densitometry is suitable for the quantification of not only human, but also porcine, SC proteins. The pattern of protein removal observed with porcine skin differs from that of human skin due to more pronounced corneocyte clustering and deep 'canyons', which necessitates specific evaluation of porcine skin samples and a working protocol that takes this into account. The presented data will facilitate future analysis of porcine SC proteins during in vitro tape stripping.

Copyright © 2011 S. Karger AG, Basel

Introduction

In the field of dermatopharmacokinetics, tape stripping is employed to establish skin penetration profiles of substances that are applied onto the skin in various vehicles. After a defined application time, the uppermost layers of stratum corneum (SC) are consecutively removed with adhesive tapes. Subsequently, all adhesive films are analyzed for their drug content as well as for the amount of removed corneocyte aggregates. Quantification of the latter is necessary to obtain an accurate penetration depth of the applied substances [1]. Formerly, time-consuming methods for the analysis of these SC proteins were employed, such as gravimetric determination [2–8], microscopic evaluation [9], or extraction and subsequent analysis with protein assays [10, 11]. More recently, optical methods for protein analysis on adhesive films have been developed. The UV absorption of proteins, directly reflecting the amount of corneocytes, was found to be too weak as opposed to the light scattering observed for the horny layer particles [6]. In contrast, optical spectroscopy in the visible range was found

V.K. and J.C.S. contributed equally to this work.

KARGER

Fax +41 61 306 12 34
E-Mail karger@karger.ch
www.karger.com

© 2011 S. Karger AG, Basel
1660–5527/11/0245–0256$38.00/0

Accessible online at:
www.karger.com/spp

Claudia Valenta
Department of Pharmaceutical Technology and Biopharmaceutics
Faculty of Life Sciences, University of Vienna
Althanstrasse 14, AT–1090 Vienna (Austria)
Tel. +43 1 4277 55410, E-Mail Claudia.valenta@univie.ac.at

to be a suitable tool for protein quantification on tapes in a manner that is undisturbed by other skin components [1, 5, 12–14]. The so-called pseudo-absorption of the proteins – which is composed of reflection, scattering and diffraction of the light by corneocytes – can be used to indirectly quantify the protein mass on the tapes [1, 5].

Recently, the compact infrared (IR) densitometer SquameScan® 850A was introduced as an efficient and simple quantification tool for adhesive tapes obtained from human volunteers in vivo [15] and in vitro [16]. The optical pseudo-absorption of SC tape strippings was shown to correlate linearly with the respective protein content. Calibration curves were obtained which can be used for the rapid and non-destructive quantification of human SC proteins.

However, no data have so far been presented to validate this method for the analysis of tape strippings obtained from porcine skin in vitro. Clinical trials performed on human volunteers often involve considerable effort in terms of logistics and time, as well as permission from an ethical committee. Furthermore, excised human skin is not always available. Therefore, in vitro tape stripping using porcine skin represents a suitable alternative to obtain basic information about the penetration behavior of new vehicles and drugs. Numerous studies have investigated the suitability of the porcine skin model for in vitro studies [7, 8, 17–19]. It is a well-accepted substitute for human skin due to similarities in epidermal thickness, lipid composition and permeability [8]. In context with tape stripping, porcine ear skin was found to be the most suitable in the in vitro model [8, 20]. Therefore, there is a need for efficient and accurate quantification methods to analyze porcine corneocytes on adhesive tapes.

The present publication aims to establish the method of IR densitometry for quantification of porcine SC proteins obtained by in vitro tape stripping. Two different brands of standardized adhesive films, Corneofix® and D-Squame® tapes, were investigated for their suitability to homogeneously remove the corneocytes of the upper skin layers. The primary objective of the study was to generate calibration curves for the quantification of porcine SC proteins. The validation of IR densitometry for this application is an important step towards paving the way for future in vitro experiments with porcine skin.

Materials and Methods

Chemicals

Sodium hydroxide (CAS No. 1310-73-2, Lot No. 437415/2) was purchased from Sigma-Aldrich Chemie GmbH (Steinheim, Germany). Hydrochloric acid (CAS No. 7647-01-0, Lot No. 41240) was obtained from Sigma-Aldrich Laborchemikalien GmbH (Seelze, Germany). Sodium chloride (CAS No. 7647-14-5, Lot No. 082409) was purchased from Herba Chemosan Apotheker AG (Vienna, Austria). The Micro BCA™ Protein Assay Kit was obtained from Pierce Biotechnology Inc. (Rockford, Ill., USA). The kit consisted of reagent A (alkaline tartrate-carbonate buffer), reagent B (bicinchoninic acid solution) and reagent C (copper sulfate solution), which were mixed according to the manufacturer's instructions. The protein standards employed were bovine γ-globulin (BGG; 2.0 mg/ml, product No. 23212, Lot No. LC142488) and bovine serum albumin (BSA; 2.0 mg/ml, product No. 23209, Lot No. LC143026) as purchased from Pierce Biotechnology Inc. Standard D-Squame adhesive tapes with a diameter of 22 mm and an area of 3.8 cm^2 were purchased from CuDerm Corp. (Dallas, Tex., USA). Standard Corneofix adhesive films with a square area of 4.0 cm^2 were obtained from Courage + Khazaka GmbH (Cologne, Germany).

Preparation of Porcine Skin

Fresh porcine ears were donated by the Clinic for Swine, University of Veterinary Medicine, Vienna. Preliminary studies showed that different storage conditions did not alter the skin barrier function or the SC properties. Tape-stripping results obtained with fresh porcine ear skin were comparable to those of refrigerated or deep-frozen material. Recently published findings confirmed these observations [16]. In order to ensure logistic feasibility and reproducibility of the experiments, all porcine ears used in this study were stored at –24°C and thawed prior to the respective experiments. After defrosting, the ears were cleaned carefully with purified water and blotted dry with soft tissue. The skin was subsequently freed from hair with scissors, and intact representative skin areas were indicated with a permanent marker. In addition, the transepidermal water loss (TEWL) of the skin was determined using the closed-chamber device AquaFlux® (Biox Ltd., London, UK) to confirm an intact skin barrier function and to monitor the defrosting process. When the TEWL reached values between 15 and 20, the tape stripping procedure was started. The TEWL measurements were performed before and after tape stripping on the respective skin areas, and the software program AquaFlux V6.2 was used for data analysis.

In vitro Tape Stripping

The tape stripping procedure was conducted with 20 sequential adhesive films for each experiment. Two different brands of adhesive tape, D-Squame and Corneofix tapes, were investigated separately. For each type of adhesive film, 12 individual experiments (n = 240, respectively) were conducted by the same technician to minimize variations [15, 21]. The in vitro tape stripping was carried out under standardized conditions, which were adapted to the different types of adhesive film. Since various factors – such as the intensity and duration of pressure application as well as the velocity of tape removal – may have a significant influence on the amount of removed SC proteins [5, 19], care was taken to ensure a reproducible working procedure. The porcine

ears were stretched out on Styrofoam plates and fixed with needles if necessary. After placing the first adhesive film on the skin, its outline was indicated with a permanent marker to ensure subsequent tape stripping on the exact same skin area. In order to apply pressure while ensuring a rolling movement to minimize the influence of wrinkles [14], pressure was applied with the thumb covered in a vinyl glove as previously described [19, 22]. The experiment was performed on a balance to ensure a constant pressure of 49 N (5 kg) in the case of Corneofix and 19 N (2 kg) in the case of D-Squame. This comparatively high pressure was a prerequisite for obtaining reproducible amounts of SC proteins, especially in the case of Corneofix tapes which possess a lower adhesive power [19]. Similar working protocols were reported for D-Squame tapes on human skin in vitro [16, 21]. A critical contact time and pressure are necessary to obtain the maximum 'tackiness' of the adhesive film [23], i.e. the maximum adhesive power, to promote reproducible removal of proteins. After applying the respective pressure for 3 s, the tape was removed in a single rapid movement. The amount of adherent SC proteins was subsequently determined by IR densitometry and the Micro BCA protein assay. The cumulative amount of SC proteins was employed to establish the depth of the complete SC as previously described [5].

Infrared Densitometry

The amount of corneocytes on each removed tape strip was determined using the infrared densitometer SquameScan™ 850A (Heiland Electronic GmbH, Wetzlar, Germany) [15]. This device measures the decrease in light intensity over an area of 15 mm. The optical pseudo-absorption of the adhesive films at a wavelength of 850 nm serves to indirectly quantify the amount of SC proteins on the tapes. The analysis is non-destructive and rapid. The absorption values (%) can be read from the display after an equilibrium time of 3 min. The linear working range of the device is between 0 and 40% of absorption with a resolution of 0.1%, as indicated by the manufacturer [15, 16].

The instrument was calibrated prior to the experiments. An empty sample holder was set as 0% of absorption, while an ambient light filter with a defined absorption of 39.0% was used to control the functionality of the device. The absorption of an empty tape was used as a reference to account for the background noise. After the tape stripping procedure, the removed tapes were placed in the sample holder with the adhesive side facing upwards and subsequently analyzed [15, 16]. The homogeneous distribution of the corneocyte aggregates on each tape strip was checked visually after removal. The existence of non-homogeneous areas was noted in the protocol as previously reported [5].

Micro BCA Protein Assay

The quantification of the porcine SC proteins removed with each tape strip was carried out according to the microplate working protocol of the Micro BCA protein assay as previously described [15]. The colorimetric reaction is based on the formation of a chelate complex of bicinchoninic acid (BCA) and cuprous ions.

After the pseudo-absorption at 850 nm of each tape strip was analyzed via IR densitometry the adhesive tapes were transferred into 1.5-ml Eppendorf tubes and incubated with 750 μl of 1 M sodium hydroxide solution to extract the proteins. To this end, the tubes were placed into an Eppendorf Thermomixer comfort (Eppendorf AG, Hamburg, Germany) and shaken at 37°C and 1,400 rpm for 1 h. After the appropriate cooling time, 500 μl of the resulting protein solutions were neutralized with 500 μl of 1 M hydrochloric acid. After mild homogenization, 100 μl of each sample was replicated into a 96-well microplate. Subsequently, 100 μl of standardized Micro BCA Protein Assay working reagent were added. The covered microplate was shaken at 300 rpm for 60 s and then incubated at 37°C for 2 h. After appropriate cooling time, the absorbance of the samples at $\lambda = 550$ nm was determined at room temperature with a UV/VIS microplate reader (Tecan Infinite™ 200, Tecan Ltd., Maennedorf, Switzerland). The protein content of each removed adhesive tape was analyzed in triplicate ($n = 3$), and the mean value was used for further evaluation. Five blank adhesive tapes ($n = 5$) were respectively extracted in exactly the same fashion as the protein-covered tapes, and analyzed with every round of analysis. The mean value of these blank tapes served as the respective control to account for background noise.

The quantification of the protein samples was performed with the help of calibration curves created by diluting protein standard solutions which were freshly prepared and analyzed with each microplate. The standard employed for this study was BGG as previously reported [15]. For reasons of comparison, standard solutions of BSA were prepared and analyzed as well. The standard solutions were prepared in the range of 2.5–40 μg/ml, which is the recommended linear working range of the employed assay. A solution of 1 M sodium chloride was employed as a solvent, which corresponds to a mixture of equal parts of 1 M sodium hydroxide and 1 M hydrochloric acid. The same solution without BGG served as a control. This blank solution was determined in triplicate on each microplate. The mean value was subtracted from the results of the standard solutions to account for the background noise.

Protein values above the linear working range of the assay can be determined via extrapolation of the calibration curve. However, the slope rather follows a linear correlation of the second order, which will lead to inaccurate results for higher protein values (fig. 1). Therefore, samples where a high protein content was anticipated due to the obtained IR densitometric values were diluted with 1 M NaCl solution (1:3 v/v) prior to analysis with the Micro BCA assay.

Statistical Data Analysis

The linear regressions as well as the coefficients of determination R^2, the correlation coefficients R, the mean values and the standard deviations were calculated using the software program Microsoft Office Excel 2003. The linear regression analysis was performed to determine the relationship between two properties of the corneocytes: the pseudo-absorption at 850 nm as determined via IR densitometry and the amount of corneocytes as determined with the Micro BCA protein assay. All other statistical tests such as the Student's t test were performed using the software program GraphPad Prism 3.

The calibration curves of the protein standards were separately evaluated both as linear correlations of the first order (linear function) and linear correlations of the second order (square function), as indicated in the Micro BCA working protocol. Since the protein values calculated with these curves were highly comparable ($p > 0.05$), it was decided that the conventional linear calibration curve provided sufficient linearity in the range of the investigated protein concentrations.

Results

Skin Barrier Function and TEWL

Determination of the TEWL was employed to assess the intactness of the skin barrier function. Mean TEWL values of 17.09 ± 2.20 $g \cdot m^{-2} \cdot h^{-1}$ (n = 24) were reached after approximately 1.5 h of thawing. At this point, the tape stripping procedure was started to avoid dehydration of the thawed tissue. Removal of 20 tape strips lead to a variable increase in TEWL to values around 51.22 ± 15.63 $g \cdot m^{-2} \cdot h^{-1}$ (n = 24). This might be due to interindividual differences in SC thickness [7], variable SC cohesion [23], as well as variable or decreased hydration of the in vitro tissue [8]. After 20 tapes, a large part of the barrier of the porcine ear SC had been removed [8]. Tape stripping of the whole SC with respectively 80–130 tapes led to a more pronounced increase in TEWL, with values up to around 70.17 ± 3.84 $g \cdot m^{-2} \cdot h^{-1}$ for Corneofix tapes and 78.78 ± 4.36 $g \cdot m^{-2} \cdot h^{-1}$ for D-Squame tapes (n = 7, respectively). The higher increase caused by D-Squame tapes is in agreement with data presented in the literature [19], and may be ascribed to the stronger adhesive force which leads to a more pronounced disruption of the skin barrier.

Protein Analysis with the IR Densitometer

All analyzed tape strips gave absorption values well within the linear working range. The limit of quantification was not reached. Since the device allows for a calibration prior to every series of measurements – thus eliminating the influence of the tapes' background absorption – no further correction of the obtained values was necessary.

Protein Analysis with the Micro BCA Protein Assay

Since previous investigations had employed different protein standards for comparable tasks [15, 16], both BGG and BSA were tested as possible standards for the quantification of porcine SC proteins. The protein absorption of the diluted standard solutions was determined at 550 nm with a microplate reader. Figure 2 shows the results of the linear regression analysis between protein content and absorption for the diluted standard solutions of BGG and BSA. Comparable calibration curves could be obtained with both protein standards. In case of BGG, the mean coefficient of determination R^2 was 0.999 ± 0.002 (n = 37), while in the case of BSA, R^2 was 0.999 ± 0.001 (n = 8). In order to provide a basis for comparison with previously published results for human skin [15], the BGG standard was employed for evaluation of all porcine protein samples. The standard curves determined for each experiment provided a linear correlation between the protein absorption at 550 nm and the protein content in the range of 2.5–40 μg/ml. Since the protein amounts obtained after removal of adhesive films were never below this concentration, no extrapolation of the data towards the lower limit of quantification was necessary.

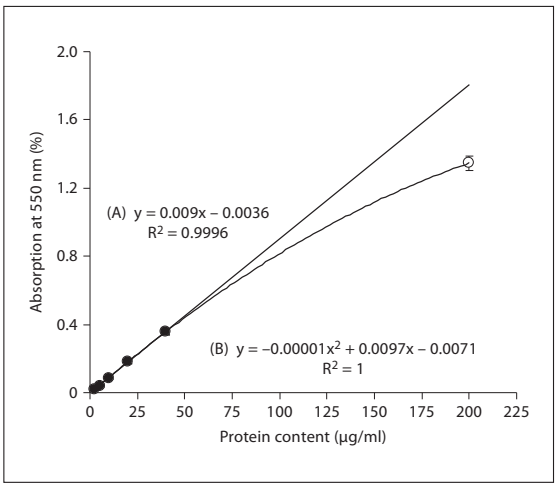

Fig. 1. Impact of the polynomial nature of protein calibration curves shown on data obtained with BGG (number of calibration series = 37). The mean protein values obtained with the standard solutions were set into correlation with the respective absorption values by linear regression using either a linear correlation curve (A; —●—) or a polynomial correlation of the second order (B; —○—), as suggested by the manufacturer's working protocol. The analyzed working range was between 2.5 and 200 μg/ml BGG for the polynomial correlation curve. The linear working range employed for the microplate working protocol was between 2.5 and 40 μg/ml.

Every microplate was evaluated separately with the respective blank tape samples and the protein standard solutions as recommended by the manufacturer. In order to examine the reproducibility of the individual experiments, an overall regression analysis was performed over all individual data points of the employed BGG standard solutions, which corresponded to 37 individually prepared samples for each concentration (n = 185). Figure 3 shows the results of the regression analysis for the absorption at 550 nm and the protein content of the BGG standard. The overall coefficient of determination R^2 was 0.9932 with a confidence interval of 95%,

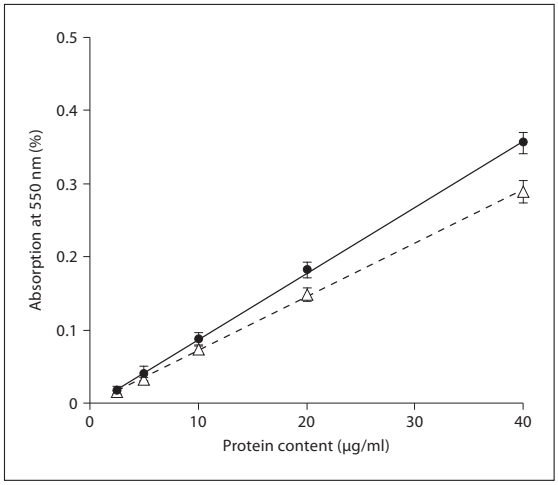

Fig. 2. Comparison of BGG and BSA as external standards for protein analysis with the Micro BCA protein assay. Defined protein solutions were employed to establish a linear correlation between protein concentration (µg/ml) and protein absorbance. The diluted protein solutions were analyzed at 550 nm with a TECAN Infinite® microplate reader. The presented values are means ± SD of individually determined calibration curves: n = 8 curves for BSA (– – Δ – –); n = 37 curves for BGG (—●—).

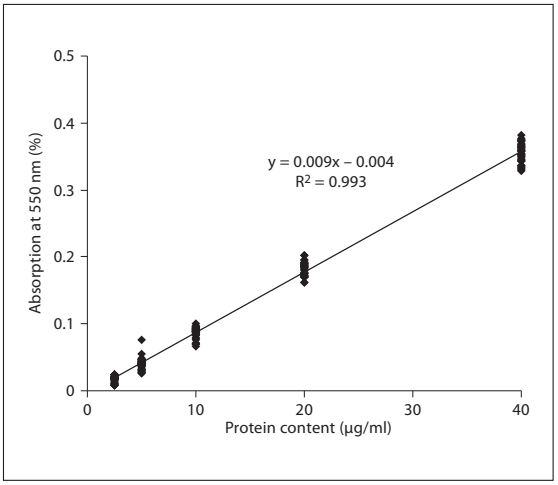

Fig. 3. Linear regression over all individual data points of 37 calibration curves obtained with BGG as a protein standard (n = 185). The confidence intervals set at 95% were within the range of 0.0089 to 0.0091 for the slope and –0.0057 to –0.0012 for the Y-intercept with a mean correlation of y = 0.0090 ± 0.0001 to 0.0035 ± 0.0012. The protein absorption values of defined standard solutions were determined with a microplate reader at room temperature.

which confirms that the described working protocol is suitable for obtaining reproducible results with the Micro BCA assay.

The absorption of the SC proteins extracted from the tapes was determined with the help of the individual calibration curves established with BGG as a protein standard. The amount of proteins extracted from each tape was quantified in this fashion, and the obtained values were employed for the linear regression analysis.

Linear Regression Analysis: Pseudo-Absorption versus Protein Content

Summarizing the experiment: tape stripping, visual control of the protein coverage on the tapes and IR densitometric analysis were performed, followed by extraction and analysis of the protein content with the Micro BCA protein assay. Despite an accurate working procedure, the porcine SC proteins were generally removed in large polygonal aggregates. Therefore, no tapes were a priori excluded from analysis in order to determine whether the specific clustering behavior of porcine SC proteins would affect the IR densitometric quantification. Inhomogeneous protein coverage was noted in the protocol for separate evaluation procedures [5, 14].

The obtained protein content of the samples as determined with the Micro BCA assay was then plotted against the previously determined IR densitometric absorption values. The regression analysis revealed a linear correlation between these data, both for Corneofix and D-Squame tapes (fig. 4; n = 240, respectively). The obtained coefficients of determination were in the same order of magnitude as previously reported for human SC proteins [15, 16], namely $R^2 = 0.812$ for Corneofix and $R^2 = 0.732$ for D-Squame tapes. An analysis of all obtained protein values irrespective of the type of adhesive film showed a similar trend (n = 480, $R^2 = 0.729$). A large number of experiments were included in the correlation to give an overview about the reproducibility of the tape stripping method using porcine ear skin. The obtained correlations confirm that quantification of porcine SC proteins is possible in the course of an everyday experimental setup without having to exclude tapes from the final evaluation. A certain variability of the data has to be anticipated for experiments conducted with biological material [24].

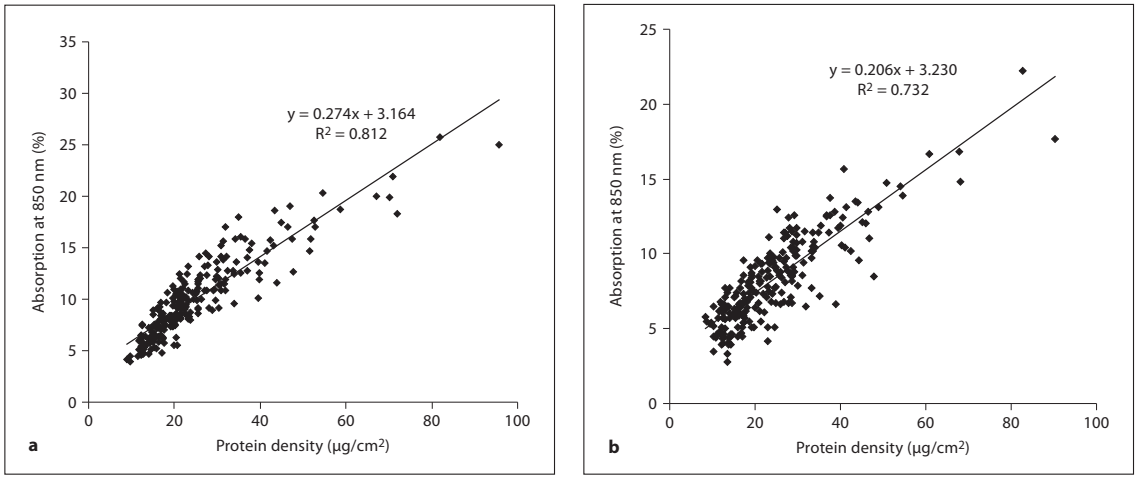

Fig. 4. Linear regression analysis of individual protein samples obtained through sequential tape stripping of porcine ear skin with either Corneofix (**a**) or D-Squame tapes (**b**). For each type of adhesive film, 12 experiments were conducted during each of which 20 sequential adhesive films were removed (n = 240 for each type of adhesive film). The protein content as determined with the Micro BCA assay was plotted against the corresponding IR densitometric data.

Determination of Porcine SC Mass

Despite the good overall correlation between IR densitometric values and the protein content of the tapes, the presented calibration curves might yield inaccurate results for adhesive films with low protein coverage. Since the amount of corneocytes removed from deeper layers of the SC becomes smaller with increasing tape numbers, higher uncertainties in quantification have to be expected [5]. Moreover, it was shown that a reliable linear regression analysis should only be conducted with selected pairs of data not disturbed by any methodological or analytical effects [1]. Otherwise, methodological limitations will lead to skewed correlations [11, 24].

Therefore, a more restrictive evaluation of the data was performed for the individual experiments following the recommendations of Weigmann et al. [1, 5]. The individual data sets were checked for experimental artifacts as previously noted during the experiment. Potentially biased samples, i.e. adhesive films with strongly inhomogeneous protein coverage and/or risk of a stack effect [5], were subsequently excluded from the linear regression analysis. Individual calibration curves for each experiment were calculated and extrapolated to the total SC depth which is represented by additional zero values for pseudo-absorption and protein content. Figure 5 shows representative examples for individual calibration curves obtained with either Corneofix or D-Squame (n = 13, respectively). The individual correlations were performed for 12 data sets for each tape brand. Since important skin parameters such as SC thickness and cohesion may vary significantly for different individuals, the data obtained for each individual were evaluated separately to obtain representative mean values of 12 experiments [5, 13]. The number of samples in the individual experiments remaining after exclusion of experimental artifacts ranged from 13 to 19 for Corneofix (34 out of 240 tapes excluded) and from 9 to 19 for D-Squame (59 out of 240 tapes excluded). It is noteworthy that the number of excluded tapes was by far larger for D-Squame than for Corneofix.

All experiments were evaluated in this fashion and highly comparable correlation curves were achieved. In the case of Corneofix, the mean R^2 was 0.940 ± 0.019 while in the case of D-Squame, a mean R^2 of 0.934 ± 0.022 was obtained (n = 12, respectively). The slopes k were 0.438 ± 0.054 for Corneofix and 0.385 ± 0.069 for D-Squame tapes. No statistical differences between the k values obtained for Corneofix and D-Squame tapes were found ($p > 0.05$). Therefore, a mean calibration curve to be used for the evaluation of undisturbed data was estab-

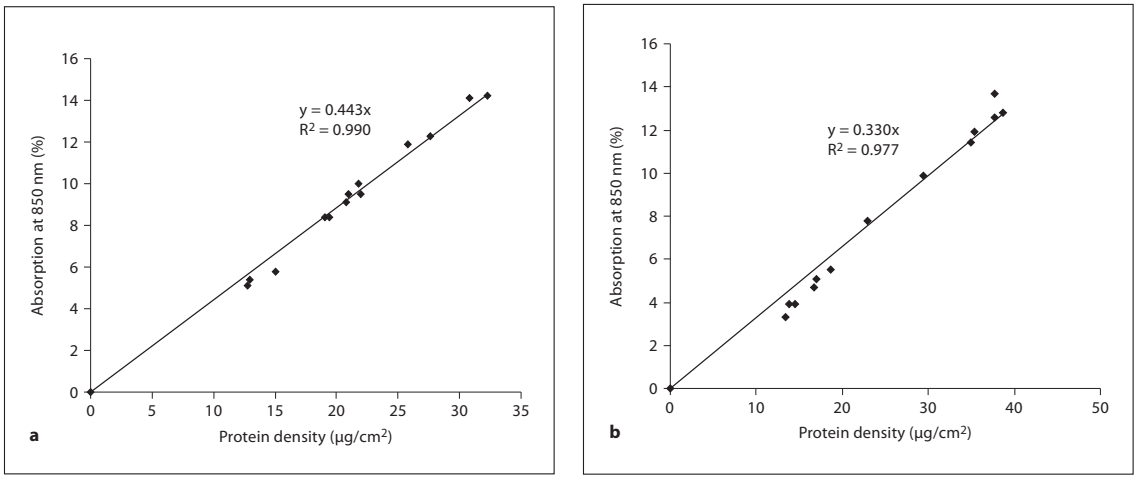

Fig. 5. Representative linear regression curves of individual protein samples obtained through 1 sequential tape stripping experiment of porcine ear skin with either Corneofix (**a**) or D-Squame tapes (**b**). Adhesive films with inhomogeneous protein coverage which would lead to biased results were excluded. The analyzed values represent undisturbed adhesive films (n = 13, respectively) with visually homogeneous protein coverage. Extrapolation of the regression curve was performed in order to allow an accurate determination of low protein values.

lished including all experiments irrespective of the tape brand used. The mean overall correlation was found as y = 0.41x with a mean coefficient of determination R^2 of 0.937 ± 0.021 (n = 24). The obtained slope k represents the mean factor of proportionality between pseudo-absorption and protein content, which was 0.41 ± 0.07 for all experiments (n = 24). This value can be employed to calculate the mass of SC proteins (*m*) after determination of their pseudo-absorption at 850 nm (*A*) for a normalized tape area of 1 cm^2 by employing the equation $m = A/0.41$ (in $\mu g/cm^2$).

As previously discussed [5], the highest accuracy in protein quantification is surely obtained with individual correlation curves which have to be established for every volunteer or every skin sample. In the case of porcine ear skin, this would be a rather time-consuming quest considering the fact that only a limited number of experiments can be performed on a single porcine ear. The use of the established overall correlation will save time while still providing sufficiently accurate results.

Determination of Porcine SC Thickness in vitro

Additional tape stripping experiments (n = 7 for D-Squame, n = 7 for Corneofix) were conducted in which the complete horny layer was removed. The number of adhesive films required for this task varied between 80 and 130 strips. The end of tape stripping was set at the limit of quantification of the IR densitometer. When the values remained constant around 0.0 ± 0.1%, the stripping procedure was stopped.

The cumulative value of pseudo-absorption was 327.44 ± 133.55 % (n = 14). The mean SC thickness was calculated using the mean proportionality factor of 0.41. The mean protein density of the tissue was assumed with 1 $g \cdot cm^{-3}$, as previously proposed for calculating the thickness of both porcine [8] and human skin [5]. The resulting mean SC thickness was found to be 7.96 ± 3.25 µm. These values are in agreement with recent data published for porcine SC thickness [7, 8, 25]. Higher values for SC thickness have been reported as well [20, 26]. This expected variability may be due to interindividual differences – such as the exact age and breed of the pigs [7], the general skin state as well as the exact location of tissue sampling and the different techniques of analysis. Various techniques such as histological sectioning after freezing [26], TEWL measurements in combination with tape stripping [8], light microscopy [20] and fluorescence microscopy [25] were proposed.

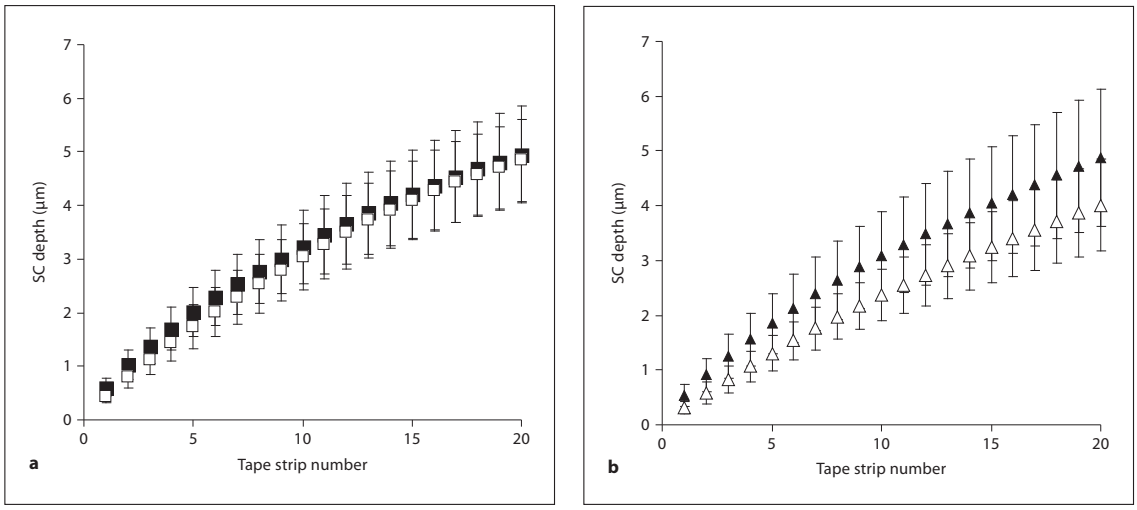

Fig. 6. Depth of the SC reached after removal of 20 sequential tape strips using Corneofix (**a**) or D-Squame tapes (**b**). The black symbols (■, ▲) represent the SC depth as calculated from the protein values obtained by direct analysis with the Micro BCA protein assay. The white symbols (□, △) represent the SC depth as calculated after indirect protein quantification by IR densitometry using the presented factor of proportionality k = 0.41. The values are means ± SD of 12 experiments.

The accuracy of the obtained results was confirmed by correlating the SC thickness as determined by the two employed methods against the respective tape strip number (fig. 6). In the case of Corneofix tapes (fig. 6a), an almost identical SC thickness was calculated using the protein amounts determined via the protein assay and the corresponding values determined via IR densitometry. This supports the validity of the applied extrapolation of the correlation curves as previously reported [5]. In the case of D-Squame tapes (fig. 6b), a slight discrepancy between the values was observed. This again confirms that tapes of lower adhesive power are more suitable for the use on porcine skin since a smaller risk of the stack effect and relatively smaller uncertainties due to inhomogeneous protein coverage occur.

It is well known that the amount of corneocytes removed with single tapes and the thickness of the horny layer can vary considerably for different individuals [1, 22, 27]. Hence during skin penetration studies, the absolute horny layer thickness should either be established for every tested individual or for a sufficiently large number of individuals for which a representative mean thickness can be calculated.

Discussion

Peculiarities of Porcine Skin during Tape Stripping

Many of the observations made during this investigation are linked to the specific properties of porcine skin and its distribution on adhesive films. In pig skin, the cells are organized in polygonal clusters or columns that comprise the whole of the epidermis and are separated by intercluster regions or 'canyons'. This structure as described and graphically demonstrated by Carrer et al. [25] might explain the distinct pattern of porcine corneocyte removal. As figure 7a, b clearly shows, the corneocytes are removed in large polygonal clusters. Since the intercluster regions start as wrinkles on the skin surface, the corresponding areas on the tape will exhibit a lower corneocyte density – thus appearing as separating barriers between the SC clusters fixed to the tape. High protein density as primarily observed for the first tape strips removed will therefore lead to comparatively inhomogeneous protein coverage. The following adhesive films showed a more homogeneous protein coverage, especially in the case of Corneofix tapes. Due to their higher adhesive power, the D-Squame tapes generally showed a more irregular pattern of protein removal. In contrast,

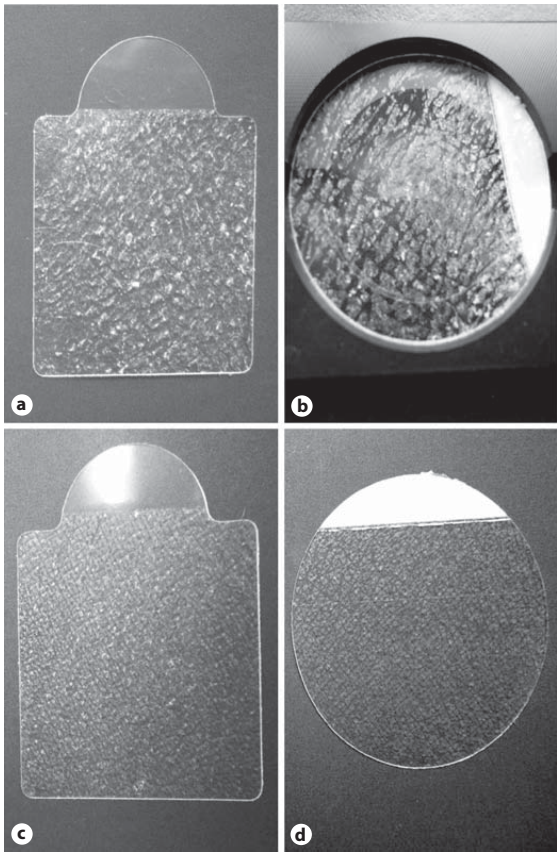

Fig. 7. Representative examples of first adhesive films to be removed from the skin surface of porcine skin (**a**, **b**) and human skin (**c**, **d**).

the first tape strips removed from human skin in vivo (fig. 7c, d; courtesy of the experimenter) show a finely distributed network of small corneocyte aggregates.

However, the distribution of the porcine protein clusters and intercluster regions is apparently of a sufficiently homogeneous nature to allow for a reasonably accurate analysis of the pseudo-absorption by IR densitometry. Previous studies have reported the successful quantification of porcine SC proteins via assessment of the pseudo-absorption by UV/VIS spectroscopy [13]. Despite the presence of the described trans-epidermal shunt pathways [25], the penetration behavior of different sunscreens was found to be nearly identical for human skin in vivo and porcine ear skin in vitro [13]. A substantial amount of research confirms the suitability of the porcine ear model as a substitute for human skin despite the inherent structural differences. A slightly higher permeability of the porcine skin has been reported [28, 29], which may be related to the presented canyons or the larger orifices of porcine hair follicles [13]. The reported observations are thus in accordance with previous opinions. In vitro tissue shows different properties compared to living skin which may affect the amount of removed SC. The presence of wrinkles may have a different effect during in vitro tape stripping even if a rolling movement is used to apply pressure [14].

Linear Regression Analysis and Tape Stripping

In recent years, various methods have been introduced for the quantification of proteins removed with adhesive films. Most of these methods have been validated by simply correlating the obtained data with the values determined by a classical protein analysis method, such as protein assays [10, 11, 15, 16] or weighing [1, 2, 6]. In this context, disturbing influences connected with the tape stripping procedure have been described in detail [1, 14]. The main challenge is to obtain a homogeneous distribution of corneocyte aggregates fixed on the individual tapes. Inhomogeneous protein coverage may be caused by the inherent heterogeneity of the skin, and might therefore not be entirely avoided [11]. On the other hand, errors caused during the working procedure can be controlled – such as incorrect positioning of the tapes or inconsistent removal – otherwise the obtained absorption values might not be representative of the amount of corneocytes on the tape [1]. To prevent such disturbing effects from biasing the correlation, the homogeneous distribution of the horny layer particles on each tape should be checked visually. If obvious disturbances are detected, the corresponding data pair should be excluded from the linear regression analysis [1, 19]. However, the distribution of the horny layer particles of porcine skin on the tapes was found to be generally more irregular than for tapes strips removed from human skin. Thus, all obtained tape strips were used for establishing an overall correlation as previously demonstrated [15, 16]. Nonetheless, discrepancies concerning the protein coverage were noted. Evaluation of the data showed that despite the irregular pattern of protein removal of porcine skin, the overall correlations obtained for the summarized 240 samples were highly satisfying when compared to data obtained with human skin [15, 16].

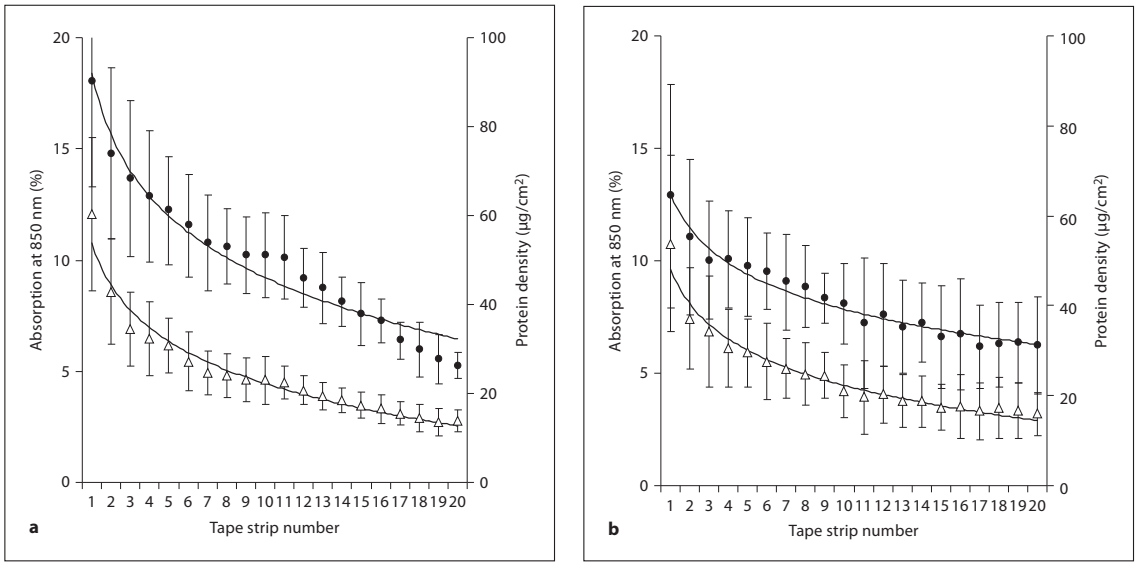

Fig. 8. Progression of the removed protein content as observed with Corneofix (**a**) and D-Squame (**b**) tapes during the tape stripping process on porcine ear skin. The presented values are the means of 12 independent experiments (means ± SD) during each of which 20 sequential tape strips were removed. The mean protein absorption at 850 nm (%; —●—) as well as the mean protein density (µg/cm²; – – Δ – –) were plotted against the respective tape strip number.

IR Densitometry: Influence of Different Tape Brands and Protein Coverage

The two investigated brands of adhesive film led to successive protein removal from the skin surface. The D-Squame tapes generally led to higher amounts of removed protein than the Corneofix tapes, despite the adapted working protocol. In addition, the protein removal process proceeded quite differently with increasing tape numbers according to the brand of adhesive film. The D-Squame tapes produced similarly high amounts of removed protein irrespective of the tape number. In contrast, the Corneofix tapes led to the removal of large amounts of protein especially on the first and second tape while subsequent tapes showed a consistent decrease in protein content. Similar observations have been reported in context with comparative studies using D-Squame and Tesafilm tapes [16].

The results of the different methods of analysis, namely the IR densitometric absorption values and protein content determined with the Micro BCA assay, are plotted against the respective tape strip number (fig. 8). The curves help visualize the change in protein content during the tape stripping procedure. Moreover, the correlation of the absorption and the protein content to the respective tape number illustrates the effect of potential disturbances. The units of the respective measurement quantities are given on the scales to the left and to the right. The curves show that both types of measured quantities, i.e. pseudo-absorption and actual protein content, correlate very well for Corneofix tapes (fig. 8a). In case of D-Squame, the high protein values on the first tape lead to slightly inconsistent results since the absorption values are comparatively low (fig. 8b).

Although the two methods deliver largely corresponding results in both cases, it becomes clear that the results obtained for the first tape strip may vary slightly, especially in the case of D-Squame. This might be ascribed to the discrepancy between the measurement area of the IR densitometer and the extracted tape strip area. While the IR densitometer assesses only around 45% of the tape strip area, the protein assay accounts for the whole area. Irregular protein coverage on the adhesive film outside the measurement area remains unnoticed during IR densitometry, but will influence the results of the protein assay. The potential discrepancies will increase with increasing protein content, as is occasionally

obtained with the first adhesive film of Corneofix, but more frequently with D-Squame tapes. This methodological issue might result in slightly inconsistent data and explains the outliers which bias the overall correlation of all samples. Even if the tape stripping procedure is conducted correctly, slight variability in protein coverage of the tapes cannot be entirely avoided when using porcine ear skin.

In addition, high protein coverage might cause an additional stack effect due to overlapping corneocyte aggregates, which might lead to erroneously low protein absorption values. The stack effect was described for UV/VIS spectroscopy [1, 5], but may affect other optical methods such as IR densitometry as well. If the density of corneocytes on the tapes is very high, cells may be piled upon each other and thus remain undetected. This leads to comparatively lower absorption values in relation to the actual protein content.

The described discrepancy between absorption and actual protein content was primarily observed for the first D-Squame tapes which possess higher adhesive power. This explains the slightly lower coefficient of determination of the original correlation obtained with D-Squame tapes. Similar observations of inhomogeneous protein coverage were reported for in vivo studies on human volunteers with D-Squame tapes [11]. The inhomogeneities were highest for the first tape strips, and decreased progressively with SC depth. It may be assumed that ideal homogeneity of the protein coverage may not be reached due to the inherent heterogeneity of SC properties, particularly for the loosely bound outer SC layers [11]. As is well known, the structure of the SC is not homogeneous in its entire thickness [2]. Likewise, it is a common experience during tape stripping that higher amounts of particles may be suddenly removed with an individual tape [1]. However, different studies indicate that accurate protein quantification is possible if both the skin material used and the working protocol are chosen with care [5, 14]. Inhomogeneous protein coverage of Tesafilm tapes occurred rarely for human skin in vivo and did not represent a significant source of error for protein quantification through UV/VIS spectroscopy [5]. It remains to be investigated whether the higher adhesive power of D-Squame tapes is indeed unfavorable in this context. In any case, attention should be paid to a consistent quality of the employed adhesive films. Unfavorable or prolonged storage conditions might impair the tackiness of the tapes and should thus be avoided.

In consideration of all discussed aspects, the obtained coefficients of determination show all the more that the correlation between pseudo-absorption and protein content of the tapes is actually of a remarkably robust nature.

Methodological Aspects Concerning the Micro BCA Protein Assay

Protein analysis with ready-to-use test kits is a practical and reliable method for evaluating the performance of a new analysis method such as IR densitometry. Important aspects that should not be neglected are the choice of the right assay that will deliver accurate results for the analyzed range of protein concentrations. In the present case, the Micro BCA assay was the method of choice since protein concentrations below 20 μg/ml were frequently observed. Since high protein values above 40 μg/ml will be determined with decreasing accuracy (fig. 1), such samples should either be diluted beforehand or excluded from the linear regression analysis. The alternative method of bisecting the respective tapes with a scalpel for separate analysis may be a source of error [11]. In addition, the first adhesive films frequently have to be discarded from the final evaluation due to comparatively larger inhomogeneities in protein coverage [19].

IR Densitometry: Differences between Human and Porcine Skin

The obtained correlations differed from those reported for human skin [15, 16]. A comparison of the calibration curves shows that the slope of the presented porcine correlations is less steep. This might be explained by two phenomena. Firstly, porcine skin might behave differently when subjected to radiation at 850 nm, leading to a different pattern in terms of light scattering, reflection and diffraction. Since protein absorption was previously reported to differ significantly between male and female human volunteers [30], it is not unlikely that porcine SC proteins exhibit a different pattern of pseudo-absorption as well. Differences between porcine and human keratin have been reported [31]. Secondly, porcine skin appears rather rough in comparison to human skin and behaves differently when subjected to the adhesive force of a tape strip. While human corneocytes are removed as a consistent layer of finely distributed protein aggregates, the porcine corneocytes are removed in large clusters or patches. On the one hand, this might lead to an increased occurrence of the stack effect [5, 14]. On the other hand, the pseudo-absorption of the proteins may be a different one for this specific pattern of protein removal.

Summarizing these findings, it can be concluded that the presented correlation curves are a useful prerequisite for rapid and efficient quantification of porcine SC proteins during in vitro tape stripping studies. The results indicate that tape strips with lower adhesive power are more suitable for IR densitometric analysis of porcine SC proteins. Although IR densitometry should be primarily employed for homogenous skin samples, it was shown that it is possible to obtain satisfyingly accurate results for porcine ear skin despite significant protein clustering. The pseudo-absorption measured by IR densitometry was found to be suitable for quantification of corneocyte aggregates on individual tapes.

Conclusion

It may be concluded that despite the obvious challenges that occur during tape stripping of porcine skin, reproducible and accurate results can be obtained if the tape stripping procedure is conducted correctly. IR densitometry as an optical method for protein quantification can be used to rapidly and efficiently determine the penetration profiles of applied substances without destroying the respective tapes. Further studies are being conducted to investigate the porcine ear model in tape stripping experiments in combination with IR densitometric protein analysis.

Acknowledgments

The authors would like to thank Rainer Voegeli, Chantal Rodgarkia-Dara and Arvid Staub for valuable discussion and technical support and Wolfgang Sipos for providing fresh porcine ears. We would also like to express our gratitude to Jürgen Lademann, Hans-Jürgen Weigmann and Sabine Schanzer for their cooperative introduction to the tape stripping method and for sharing their experience.

Disclosure Statement

The authors report no conflicts of interest. No external funding was received and the authors alone are responsible for the content and writing of the paper.

References

1 Weigmann HJ, Lademann J, Meffert H, Schaefer H, Sterry W: Determination of the horny layer profile by tape stripping in combination with optical spectroscopy in the visible range as a prerequisite to quantify percutaneous absorption. Skin Pharmacol Appl Skin Physiol 1999;12:34–45.
2 Bommannan I, Potts RO, Guy RH: Examination of stratum corneum barrier function in vivo by infrared spectroscopy. J Invest Dermatol 1996;95:403–408.
3 Kalia YN, Pirot F, Guy RH: Homogeneous transport in a heterogeneous membrane: water diffusion across human stratum corneum in vivo. Biophys J 1996;71:2692–2700.
4 Kalia YN, Alberti I, Sekkat N, Curdy C, Naik A, Guy RH: Normalization of stratum corneum barrier function and transepidermal water loss in vivo. Pharm Res 2000;17:1148–1150.
5 Weigmann HJ, Lindemann U, Antoniou C, Tsikrikas GN, Stratigos AI, Katsambas A, Sterry W, Lademann J: UV/VIS absorbance allows rapid, accurate, and reproducible mass determination of corneocytes removed by tape stripping. Skin Pharmacol Appl Skin Physiol 2003;16:217–227.
6 Marttin E, Neelissen-Subnel MT, De Haan FH, Bodde HE: A critical comparison of methods to quantify stratum corneum removed by tape stripping. Skin Pharmacol 1996;9:69–77.
7 Herkenne C, Naik A, Kalia YN, Hadgraft J, Guy RH: Pig ear skin ex vivo as a model for in vivo dermatopharmacokinetic studies in man. Pharm Res 2006;23:1850–1856.
8 Sekkat N, Kalia YN, Guy RH: Biophysical study of porcine ear skin in vitro and its comparison to human skin in vivo. J Pharm Sci 2002;91:2376–2381.
9 Lindemann U, Wilken K, Weigmann HJ, Schaefer H, Sterry W, Lademann J: Quantification of the horny layer using tape stripping and microscopic techniques. J Biomed Opt 2003;8:601–607.
10 Dreher F, Arens A, Hostynek JJ, Mudumba S, Ademola J, Maibach HI: Colorimetric method for quantifying human stratum corneum removed by adhesive-tape stripping. Acta Derm Venereol 1998;78:186–189.
11 Dreher F, Modjtahedi BS, Modjtahedi SP, Maibach HI: Quantification of stratum corneum removal by adhesive tape stripping by total protein assay in 96-well microplates. Skin Res Technol 2005;11:97–101.
12 Weigmann HJ, Jacobi U, Antoniou C, Tsikrikas GN, Wendel V, Rapp C, Gers-Barlag H, Sterry W, Lademann J: Determination of penetration profiles of topically applied substances by means of tape stripping and optical spectroscopy: UV filter substance in sunscreens. J Biomed Opt 2005;10:14009.
13 Weigmann HJ, Schanzer S, Patzelt A, Bahaban V, Durat F, Sterry W, Lademann J: Comparison of human and porcine skin for characterization of sunscreens. J Biomed Opt 2009;14:24–27.
14 Lademann J, Jacobi U, Surber C, Weigmann HJ, Fluhr JW: The tape stripping procedure – evaluation of some critical parameters. Eur J Pharm Biopharm 2009;72:317–323.
15 Voegeli R, Heiland J, Doppler S, Rawlings AV, Schreier T: Efficient and simple quantification of stratum corneum proteins on tape strippings by infrared densitometry. Skin Res Technol 2007;13:242–251.
16 Hahn T, Hansen S, Neumann D, Kostka KH, Lehr CM, Muys L, Schaefer UF: Infrared densitometry: a fast and non-destructive method for exact stratum corneum depth calculation for in vitro tape-stripping. Skin Pharmacol Physiol 2010;23:183–192.
17 Sekkat N, Guy RH: Biological models to study skin permation; in Testa B, Van de Waterbeemd H, Folkers G, Guy RH (eds): Pharmacokinetic Optimization in Drug Research. Zuerich, Wiley-VCH and VHCA, 2001, pp 155–172.
18 Tiemessen H: Percutaneous absorption: Animal skin models versus in vitro models using human skin; in Gurny R, Teubner A (eds): Dermal and Transdermal Drug Delivery. Stuttgart, Wissenschaftliche, 1993, pp 101–117.

19 Breternitz M, Flach M, Prassler J, Elsner P, Fluhr JW: Acute barrier disruption by adhesive tapes is influenced by pressure, time and anatomical location: integrity and cohesion assessed by sequential tape stripping. A randomized, controlled study. Br J Dermatol 2007;156:231–240.
20 Jacobi U, Kaiser M, Toll R, Mangelsdorf S, Audring H, Otberg N, Sterry W, Lademann J: Porcine ear skin: an in vitro model for human skin. Skin Res Technol 2007;13:19–24.
21 Wagner H, Kostka KH, Lehr CM, Schaefer UF: Drug distribution in human skin using two different in vitro test systems: comparison with in vivo data. Pharm Res 2000;17:1475–1481.
22 Dickel H, Goulioumis A, Gambichler T, Fluhr JW, Kamphowe J, Altmeyer P, Kuss O: Standardized tape stripping: a practical and reproducible protocol to uniformly reduce the stratum corneum. Skin Pharmacol Physiol 2010;23:259–265.
23 Loeffler H, Dreher F, Maibach HI: Stratum corneum adhesive tape stripping: influence of anatomical site, application pressure, duration and removal. Br J Dermatol 2004;151:746–752.
24 Alberti I, Kalia YN, Naik A, Bonny JD, Guy RH: In vivo assessment of enhanced topical delivery of terbinafine to human stratum corneum. J Control Release 2001;71:319–327.
25 Carrer DC, Vermehren C, Bagatolli LA: Pig skin structure and transdermal delivery of liposomes: a two photon microscopy study. J Control Release 2008;132:12–20.
26 Meyer W, Zschemisch NH: Skin layer thickness at the ear of the domesticated pig, with special reference to the use of the ear integument for human dermatological research. Berl Muench Tierarztl Wochenschr 2002;115:401–406.
27 García Ortiz P, Hansen SH, Shah VP, Sonne J, Benfeldt E: Are marketed topical metronidazole creams bioequivalent? Evaluation by in vivo microdialysis sampling and tape stripping methodology. Skin Pharmacol Physiol 2011;24:44–53.
28 Singh S, Zhao K, Singh J: In vitro permeability and binding of hydrocarbons in pig ear and human abdominal skin. Drug Chem Toxicol 2002;25:83–92.
29 Godin B, Touitou E: Transdermal skin delivery: predictions for humans from in vivo, ex vivo and animal models. Adv Drug Deliv Rev 2007;59:1152–1161.
30 Jacobi U, Gautier J, Sterry W, Lademann J: Gender-related differences in the physiology of the stratum corneum. Dermatology 2005;211:312–317.
31 Bouwstra JA, Gooris GS, Bras W, Downing DT: Lipid organization in pig stratum corneum. J Lipid Res 1995;36:685–695.

Pharmaceutics **2011**, *3*, 275-306; doi:10.3390/pharmaceutics3020275

OPEN ACCESS

pharmaceutics

ISSN 1999-4923

www.mdpi.com/journal/pharmaceutics

Article

Semi-solid Sucrose Stearate-Based Emulsions as Dermal Drug Delivery Systems

Victoria Klang [1], Julia C. Schwarz [2], Nadejda Matsko [3], Elham Rezvani [4], Nivine El-Hagin [1], Michael Wirth [1] and Claudia Valenta [1,2,*]

[1] Department of Pharmaceutical Technology and Biopharmaceutics, Faculty of Life Sciences, University of Vienna, Althanstraße 14, 1090 Vienna, Austria; E-Mail: victoria.klang@univie.ac.at (V.K.)

[2] Research Platform "Characterisation of Drug Delivery Systems on Skin and Investigation of Involved Mechanisms", University of Vienna, 1090 Vienna, Austria; E-Mail: julia.schwarz@univie.ac.at

[3] Institute for Electron Microscopy and Fine Structure Research, Graz University of Technology and Centre for Electron Microscopy Graz, 8010 Graz, Austria; E-Mail: nadejda.matsko@felmi-zfe.at

[4] Department of Food Sciences and Technology, BOKU-University of Natural Resources and Applied Life Sciences Vienna, 1190 Vienna, Austria; E-Mail: elham.rezvani@boku.ac.at

* Author to whom correspondence should be addressed: E-Mail: Claudia.valenta@univie.ac.at; Tel.: +43 1 4277 55 410; Fax: +43 1 4277 9554.

Received: 7 April 2011; in revised form: 20 May 2011 / Accepted: 30 May 2011 / Published: 30 May 2011

Abstract: Mild non-ionic sucrose ester surfactants can be employed to produce lipid-based drug delivery systems for dermal application. Moreover, sucrose esters of intermediate lipophilicity such as sucrose stearate S-970 possess a peculiar rheological behavior which can be employed to create highly viscous semi-solid formulations without any further additives. Interestingly, it was possible to develop both viscous macroemulsions and fluid nanoemulsions with the same chemical composition merely by slight alteration of the production process. Optical light microscopy and cryo transmission electron microscopy (TEM) revealed that the sucrose ester led to the formation of an astonishing hydrophilic network at a concentration of only 5% w/w in the macroemulsion system. A small number of more finely structured aggregates composed of surplus surfactant were likewise detected in the nanoemulsions. These discoveries offer interesting possibilities to adapt the low

Pharmaceutics **2011**, *3* **276**

viscosity of fluid O/W nanoemulsions for a more convenient application. Moreover, a simple and rapid production method for skin-friendly creamy O/W emulsions with excellent visual long-term stability is presented. It could be shown by franz-cell diffusion studies and *in vitro* tape stripping that the microviscosity within the semi-solid formulations was apparently not influenced by their increased macroviscosity: the release of three model drugs was not impaired by the complex network-like internal structure of the macroemulsions. These results indicate that the developed semi-solid emulsions with advantageous application properties are highly suitable for the unhindered delivery of lipophilic drugs despite their comparatively large particle size and high viscosity.

Keywords: sucrose stearate S-970; O/W emulsion; semi-solid; nanoemulsion; particle size; skin penetration

1. Introduction

Sucrose fatty acid esters have been known as additives in the fields of nutrition, cosmetics and pharmacy for a long time [1-4]. However, it is only recently that their potential as mild non-ionic surfactants in the production of topical lipid-based drug delivery systems has been investigated more thoroughly. Different sucrose esters of various HLB values have been investigated for their potential to form O/W nanoemulsions [5-7] and to increase [8-10] or retard [11] the skin permeation of incorporated drugs. We have recently demonstrated the superiority of sucrose stearate S-970 over a comparable lecithin mixture to produce highly stable and homogeneous O/W nanoemulsions for dermal application [7]. In this context we found that the employed emulsifier sucrose stearate S-970 exhibited a peculiar rheological behavior when processed in a specific way. The astonishing gel-forming ability of sucrose stearate mixtures of intermediate hydrophilic/lipophilic balance (HLB value) around 9 to 11 has been reported in earlier literature [12,13] as well as recently [11,14,15]. However, no attempt has been made so far to design semi-solid multiphase vehicles which are stabilized in this fashion and can be used for incorporation of lipophilic drugs. The properties of a sucrose stearate/water dispersion were recently investigated [15], but no approach to incorporate additional excipients has been reported. However, incorporation of oil or model drugs may have a significant effect on the gelling properties of the sucrose ester and thus the microstructure of the resulting vehicles. Likewise, the drug release properties of such viscous sucrose ester-stabilized formulations have not been explored yet. Since these aspects are of great practical interest for the development of new formulations, the present work addresses these points.

A simple and skin-friendly sucrose stearate-based O/W emulsion was developed. Optical light microscopy, cryo transmission electron microscopy, rheological investigations and laser diffractometry were employed to characterize the microstructure of the novel system. Three lipophilic model drugs were incorporated and the effect of formulation microstructure and viscosity on the release profile of the system was investigated *in vitro* using franz-type diffusion cells and tape stripping experiments on porcine ears. Since a large particle size and high viscosity of a topically applied formulation are

frequently associated with decreased or sustained drug release, we decided to compare the novel systems to corresponding O/W nanoemulsions. Through a slight alteration of the production process and subsequent high-pressure homogenization it was possible to develop fluid O/W nanoemulsions of the exact same composition as the novel macroemulsions and the same content of sucrose stearate, namely 5% (w/w). Microscopic and rheological investigations were performed on these systems as well. Dynamic light scattering and laser Doppler electrophoresis were employed to further characterize the nanoemulsions.

Overall, the aim of the present study was to explore the astonishing gel-forming properties of sucrose stearate S-970 in colloidal multiphase drug delivery systems and to characterize the nature of the resulting semi-solid vehicles. In addition, the drug release profile of these novel O/W emulsions was evaluated by comparing them to fluid nano-sized emulsions of identical chemical composition.

2. Experimental Section

2.1. Materials

Sucrose stearate (Ryoto Sugar Ester® S-970) was supplied by Mitsubishi-Kagaku Food Corporation (Tokyo, Japan). PCL-liquid (cetearyl ethylhexanoate, isopropyl myristate) was purchased from Dr.Temt Laboratories (Vienna, Austria). The preserving agent potassium sorbate was obtained from Herba Chemosan Apotheker-AG (Vienna, Austria). Flufenamic acid (CAS: 530-78-9, Batch No. 1619) and diclofenac acid (CAS: 15307-86-5, Batch No. 080304) were obtained from Kemprotec Limited (Middlesbrough, UK). Curcumin (CAS: 458-37-7, Batch No. 079K1756) was purchased from Sigma Aldrich (St. Louis, USA). Standard Corneofix® adhesive films with a square area of 4.0 cm² were obtained from Courage + Khazaka GmbH (Cologne, Germany). All further chemicals used were of analytical reagent grade and used without further purification.

2.2. Formulations

Different concentrations of 1 to 5% w/w sucrose stearate S-970 were tested for their emulsifying potential in O/W emulsions. An increase in viscosity in dependence of the preparation method had been noticed especially for 5% w/w of sucrose stearate. At surfactant concentrations above 5% w/w, highly viscous creamy emulsions had been obtained irrespective of the preparation method, *i.e.* the emulsion microstructure had been too viscous to pass it through a high-pressure homogenizer even if heated. Therefore, an amount of 5% w/w of sucrose stearate was chosen for the final formulations.

The produced viscous macroscopic emulsions and the corresponding fluid nanoemulsions were identical in their composition, which is given in Table 1.

The preparation of a separate water and oil phase was the same in both cases. The aqueous phase, consisting of freshly distilled water and potassium sorbate, as well as the oil phase, consisting of the cosmetic oil PCL-liquid, were respectively stirred at 50 °C. Blank and drug-loaded formulations were prepared. The lipophilic model drugs flufenamic acid, diclofenac acid and curcumin were respectively dissolved in the oil phase at a concentration of 0.5% (w/w).

Table 1. Basic composition of macroemulsions (E) and nanoemulsions (NE).

Excipients	Emulsion composition (% w/w) E = NE
PCL-liquid	20
Sucrose stearate S-970	5.0
Potassium sorbate	0.1
Model drug	0.5
Distilled water to	100

In case of the macroemulsions, sucrose stearate S-970 was dissolved in the oil phase. A highly viscous macroemulsion was obtained upon slow admixture of the aqueous phase, further stirring for 10 minutes and subsequent treatment with an ultra-turrax (Omni 500, 2500 rpm, 4 minutes). Refrigerated storage appeared to favor the observed gelling effect.

In case of the nanoemulsions, sucrose stearate S-970 was dissolved in the aqueous phase in order to maintain low viscosity of the system. The oil phase was subsequently added slowly to the aqueous phase for the same reason. The mixture was stirred for further 10 minutes, then pre-homogenized with an ultra-turrax (Omni 500, 2,500 rpm, 4 minutes). The mixture was stirred and heated to 50 °C before homogenization with a high-pressure homogeniser (EmulsiFlex C3, Avestin) for 16 homogenization cycles at 750 bars. Process parameters such as homogenization pressure and homogenization time had been optimized during previous studies [7]. Care was taken to process the mixture under mildly pre-heated conditions to avoid any sudden cooling and associated gelling within the device.

2.3. Emulsion Characterization

2.3.1. Visual characterization

Both macroemulsions and nanoemulsions were investigated for the presence of structures visible to the eye as well as for their texture and skin feeling.

2.3.2. Particle size

The macroemulsions were investigated for their particle size and particle size distribution by laser diffractometry (laser diffraction, static laser light scattering). Measurements were performed in triplicate on a Mastersizer 2000 (Malvern, UK). The instrument was operated with the HydroS 2000 sample dispersion unit (Malvern, UK) and software version 5.60 at 25 °C. The samples were diluted with distilled water (1:1000 v/v) and stirred slightly prior to analysis. All samples were analyzed in triplicate (n = 3). No sonification of the samples was performed prior or during the measurements to avoid the destruction of possible aggregates which may provide information about the microstructure as well as destabilization phenomena [16,17]. Laser diffraction measurements yield volume-weighted diameters as results for droplet sizes up to 2000 µm [16]. The parameters obtained in the present experiments were the d(v, 0.1), d(v, 0.5) and d(v, 0.9). Likewise, the volume weighted mean D [4,3] and the surface weighted mean D [3,2] were obtained. The d(v, 0.5) or volume median diameter marks the size where 50% of the distribution is above and 50% is below this value. The d(v, 0.1) represents

the point where 10% of the volume distribution is below this value. In analogy, the d(v, 0.9) marks the point where 90% of the volume distribution is below this value. The d(v, 0.9) can be employed to quantify larger droplets which might be present in the sample such as aggregates formed due to internal processes or destabilization [16]. The volume weighted mean or volume mean diameter D [4,3] corresponds to the mean diameter of spheres with the same volume as the analyzed droplets and is calculated by $d_{4,3} = \sum n_i d_i^4 / \sum n_i d_i^3$, where n_i is the number of particles with diameter d_i [17]. In analogy, the surface weighted mean D [3,2] represents the mean diameter of the spheres with the same surface area as the analyzed droplets. In addition, the span was automatically calculated for all samples. This dimensionless number represents the width of the droplet size distribution based on the 10%, 50% and 90% quantile. A wide particle size distribution will yield a comparatively large span. All parameters were calculated automatically using the Mie theory with a refractive index of 1.52 and a particle absorption value of 0.1. Measurements were conducted immediately after production and after six months of storage time.

The nanoemulsions were investigated for their particle size and particle size distribution by dynamic light scattering (DLS, photon correlation spectroscopy) using a Zetasizer Nano ZS (Malvern, UK) at 25 °C. Samples were diluted with freshly distilled water 1:100 (v/v) to diminish opalescence. The obtained parameters were the hydrodynamic diameter expressed as z-average value of the samples as well as the polydispersity index (PDI). The z-average value is an intensity weighted mean diameter of the bulk population of the sample while the PDI represents the particle size distribution within the formulations. PDI values below 0.2 indicate a narrow size distribution and thus good long-term stability [18]. The approximate measuring range of this instrument is from 3 nm to 3 µm [19]. All samples were analyzed in triplicate (n = 3). Each individual result was automatically calculated as the average of 3 measurements with 20 sub-measurements each. The particle size and PDI of the nanoemulsions were measured immediately after preparation and in regular intervals over a period of six months. In order to detect the presence of potential larger droplets or aggregates, both optical light microscopy and cryo TEM were employed.

2.3.3. Particle surface charge (zeta potential)

The particle surface charge of the nanoemulsions was determined by laser Doppler electrophoresis using a Zetasizer Nano ZS (Malvern, UK). The electrophoretic mobility of the droplets was determined and automatically converted into the zeta potential using the Helmholtz-Smoluchowski equation by the Malvern data analysis software [16]. Zeta potential (ZP) values of the formulations were determined at 25 °C. Samples were diluted with distilled water (1:100 v/v) containing sodium chloride (0.01 mmol) in order to ensure constant conductivity below 0.05 ms/cm and thus reproducible measurement conditions [16,18,20]. The ZP roughly characterizes the surface charge of the emulsion droplets in solution. High absolute values above 30 mV lead to repulsive forces between the droplets which may improve the physical stability of multiphase systems [20]. Absolute ZP values above 60 mV indicate excellent electrochemical stability [16]. Zeta potential values were determined in triplicate for all nanoemulsions (n = 3) after production and in regular intervals over six months.

2.3.4. Physical stability

The physical stability of both macroemulsions and nanoemulsions was compared by determination of the particle size after an observation period of six months. All formulations were stored at 4 °C. A visual control was regularly performed to detect any signs of instability. In case of the nanoemulsions, additional control measurements were performed in regular intervals over the whole observation period as well.

2.3.5. Drug content, chemical stability and pH value

The drug content of all formulations was analyzed immediately after preparation to ensure appropriate drug incorporation. Briefly, 10 mg of the emulsion were dissolved in 1 mL of methanol, centrifuged for 6 minutes at 12,000 rpm (Hermle Z323K, MIDSCI, USA) and analyzed by HPLC or UV/Vis spectroscopy. Samples were taken at least in triplicate ($n \geq 3$). In case of flufenamic acid and diclofenac acid, further samples were taken in regular intervals over three months to obtain a rough overview about the chemical stability of the acidic drugs and their homogeneous dispersion within the systems. Since curcumin is known to undergo a variety of degradation processes which would require more specific methods of analysis, no attempt was made to cover this aspect in the scope of the present work. The obtained data should merely ensure the use of representative and intact formulations for all further studies.

The pH value of the formulations was determined using a pH meter (Orion 420A, Bartelt, Austria). The pH of all formulations was determined at room temperature (25 °C) in regular intervals to detect destabilization phenomena induced by chemical degradation through hydrolysis or oxidation, which result in a decrease of pH [21].

2.3.6. Optical light microscopy

Optical light microscopy was employed to obtain an overview about the presence of structures within the micrometer size range, which was especially interesting in the case of the macroemulsion morphology. In case of nanoemulsions, optical light microscopy served as a quality control to ensure the absence of larger structures. The microscopic analysis was carried out using a photo microscope (Zeiss Axio Observer.Z1 microscopy system, Carl Zeiss, Oberkochen, Germany) equipped with phase contrast and differential interference contrast (DIC) and using LD Plan-Neofluar objectives. A small amount of fresh or stored sample of the macroemulsions and nanoemulsions was respectively placed on an object slide, covered and analyzed immediately. Images were taken in conventional bright field mode, with phase contrast and with DIC while 5, 10, 20 and 40-fold magnifications were employed for all samples.

2.3.7. Transmission electron microscopy (TEM): Cryo TEM and negative staining for conventional TEM

The structure of blank macroemulsions and nanoemulsions containing 5% (w/w) sucrose stearate was visualized using cryo TEM. To this end, several vitrified specimens were prepared for each

formulation type. In case of the macroemulsion, a fresh glow-discharge copper grid covered with a perforated carbon film was placed on the sample, polished by filter paper in order to remove excess material and immediately plunged into liquid ethane. The macroemulsion samples were observed in an undiluted state so as not to destroy the internal structure. In case of the nanoemulsion, the sample was dissolved in distilled water (1:10 v/v). Subsequently, a 4 µm drop of the solution was placed on a fresh glow-discharge TEM copper grid covered with a perforated carbon film (Pelco International) and blotted with a filter paper to form a thin liquid film of the sample (thickness of 100–250 nm). The thinned sample was plunged into liquid ethane at its freezing temperature (−183 °C) to form a vitrified specimen, and was then transferred to liquid nitrogen (−196 °C) for storage until examination. Vitrified specimens were examined in a Philips T12 transmission electron microscope (Philips) operating at an accelerating voltage of 120 kV using an Oxford CT3500 (Oxford Instruments) cryo holder that maintained the vitrified specimens at −160 °C during sample observation. Images were recorded digitally on a cooled Gatan BioScan CCD camera (Gatan) using the DigitalMicrograph 3.4 software (Gatan) in low-dose imaging mode to minimize beam exposure and electron beam radiation damage.

In addition, conventional TEM analysis was performed for both samples after negative staining with uranyl acetate as previously described [22]. To this end, a carbon coated mesh was hydrophilized by glow discharge and a drop of the respective undiluted emulsion was deposited on the mesh. An aqueous solution of 1% (v/v) of the negative staining agent uranyl acetate was subsequently applied on the mesh to facilitate observation.

2.3.8. Rheological characterization

The rheological properties of both macroemulsions and nanoemulsions were investigated. All experiments were performed on a Bohlin CVO Rheometer (Malvern Instruments, UK) with a thermostatic control system (Bohlin KTB30, Malvern, UK). The employed rheometer tools were a thermostatically controlled cone and plate tool with 40 mm in diameter and a 4° angle (CP 4°/40 mm) for the macroemulsions and a coaxial cylinder system with 25 mm in diameter (cup and bob C25) for the nanoemulsions. The temperature for both tools was maintained at 25 ± 0.5 °C throughout all experiments. The applied amount of sample was around 2 g for macroemulsions and around 15 g for nanoemulsions. Both blank and drug-loaded formulations were investigated. All measurements were performed at least in triplicate ($n \geq 3$). Values given in figures and tables are the average values.

Flow curves were established for all systems. The flow properties of both blank and drug-loaded macroemulsions and nanoemulsions were investigated by measuring the dynamic viscosity η (in Pa·s) under shear stress. Rheological experiments in a controlled-rate mode were performed. A controlled shear rate γ was employed at a constant temperature of 25 ± 0.5 °C to determine the viscosity of the samples as a function of the shear rate ranging from 0.1 s^{-1} to 100 s^{-1}. The obtained flow curves of both macroemulsions and nanoemulsions were compared to the power law model (Ostwald model) defined as $\eta = m\,\gamma^{(n-1)}$ where η represents the shear viscosity, m equals the consistency coefficient, γ represents the shear rate and n is the flow behavior index. Values of $n = 1$ are indicative for Newtonian fluids while values of $n < 1$ are representative for shear-thinning, *i.e.* pseudoplastic fluids. Values of $n > 1$ are found for shear-thickening dilatant fluids [23,24].

Moreover, oscillatory shear experiments were performed for all systems. In the oscillatory mode, a sinusoidal stress is applied to the sample and the response in form of the induced strain is measured [25,26]. To this end, the rheometer tool is moved forward and backward in a defined sinusoidal motion. After identification of the linear viscoelastic region the samples were investigated over a frequency of 1–10 Hz. Crucial parameters were determined as a function of the oscillatory frequency (*v*, in Hz). The parameters obtained in this fashion are the elastic modulus G', the viscous modulus G'', the complex modulus G* and the dynamic viscosity η'.

The elastic modulus or storage modulus G' is defined as G' = G* cos (δ) and describes the recoverable energy that is stored within an elastic system. The viscous modulus or loss modulus G´´ is calculated by G´´ = G* sin (δ) and represents the energy that is dissipated in the viscous flow and transformed into heat. These moduli represent the real and imaginary parts of the complex dynamic shear modulus G* [25-27]. The dynamic viscosity η' is defined as $\eta' = G''/\omega$, where ω is the angular velocity of the oscillatory stress which is in turn related to the oscillatory frequency by the relationship $\omega=2\pi v$. The related phase angle is expressed as δ [25,26].

2.4. Skin permeation experiments using franz-type diffusion cells

In vitro skin permeation studies were performed using standard franz-type diffusion cells (Permegear, USA). Thus, the potential influence of the different formulation properties of macroemulsions and nanoemulsions on the skin permeation of the three model drugs flufenamic acid, diclofenac acid and curcumin was investigated. Porcine abdominal skin was chosen as model membrane because of its morphology and permeability, which are similar to those of human skin [9,28]. The porcine abdominal skin was freed from hair and treated with a dermatome (GB 228R, Aesculap) set at 1.2 mm. The skin was stored at −20 °C until use and thawed prior to the experiments. Appropriate skin patches were clamped between the donor and the receptor chamber of the diffusion cells having a permeation area of 1.13 cm^2. The receptor compartment was filled with 2 mL of phosphate buffer (pH 7.4, 0.012M) in case of flufenamic acid and diclofenac acid [29]. In case of curcumin, a mixture of distilled water/ethanol (50/50 % v/v) was employed to ensure sink conditions [30,31]. The diffusion cells were kept at skin surface temperature (32 °C) and stirred with magnetic bars for 24 hours. The formulation (0.6 g) was placed on the excised skin in the donor chamber. Samples of 200 µL were removed at defined time intervals for analysis and were replaced by fresh receptor medium. At least five parallel experiments were performed for each formulation ($n \geq 5$). The samples were analyzed for their drug content by HPLC in case of flufenamic acid and diclofenac acid or by UV/Vis spectroscopy in case of curcumin. Permeation profiles of the drugs were constructed by plotting time (hours) against the cumulative amount of the drug (µg/cm²) as measured in the receptor solution. In addition, the steady state flux (J, $\mu g \cdot cm^{-2} \cdot h^{-1}$) was calculated by linear regression after the respective lag-times.

2.5. Skin penetration experiments via in vitro tape stripping

In order to obtain penetration profiles of the three model drugs from both macroemulsions and corresponding nanoemulsions at least six individual tape-stripping experiments were performed for

each formulation ($n \geq 6$) on porcine ear skin. Fresh porcine ears were donated by the Clinic for Swine, University of Veterinary Medicine, Vienna. Since previous studies had shown that frozen storage does not alter the skin barrier function or the stratum corneum properties in the context of tape stripping experiments [32,33], the ears were stored at −24 °C and thawed prior to the respective experiments. After defrosting, the ears were cleaned carefully with purified water and blotted dry with soft tissue. The skin was subsequently freed from hair with scissors and intact, representative skin areas were indicated with a permanent marker. In addition, the transepidermal water loss (TEWL) of the skin was determined using the closed-chamber device AquaFlux® (Biox Ltd., London, UK) to confirm an intact skin barrier function and to monitor the defrosting process [33]. The software program AquaFlux® V6.2 was used for analysis of these data. When the TEWL reached values between 15 and 20 g m^{-2} h^{-1} the experiment was started. To this end, the porcine ears were stretched out on styrofoam plates and fixed with needles if necessary. The respective formulation was applied onto the marked skin area at a concentration of 6 mg·cm^{-2} with a saturated vinyl glove finger and was gently distributed and massaged for 30 seconds. After a penetration time of 1 hour the tape stripping procedure was started.

The adhesive films employed to remove the superficial stratum corneum layers were standard Corneofix® tapes. Care was taken to ensure a reproducible working procedure. After placing the first adhesive film on the skin its outline was indicated with a permanent marker to ensure subsequent tape stripping on the exact same location. Pressure was applied with the thumb covered in a vinyl glove as previously reported [34] to ensure a rolling movement and thus minimize the influence of wrinkles [35]. The experiment was performed on a balance to ensure a constant pressure of 49 N (5 kg) which is a prerequisite for the removal of reproducible amounts of stratum corneum proteins [33]. After applying pressure for 3 seconds, the tape was removed in a single rapid movement. In this fashion, 20 sequential adhesive films were removed per experiment. The amount of adherent corneocytes was subsequently determined by IR-densitometry using the infrared densitometer SquameScan™ 850A (Heiland electronic GmbH, Wetzlar, Germany) [36]. Briefly, the optical pseudo-absorption of the adhesive films at a wavelength of 850 nm is employed to quantify the amount of stratum corneum proteins on the tapes. The absorption values in % can be read from the display and the corresponding mass of proteins can be determined using the correlation factor of 0.41 which was previously established for analysis of porcine ear skin [33]. This value can be employed to calculate the mass of SC proteins (*m*) after determination of their pseudo-absorption at 850 nm (*A*) for a normalized tape area of 1 cm^2 by employing the equation $m = A / 0.41$ (in µg·cm^{-2}).

The mean cumulative amount of removed stratum corneum proteins was employed to establish the penetration depth of the applied drugs in relation to the complete stratum corneum thickness. The latter was determined by continuous stripping of the complete stratum corneum in four of the experiments ($n = 4$) until the detection limit of the IR-densitometer was reached.

2.6. HPLC analysis

The formulations or samples containing flufenamic acid or diclofenac acid were analyzed for their drug content by HPLC (Series ISS-200, Perkin Elmer, USA), consisting of an auto sampler, a lc pump and an UV-diode array detector (235C). Previously reported methods were used using a Nucleosil 100-5 C18 column (250 mm × 4 mm, Macherey-Nagel, USA) plus a Nucleosil 100-5 C18 pre-column

(CC8/4, 40 mm × 4 mm, Macherey-Nagel, USA). For all analyses, the oven temperature was set at 50 °C and the injection volume was 20 µL. The analysis of the data was performed using the TotalChrom Navigator 6.2.0 software. Standard solutions of the drugs were prepared and calibration curves were calculated by plotting the analyzed drug concentrations against the obtained peak area values.

The quantification of flufenamic acid and diclofenac acid was conducted according to previously described methods [29,37]. For both drugs, the mobile phase consisted of methanol/water (75/25 w/w); glacial acetic acid was added until a pH value of 3.2 was reached. The flow rate was 1.0 mL/min in both cases. For flufenamic acid, the detection wavelength was set at 245 nm with a retention time of 4.5 minutes. A calibration curve was calculated based on peak area measurements of diluted standard solutions ranging from 0.09 µg/mL to 110.50 µg/mL with a coefficient of determination $R^2 = 0.9999$. The limit of detection for flufenamic acid was found to be around 0.04 µg/mL; the limit of reasonable quantification was set at 0.09 µg/mL. For diclofenac acid, the detection wavelength was set at 280 nm with a retention time of 10 minutes. The measurement range of the diluted standard solutions employed for the calibration curve was between 0.06 µg/mL and 28.97 µg/mL with $R^2 = 1$. The limit of detection for diclofenac acid was, likewise, around 0.04 µg/mL; the limit of quantification was set at 0.06 µg/mL.

2.7. UV/VIS spectroscopic analysis

The quantification of curcumin was performed as previously reported [30] using a double beam UV/Vis spectrophotometer (Spectrophotometer U-3010, Hitachi, Japan). A correlation curve was established for standard solutions of curcumin in pure ethanol (96% v/v) ranging from 0.31 µg/mL to 5.01 µg/mL with $R^2 = 0.9952$. The curcumin content of the samples filled into quartz cuvettes was determined at 425 nm. Samples containing a higher curcumin content were diluted prior to the analysis until values within the linear range of the calibration curve were obtained. This was frequently the case for samples extracted from the first two adhesive films of the tape stripping experiments.

2.8. Statistical data analysis

Results are expressed as means of at least three experiments ± SD. Statistical data analyses were performed with the software program GraphPadPrism3. Parametric data were analyzed using the Student's t-test with $P < 0.05$ as minimum level of significance while non-parametric data were analyzed using the Mann-Whitney test or the Wilcoxon signed rank test with $P < 0.05$, respectively.

3. Results and Discussion

3.1. Formulations and production aspects

The optimal surfactant concentration to produce both highly viscous macroemulsions and fluid nanoemulsions was found to be 5% w/w. Despite the increasing viscosity, considerate sample preparation still allowed for high-pressure homogenization of the mixture in case of the nanoemulsions. Thus, the physicochemical properties of emulsions stabilized by 5% w/w of sucrose stearate could be varied by modification of the production process.

As anticipated, conductivity measurements confirmed the nature of the obtained emulsions as being of the O/W type. The temperature seemed to play a crucial role during processing of the sucrose stearate-based emulsions. If the fluid mixture was kept at 40–50 °C, further homogenization was feasible. If the mixture was cooled, some sort of gelling effect took hold and transformed the system into a semi-solid emulsion. This was especially pronounced if the mixture was cooled down rapidly. Similar behavior has been reported for aqueous sucrose stearate dispersions [15]. Moreover, the different ways of emulsion preparation as described in the literature [22] may have had an additional influence on the properties of the resulting mixture and thus either allowed for further high-energy processing or not. The variation in the mixing protocol of the compounds apparently influenced the viscosity of the pre-emulsion, which plays an important role for later processing [19].

3.2. Visual characterization

Creamy, thick macroemulsions were produced by dissolving the sucrose ester in the oil phase. The low density of the emulsions suggested that large amounts of air were incorporated to provide a fluffy appearance. All formulations had an appealing, homogeneous appearance which was retained over the whole observation period.

In contrast, fluid if slightly gel-like nanoemulsions were produced by dissolving the surfactant in the aqueous phase and subsequent high-pressure homogenization. Figure 1 shows the visual appearance of the viscous macroscopic emulsions in contrast to the fluid nanoemulsions. Upon closer inspection, small white aggregates could be detected in the otherwise homogeneous whitish to bluish nanoemulsions. These were most likely composed of surfactant aggregates formed during or after high-pressure homogenization and can be ascribed to the comparatively high surfactant concentration as opposed to our previous studies [7]. These structures did however not impair the performance or physical stability of the formulations in any way. Upon cooled storage at 4 °C, they appeared to contribute to the increasingly gel-like texture of the nanoemulsions. Indeed, low storages temperatures have previously been reported to cause gelation of nanoemulsions of certain compositions [38].

Figure 1. Visual appearance of a sucrose stearate-based macroemulsion (E) and a corresponding nanoemulsion (NE). Age of the presented formulations: 9 months.

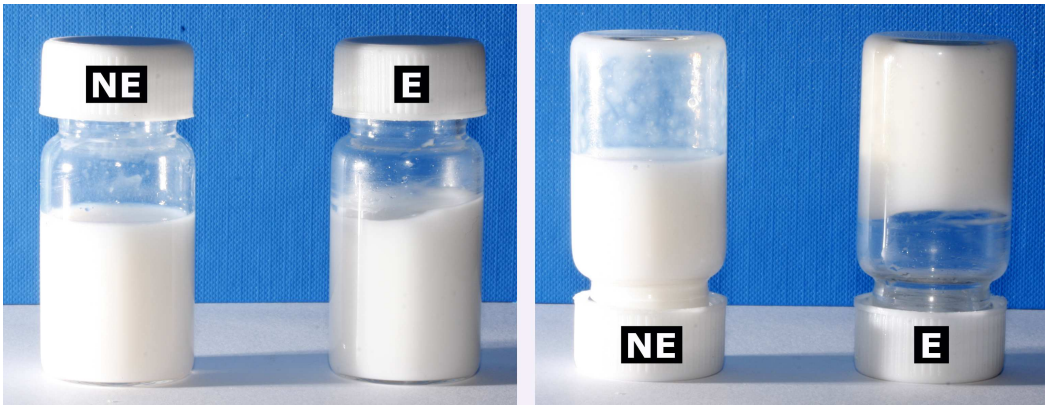

3.3. Particle size

In case of the macroemulsions, the mean particle sizes were in the micrometer range as shown in Table 2A and 2B.

Table 2. Physicochemical properties of fresh **(2A)** and stored **(2B)** blank and drug-loaded macroemulsions (E) after high-shear dispersion with an ultra-turrax. Measurements were performed in triplicate on a Mastersizer 2000 (Malvern, UK) at 25 °C. The samples were diluted with distilled water (1:1000 v/v) and stirred slightly prior to analysis. The parameters shown are the mean particle size expressed as volume weighted mean D [4,3], surface weighted mean D [3,2] and volume median diameter d(0.5) as well as the d(0.1) and d(0.9) values and the span. All values represent the mean of three formulations (n = 3) in µm and are given ± SD.

(2A) Freshly prepared samples				
Parameters	E blank	E curc	E fluf	E diclo
D [4,3]	06.94 ± 0.97	09.72 ± 1.92	08.56 ± 0.05	11.80 ± 0.42
D [3,2]	03.70 ± 0.15	04.14 ± 0.04	04.46 ± 0.02	05.43 ± 0.36
d (v, 0.1)	01.74 ± 0.04	01.73 ± 0.01	01.72 ± 0.01	02.04 ± 0.16
d (v, 0.5)	05.16 ± 0.26	06.80 ± 0.07	08.26 ± 0.04	11.29 ± 0.45
d (v, 0.9)	12.58 ± 2.25	14.55 ± 0.41	15.44 ± 0.09	22.09 ± 0.42
Span	02.09 ± 0.31	01.89 ± 0.04	01.66 ± 0.01	01.78 ± 0.05
(2B) After 6 months of storage				
Parameters	E blank	E curc	E fluf	E diclo
D [4,3]	25.81 ± 2.44	26.46 ± 08.27	35.33 ± 2.35	33.03 ± 3.89
D [3,2]	08.71 ± 0.38	06.57 ± 00.72	11.25 ± 0.88	08.79 ± 0.41
d (v, 0.1)	04.18 ± 0.25	02.56 ± 00.25	06.88 ± 0.65	03.41 ± 0.18
d (v, 0.5)	20.04 ± 2.29	13.41 ± 02.57	21.53 ± 1.49	23.54 ± 1.57
d (v, 0.9)	55.31 ± 5.96	49.66 ± 16.30	77.37 ± 3.01	73.61 ± 6.74
Span	02.55 ± 0.05	03.45 ± 00.51	03.28 ± 0.13	02.98 ± 0.08

All parameters of importance are given, namely the D [4,3], D [3,2], d(v, 0.1), d(v, 0.5) and d(v, 0.9) values as well as the span. The span, which describes the width of the particle size distribution, was comparatively large for both blank and drug-loaded formulations. This indicates that various emulsion droplet sizes, ranging from the nanometer up to the micrometer scale, were present in the mixture. This could also be derived from a visual observation of the obtained distribution curves, which indicated a highly polydisperse nature of the samples with droplet sizes ranging from 0.7 up to several hundred micrometers. This was especially pronounced after 6 months of storage. In particular the strong increase in d(v, 0.9) values points to a small population of increasingly large individual droplets.

Since the samples were diluted prior the measurements, it is unclear whether these data merely give an overview about the oil droplet size distribution within the emulsion, or also about remnants of the hydrophilic network which provides the basis for the high viscosity of the systems. Likewise, since the results obtained with this technique are volume-based, the presence of a few individual larger droplets may skew the correlation considerably since the presence of very small droplets may easily be

outweighed by the far more voluminous larger droplets. Thus, an additional microscopic analysis was performed.

In case of the nanoemulsions, the mean particle sizes as determined by DLS were in the lower submicron range for both blank and drug-loaded formulations (Table 3).

Table 3. Physicochemical properties of blank and drug-loaded nanoemulsions (NE) after 16 cycles of high-pressure homogenization. Measurements were performed in triplicate on a Zetasizer Nano ZS (Malvern, UK) at 25 °C. Samples were diluted with distilled water (1:100 v/v) containing sodium chloride (0.01 mmol) before the experiments to ensure constant conductivity below 0.05 ms/cm. Parameters shown are mean particle size (MPS), zeta potential (ZP), conductivity (cond) and polydispersity index (PDI). Values represent the mean of at least three formulations ($n \geq 3$) and are given ± SD.

Parameters	**NE blank**	**NE curc**	**NE fluf**	**NE diclo**
Particle size (nm)	116.40 ± 10.22	124.69 ± 2.58	128.33 ± 11.34	114.44 ± 2.42
Zeta potential (mV)	−58.89 ± 14.48	−47.11 ± 1.49	−51.36 ± 2.71	−54.12 ± 4.83
Conductivity (mS/cm)	0.024 ± 0.005	0.017 ± 0.004	0.025 ± 0.005	0.023 ± 0.003
PDI	0.11 ± 0.03	0.25 ± 0.03	0.09 ± 0.01	0.11 ± 0.02

The narrow intensity-based distribution curves indicated a monodisperse nature of the samples. The PDI values were below 0.2 except for curcumin-loaded formulations, which indicates a narrow droplet size distribution and thus good long-term stability. Individual whitish aggregates detected among visual inspection were not detected with these measurements since they were most likely dissolved upon dilution of the samples. It is likewise known that DLS alone may fail to detect the presence of individual larger oil droplets or vesicles and may thus provide incomplete information [39]. Therefore, as for the macroemulsions, an emphasis was placed on microscopic examination techniques to obtain more accurate information about the actual microstructure of the formulations.

In context with the DLS measurements it has to be mentioned that the highly lipophilic drug curcumin was rather dispersed than dissolved within the oil phase. The presence of undissolved drug did not disturb the particle size measurements, as previously reported [40]. Merely a slight increase of the PDI value was noticed. Homogeneous distribution of the drug could be obtained after re-homogenization of the system by slight shaking. In case of the corresponding macroemulsions with curcumin the drug was homogeneously distributed within the system and no dispersed drug aggregates were visible within the homogeneous orange emulsion.

Overall, the droplet size in equilibrated emulsions is mainly determined by the intensity of mechanical agitation, the amount and interfacial properties of the surfactants, the interfacial tension and the physical properties of the oil and aqueous phases [17,41]. The properties of an emulsion will change significantly with the type of emulsification process used [41], as was impressively demonstrated in the present study. Thus, care should be taken to ensure an exact mixing procedure, since any irregularity may lead to changes in formulation microstructure.

3.4. Particle surface charge of nanoemulsions

The ZP values of blank and drug-loaded nanoemulsions are given in Table 3. The surface charge of sucrose stearate-based nanoemulsions was in the range around −50 to −60 mV, which indicates high electrochemical stabilization of the system. These high negative values are most likely caused by the presence of residual free fatty acids at the interface [7].

3.5. Physical stability

The physical long-term stability of all systems was highly satisfying. As anticipated in case of the macroemulsions, a notable increase in mean particle size after six months was observed (Figure 2A). However, the formulation remained visually stable and showed no signs of phase separation or microbial contamination upon conventional storage at 4 °C in a receptacle for ointments.

In case of the nanoemulsions (Figure 2B), the mean particle sizes remained highly constant in the course of six months as confirmed by regular measurements.

Figure 2. Mean droplet size of blank and drug-loaded macroemulsions (E, **2A**) and corresponding nanoemulsions (NE, **2B**) as determined immediately after production and after 6 months. The diluted samples were analyzed in triplicate at 25 °C on a Mastersizer 2000 (Malvern, UK) in case of the macroemulsions and a Zetasizer Nano ZS (Malvern, UK) in case of the nanoemulsions. The parameters shown are the volume weighted mean D [4,3] for macroemulsions and the mean droplet diameter as z-average for nanoemulsions. Values represent the mean of at least three formulations ($n \geq 3$) and are given ± SD.

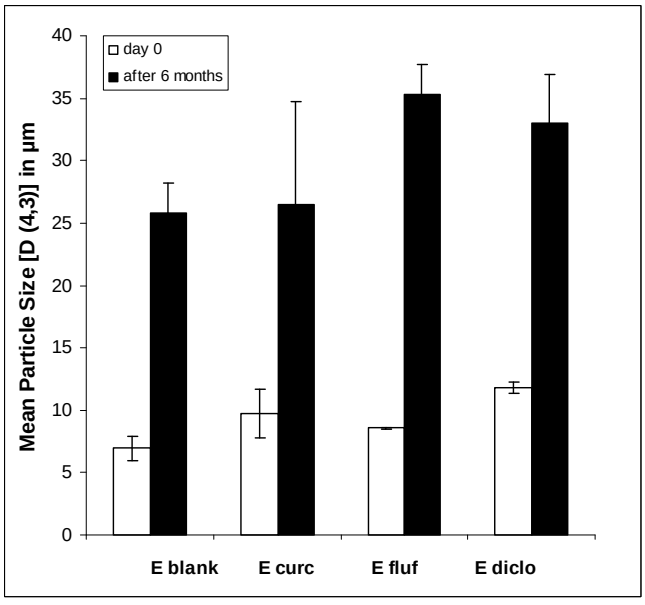

(2A)

Figure 2. *Cont.*

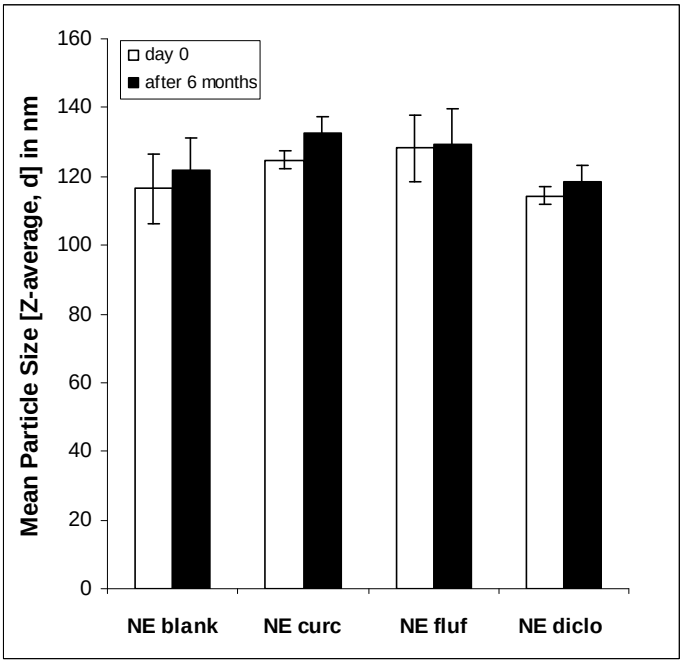

(2B)

As can be seen in Table 4, this was the case for both blank and drug-loaded nanoemulsions, shown on representative formulations containing flufenamic acid. The mean ZP values of the nanoemulsions increased slightly (Table 4A and 4B), most likely due to chemical changes within the formulations such as hydrolysis of surfactant molecules or excipients of the oil phase. This process results in the release of free fatty acids and thus an increased amount of negative charges at the interface. Since a certain surplus of surfactant was employed, the chemical degradation of the latter may have been more apparent than in our previous studies [7]. At the same time, this surplus of surfactant might be responsible for the individual whitish aggregates that were observed within the nanoemulsions. The number of these aggregates visible to the eye increased over time.

In summary, particle size measurements of submicron-sized emulsions by light scattering techniques are not always sufficient to monitor the actual physical stability of such formulations. Visible destabilization phenomena such as separation of oil droplets or formation of a precipitate might remain undetected [40]. Thus, carefully visual inspection of the samples is necessary. Additional and more precise information can be gained by microscopic investigations.

Table 4. Physical stability of blank **(4A)** and drug-loaded nanoemulsions (**4B**, shown on systems containing flufenamic acid). Similar results were obtained for all drug-loaded formulations. Experiments were performed in triplicate (n = 3) in regular intervals over an observation period of six months. The indicated parameters are the mean particle size (MPS), polydispersity index (PDI) and zeta potential (ZP). Numbers are given as means ± SD.

(4A)			
time		**NE blank**	
(weeks)	**MPS (nm) ± SD**	**PDI ± SD**	**ZP (mV) ± SD**
0	116.40 ± 10.22	0.11 ± 0.03	−61.73 ± 10.50
4	116.07 ± 09.93	0.12 ± 0.03	−64.13 ± 07.10
8	116.53 ± 08.56	0.13 ± 0.02	−60.91 ± 04.08
12	118.31 ± 08.28	0.12 ± 0.02	−61.27 ± 16.41
16	117.28 ± 08.05	0.13 ± 0.01	−60.70 ± 06.09
20	120.11 ± 08.93	0.13 ± 0.02	−64.69 ± 04.00
24	121.71 ± 09.61	0.15 ± 0.04	−64.76 ± 06.03
(4B)			
time		**NE fluf**	
(weeks)	**MPS (nm) ± SD**	**PDI ± SD**	**ZP (mV) ± SD**
0	128.28 ± 09.61	0.09 ± 0.01	−49.03 ± 00.37
4	128.01 ± 10.01	0.10 ± 0.01	−49.86 ± 02.05
8	125.06 ± 10.06	0.10 ± 0.01	−49.73 ± 04.38
12	126.55 ± 09.16	0.09 ± 0.01	−50.77 ± 04.64
16	129.94 ± 10.47	0.09 ± 0.01	−52.16 ± 05.13
20	132.92 ± 11.46	0.09 ± 0.02	−48.38 ± 02.13
24	129.12 ± 10.78	0.08 ± 0.01	−55.20± 04.40

3.6. Drug content, chemical stability and pH value

The initially determined drug contents of all formulations as well as the chemical stability of flufenamic acid and diclofenac acid remained satisfying over the course of a limited observation period of three months. No further attention was devoted to this topic since a more thorough analysis of the chemical stability of the incorporated drugs, especially in case of curcumin, was not an emphasis of this study.

The pH values of blank formulations were around 6.80 ± 0.04 for macroemulsions and 6.89 ± 0.01 for nanoemulsions (n = 3, respectively). Drug incorporation led to slightly lower pH values in case of flufenamic acid and diclofenac acid (data not shown). However, all pH values were in an acceptable range for dermal application.

Interestingly, chemical degradation processes appeared to affect the nanoemulsions to a greater extent than the corresponding macroemulsions irrespective of drug incorporation. After a storage time of 6 months, the overall mean pH value of all formulations was 6.40 ± 0.20 in case of the macroemulsions and 6.01 ± 0.11 in case of the nanoemulsions (n = 13, respectively). This observation is in agreement with previously reported data which indicate that lipid oxidation in nanoemulsions

proceeds more rapidly than in conventional emulsions due to the increased surface area of the nano-sized droplets [17].

3.7. Optical light microscopy

Optical light microscopy was conducted to obtain an overview about larger structures present in the different formulations. The images were in good agreement with the visual observations of the samples as well as the particle size measurements.

Figure 3. Images of fresh as well as stored macroemulsions as observed by optical light microscopy. Images **3A, 3B and 3C** show a blank macroemulsion directly after preparation while the corresponding images **3D, 3E and 3F** show the same formulation after 6 months of storage. The employed microscopic modes were 10x magnification/bright field (3A, 3D), 20x magnification/DIC (3B, 3E and 3G, 3H, 3I) and 40x magnification/bright field (3C, 3F). The indicated scale bars represent 50 µm. Images **3G, 3H and 3I** represent artefacts of fresh macroemulsions obtained after 20 minutes of storage of the object slide.

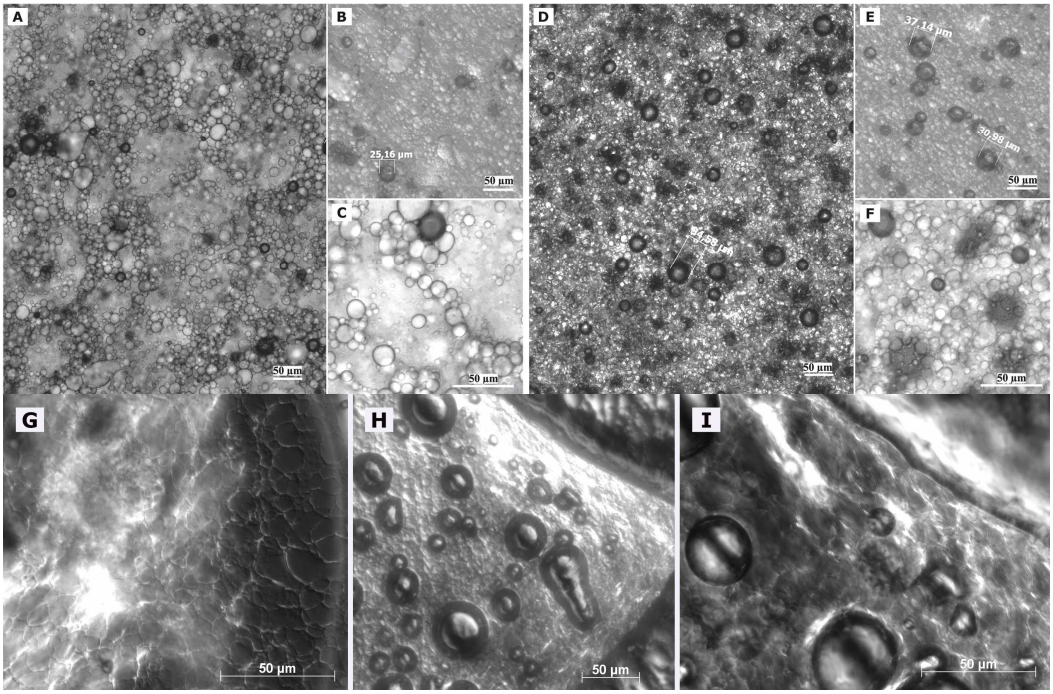

In case of freshly prepared blank macroemulsions a complex network of hydrophilic spherical structures presumably composed of sucrose ester/water aggregates was observed (Figure 3A to 3C). Large spherical interconnected aggregates formed a net-like structure which surrounded the darker oil droplets. In between the large “meshes” of this network, smaller spherical aqueous structures were observed which filled up the space. Likewise, it may be assumed that large amounts of air are incorporated as well. Overall, the particle sizes observed for the different surfactant aggregates varied

from around 30 µm for the large network-forming structures down to 0.6 µm for the smaller aggregates filling up the spaces in between. The oil droplets were of variable size and their diameter ranged mostly within the micrometer range, as already indicated by the laser diffraction measurements. Although these particle size measurements were conducted with highly diluted samples, it is unclear whether the sucrose ester aggregates were included in the analysis. If this was the case, it would account for the high polydispersity of the analyzed samples. Particle sizes as small as 600 nm have likewise been reported for the structural compounds of aqueous gel-like dispersions of sucrose stearate [15]. However, the values reported by Ullrich and co-workers were based on DLS analysis of highly polydisperse and undiluted samples, which renders an interpretation difficult.

Interestingly, the nature of the viscous macroemulsions changed upon storage. Images that were taken after a storage time of over 6 months revealed an increasingly dense aggregate network with less free space between the aggregate "meshes" of the network (Figure 3D to 3F). This increase in density of the network might have been caused by a minor separation of water condensation on the lid of the storage receptacle. Likewise, the influence of gravity might have caused incorporated air to escape from the emulsion bulk phase. As anticipated by particle size measurements, the average size of the dispersed oil droplets showed a definite increase with oil droplet diameters frequently larger than 30 µm. Individual oil droplets of up to 160 µm in diameter were observed as well. It may be assumed that the presence of such individual large droplets remained undetected in the laser diffraction measurements due to methodological limitations [42]. Despite this obvious change in the internal formulation structure, the visual appearance of the semi-solid vehicles remained intact.

Interesting additional information was gained from observation of changes in formulation microstructure upon manipulation on an object plate. After prolonged presence of the macroemulsions on the object plate, a dried network became visible which covered the dried out area around residual water droplets (Figure 3G). In addition, the potential of the sucrose ester mixture to form liquid crystalline structures became more apparent as increasingly large areas, also along the dried network structure, showed birefringence under polarized light (Figure 3G, 3H, 3I). These observations indicate that the network structure of the viscous formulation might be at the margin of a weak liquid crystalline matrix.

Overall, the observed network of unilamellar vesicles bears a certain resemblance to a cubic gel phase observed in previous studies [43,44]. Despite the apparent differences in formulation composition and size range when compared to our macroemulsions, similar general observations were reported. A system of high viscosity was obtained with no other compounds than a dispersed phase fraction of 5–15% w/w. The vesicular unilamellar spheres responsible for the system's properties consisted of amphiphilic material only. Dilution of the gel phase led to the formation of a viscous, but not gel-like phase which was unfortunately not further characterized. The fact that the macroemulsion structure is not as ordered as the cubic gel structure might be due to the fact that much larger amounts of water and less surfactant are present. Our system might thus be comparable to the described diluted cubic phase system. Another explanation might point to a resemblance to self-standing gel-like emulsions. However, larger amounts of internal phase are usually reported for such systems [45].

In case of the freshly prepared nanoemulsion (Figure 4A), constant background movement indicated the presence of nano-sized oil droplets subjected to Brownian motion [22]. The samples were highly

homogeneous except for a few larger vesicular structures and individual surfactant aggregates. These structures which were visible to the naked eye as whitish flakes appeared as irregularly shaped "islands" within the formulation. However, their number was highly limited after production. These aggregates remained undetected during the DLS measurements of the diluted samples.

Figure 4. Images of fresh, as well as stored, nanoemulsions as observed by optical light microscopy. All images were taken with 40 x magnification/DIC. Image **4A** shows the blank nanoemulsion directly after preparation. Figure **4C** shows the same formulation after 6 months of storage. Image **4B** shows an artefact obtained with a fresh nanoemulsion sample due to evaporation effects on the object slide. The indicated scale bars represent 50 µm.

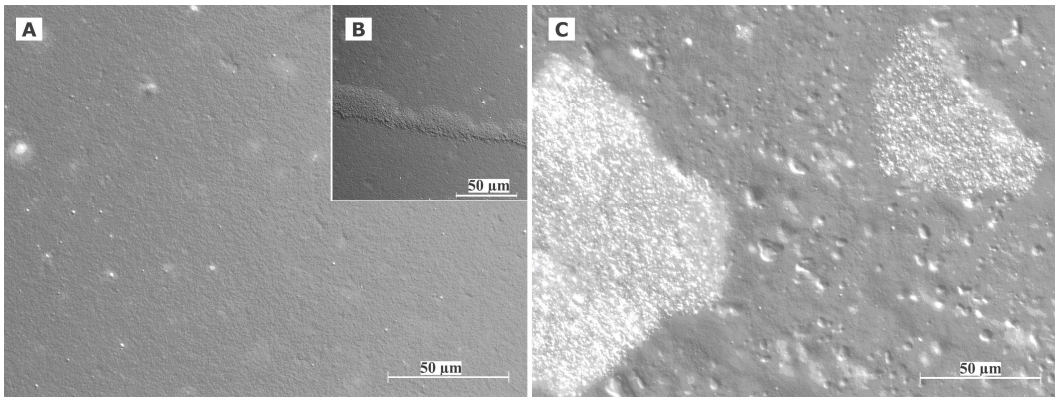

The nature of the fluid nanoemulsions changed upon storage. Images that were taken of samples after 6 months of storage time (Figure 4C) revealed a much larger number of the described shapeless aggregates. It may be assumed that these aggregates represent separated fractions of surplus sucrose ester. For blank nanoemulsions, the viscosity of the sample appeared to be increased as compared to the fresh one due to gelling effects of the surfactant. No such gelling effect upon storage was observed for the more fluid nanoemulsions with flufenamic acid and diclofenac acid. This aspect is currently being investigated in rheological studies over prolonged observation periods and will be reported in a separate context. Overall, nanoemulsions apparently suffered notable changes in formulation microstructure despite the fact that the particle size measurements suggested otherwise.

Again, observation of the sample's behavior on the object plate provided useful information. The nanoemulsion droplet started gelling immediately upon application on the plate. After covering of the sample, a structured dispersed film remained at the edges of the droplet (Figure 4B). Again, this rather ordered structural network may be situated at the margin of a weak liquid crystalline network [15]. Similar behavior can be observed upon positioning of a microemulsion on an object plate, where growth of liquid crystals can be observed at the margin of the sample due to evaporation of volatile compounds.

Although the peculiar rheological behavior of colloidal sucrose ester suspensions in water has recently attracted attention [11,14], the microstructure of these systems is still somewhat unclear [15].

Microscopic data exists mostly for suspensions with higher concentrations of sugar surfactant, which consequently contain increasing amount of liquid crystalline structures [13]. Interestingly, for a suspension of another sucrose stearate mixture with a slightly higher HLB value of 12, liquid crystalline structures were already observed at a concentration of 4% w/w [46]. Although information on the structure of O/W emulsions co-stabilized by alkylpolyglucosides, a frequently employed type of sugar surfactant, can be found [47], no such data exist for O/W emulsions stabilized by a sucrose ester mixture alone.

3.8. Cryo TEM and TEM after negative staining

Cryo TEM investigations of freshly prepared formulations were additionally performed to visualize the structural differences between the two original systems on a nano-scale level. In case of the macroemulsion (Figure 5A), a dense structural network was observed which appeared to consist of closely located or connected spherical aggregates with mean diameters as small as a few hundred nanometers (marked areas). These aggregates formed the larger droplets which had been visualised by light microscopy. Since the sample was observed in its original state without dilution and the TEM image is merely a 2D projection, the borders of the smaller aggregates could not be clearly distinguished. However, the images serve to confirm the rich internal structure of the macroemulsion. The structural network appeared to be remarkably homogeneous, since the ice crystals commonly observed during cryo-preparation emerged in a highly ordered and regular fashion. Additional analysis with conventional TEM sample preparation and negative staining confirmed these observations (Figure 5B). Droplets of various sizes could be distinguished.

Figure 5. Analysis of the microstructure of blank macroemulsions by cryo TEM **(5A)** and conventional TEM after negative staining with uranyl acetate **(5B)**. The magnification is illustrated by the black scale bars.

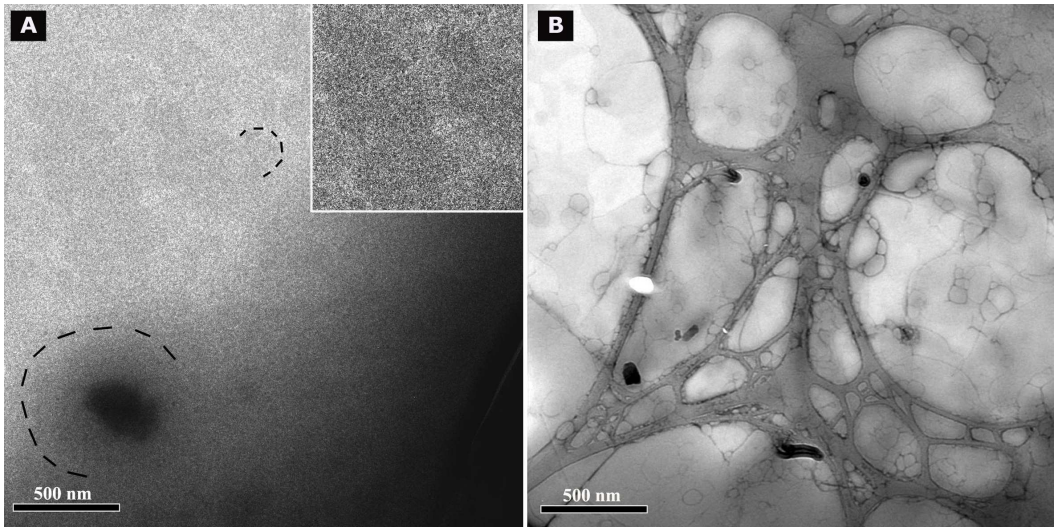

In case of the nanoemulsion, a common if highly crowded internal structure was revealed despite the dilution of the sample (Figure 6A). The nano-sized oil droplets appeared to be partially deformed or collapsed, which is not entirely unexpected given the high surfactant concentration and resulting high viscosity of the formulation. Likewise, the shape of the deformable nanodroplets can be influenced by the oil volume fraction [48]. At high oil volume fractions, the surfaces of the crowded droplets strongly repel each other. This can cause the droplets to deform and become non-spherical [49]. In addition, individual shapeless aggregates most likely composed of sucrose stearate/water were detected in the nanoemulsion sample, which confirmed the optical light microscopy data. The rheological properties of the sample influence the processing conditions during high-pressure homogenization. The equilibrium between the rupturing of oil droplets and coalescence events which occur within the device are governed by the viscosity of the processed colloidal system [50,51]. In terms of viscosity, the employed pre-homogenized mixture surely resides at the margin of the device's working capacity. The surplus of surfactant which is subjected to the high-pressure homogenization procedure is apparently united in the described shapeless aggregates. Conventional TEM analysis after negative staining confirmed the above observations (Figure 6B). A noteworthy observation regarding the conventional TEM analysis is the fact that a largely intact emulsion structure could be visualized despite the high vacuum and the potential risk of beam damage imminent to this technique. This aspect will be the subject of further investigations.

Figure 6. Analysis of the microstructure of blank nanoemulsions by cryo TEM **(6A)** and conventional TEM after negative staining with uranyl acetate **(6B)**. The magnification is illustrated by the black scale bars.

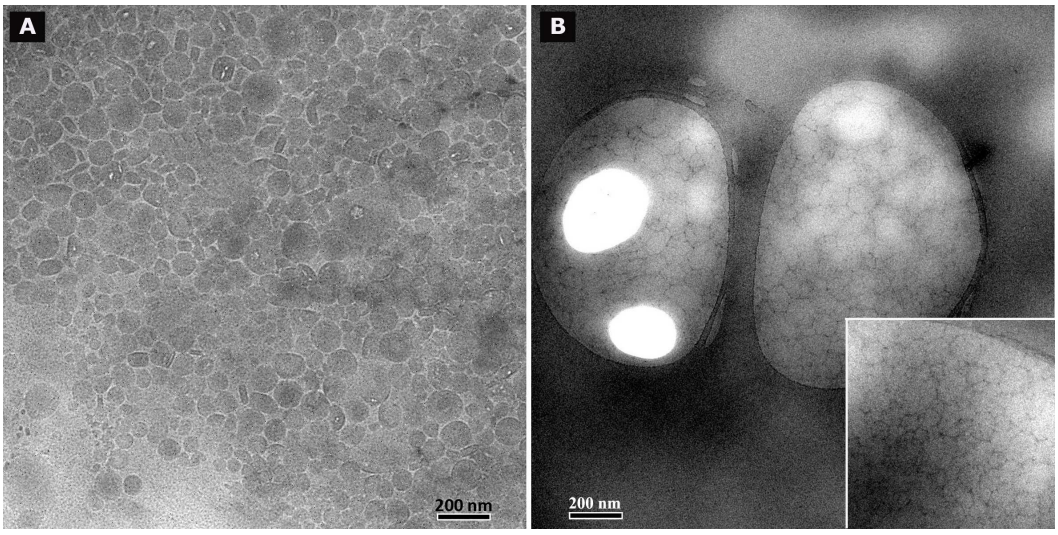

Summarizing the main conclusions of the microscopic observations, it may be assumed that the highly viscous and dense structure of the macroemulsions is caused by a network of excess surfactant. In case of the nanoemulsion, smaller droplet sizes are created which possess a larger surface area covered by surfactant molecules. Thus, only a small amount of surplus surfactant is left after

production which subsequently leads to the observed aggregates which increase in number and size during storage. In case of the macroemulsion, the droplet sizes remain in the micrometer range, thus providing less surface area to be covered by surfactant molecules. Consequently, a larger amount of free surfactant is left which then forms the network-like structure via self-assembly into vesicles or similar structures, possibly approaching a weak liquid crystalline state.

3.9. Rheological investigations

The rheological properties of a colloidal system strongly depend on its composition and, more importantly in this case, on the processing conditions. The analysis of these properties is a simple tool to characterize the macroscopic properties of a formulation in an objective way and thus to confirm visual observations [52]. The rheological properties of emulsions are crucial for their application on skin as well as their physical stability. Especially in case of the presented macroemulsions, it may be assumed that the coalescence of oil droplets or other potential destabilization phenomena strongly depend on the rheological properties of the system. These properties are influenced by the oil volume fraction, the droplet size and particle charge as well as by colloidal interactions [53]. In order to obtain an overview about the rheological properties of the different systems, the flow behavior as well as the viscoelastic properties of both blank and drug-loaded systems were analyzed.

In case of the macroemulsions, the flow curves revealed that the dynamic viscosity of the systems decreased with increasing shear rates. This pseudoplastic or shear-thinning flow behavior was found for both blank and drug-loaded macroemulsions. The incorporation of the model drugs led to an increase in viscosity at all shear rates. Figure 7 demonstrates the advantageous effect of drug incorporation on the viscosity of the macroemulsions in an exemplary manner at a shear rate of 15 s^{-1}. The apparent viscosity of the macroemulsions at this shear rate was between 2.26 ± 0.10 and 7.92 ± 0.02 Pa·s.

Figure 7. Comparison of the apparent viscosity of macroemulsions (E) and corresponding nanoemulsions (NE) with and without incorporated drug at a shear rate of 15 s^{-1}. The effect of the incorporated drugs curcumin (cu), flufenamic acid (fl) and diclofenac acid (di) is demonstrated. Values represent the mean of three formulations (n = 3) and are given ± SD.

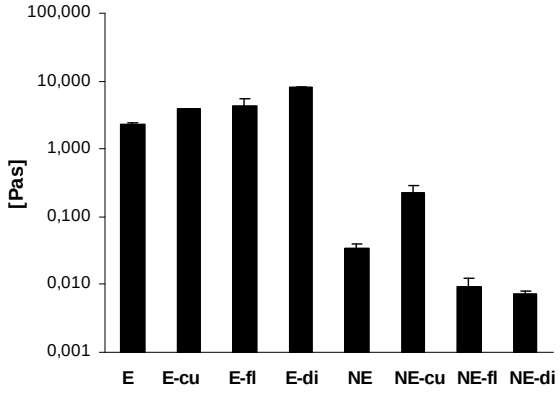

A minor shear-thinning effect was also observed for blank nanoemulsions and nanoemulsions with curcumin. As already indicated, curcumin was partly dispersed in the system, thus changing its overall properties and leading to an increased viscosity and shear-thinning behavior of the nanoemulsion. For all other drug-loaded nanoemulsions, the dynamic viscosity was entirely independent of the applied shear rate which is characteristic for Newtonian flow behavior. Except in the case of curcumin, the incorporation of drugs into the sucrose stearate nanoemulsion led to a decrease of viscosity at all shear rates (Figure 7): nanoemulsions with flufenamic acid and diclofenac acid exhibited an apparent viscosity of 0.01 ± 0.001 Pa·s at all shear rates.

Overall, it was apparent that the viscosity of the macroemulsions was several orders of magnitude higher than that of the nanoemulsions. The apparent viscosity of the blank nanoemulsion was 0.03 ± 0.001 Pa·s at the presented shear rate, while the viscosity of the corresponding blank macroemulsion was 2.26 ± 0.10 Pa·s, which corresponds to a 64-fold increase in viscosity.

An analysis of the flow curves of both macroemulsions and nanoemulsions using the power law model confirmed the above discussed observations. In case of the nanoemulsions, the value of the flow behavior index n was in the order NE diclo > NE fluf > NE blank > NE curc, where especially the values of the nanoemulsions with diclofenac acid and flufenamic acid were close to 1 (n = 0.98 ± 0.03 and n = 0.92 ± 0.08), thus confirming Newtonian flow behavior. In contrast, the flow behavior index n of blank macroemulsions was 0.10 ± 0.01 and was decreased further by incorporation of either drug. A value of n close to zero indicates pronounced shear-thinning behavior of the samples.

Overall, the shear-thinning effect observed for macroemulsions and, to a minor extent, for blank and curcumin-loaded nanoemulsions is consistent with literature. The pseudoplastic nature of the macroemulsions can be explained by the deformation of the emulsion droplets under increasing shear which facilitates their flow. Likewise, nanoemulsions may exhibit shear-thinning behavior due to changes in the droplet shape along the flow channel [22]. In this case, the incorporation of flufenamic acid and diclofenac acid apparently eliminated any such effect by lowering the viscosity of the blank nanoemulsion system, possibly by interacting with surplus amounts of surfactant.

In addition, oscillatory measurements were performed. In case of the macroemulsions, the elastic modulus G’ was strongly dominating over the viscous modulus G’’ at all oscillatory frequencies, which is favorable in terms of physical stability. A comparison of G’ and G’’ for all systems at a frequency of 1 Hz is given in Figure 8. The elastic modulus G’ ranged from approximately 250 to 1300 Pa while the viscous modulus G’’ ranged from 70 to 380 Pa. Drug incorporation generally increased the values of G’ and G’’. The only exception was the curcumin-loaded formulation where G’’ was decreased. Overall, both parameters increased at an increasing oscillatory frequency. An increase in the elastic modulus with increasing frequency has been related to the closer packing of microgelled colloidal particles and the resulting larger friction forces between the droplets subjected to shear [54].

Figure 8. Comparison of the elastic modulus G' (black bars) and the viscous modulus G'' (grey bars) of macroemulsions (E) and corresponding nanoemulsions (NE) with and without incorporated drug at an oscillatory frequency of 1 Hz. The effect of the incorporated drugs curcumin (cu), flufenamic acid (fl) and diclofenac acid (di) is demonstrated. Values represent the mean of three formulations (n = 3) and are given ± SD.

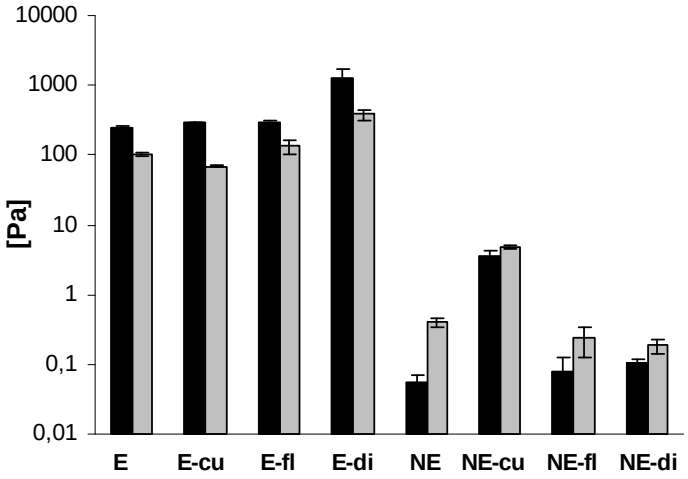

In case of the nanoemulsions, the viscous modulus G'' clearly dominated over the elastic modulus G' (Figure 8). In case of flufenamic acid and diclofenac acid, drug incorporation led to a decrease of the viscous modulus G'', thus confirming their fluidizing effect on the nanoemulsions. In case of curcumin, incorporation led to an increase of the viscous modulus G'' due to undissolved drug. The elastic modulus G' was increased by drug incorporation in all cases. Again, both parameters G'' and G' increased with increasing oscillatory frequency. Needless to say, both the elastic and viscous modulus were again several orders of magnitude larger for macroemulsions than for nanoemulsions. While the elastic modulus G' of blank nanoemulsions was 0.06 ± 0.01 Pa, the corresponding value for blank macroemulsons was 248.01 ± 14.97 Pa. This corresponds to a 4409-fold increase in the formulation's elasticity. Likewise, the viscous modulus G'' of blank macroemulsions was 256 times larger than for blank nanoemulsions (0.40 ± 0.05 *versus* 101.83 ± 3.68 Pa).

Overall, the rheological data confirmed that the employed sucrose stearate mixture led to the formation of entirely different emulsion bulk structures by alteration of the production process. A thorough understanding of the bulk structure of an emulsion is necessary to accurately describe its macroscopic mechanical properties. If the droplets within an emulsion are concentrated enough to be deformed, as is obviously the case for the present systems, the mechanical properties of the system can change from viscous to elastic during production due to increased deformation through osmotic pressure [55]. The application of a small shear strain works against the interfacial tension and causes the packed droplets to deform, thereby creating additional interfacial area and storage energy [55]. Likewise, as indicated by the cryo TEM experiments, the macroemulsion structure appeared to be highly symmetrical in terms of distribution of water and oil phase, which may contribute to increasing viscosity and elasticity [56].

The potential of the sucrose ester mixture to stabilize highly elastic macroemulsions is worthy of further investigation. So far, it may be assumed that the ability of the employed sucrose ester to increase the viscosity of emulsions may be related to its potential to self-assembly and the ability of sucrose to form hydrogen bonds and bind water [17].

3.10. In vitro skin permeation: franz-cells

The cumulative permeated drug amounts after 24 hours as well as the corresponding drug fluxes for all three model drugs are given in Table 5.

Table 5. Skin permeation rates of curcumin (curc), flufenamic acid (fluf) and diclofenac acid (diclo) from macroemulsions (E) and nanoemulsions (NE) expressed as cumulative permeated drug amounts ($\mu g \cdot cm^{-2}$) and mean drug fluxes (J, $\mu g \cdot cm^{-2} \cdot h^{-1}$). At least five experiments were performed for each formulation ($n \geq 5$); indicated values are means ± SD.

Formulation	Cumulative drug amount after 24h ± SD ($\mu g \cdot cm^{-2}$)	Mean drug flux ± SD (J, $\mu g \cdot cm^{-2} \cdot h^{-1}$)
E curc	n.d.	n.d.
NE curc	0.71 ± 0.96	0.04 ± 0.06
E fluf	27.27 ± 7.18	1.28 ± 0.34
NE fluf	24.48 ± 5.13	1.15 ± 0.24
E diclo	140.30 ± 27.36	6.66 ± 1.28
NE diclo	147.37 ± 31.05	6.92 ± 1.44

As can be seen, the corresponding macroemulsions and nanoemulsions performed equally well in this experimental setup, leading to highly similar release profiles in all three cases. No statistically significant differences between the different formulation types were obtained in terms of either cumulative drug amounts or drug fluxes ($P > 0.05$, respectively). In case of curcumin, the achieved permeation rates were negligible despite the adapted acceptor medium. This can be ascribed to the high lipophilicity of curcumin, which is known to be problematic in terms of formulation development and drug delivery [30,31]. However, the skin permeation experiments were not perpetuated for a longer time span so as not to allow maceration effects to take hold.

The small droplet size of the nanoemulsions is associated with a large surface area, which has frequently been reported to result in an enhanced or accelerated release of incorporated drugs and thus an increased biological effect [51,57,58]. Interestingly, no such effect was observed in the present experiments. Indeed, literature shows that a smaller particle size is not necessarily associated with improved drug delivery [59]. In this case, the skin penetration of the model drugs rather appears to be governed by the employed excipients.

Another interesting aspect in this context is the fact that the skin permeation rates of the drugs were not influenced by the strongly increased viscosity of the macroemulsion systems. The microviscosity of the macroemulsions appeared to be comparable to that of the fluid nanoemulsions despite the significant difference in macroviscosity. This phenomenon has been investigated and confirmed in a recent study dealing with gel-like colloidal dispersions of a comparable sucrose stearate mixture [15].

It may thus be assumed that the loose interconnected hydrophilic network observed for the macroemulsions in our study is of a similar nature despite the presence of additional oil droplets. The release of all three model drugs remained impaired by the complex network-like macroemulsion structure.

3.11. In vitro skin penetration: tape stripping

The results of the tape stripping experiments were in good agreement with the results obtained with the franz-cell studies. In summary, neither the particle size nor the viscosity appeared to exert any influence on the penetration behavior of the three model drugs. The penetration depth of the drugs was found to be highly similar for corresponding macroemulsions and nanoemulsions in case of all three model substances ($P > 0.05$, respectively). The same tendency was observed for the accumulated amounts of drug in the SC as determined by summarizing the drug quantities recovered from the individual tape strips ($P > 0.05$, respectively). Merely in case of diclofenac acid, slightly if significantly larger drug amounts were recovered from the skin treated with the macroemulsion due to a surplus of drug on the first adhesive film ($P < 0.05$). Table 6 shows a comparison of the macroemulsions and nanoemulsions in terms of penetrated drug amounts and the penetration depth of the drugs. The latter is expressed both in absolute values (µm) and as percentage of the entire SC thickness, which was found to be 6.59 ± 0.47 µm for the employed porcine ears after removal of the entire SC via tape stripping ($n = 4$).

Table 6. Skin penetration data of curcumin (curc), flufenamic acid (fluf) and diclofenac acid (diclo) from macroemulsions (E) and nanoemulsions (NE) as determined by tape stripping. At least six experiments were performed for each formulation ($n \geq 6$); indicated values are means ± SD.

Formulation	Penetrated drug amount [µg/cm²]	Penetration depth [µm]	[% of SC]
E curc	45.22 ± 6.61	3.75 ± 0.53	56.79 ± 08.01
NE curc	51.07 ± 4.17	3.21 ± 0.81	48.61 ± 12.24
E fluf	21.93 ± 6.29	3.08 ± 1.29	46.65 ± 19.62
NE fluf	24.02 ± 7.03	3.61 ± 0.95	54.67 ± 14.36
E diclo	27.98 ± 4.43	5.62 ± 0.65	85.22 ± 09.83
NE diclo	20.72 ± 2.58	4.79 ± 0.95	72.70 ± 14.40

A graphical illustration of the penetration profiles for flufenamic acid from both macroemulsions and nanoemulsions is given in Figure 9A/9B as a representative example.

The highest skin penetration depth was achieved by by diclofenac acid, which was in good agreement with the results of the franz-cell studies. Concerning curcumin it is interesting to note that unlike the results derived from the franz-cell diffusion studies, satisfying skin penetration was reached in this experimental setup which was comparable to that of flufenamic acid. It may thus be assumed that *in vitro* tape stripping is a more suitable approach to investigate the skin penetration of highly lipophilic drugs such as curcumin. Additional *in vivo* tape stripping studies will be conducted with the curcumin-loaded formulations to confirm these results.

Figure 9. *In vitro* skin penetration profiles of flufenamic acid applied topically in macroemulsions **(9A)** and nanoemulsions **(9B)**. The data were obtained via tape stripping using porcine ear skin (n = 8, respectively).

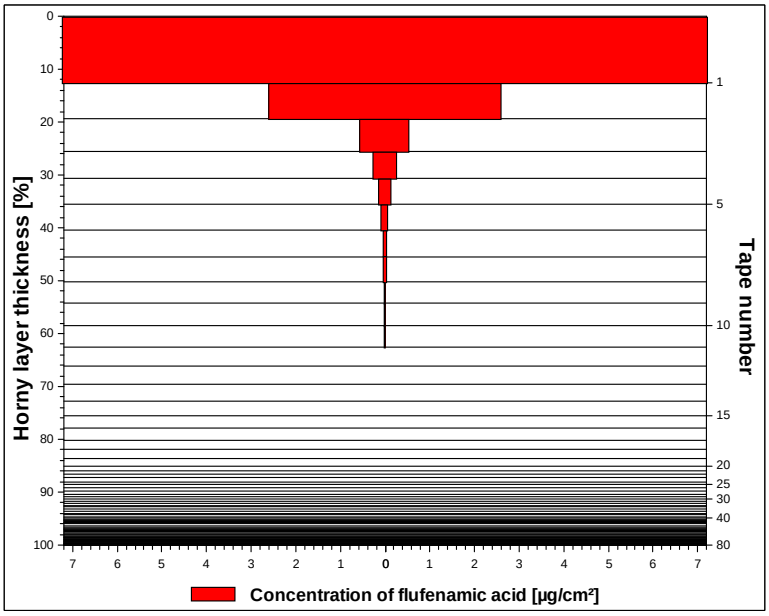

(9A)

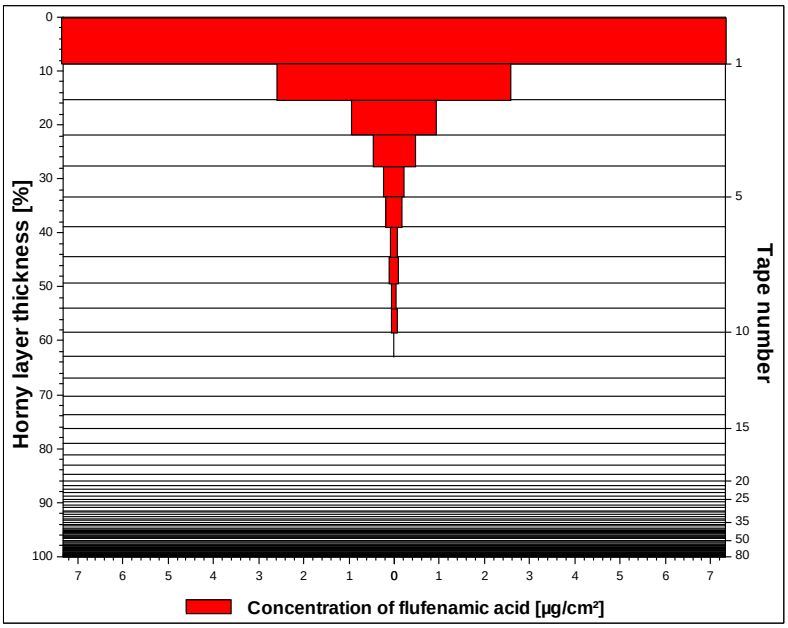

(9B)

3.12. Comparison of in vitro studies: franz-cells vs. tape stripping

Since the classical experimental set-up using franz-type diffusion cells may be influenced by interactions between the receptor medium and the model skin which may affect the barrier properties [60], additional tape stripping experiments were performed to avoid the influence of the receptor medium and to provide a more practically orientated experimental setup with a short finite-dose application.

Under *in vivo* conditions, there is of course a high tissue clearance due to the bloodstream which cannot be simulated with the excised porcine ear. However, the results of our study showed that in the case of curcumin, hardly any skin diffusion was obtained with franz-type diffusion cells over the course of 24 hours despite the presence of a large amount of ethanol in the receptor medium, which offers a high solubilizing capacity for curcumin. In contrast, a penetration profile similar to that of the other drugs was achieved by *in vitro* tape stripping.

As expected, the skin penetration and skin permeation data obtained by the different experimental setups were not entirely comparable in terms of numerical values. In case of curcumin, a reasonable penetration into the stratum corneum was determined by tape stripping (around 50 µg cm^{-2}) while no transdermal permeation was observed with franz-type diffusion cells despite the adapted receptor medium. In case of flufenamic acid, the amounts detected in the skin by tape stripping and in the receptor medium after 24 hours were of a similar order of magnitude (around 25 µg cm^{-2}, respectively). In case of diclofenac acid, a comparatively smaller amount of drug was obtained by tape stripping (around 25 µg cm^{-2}) than was recovered from the receptor medium (around 145 µg cm^{-2}). Since it is well-known that diclofenac as an acid is difficult to deliver, it may be assumed that as for curcumin, the results obtained with franz-type diffusion cells are not representative of the *in vivo* situation. In case of curcumin, an underestimation of the skin penetration potential resulted while in case of diclofenac, an overestimation was obtained. The inconsistent experimental results for diclofenac might be related to the different types of setup, the different types of skin employed for the experiments and related differences in pH gradients across the skin [61]. Overall, it may be concluded that tape stripping experiments deliver by far more realistic data than franz-type diffusion cell studies. Comparative *in vivo* tape stripping experiments are envisioned in order to confirm the relevance of the data obtained by *in vitro* tape stripping.

4. Conclusions

Sucrose stearate of an intermediate HLB value can be employed to design innovative lipid-based drug delivery systems which possess improved texture for dermal application while at the same time providing unimpeded drug release properties. The exact nature of the fluffy hydrophilic network surrounding the O/W emulsion droplets of various sizes should be subject to further investigations in order to specifically create desired properties of similar new vehicles. In the context of our investigations, additional *in vivo* tape stripping experiments are planned to gain a more realistic estimation of the penetration behavior of the newly developed formulations.

Acknowledgements

The authors would like to thank Wolfgang Sipos and the Veterinary University of Vienna for providing fresh porcine ears and Gerhard Schleining for valuable discussion. The financial support of the research platform "Characterisation of Drug Delivery Systems on Skin and Investigation of Involved Mechanisms" is gratefully acknowledged.

References and Notes

1. Desai, N.B. Sucrose esters - an interesting class of substances for cosmetics. *Parfuemerie Kosmet.* **1985**, *66*, 629-632.
2. Thevenin, M.A.; Grossiord, J.L.; Poelman, M.C. Sucrose esters/cosurfactant microemulsion systems for transdermal delivery: Assessment of bicontinuous structures. *Int. J. Pharm.* **1996**, *137*, 177-186.
3. Hill, K.; Rhode, O. Sugar-based surfactants for consumer products and technical applications. *Fett/Lipid* **1999**, *101*, 25-33.
4. Carlotti, M.E.; Sapino, S.; Ugazio, E.; Peira, E.; Gallarate, M. O/W Moisturizing Emulsions with Saccharose Palmitate and Saccharose Stearate. *J. Disp. Sci. Technol.* **2008**, *29*, 375-386.
5. Takegami, S.; Kitamura, K.; Kawada, H.; Matsumoto, Y.; Kitade, T.; Ishida, H.; Nagata, C. Preparation and characterization of a new lipid nano-emulsion containing two cosurfactants, sodium palmitate for droplet size reduction and sucrose palmitate for stability enhancement. *Chem. Pharm. Bull. (Tokyo)* **2008**, *56*, 1097-1102.
6. Klang, V.; Matsko, N.; Zimmermann, A.M.; Vojnikovic, E.; Valenta, C. Enhancement of stability and skin permeation by sucrose stearate and cyclodextrins in progesterone nanoemulsions. *Int. J. Pharm.* **2010**, *393*, 152-160.
7. Klang, V.; Matsko, N.; Raupach, K.; El-Hagin, N.; Valenta, C. Development of sucrose stearate-based nanoemulsions and optimisation through gamma-cyclodextrin. *Eur. J. Pharm. Biopharm.* **2011**, in press.
8. Calderilla-Fajardo, S.B.; Cazares-Delgadillo, J.; Villalobos-Garcia, R.; Quintanar-Guerrero, D.; Ganem-Quintanar, A.; Robles, R. Influence of sucrose esters on the *in vivo* percutaneous penetration of octyl methoxycinnamate formulated in nanocapsules, nanoemulsion, and emulsion. *Drug Dev. Ind. Pharm.* **2006**, *32*, 107-113.
9. Cazares-Delgadillo, J.; Naik, A.; Kalia, Y.N.; Quintanar-Guerrero, D.; Ganem-Quintanar, A. Skin permeation enhancement by sucrose esters: A pH-dependent phenomenon. *Int. J. Pharm.* **2005**, *297*, 204-212.
10. Csoka, G.; Marton, S.; Zelko, R.; Otomo, N.; Antal, I. Application of sucrose fatty acid esters in transdermal therapeutic systems. *Eur. J. Pharm. Biopharm.* **2007**, *65*, 233-237.
11. Szuts, A.; Budai-Szucs, M.; Eros, I.; Ambrus, R.; Otomo, N.; Szabo-Revesz, P. Study of thermo-sensitive gel-forming properties of sucrose stearates. *J. Excipients Food Chem.* **2010**, *1*, 13-20.
12. Gallegos, C.; Calahorro, C.; Munoz, J.; Berjano, M.; Guerrero, A. High-HLB sucrose esters: A peculiar viscous behaviour. *Comun. Jorn. Com. Esp. Deterg.* **1991**, *22*, 283-295.
13. Calahorro, C.; Munoz, J.; Berjano, M.; Guerrero, A.; Gallegos, C. Flow behavior of sucrose stearate/water systems. *J. Am. Oil Chem. Soc.* **1992**, *69*, 660-666.

14. Szuts, A.; Budai-Szucs, M.; Eros, I.; Otomo, N.; Szabo-Revesz, P. Study of gel-forming properties of sucrose esters for thermosensitive drug delivery systems. *Int. J. Pharm.* **2010**, *383*, 132-137.
15. Ullrich, S.; Metz, H.; Maeder, K. Sucrose ester nanodispersions: Microviscosity and viscoelastic properties. *Eur. J. Pharm. Biopharm.* **2008**, *70*, 550-555.
16. Mishra, P.R.; Al Shaal, L.; Mueller, R.H.; Keck, C.M. Production and characterization of Hesperetin nanosuspensions for dermal delivery. *Int. J. Pharm.* **2009**, *371*, 182-189.
17. Lee, S.J.; Choi, S.J.; Li, Y.; Decker, E.A.; McClements, D.J. Protein-stabilized nanoemulsions and emulsions: Comparison of physicochemical stability, lipid oxidation, and lipase digestibility. *J. Agr. Food Chem.* **2011**, *59*, 415-427.
18. Yilmaz, E.; Borchert, H.H. Design of a phytosphingosine-containing, positively-charged nanoemulsion as a colloidal carrier system for dermal application of ceramides. *Eur. J. Pharm. Biopharm.* **2005**, *60*, 91-98.
19. Saupe, A.; Gordon, K.C.; Rades, T. Structural investigations on nanoemulsions, solid lipid nanoparticles and nanostructured lipid carriers by cryo-field emission scanning electron microscopy and Raman spectroscopy. *Int. J. Pharm.* **2006**, *314*, 56-62.
20. Mueller, R.H. *Zetapotential und Partikelladung in der Laborpraxis*; Wissenschaftliche Verlagsgesellschaft mbH: Stuttgart, Germany, 1996; Band 37, Paperback APV.
21. Wabel, C. *Influence of Lecithin on Structure and Stability of Parenteral Fat Emulsions*, PhD Thesis; Friedrich-Alexander-Universität, Erlangen-Nürnberg, Germany, 1998.
22. Schalbart, P.; Kawaji, M.; Fumoto, K. Formation of tetradecane nanoemulsion by low-energy emulsification methods. *Int. J. Refr.* **2010**, *33*, 1612-1624.
23. Rao, M.A. *Rheology of Fluid and Semisolid Foods: Principles and Applications*; Aspen Publishers Inc.: Gaithersburg, MD, USA, 1999.
24. Taherian, A.R.; Fustier, P.; Ramaswamy, H.S. Effect of added oil and modified starch on rheological properties, droplet size distribution, opacity and stability of beverage cloud emulsions. *J. Food Eng.* **2006**, *77*, 687-696.
25. Valenta, C.; Kast, C.E.; Harich, I.; Bernkop-Schnuerch, A. Development and *in vitro* evaluation of a mucoadhesive vaginal delivery system for progesterone. *J. Control. Release* **2001**, *77*, 323-332.
26. Valenta, C.; Schultz, K. Influence of carrageenan on the rheology and skin permeation of microemulsion formulations. *J. Control. Release* **2004**, *95*, 257-265.
27. Klang, S.H.; Baszkinb, A.; Benita, S. The stability of piroxicam incorporated in a positively-charged submicron emulsion for ocular administration. *Int. J. Pharm.* **1996**, *132*, 33-44.
28. Michniak-Kohn, B.B.; Wertz, P.W.; Al-Khalili, M.; Meidan, V.M. Skin: Physiology and Penetration Pathways. In *Delivery System Handbook for Personal Care and Cosmetic Products*; Rosen, M.R., Ed.; William Andrew Inc.: New York, NY, USA, 2005; pp. 77-100.
29. Hoeller, S.; Valenta, C. Effect of selected fluorinated drugs in a "ringing" gel on rheological behaviour and skin permeation. *Eur. J. Pharm. Biopharm.* **2007**, *66*, 120-126.
30. Lin, C.; Lin, H.; Chenc, H.; Yu, M.; Lee, M. Stability and characterisation of phospholipid-based curcumin-encapsulated microemulsions. *Food Chem.* **2009**, *116*, 923-928.

31. Maiti, K.; Mukherjee, K.; Gantait, A.; Saha, B.P.; Mukherjee, P.K. Curcumin-phospholipid complex: Preparation, therapeutic evaluation and pharmacokinetic study in rats. *Int. J. Pharm.* **2007**, *330*, 155-163.
32. Hahn, T.; Hansen, S.; Neumann, D.; Kostka, K.H.; Lehr, C.M.; Muys, L.; Schaefer, U.F. Infrared densitometry: A fast and non-destructive method for exact stratum corneum depth calculation for *in vitro* tape-stripping. *Skin Pharmacol. Physiol.* **2010**, *23*, 183-192.
33. Klang, V.; Schwarz, J.C.; Hartl, A.; Valenta, C. Facilitating *in vitro* tape stripping: Application of infrared densitometry for quantification of porcine stratum corneum proteins. *Skin Pharmacol. Physiol.* **2011**, in press.
34. Breternitz, M.; Flach, M.; Prassler, J.; Elsner, P.; Fluhr, J.W. Acute barrier disruption by adhesive tapes is influenced by pressure, time and anatomical location: Integrity and cohesion assessed by sequential tape stripping. A randomized, controlled study. *Br. J. Dermatol*. **2007**, *156*, 231-240.
35. Lademann, J.; Jacobi, U.; Surber, C.; Weigmann, H.J.; Fluhr, J.W. The tape stripping procedure--evaluation of some critical parameters. *Eur. J. Pharm. Biopharm.* **2009**, *72*, 317-323.
36. Voegeli, R.; Heiland, J.; Doppler, S.; Rawlings, A.V.; Schreier, T. Efficient and simple quantification of stratum corneum proteins on tape strippings by infrared densitometry. *Skin Res. Technol.* **2007**, *13*, 242-251.
37. Hanyšová, L.; Mokrý, M.; Kastner, P.; Klimeš, J. HPLC Evaluation of Diclofenac in the Various Forms of Therapeutic Preparations. *Chem. Pap.* **2005**, *59*, 103-108.
38. Rao, J.; McClements, D.J. Stabilization of phase inversion temperature nanoemulsions by surfactant displacement. *J. Agr. Food Chem.* **2010**, *58*, 7059-7066.
39. Benita, S.; Levy, M.Y. Submicron emulsions as colloidal drug carriers for intravenous administration: Comprehensive physicochemical characterization. *J. Pharm. Sci.* **1993**, *82*, 1069-1079.
40. Sznitowska, M.; Janicki, S.; Dabrowska, E.; Zurowska-Pryczkowska, K. Submicron emulsions as drug carriers. Studies on destabilization potential of various drugs. *Eur. J. Pharm. Sci.* **2001**, *12*, 175-179.
41. Jahanzad, F.; Josephides, J.; Mansourian, A.; Sajjadi, S. Dynamics of Transitional Phase Inversion Emulsification: Effect of Addition Time on the Type of Inversion and Drop Size. *Ind. Eng. Chem. Res.* **2010**, *49*, 7631-7637.
42. Keck, C.M.; Mueller, R.H. Size analysis of submicron particles by laser diffractometry--90% of the published measurements are false. *Int. J. Pharm.* **2008**, *355*, 150-163.
43. Gradzielski, M.; Bergmeier, M.; Mueller, M.; Hoffmann, H. Novel Gel Phase: A Cubic Phase of Densely Packed Monodisperse, Unilamellar Vesicles. *J. Phys. Chem. B* ***1997***, *101*, 1719-1722.
44. Gradzielski, M.; Mueller, M.; Bergmeier, M.; Hoffmann, H.; Hoinkis, E. Structural and Macroscopic Characterization of a Gel Phase of Densely Packed Monodisperse, Unilamellar Vesicles. *J. Phys. Chem. B* ***1999***, *103*, 1416-1424.
45. Kawada, H.; Kume, T.; Matsunaga, T.; Iwai, H.; Sano, T.; Shibayama, M. Structure and Rheology of a Self-Standing Nanoemulsion. *Langmuir* **2009**, *26*, 2430-2437.
46. Sadtler, V.M.; Guely, M.; Marchal, P.; Choplin, L. Shear-induced phase transitions in sucrose ester surfactant. *J. Colloid. Interface Sci.* **2004**, *270*, 270-275.

47. Savic, S.D.; Savic, M.M.; Vesic, S.A.; Vuleta, G.M.; Mueller-Goymann, C.C. Vehicles based on a sugar surfactant: Colloidal structure and its impact on *in vitro*/*in vivo* hydrocortisone permeation. *Int. J. Pharm.* **2006**, *320*, 86-95.
48. Mason, T.G.; Graves, S.M.; Wilking, J.N.; Lin, M.Y. Extreme emulsification: Formation and structure of nanoemulsions. *Condens. Matter Phys.* **2006**, *1*, 193-199.
49. Graves, S.; Meleson, K.; Wilking, J.; Lin, M.Y.; Mason, T.G. Structure of concentrated nanoemulsions. *J. Chem. Phys.* **2005**, *122*, 134703-1-134703-16.
50. Cortés-Muñoz, M.; Chevalier-Lucia, D.; Dumay, E. Characteristics of submicron emulsions prepared by ultra-high pressure homogenisation: Effect of chilled or frozen storage. *Food Hydrocolloid.* **2009**, *23*, 640-654.
51. Tadros, T.; Izquierdo, P.; Esquena, J.; Solans, C. Formation and stability of nano-emulsions. *Adv. Colloid Interface Sci.* **2004**, *108-109*, 303-318.
52. Heuschkel, S. *Untersuchungen zum Mechanismus der Penetrationserhöhung durch Mikroemulsionen und neue Enhancer bei der dermalen Applikation von Wirkstoffen*, PhD Thesis; Martin-Luther-University, Halle-Wittenberg, Germany, 2009.
53. McClements, D.J. *Food Emulsions: Principles, Practices, and Techniques*; CRC Press: Boca Raton, FL, USA, 2005.
54. Valdez, M.A.; Acedo-Carrillo, J.I.; Rosas-Durazo, A.; Lizardi, J.; Rinaudo, M.; Goycoolea, F.M. Small-deformation rheology of mesquite gum stabilized oil in water emulsions. *Carbohyd. Polym.* **2006**, *64*, 205-211.
55. Mason, T.G.; Graves, S.M.; Wilking, J.N.; Lin, M.Y. Effective structure factor of osmotically deformed nanoemulsions. *J. Phys. Chem. B* **2006**, *110*, 22097-22102.
56. Lee, C.H.; Moturi, V.; Lee, Y. Thixotropic property in pharmaceutical formulations. *J. Control. Release* **2009**, *136*, 88-98.
57. Friedman, D.I.; Schwarz, J.S.; Weisspapir, M. Submicron emulsion vehicle for enhanced transdermal delivery of steroidal and nonsteroidal antiinflammatory drugs. *J. Pharm. Sci.* ***1995***, *84*, 324-329.
58. Bouchemal, K.; Briancon, S.; Perrier, E.; Fessi, H. Nano-emulsion formulation using spontaneous emulsification: Solvent, oil and surfactant optimisation. *Int. J. Pharm.* **2004**, *280*, 241-251.
59. Wu, X.; Biatry, B.; Cazeneuve, C.; Guy, R.H. Drug delivery to the skin from sub-micron polymeric particle formulations: Influence of particle size and polymer hydrophobicity. *Pharm. Res*. **2009**, *26*, 1995-2001.
60. Wagner, H.; Kostka, K.H.; Lehr, C.M.; Schaefer, U.F. Drug distribution in human skin using two different *in vitro* test systems: Comparison with *in vivo* data. *Pharm. Res*. **2000**, *17*, 1475-1481.
61. Stracke, F.; Weiss, B.; Lehr, C.M.; Koenig, K.; Schaefer, U.F.; Schneider, M. Multiphoton microscopy for the investigation of dermal penetration of nanoparticle-borne drugs. *J. Invest. Dermatol*. **2006**, *126*, 2224-2233.

© 2011 by the authors; licensee MDPI, Basel, Switzerland. This article is an open access article distributed under the terms and conditions of the Creative Commons Attribution license (http://creativecommons.org/licenses/by/3.0/).

ARTICLE IN PRESS

European Journal of Pharmaceutics and Biopharmaceutics xxx (2011) xxx–xxx

Contents lists available at SciVerse ScienceDirect

European Journal of Pharmaceutics and Biopharmaceutics

journal homepage: www.elsevier.com/locate/ejpb

Research paper

In vitro vs. in vivo tape stripping: Validation of the porcine ear model and penetration assessment of novel sucrose stearate emulsions

Victoria Klang [a], Julia C. Schwarz [b], Barbara Lenobel [a], Martina Nadj [a], Josef Auböck [c], Michael Wolzt [d], Claudia Valenta [a,b,*]

[a] University of Vienna, Department of Pharmaceutical Technology and Biopharmaceutics, Faculty of Life Sciences, Vienna, Austria
[b] University of Vienna, Research Platform "Characterisation of Drug Delivery Systems on Skin and Investigation of Involved Mechanisms", Vienna, Austria
[c] Allgemeines Krankenhaus der Stadt Linz, Abteilung für Dermatologie und Venerologie, Linz, Austria
[d] Universitätsklinik für Klinische Pharmakologie, AKH Wien und Medizinische Universität Wien, Vienna, Austria

ARTICLE INFO

Article history:
Received 11 August 2011
Accepted in revised form 10 November 2011
Available online xxxx

Keywords:
Tape stripping
Porcine ears
Skin penetration
Sucrose stearate
Nanoemulsion

ABSTRACT

Porcine ear skin is frequently used as a substitute for human skin in dermatological research and is especially useful for tape stripping experiments where the penetration of active substances into the uppermost skin layers is investigated. However, certain differences between the surface properties of these skin types exist, and reports on the comparability of tape stripping data obtained in vitro using porcine ear skin and data obtained in vivo on human forearm skin are scarce. Thus, we performed comparative tape stripping experiments in which the skin penetration of curcumin and fluorescein sodium from conventional microemulsions and hydrogels was investigated. In this context, the skin penetration potential of novel semi-solid macroemulsions and fluid nanoemulsions based on sucrose stearate was evaluated as well. The removed corneocytes were quantified by NIR-densitometry using recent correlation data for human and porcine proteins. The trends observed for the skin penetration into porcine ear skin were highly representative for the in vivo situation on human skin, confirming that the porcine ear is an excellent in vitro model for tape stripping experiments. Moreover, the validity of the NIR-densitometric approach for the quantification of both human and porcine stratum corneum proteins was confirmed in this study for the first time.

© 2011 Elsevier B.V. All rights reserved.

1. Introduction

Tape stripping is a well-established method to investigate the skin penetration of topically applied substances. The superficial layers of the stratum corneum (SC) are removed with adhesive films, which are subsequently analysed for their drug and protein content. Thus, the amount of penetrated drug and the penetration depth into the skin can be determined [1,2]. Recently, near-infrared densitometry (NIR-densitometry) has been shown to possess great potential for the analysis of the SC proteins removed with each tape and has subsequently been validated for in vivo [3] and in vitro [4] tape stripping on human skin. However, in vivo studies may be associated with significant organisational and legislative issues, and the sources for excised human skin for in vitro studies are limited. In tape stripping experiments, the excised porcine ear has been shown to be a suitable skin substitute for human skin in vivo [2] since the ear skin, which remains on the cartilage during the experiments, does not contract [5]. In fact, this renders porcine ear skin even more suitable for in vitro tape stripping than excised human skin or excised porcine skin from other areas [6]. Thus, the NIR-densitometric method of protein quantification has been validated for this application as well [7].

Valuable information on the porcine ear skin model in general can be found [5]. However, only few reports deal with the use of porcine ear skin for in vitro tape stripping [8,9] and quantification of the porcine proteins removed with the tapes [2,10]. There is a surprising lack of comparative studies, which deal with conventional vehicles applied in a non-occluded fashion, although it may be assumed that a vast majority of topical formulations is applied in this manner. Validation of the porcine ear model under these conditions using different formulations of practical relevance seems essential to legitimate its use for in vitro tape stripping.

Abbreviations: SC, stratum corneum; NIR-densitometry, near-infrared densitometry; TEWL, transepidermal water loss.

* Corresponding author. University of Vienna, Department of Pharmaceutical Technology and Biopharmaceutics, Althanstrasse 14, 1090 Vienna, Austria. Tel.: +43 1 4277 55 410; fax: +43 1 4277 9554.

E-mail addresses: victoria.klang@univie.ac.at (V. Klang), julia.schwarz@univie.ac.at (J.C. Schwarz), josef.auboeck@akh.linz.at (J. Auböck), michael.wolzt@meduniwien.ac.at (M. Wolzt), Claudia.valenta@univie.ac.at (C. Valenta).

0939-6411/$ - see front matter © 2011 Elsevier B.V. All rights reserved.
doi:10.1016/j.ejpb.2011.11.009

Please cite this article in press as: V. Klang et al., In vitro vs. in vivo tape stripping: Validation of the porcine ear model and penetration assessment of novel sucrose stearate emulsions, Eur. J. Pharm. Biopharm. (2011), doi:10.1016/j.ejpb.2011.11.009

Detailed comparative information should be obtained through parallel tape stripping on human and porcine skin with substances of different log*P* values.

Thus, the aim of this study was to compare the skin penetration of two well-established model substances, namely the lipophilic dye curcumin and the hydrophilic dye fluorescein sodium, from different formulations applied on porcine ear skin in vitro and human skin in vivo. Classical formulations such as a microemulsion and an alcoholic hydrogel were employed as vehicles for this task. Recently developed skin-friendly O/W macroemulsions and nanoemulsions were additionally tested for their drug delivery potential in vivo. Interestingly, these formulations of identical composition had yielded highly comparable skin penetration rates in vitro despite significant differences in particle size and viscosity [11]. Thus, in vivo tape stripping should reveal whether this phenomenon was confined to the realms of in vitro set-ups or would be observed in vivo as well.

In summary, the present work aims to validate the porcine ear skin model for in vitro tape stripping experiments while using the novel technique of NIR-densitometry for protein quantification of both porcine and human skin. Since differences in the pattern of wrinkles, the corneocyte distribution and the pseudo-absorption at 850 nm of porcine and human corneocytes have been reported [7,12], the present study should elucidate whether these factors would impair the comparability of porcine and human skin penetration profiles. Determination of the transepidermal water loss (TEWL) as a biophysical skin analysis technique was additionally employed to ensure integrity of the skin of both volunteers and porcine ears. Long-term monitoring of the TEWL of human volunteers was conducted to determine the physiological TEWL range and to ensure representative skin properties for later tape stripping.

2. Materials and methods

2.1. Materials

Standard Corneofix® adhesive films with a square area of 4.0 cm^2 were obtained from Courage + Khazaka GmbH (Cologne, Germany). Curcumin (CAS: 458-37-7), fluorescein sodium salt (CAS: 518-47-8) and potassium sorbate (CAS: 24634-61-5) were purchased from Sigma Aldrich (St. Louis, USA). Sucrose stearate (Ryoto Sugar Ester® S-970) was supplied by Mitsubishi-Kagaku Food Corporation (Tokyo, Japan). PCL-liquid (cetearyl ethylhexanoate/isopropyl myristate, CAS: 90411-68-0) and propylene glycol (1,2-propanediol, CAS: 57-55-6) were purchased from Dr. Temt Laboratories (Vienna, Austria). Oleic acid (CAS: 112-18-1), carbopol® 940 polymer (CAS: 9063-87-0) and TRIS (tris(hydroxymethyl)-aminomethane 2% w/w buffer solution, CAS: 77-86-1) were obtained from Herba Chemosan Apotheker-AG (Vienna, Austria). The lecithin mixture lipoid S-75 was kindly donated by Lipoid GmbH (Ludwigshafen, Germany). Ultraphil® amphiphilic cream was purchased from Intendis Austria GmbH (Vienna, Austria). According to the manufacturer, the compounds of this cream are glycerol distearate, glycerol monostearate, liquid paraffin, polyoxyethylene 100 stearate, polyoxyethylene 2 and 21 stearyl alcohol, white vaseline, distilled water, benzyl alcohol and perfume oil. The traditional Austrian product spiritus vini gallici 60% (Franzbranntwein) was prepared according to the Codex Alimentarius Austriacus (Chapter B33) by diluting an extract (Urkörper Gallhuber 60%, Herba Chemosan Apotheker-AG, Vienna, Austria) with appropriate amounts of ethanol, menthol and distilled water (1:10/0.2/10 w/w). All further chemicals such as the solvents ethanol (CAS: 64-17-5) and isopropanol (CAS: 67-63-0) used were of analytical reagent grade and used as obtained from Sigma Aldrich (St. Louis, USA).

2.2. Formulations

Established formulations were employed for the comparative tape stripping experiments on porcine ear skin in vitro and human skin in vivo, namely a lecithin-based microemulsion [13] and an alcoholic hydrogel. The amphiphilic cream ultraphil® was employed for preliminary in vitro studies. The novel sucrose stearate-based emulsions were evaluated only by in vivo tape stripping since their penetration behaviour in vitro had already been established [11]. The composition of the individual formulations is given in Table 1.

The microemulsion was prepared by dissolving the lecithin mixture in isopropanol, ethanol and oleic acid. Distilled water was slowly added during magnetic stirring.

The hydrogel was prepared by dissolving the polymer carbopol® 940 in a mixture of spiritus vini gallici, propylene glycol and isopropanol. A homogeneous gel network was formed upon addition of the TRIS buffer solution under mild mechanical stirring.

The sucrose stearate-based macroemulsions and corresponding nanoemulsions were prepared as described [11]. The separate oil and aqueous phases were mixed and stirred with an ultra-turrax (Omni 500, 2500 rpm, 4 min). In case of the fluid nanoemulsions, the mixture was further treated with a high-pressure homogeniser (EmulsiFlex C3, Avestin) for 20 cycles at 750 bars.

The model drug curcumin was incorporated into all above mentioned formulations at 0.5% (w/w), respectively. The hydrophilic model drug fluorescein sodium was dissolved in the microemulsion for comparative investigation at 0.5% (w/w). The drug content of all formulations was determined after preparation to confirm drug incorporation. In case of curcumin, 10 mg of the respective formulation was dissolved in 1 ml of ethanol (96% v/v). The samples were homogenised in an ultrasonic bath at 30 kHz (US Starsonic 60, Liarre, Italy) for 20 min and then centrifuged for 6 min at 12,000 rpm (Hermle Z323 K, MIDSCI, USA). Subsequently, 0.5 ml of each sample was further diluted with ethanol (96% v/v, 1:10) and analysed by UV/Vis spectroscopy as described in Section 2.10. In case of fluorescein sodium, the same procedure was conducted with phosphate buffer (pH 7.4, 0.012 M) instead of ethanol. For drug quantification, 100 μl of the diluted samples was transferred into a microtiter plate in triplicate and analysed by fluorescence spectroscopy as described in Section 2.11. Samples were always taken at least in triplicate ($n \geqslant 3$).

2.3. Skin tissue

Fresh porcine ears were obtained from the Clinic for Swine at the University of Veterinary Medicine Vienna, Austria. The age of the slaughtered pigs was around 6 months. To ensure integrity of the skin barrier, the ears were removed before the carcass was exposed to any high-temperature cleaning procedure [9]. The ears were washed carefully under cold running water and blotted dry with soft tissue. All ears were stored at −20 °C and thawed prior to the experiments since the main penetration barrier, the non-vital superficial SC layer, is not influenced by frozen storage [4,14]. All experiments were carried out at room temperature. The skin remained on the isolated ear. In addition, porcine abdominal skin was tested in preliminary studies, but was found unsuitable for tape stripping experiments. The SC of porcine abdominal skin is thinner than that of the dorsal side of porcine ears [15], thus rendering the acquisition of accurate skin penetration data difficult.

2.4. Test persons and experimental conditions

Long-term evaluation of the TEWL on the volar forearms and the forehead of human volunteers was performed on a population

Please cite this article in press as: V. Klang et al., In vitro vs. in vivo tape stripping: Validation of the porcine ear model and penetration assessment of novel sucrose stearate emulsions, Eur. J. Pharm. Biopharm. (2011), doi:10.1016/j.ejpb.2011.11.009

ARTICLE IN PRESS

Table 1
Composition of all investigated formulations in % (w/w) and abbreviations.

Microemulsion		Hydrogel		Macroemulsion/nanoemulsion	
Excipients	% (w/w)		% (w/w)		% (w/w)
Lipoid S-75	40	Propylene glycol	10	PCL-liquid	20
Isopropanol	35	Isopropanol	10	Sucrose stearate	5
Oleic acid	9.5	TRIS 2%	5.1	Potassium sorbate	0.1
Ethanol 96% v/v	5	Carbopol® 940	0.6	Model drug	0.5
Model drug	0.5	Model drug	0.5	Distilled water	74.4
Distilled water	10	Spiritus vini gallici	73.8		

Abbreviations: ME microemulsion; GE hydrogel; E macroemulsion; NE nanoemulsion.

of 26 male and female volunteers aged between 18 and 44. Written informed consent for this non-invasive procedure was obtained from all participants. Measurements were taken over 4 months.

For the tape stripping experiments, twelve healthy volunteers aged 18–44 were included after giving their written informed consent. They did not suffer from skin diseases or allergies. The study was approved by the ethics committee of the medicinal university of Vienna (EK-Nr. 503/2011). All experiments were performed according to the same protocol. The volunteers were required not to apply cosmetic or skin care products up to 12 h prior to the experiment and to avoid excessive consumption of coffee, tea or alcohol [16]. Furthermore, they were asked not to engage in physical activity prior to the experiments and to remain seated for 15 min after entering the test area with constant ambient temperature (24 ± 1 °C) and humidity (50 ± 4% relative humidity).

The steps of the working protocol for in vitro and in vivo experiments were the same: after application of a formulation, the penetration behaviour of the respective model drug was determined by tape stripping and subsequent analysis of both protein content and drug amounts found on the individual tape strips. The tape stripping procedure in combination with sensitive analytical methods allows an exact localisation of the applied drugs in the SC [17].

2.5. Transepidermal water loss (TEWL)

The TEWL of the skin was determined using the closed-chamber device AquaFlux® (Biox Ltd., London, UK) and the AquaFlux® V6.2 program for data analysis. In case of porcine ear skin, TEWL measurements were taken as a quality control to exclude areas with altered skin barrier function. Although the TEWL of excised porcine ears is hardly representative of the in vivo situation, it can serve to monitor the defrosting process and to ensure a standardised working protocol [7,8,18]. The presence of small lesions and scars can be detected since such areas exhibit noticeably higher TEWL values.

Prolonged storage of fresh or defrosted porcine ears at ambient conditions will inevitably lead to dehydration of the tissue and thus to a constant decrease in the TEWL. However, there is a sufficiently long time frame for fresh or defrosted porcine ears with average TEWL values around 15 g m^{-2} h^{-1} that represents a suitable starting point for tape stripping experiments. Therefore, the TEWL of the porcine ears was determined for all samples before the tape stripping procedure. Assessment of the TEWL after tape stripping provided additional information about changes in skin barrier function [15].

In case of human skin in vivo, determination of the TEWL is an established method for skin integrity testing [19,20]. Substantiated TEWL monitoring of human volunteers was performed to establish a database of physiologically acceptable TEWL values for different skin areas such as the volar forearms and the forehead. These data served to provide a basis for comparison to identify unsuitable skin areas or skin types prior to the tape stripping experiments. Measurements were taken in regular intervals over a period of 4 months. Volunteers were advised not to treat their skin differently than usual and not to use skin care products immediately before the measurements. The influence of parameters such as age, sex, the frequent use of skin care products, inclination to sweat, skin type and the season on the skin barrier function was evaluated in this context. Information on subjective parameters, such as the use of skin care products and the inclination to sweat of the individual volunteers, was gained by means of a questionnaire.

2.6. Preliminary experiments: optimisation of tape stripping working protocol

Preliminary experiments were performed to identify the most suitable working protocol for in vitro tape stripping. The effect of different application times was investigated. To this end, tape stripping was performed after 1 and 4 h following the application of the respective formulation. The selected model formulations used were the microemulsion, the hydrogel and the amphiphilic cream ultraphil® with curcumin.

2.7. In vitro tape stripping

In vitro skin penetration profiles were established for the curcumin-loaded microemulsion, hydrogel and ultraphil® cream as well as for the microemulsion with fluorescein sodium. At least six individual tape stripping experiments were performed for each formulation on porcine ear skin ($n \geqslant 6$, respectively). After defrosting and cleaning, the skin was blotted dry with soft tissue and freed from visible hair with scissors. The ears were stretched out on styrofoam plates and fixed with needles. Intact, representative skin areas of 15 cm^2 were indicated with a permanent marker. The TEWL of the skin was determined with the AquaFlux® device (Biox Ltd., London, UK) to confirm an intact skin barrier function [7]. When the TEWL reached values between 15 and 20 g m^{-2} h^{-1}, the respective formulation was applied onto the skin by means of a saturated glove finger at a concentration of 2 mg cm^{-2} and gently distributed for 30 s. After an application time of 1 or 4 h, the tape stripping procedure was started.

The adhesive films employed to remove the superficial SC layers were standard Corneofix® tapes. Care was taken to ensure a reproducible working procedure [3,21]. The outline of the first adhesive film was indicated with a permanent marker to facilitate subsequent tape stripping on the same location. Pressure was applied with the thumb covered in a vinyl glove [22] to ensure a rolling movement and thus minimise the influence of wrinkles [1]. While a roller is among the most suitable devices to flatten out the skin during in vivo tape stripping, the skin of excised pig ears provides less space for handling a roller. Experience has shown that a rolling movement performed by the thumb leads to the most efficient and homogeneous removal of porcine corneocytes in vitro [7,22]. Thus, this working protocol was

Please cite this article in press as: V. Klang et al., In vitro vs. in vivo tape stripping: Validation of the porcine ear model and penetration assessment of novel sucrose stearate emulsions, Eur. J. Pharm. Biopharm. (2011), doi:10.1016/j.ejpb.2011.11.009

adopted for the in vitro experiments. A piece of paper was placed between the tape and the thumb to avoid a transfer of emulsion from the adjacent skin parts to the adhesive film [23]. The experiment was performed on a balance to ensure a constant pressure of 49 N (5 kg) [7]. After applying pressure for 3 s, the tape was removed in a single rapid movement. In case of curcumin-loaded formulations, 20 sequential tape strips were removed. Since a higher penetration depth was anticipated for fluorescein sodium, 40 tape strips were removed in this case.

2.8. In vivo tape stripping

In vivo skin penetration experiments were performed on 12 healthy test persons. The penetration profiles were established for the curcumin-loaded microemulsion and hydrogel as well as for the microemulsion with fluorescein sodium. Moreover, the novel curcumin-loaded macroemulsion and nanoemulsion were investigated in the same fashion. Six individual experiments on the human flexor forearm were performed for each formulation ($n = 6$, respectively).

Representative intact skin areas of 15 cm^2 were indicated with a permanent marker. The TEWL of the skin was determined as described above. The respective formulation was then applied onto the skin by means of a saturated glove finger at a concentration of 2 mg cm^{-2} and gently distributed for 30 s. After an application time of 30 min, the tape stripping procedure was conducted. In this case, pressure was applied with a roller [1,23]. Except for the means and intensity of pressure application and the application time, the working procedure was identical to that employed for the porcine ears.

2.9. Protein quantification by NIR-densitometry

We recently validated NIR-densitometry for the quantification of porcine skin during in vitro tape stripping [7]. In the present work, we tested the proposed method for in vitro tape stripping experiments on porcine skin for comparison with in vivo data, for the first time using different formulations.

The amount of corneocytes removed with the individual adhesive films was analysed using the infrared densitometer SquameScan™ 850A (Heiland electronic GmbH, Wetzlar, Germany). The removed tape strips were measured at a wavelength of 850 nm as previously described using an empty tape strip as a reference [3,4]. Thus, the optical pseudo-absorption of the adhesive films that is caused by an interaction of the corneocyte aggregates with light via scattering, diffraction and reflection was determined [23]. Since the device has been validated separately for porcine and human skin, the respective calibration data were used for protein quantification. In case of porcine skin, the mass of SC proteins (m) can be calculated after determination of their pseudo-absorption (A) for a normalised tape area of 1 cm^2 by employing the equation $m = A/0.41$ (in μg cm^{-2}) [7]. In case of human proteins, the equation derived from the respective calibration curve can be employed for this task, namely $m = (A - 2.703)/0.623$ (in μg cm^{-2}) [3]. The mean cumulative amount of removed SC proteins was employed to establish the penetration depth of the applied drugs in relation to the complete SC thickness. Experience has shown that the SC thickness of both human forearm skin and pig ear skin can vary considerably for each individual [7,9]. Since removal of the entire SC in each case is too much organisational effort and an additional strain for the volunteers, we employed well-established reference values for the entire SC thickness in accordance with the literature [9]. Thus, the thickness of the SC of porcine ear skin was assumed with 8.2 μm and the thickness of human SC of the volar forearm with 11.0 μm.

2.10. Curcumin quantification by UV/Vis spectroscopic analysis

After NIR analysis, the individual tapes containing corneocytes and curcumin were dissolved in 4 ml of ethanol (96% v/v). The samples were homogenised in an ultrasonic bath at 30 kHz (US Starsonic 60, Liarre, Italy) for 20 min and centrifuged for 6 min at 12,000 rpm (Hermle Z323K, MIDSCI, USA). The resulting curcumin solutions were analysed by UV/Vis spectroscopy. The quantification was performed as previously reported [17,24] using a double beam UV/Vis spectrophotometer (Spectrophotometer U-3010, Hitachi, Japan). A calibration curve was established for standard solutions of curcumin in ethanol (96% v/v) ranging from 0.31 μg/ml to 5.01 μg/ml with $R^2 = 0.9952$. The curcumin content of the samples filled into quartz cuvettes was determined at 425 nm against a control sample of an extracted blank tape strip. Samples containing higher curcumin content were diluted prior to analysis until values within the linear range of the calibration curve were obtained. This was occasionally the case for samples extracted from the first adhesive film of the experiments.

2.11. Fluorescein sodium quantification by fluorescence spectroscopy

After NIR analysis, the tapes containing corneocytes and fluorescein sodium were dissolved in 4 ml of phosphate buffer (pH 7.4, 0.012 M). As described above for curcumin, the samples were homogenised and centrifuged. The resulting fluorescein sodium solutions were analysed by fluorescence spectroscopy. The quantification was conducted using a microplate reader (Tecan™ infinite 200, Tecan Ltd., Maennedorf, Switzerland) at an excitation wavelength of 485 nm, an emission wavelength of 535 nm and a constant gain of 78. A calibration curve was established for standard solutions of fluorescein sodium in phosphate buffer (pH 7.4, 0.012 M) ranging from 0.04 μg/ml to 5.07 μg/ml with $R^2 = 0.9992$ to quantify the drug content of the samples. Samples containing a higher content of fluorescein sodium were diluted prior to analysis. For drug quantification, 100 μl of the diluted samples was pipetted into a microtiter plate in triplicate and analysed against control solutions of extracted blank adhesive films.

2.12. Statistical data analysis

Results are generally expressed as means of three or more experiments ± SD. Statistical data analyses were performed with the program GraphPadPrism3 while using $P < 0.05$ as a minimum level of significance in all cases. Parametric data were analysed using the Student's t test or ANOVA, while non-parametric data were analysed using the Mann–Whitney test or the Kruskal–Wallis test.

3. Results and discussion

In summary, both visual inspection and analysis of the drug content of the formulations confirmed their suitability for the subsequent experiments (data not shown). The following sections deal with the results of the in vitro experiments, followed by the results obtained in vivo and conclusive remarks on the similarities and differences between the data.

3.1. In vitro experiments: porcine ear skin

3.1.1. Transepidermal water loss (TEWL)

The TEWL of fresh or defrosted porcine ear skin in vitro can be employed as an indicator for the intactness of the SC barrier function [25,26]. Since the excised ear does not possess any metabolism, the determined values will of course differ from those

Please cite this article in press as: V. Klang et al., In vitro vs. in vivo tape stripping: Validation of the porcine ear model and penetration assessment of novel sucrose stearate emulsions, Eur. J. Pharm. Biopharm. (2011), doi:10.1016/j.ejpb.2011.11.009

ARTICLE IN PRESS

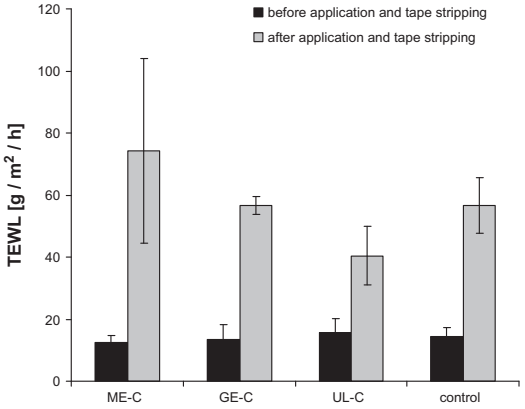

Fig. 1. TEWL of porcine ear skin in vitro measured before and after tape stripping. The influence of the applied formulation on the extent of SC barrier disruption is demonstrated. The TEWL before and after tape stripping of the area treated with the microemulsion containing curcumin is given on the left (ME-C, 20 tapes), followed by the corresponding data for the curcumin-loaded hydrogel (GE-C, 20 tapes) and ultraphil® (UL-C, 20 tapes). The respective values represent the means ± SD of at least seven experiments ($n \geqslant 7$). An untreated skin site, respectively, served as a control (20 tapes, $n = 23$).

in vivo. Nevertheless, experience has shown that lesions or irregularities in the SC barrier function can be identified. The results of the TEWL measurements conducted during in vitro tape stripping are given in Fig. 1. The TEWL value of intact porcine ear skin before tape stripping was always between 10 and 20 g m^{-2} h^{-1}. The experiments were then started immediately to prevent dehydration of the tissue. Upon removal of 20 adhesive films from untreated skin regions, the TEWL increased significantly ($P < 0.05$). However, as can be derived from the large standard deviation, this increase can vary to a large extent due to inter-individual differences. Such differences tend to become negligible upon further tape stripping of the same area. After the removal of 40 tapes from the untreated skin site, the TEWL values reached a peak around 80 g m^{-2} h^{-1}. It may be assumed that the majority of the SC was removed at this point. Removal of further tapes until the complete SC was removed only led to minor increase in the TEWL after this point (data not shown). These findings confirm previous data [7].

Apart from these observations regarding the TEWL of untreated tape stripped skin, the effect of the different formulations applied before tape stripping was investigated (Fig. 1). Apparently, the different formulations influenced the extent of SC barrier disruption during tape stripping in accordance with the employed excipients. The microemulsion, containing large amounts of surfactant and solvents, led to a significantly larger increase in the TEWL after the removal of 20 tapes when compared to the corresponding control site ($P < 0.05$). In contrast, the TEWL values obtained after the removal of 20 tapes from skin sites treated with the hydrogel were comparable to the control ($P > 0.05$). The lowest increase in TEWL was observed after treatment for the skin with ultraphil® cream, which was even lower than the value of the control site ($P < 0.05$). The extent of the SC barrier disruption in vitro can thus be ranked as ME > GE/Control > ultraphil®.

3.1.2. Influence of application time on in vitro skin penetration

Different application times of 1 and 4 h were tested in corresponding experiments with the curcumin-loaded microemulsion, the hydrogel and the ultraphil® cream. The results of these studies are given in Table 2. No significant differences in penetration depth or recovered drug amounts were found for the microemulsion or the hydrogel after 1 and 4 h of application time ($P > 0.05$, respectively). However, a slight tendency towards lower values of penetration depth and drug amounts was generally observed. This indicates that the prolonged application time in vitro does not necessarily yield higher skin penetration. On the contrary, lateral diffusion of the drug may occur [27–29] and dehydration effects may take hold. It was thus decided that 1 h of application time was sufficient for the envisioned experiments. Comparable working protocols have been successfully employed in previous in vitro studies [2]. The phenomenon of the potential lateral spreading effect after prolonged application will be subject of further studies.

In case of the ultraphil® cream, the extent of skin penetration was highly unsatisfying after 1 h. Merely, a prolonged application time of 4 h led to noticeable skin penetration of the drug while a significant amount of formulation still remained on the skin surface. It was apparent that the penetration depth of curcumin when applied in this vehicle was significantly lower even after 4 h of application time than from the other formulations ($P < 0.05$, respectively). Besides, remnants of the formulation still impaired the tackiness of the first adhesive films. Due to its lack of penetration and spreading, ultraphil® cream was thus excluded from further experiments. Modification of the working protocol towards cleaning of the skin surface was not deemed appropriate within the context of the envisioned comparative studies, but this aspect will be investigated separately at a later point.

Regarding the rank order of penetration depth of the compared formulations, an obvious tendency was apparent, namely microemulsion ⩾ hydrogel > ultraphil® cream. Both the microemulsion and the hydrogel yielded significantly higher skin penetration depths than the ultraphil® cream ($P < 0.05$). A statistically significant difference between the penetration depth of the microemulsion over the hydrogel was only reached after 4 h of application time ($P < 0.05$).

Summarising our experiences with different application times, only a slightly longer treatment for the skin than for in vivo experiments seemed most appropriate. The excised porcine ear lacks circulation and is subjected to constant dehydration during the experiment. Insufficient application times might lead to erroneously low penetration depths, which do not represent the in vivo situation. Prolonged application times may yield representative results, but may also promote unphysiological dehydration of the tissue and lateral spreading [27,30]. The decreased skin hydration, accompanied by lower TEWL values, leads to decreased skin diffusion of drugs. This effect might annihilate the positive effect of a longer application time [31]. Although the isolated porcine ear is a suitable and representative model for short-time studies, it appears to be less adequate for longer application periods, especially for highly lipophilic drugs. Appropriate sink conditions may not be reached due to the lack of cutaneous circulation [9]. Thus, decreased penetration rates of model drugs after prolonged penetration times may occur [32].

3.1.3. In vitro skin penetration profiles

The results of the in vitro tape stripping experiments for both curcumin and fluorescein sodium after 1 h of application time are summarised in Table 2. Overall, the amount of penetrated drug was highly comparable for all in vitro experiments irrespective of the lipophilicity of the investigated drug and the type of formulation ($P > 0.05$). In contrast, the penetration depth of the different drugs was influenced by both the excipients of the formulations and the log P value of the drug. The hydrophilic fluorescein sodium achieved deeper skin penetration than the lipophilic curcumin from the corresponding microemulsion ($P < 0.05$), reaching values around 50% of the entire SC. This might be due to the different solubilities of the drugs within the microemulsions. After

Please cite this article in press as: V. Klang et al., In vitro vs. in vivo tape stripping: Validation of the porcine ear model and penetration assessment of novel sucrose stearate emulsions, Eur. J. Pharm. Biopharm. (2011), doi:10.1016/j.ejpb.2011.11.009

ARTICLE IN PRESS

Table 2
In vitro skin penetration data for the different investigated formulations after application of 2 mg/cm^2 on porcine ear skin. The influence of different application times of 1 and 4 h on skin penetration of curcumin is shown. The given values are means ± SD of at least six individual experiments for each formulation ($n \geqslant 6$).

Formulation	Application time (h)	Penetrated drug amount (μg/cm^2)	Penetration depth (μm)	Penetration depth (% of SC)
ME curc	1	7.48 ± 1.32	2.26 ± 0.85	27.56 ± 10.37
ME curc	4	6.71 ± 1.76	1.82 ± 0.65	22.20 ± 7.93
GE curc	1	8.25 ± 3.84	1.26 ± 0.69	15.37 ± 8.41
GE curc	4	7.26 ± 1.97	0.91 ± 0.36	11.10 ± 4.39
UL curc	1	Not feasible		
UL curc	4	6.58 ± 1.57	0.39 ± 0.14	4.76 ± 1.71
ME fluor	1	7.65 ± 1.56	3.82 ± 0.88	46.59 ± 10.73

application of the formulations, volatile compounds evaporate and the drugs may re-crystallise due to the destruction of the formulation structure. Since crystallised drug is no longer available for penetration, this might hinder the achieved penetration depth especially in case of lipophilic drugs that are mainly dissolved by the involved solvents (verbal communication with Dr. Thomas Franz, 2011). In case of the different curcumin-loaded formulations, an effect of the vehicle on the penetration depth of the lipophilic drug was noticeable. As already discussed, higher penetration of curcumin was obtained with the microemulsion than with the hydrogel. After 1 h of application time, these differences did not quite reach significant levels due to the strong inter-individual variability within the experiments ($P > 0.05$, with $P = 0.0505$). Nevertheless, the general tendency was apparent.

3.1.4. Influence of the formulation on the amount of removed SC proteins in vitro

An additional aspect that was investigated was the influence of the applied formulation on the amount of removed SC proteins. Fig. 2 shows the comparison between the amount of SC proteins removed from untreated porcine skin as a control and the amount of SC proteins that was removed after application of the different formulations. As can be seen in Fig. 2a, the microemulsion rapidly penetrated into the skin without leaving significant traces of formulation on the skin surface. Thus, the removal of SC proteins was not hindered by the application of the formulation when compared to the control ($P > 0.05$). In case of the hydrogel (Fig. 2b), a significant influence of the formulation on the amount of removed corneocytes was found until the 7th removed adhesive film ($P < 0.05$, respectively). Slightly lower amounts of SC were removed, possibly due to decreased tackiness of the tapes. Interestingly, no weakening of the cohesion between corneocytes caused by the ethanol within the microemulsion and the hydrogel was observed, which would have led to higher amounts of removed corneocytes [30]. The subsequent tapes were not impaired in their tackiness by the remnants of the formulation when compared to the control ($P > 0.05$). In case of ultraphil®, significantly less corneocytes were removed with all 20 adhesive films as opposed to the control ($P < 0.05$, Fig. 2c). This pronounced influence of the formulation on the tape stripping process can be ascribed to the insufficient penetration of the formulation, in particular the lipophilic compounds, which remained on the skin surface and impaired the tackiness of the tapes [30]. In such cases, cleaning of the skin surface prior to the tape stripping process appears essential to obtain reliable results. The cleaning of the skin surface with solvents may likewise influence the results obtained with the first adhesive tapes. Thus, an acceptable compromise has to be found in accordance with the respective formulation properties.

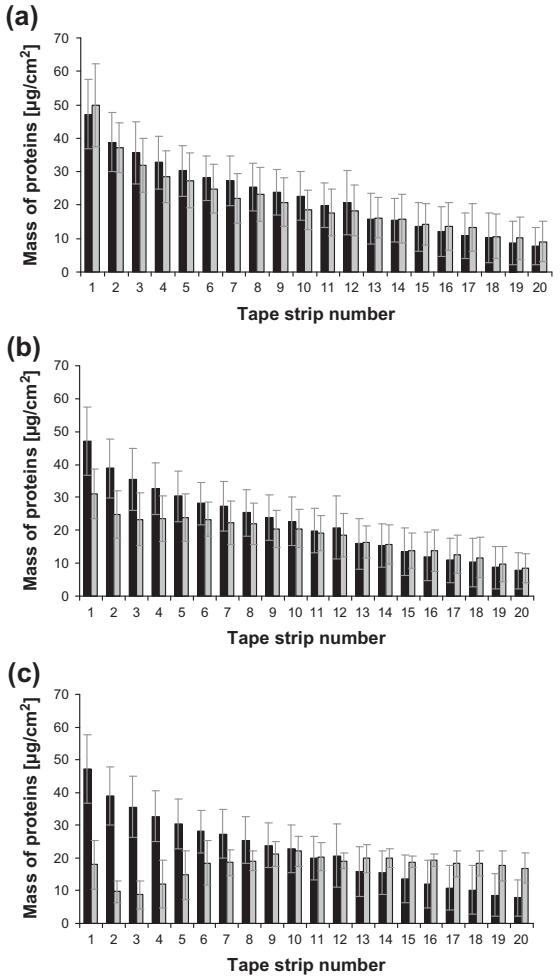

Fig. 2. Influence of the applied formulation on the amount of removed porcine SC proteins in vitro. The black bars, respectively, represent the amount of SC proteins removed from untreated skin areas (control). The grey bars, respectively, represent the amounts of SC proteins removed after the application of a microemulsion (a, after 1 h), a hydrogel (b, after 1 h) or ultraphil® cream (c, after 4 h). The given values represent the mean of at least six experiments ($n \geqslant 6$).

3.2. In vivo experiments: human forearm skin

3.2.1. Transepidermal water loss (TEWL)

The TEWL can be employed to characterise the skin barrier function of human volunteers in vivo [25,26]. The results of the long-term in vivo monitoring of the TEWL of human volunteers are given in Table 3 panels a and b. The TEWL of each volunteer was determined over the course of 4 months in regular intervals both on the forehead as well as the left and right forearm. At least 29 independent measurements were taken for each person

Please cite this article in press as: V. Klang et al., In vitro vs. in vivo tape stripping: Validation of the porcine ear model and penetration assessment of novel sucrose stearate emulsions, Eur. J. Pharm. Biopharm. (2011), doi:10.1016/j.ejpb.2011.11.009

Table 3
TEWL of human volunteers. The TEWL of each volunteer was determined over the course of 4 months by means of at least 29 independent measurements per person ($n \geqslant 29$), which were conducted in regular intervals. The mean of these TEWL values was, respectively, considered as representative for each individual. Table 2a shows the mean TEWL values in g m^{-2} h^{-1} ± SD as determined for all volunteers. The data were evaluated in regard to different criteria as detailed below. Table 2b demonstrates the mean TEWL in g m^{-2} h^{-1} ± SD of all measurements conducted during the course of each month.

Panel 3a				
Investigated group	Number of volunteers	Mean TEWL (g/m^2 h) ± SD		
		Left forearm	Right forearm	Forehead
All volunteers	n = 26	11.67 ± 2.68	12.31 ± 2.85	24.16 ± 4.04
Female Volunteers	n = 15	10.79 ± 1.85	11.11 ± 1.97	24.37 ± 3.74
Male Volunteers	n = 11	12.87 ± 3.23	13.95 ± 3.12	23.89 ± 4.60
Age 18–25	n = 12	12.10 ± 3.47	12.52 ± 3.71	24.19 ± 4.09
Age 26–55	n = 14	11.42 ± 1.83	12.10 ± 2.04	24.06 ± 4.31
Skin care products	n = 18	11.00 ± 2.05	11.64 ± 2.56	24.14 ± 3.54
No skin care product	n = 08	13.16 ± 3.44	13.82 ± 3.04	24.23 ± 5.28
Sweating	n = 15	11.90 ± 2.25	12.69 ± 2.91	24.40 ± 4.00
No sweating	n = 11	11.35 ± 3.27	12.00 ± 2.94	24.35 ± 4.12
Skin type I	n = 03	10.58 ± 1.11	11.67 ± 0.80	20.94 ± 1.65
Skin type II	n = 10	11.69 ± 3.38	11.96 ± 3.14	23.18 ± 3.71
Skin type III	n = 10	12.05 ± 2.55	13.08 ± 3.19	25.65 ± 4.26
Skin type IV	n = 03	11.03 ± 0.62	11.44 ± 0.78	24.94 ± 4.96
Panel 3b				
Month	Number of measurements	Mean TEWL (g/m^2 h) ± SD		
		Left forearm	Right forearm	Forehead
February	n = 85	10.81 ± 3.32	11.54 ± 3.70	22.36 ± 5.50
March	n = 109	12.05 ± 3.18	12.44 ± 3.34	23.86 ± 5.61
April	n = 170	11.67 ± 3.32	12.48 ± 3.74	24.43 ± 5.26
May	n = 155	10.80 ± 2.88	11.60 ± 3.46	25.24 ± 5.51

($n \geqslant 29$). The mean of these TEWL values was considered as representative for each volunteer. The resulting final TEWL values of the volunteers were then evaluated in regard to different criteria to elucidate the potential influence of parameters such as sex, age, the use of skin care products, sweating, skin type (Table 3 panel a) or the season (Table 3 panel b) on the skin barrier function.

As expected, the TEWL of the different investigated skin regions varied for the forehead and the forearm regions. The determined absolute values were around 11–12 g m^{-2} h^{-1} for the forearm skin and around 25 g m^{-2} h^{-1} for the thinner skin region covering the forehead, which is in accordance with previous findings [26]. The higher TEWL of regions with increased permeability can be related to the smaller corneocytes size [26,33], the smaller number of SC cell layers [20] and the density of eccrine sweat glands [16].

No significant difference was found between the TEWL of the left and right forearm ($P > 0.05$). Likewise, no significant difference was found between the TEWL of the respective regions for male and female or younger and older volunteers ($P > 0.05$, respectively). This indicates that neither gender nor age influence the TEWL, which is in accordance with previous reports dealing with the effect of ethnicity, age and sex on the TEWL [26,34]. However, other opinions can be found [35]. None of the other investigated criteria, such as the regular use of skin care products, the inclination to sweating or the skin type of the participants according to the Fitzpatrick scale [36] proved to be of significance regarding the TEWL ($P > 0.05$ in all cases).

Monitoring of the TEWL results for all volunteers as determined during the course of several months revealed a slight, if significant variation of the TEWL during this time ($P < 0.05$, Table 3 panel b). In case of the forehead, it may be assumed that the increasing external temperature might have an effect on the TEWL despite air conditioned laboratory surroundings. In case of the forearms, however, no clear tendency in this respect could be observed, which indicates that a slight variation of the TEWL values can be regarded as normal during long-term observation. The results of evaporimetric methods even with closed-chamber systems may be influenced by the microclimate near the skin surface, which in turn is inevitably influenced by the present overall climate at a given time of the year [37]. In summary, no significant effects of the different subject-related variables on the TEWL were found in the long-term study apart from the obvious difference between the anatomical sites. The season of the measurements was found to have a slight impact on the TEWL, as confirmed by literature where seasonal variations in biophysical and biological characteristics of the SC have been reported [35,38].

Apart from this long-term observation, the TEWL before and after tape stripping was determined as an indicator for the barrier function of the skin [17]. The TEWL of untreated skin was in accordance with the results of the long-term monitoring and previous

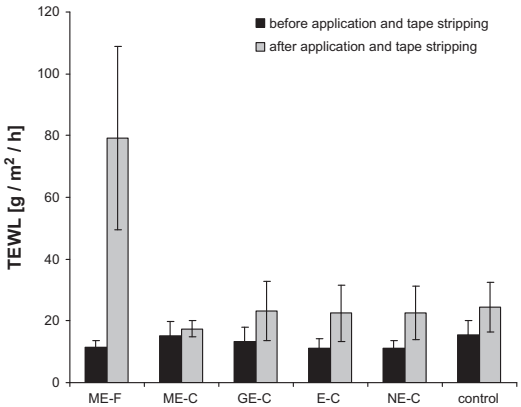

Fig. 3. TEWL of human forearm skin in vivo measured before and after tape stripping. The TEWL before and after tape stripping of the area treated with the microemulsion containing fluorescein sodium is given on the left (ME-F, 40 tapes), followed by the corresponding data for the curcumin-loaded microemulsion (ME-C, 20 tapes), hydrogel (GE-C, 20 tapes), macroemulsion (E-C, 20 tapes) and nanoemulsion (NE-C, 20 tapes). An untreated skin site served as a control. Values represent the means ± SD of six experiments (n = 6).

Please cite this article in press as: V. Klang et al., In vitro vs. in vivo tape stripping: Validation of the porcine ear model and penetration assessment of novel sucrose stearate emulsions, Eur. J. Pharm. Biopharm. (2011), doi:10.1016/j.ejpb.2011.11.009

ARTICLE IN PRESS

studies [26,33]. Interestingly, the in vivo TEWL values observed after the removal of 20 adhesive tapes were highly comparable for both untreated skin and skin treated with the different formulations (Fig. 3). Thus, in contrast to the in vitro results, only a slow increase in TEWL was observed in vivo, which was not influenced by the presence of topical formulations. Literature confirms that a slow and variable increase in TEWL of human skin is observed during the initial tape stripping process. Only when a major part of the SC is removed, the TEWL increases strongly [39], as can be seen for the microemulsion with fluorescein sodium where 40 adhesive tapes were removed (Fig. 3). The initial changes depend largely on the condition of the SC as well as on the exact tape stripping procedure. Inter-individual variations might be related to site-dependent differences in spontaneous desquamation and SC cohesion [20].

3.2.2. In vivo skin penetration profiles

The results of the in vivo tape stripping experiments are given in Table 4. As for the in vitro experiments, the skin penetration of fluorescein sodium from the microemulsion was higher than that of curcumin from the same or other vehicles ($P < 0.05$). Overall, the same tendencies as for the in vitro experiments were found. The penetration of curcumin tended to be higher from the microemulsion than from the hydrogel or the macro- and nanoemulsions. However, none of these differences reached a significant level ($P > 0.05$, respectively). As already observed in previous in vitro studies [11], the skin penetration behaviour of the macroemulsion and the nanoemulsion was highly comparable despite the marked difference in particle size and rheological properties ($P > 0.05$). For all formulations, no statistically significant differences were found when comparing the results of the tape stripping experiments performed on female and male volunteers ($P > 0.05$).

3.2.3. Influence of the formulation on the amount of removed SC proteins in vivo

The observed tendencies were in agreement with previous in vivo investigations reporting an obvious influence of the applied formulation on the amount of removed corneocytes [29]. In case of the microemulsion and the hydrogel, slight if significant differences were noticeable for the first few tapes ($n = 6$, $P < 0.05$, respectively) in accordance with the effects discussed and depicted for the in vitro data. In case of the macroemulsion and the nanoemulsion, significant differences were also noticeable for the first few tapes ($n = 6$, $P < 0.05$, respectively). However, more corneocytes were apparently removed with the first few tapes after application of these formulations when compared to the control. It may be assumed that the cohesion of the corneocytes might have been decreased after application of the highly hydrophilic systems. Moisturising O/W creams can cause acute hydration of the SC, an increase in TEWL and weakened SC cohesion. Thus, higher amounts of protein are removed though tape stripping [16,20,22].

In summary, the amount of removed corneocytes both in vivo and in vitro may be influenced in different ways. The applied formulations may lead to reduced tackiness of the tapes, especially if highly lipophilic creams with slow skin penetration or solvents are applied. In this case, modification of the working protocol towards cleaning of the skin should be considered. On the other hand, moisturising or occlusive formulations may lead to increased skin hydration, thus causing facilitated removal of corneocytes due to reduced cohesion. These findings once again confirm the need for the quantification of the removed corneocytes on each individual tape.

Table 4
In vivo skin penetration data for the different investigated formulations after application of 2 mg/cm^2 on human volar forearm skin for 30 min. Six experiments were performed for each formulation ($n = 6$), values are given as means ± SD.

Formulation	Penetrated drug amount (μg/cm^2)	Penetration depth (μm)	Penetration depth (% of SC)
ME curc	6.45 ± 2.28	3.08 ± 1.13	28.00 ± 10.27
GE curc	8.68 ± 1.08	2.70 ± 0.68	24.55 ± 06.18
E curc	7.03 ± 1.17	2.52 ± 0.47	22.91 ± 04.27
NE curc	6.60 ± 1.50	2.36 ± 0.62	21.45 ± 05.64
ME fluor	12.89 ± 2.81	5.61 ± 1.35	51.00 ± 12.27

3.3. Validity of the porcine ear model

Different in vitro models exist to mimic human skin penetration in vivo. The benefits of ex vivo investigations are manifold: ethical approval is not required, multiple replicate experiments are more easily performed and toxic compounds can be evaluated [9].The difference between in vivo and in vitro data using excised human skin may become very small if working protocols are harmonised [40]. However, in vitro studies using excised human skin usually rely on material obtained from the abdomen after liposuction, while in vivo studies are conducted on the human forearm. Thus, the obtained data will exhibit certain differences, especially if the skin has been subjected to heat-separation [40]. Therefore, porcine ear skin may be equally if not more suitable as an in vitro model, delivering good correlations [41]. Pig skin shares essential permeation characteristics with human skin, especially for lipophilic components [18]. The physiological conditions of porcine ear skin can be kept almost constant since the porcine ear skin remains on the ear cartilage, the skin barrier is not interrupted, dehydration is decelerated and no contraction occurs [1]. The accuracy of the data depends on the use of proper methodology that has to be standardised and optimised for each in vitro set-up [41]. Previous studies have shown that porcine ear skin is a suitable substitute for human skin when performing in vitro experiments [2,9,42].

In the present study, comparable tendencies were observed after in vivo and in vitro tape stripping, which confirms that the porcine ear model is suitable for conducting comparative studies to evaluate skin penetration of different vehicles. Fig. 4 shows the respective penetration profiles of the curcumin-loaded microemulsion in vivo and in vitro. Both penetration depth in regard to the entire horny layer thickness and the recovered drug amounts were highly comparable. As can be seen from the profiles, very similar amounts of corneocytes were removed with every tape during the tape stripping process from the human forearm skin in vivo (Fig. 4A). As a consequence of this very constant removal process, the drug amounts on the individual tapes were equally homogeneously distributed, as can be derived from the very homogeneous thickness of the individual bars in Fig. 4A. In contrast, the corneocytes of the porcine skin surface appeared to be less densely packed. As can be seen in Fig. 4B, large amounts of corneocytes and, consequently, adherent penetrated drug were removed with the first adhesive films. The number of removed corneocytes and drug per tape decreased constantly with increasing tape number, which might be ascribed to the increasing corneocyte adhesion in the deeper cell layers and an increasingly homogeneous skin structure. Indeed, this more irregular surface structure of the porcine skin with loose cell clusters and canyons has already been reported [7] and is well reflected in the presented results.

Despite these general differences regarding corneocyte removal, the overall trends regarding skin penetration were remarkably comparable for in vitro and in vivo experiments (Fig. 5), especially in the case of the microemulsions both with fluorescein sodium and curcumin. A certain level of variability in individual skin penetration depths was observed both in vivo and in vitro, which should however be acceptable for practical application [9,43]. Determination of six individual samples is generally sufficient to

Please cite this article in press as: V. Klang et al., In vitro vs. in vivo tape stripping: Validation of the porcine ear model and penetration assessment of novel sucrose stearate emulsions, Eur. J. Pharm. Biopharm. (2011), doi:10.1016/j.ejpb.2011.11.009

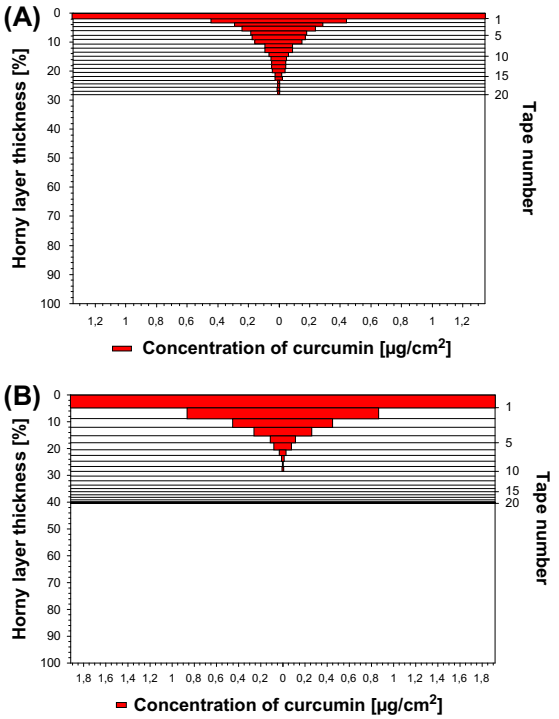

Fig. 4. Skin penetration profiles of curcumin from a microemulsion: comparison of data obtained on human forearm skin in vivo (A) and porcine skin in vitro (B). The depicted values are means of six individual experiments ($n = 6$, respectively). (For interpretation of the references to colour in this figure legend, the reader is referred to the web version of this article.)

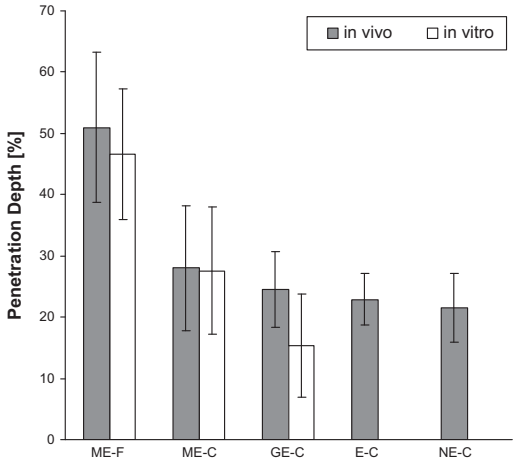

Fig. 5. Comparison of in vivo and in vitro skin penetration of the model drugs fluorescein sodium (F) and curcumin (C) from different formulations. The penetration depth of fluorescein sodium from the microemulsion is given on the left (ME-F), followed by the corresponding penetration data for curcumin from the microemulsion (ME-C), the hydrogel (GE-C), the macroemulsion (E-C) and the nanoemulsion (NE-C). The given values, respectively, represent the means ± SD of 6 individual experiments for both in vitro and in vivo studies.

obtain representative tendencies [2]. Regarding the penetrated drug amounts, the respective values obtained with the curcumin-loaded microemulsion and hydrogel were highly comparable for the in vitro and in vivo studies ($P > 0.05$, respectively). This confirms that the delivered drug load is primarily dependent on passive diffusion, which appears to be in the same order of magnitude for porcine and human skin at the chosen experiment times. Merely, in case of the fluorescein-loaded microemulsion, a slight if statistically significant difference was found between the permeated drug amounts in vitro and in vivo ($P < 0.05$). The higher penetrated drug amount in vivo might be related to the physiological skin hydration, which is continually decreasing in the excised porcine ear tissue and influences the penetration of hydrophilic drugs more than lipophilic ones [17].

When regarding the numerical values represented in Fig. 5 and detailed in Tables 2 and 4, the microemulsion with fluorescein sodium penetrated the SC in vitro to an extent of 46.59 ± 10.73%, while the in vivo penetration reached values of 51.00 ± 12.27%. Thus, the in vitro penetration achieved 91.34% of the actual in vivo values. In case of the microemulsion with curcumin, the in vitro values represented 98.43% of the actual in vivo penetration. In case of the hydrogel, a slight underestimation was reached in vitro with 62.60% of the penetration depth in vivo. Such an underestimation may be observed in vitro with porcine ear skin especially if the follicular pathway of penetration is involved, which is impaired in vitro due to the lack of physiological movement that may favour penetration via this route [42]. Dehydration of the tissue may play an additional role. The macroemulsion and the nanoemulsion, which were evaluated for in vivo application, achieved only slightly lower penetration depths than the other formulations.

Overall, the good in vivo/in vitro correlation obtained for the microemulsions and the hydrogel suggests that in vitro tape stripping experiments may be sufficiently representative to replace in vivo tape stripping for further studies with these formulations.

3.4. Skin penetration of macroemulsion vs. nanoemulsion in vivo

Colloidal systems stabilised by carbohydrate-based surfactants possess great potential for dermal drug delivery [44,45]. Recently, both macroemulsions and nanoemulsions stabilised by sucrose stearate were developed [11]. Interestingly, their in vitro skin penetration behaviour was highly comparable despite the significant differences in particle size and viscosity. Since the outcome of in vitro studies may be influenced by the experimental set-up, we decided to confirm the obtained results by tape stripping experiments conducted in vivo. Overall, few reports deal with the actual skin penetration potential of submicron-sized emulsions in vivo and no such data exist for the novel semi-solid and liquid formulations based on sucrose stearate.

The presented in vivo results confirmed the tendencies observed in vitro [11], namely identical skin penetration potential of both systems ($P > 0.05$, Fig. 5). This is in contrast to numerous reports on the superior skin penetration of nanosized colloidal systems [46–48]. Possibly, the large droplets of the macroemulsion exhibit a larger contact area that fosters penetration of drugs into the skin [15]. This aspect might make up for the comparatively smaller droplet surface area of the macroemulsion in comparison with the nanoemulsion, which is usually held accountable for improved skin penetration of nanosized vehicles. Surprisingly, both systems achieved skin penetration rates that were comparable to those of the microemulsion and the hydrogel ($P > 0.05$) although the latter formulations contain large amounts of surfactants and solvents. It may thus be assumed that these emulsions represent a skin-friendly alternative to the classic vehicles.

Please cite this article in press as: V. Klang et al., In vitro vs. in vivo tape stripping: Validation of the porcine ear model and penetration assessment of novel sucrose stearate emulsions, Eur. J. Pharm. Biopharm. (2011), doi:10.1016/j.ejpb.2011.11.009

ARTICLE IN PRESS

4. Conclusion

The presented data confirm that porcine ear skin is a highly suitable model for in vitro tape stripping. The penetration profiles of curcumin and fluorescein sodium obtained after a finite-dose application of different vehicles were in excellent agreement with the corresponding in vivo data. The results can be regarded as a complementary validation of the different NIR-densitometric calibration data for the quantification of human and porcine SC proteins. Moreover, it was confirmed that the skin penetration potential of recently developed semi-solid sucrose stearate-based macroemulsions is comparable to that of fluid nanoemulsions of identical composition despite significant differences in particle size and viscosity.

Acknowledgements

The authors would like to thank Robert Knobler, Anita Vamosi and Carola Fuchs, AKH Vienna, as well as Magdalena Hoppel and Andrea Hartl, University of Vienna, and Jürgen Lademann and his working group of the Charité Berlin for technical assistance. We would also like to express our gratitude to Wolfgang Sipos and the Clinic for Swine, Veterinary University of Vienna, for providing fresh porcine ears.

References

[1] J. Lademann, U. Jacobi, C. Surber, H.J. Weigmann, J.W. Fluhr, The tape stripping procedure – evaluation of some critical parameters, Eur. J. Pharm. Biopharm. 72 (2009) 317–323.
[2] H.J. Weigmann, S. Schanzer, A. Patzelt, V. Bahaban, F. Durat, W. Sterry, J. Lademann, Comparison of human and porcine skin for characterization of sunscreens, J. Biomed. Opt. 14 (2009) 24–27.
[3] R. Voegeli, J. Heiland, S. Doppler, A.V. Rawlings, T. Schreier, Efficient and simple quantification of stratum corneum proteins on tape strippings by infrared densitometry, Skin Res. Technol. 13 (2007) 242–251.
[4] T. Hahn, S. Hansen, D. Neumann, K.H. Kostka, C.M. Lehr, L. Muys, U.F. Schaefer, Infrared densitometry: a fast and non-destructive method for exact stratum corneum depth calculation for in vitro tape-stripping, Skin Pharmacol. Physiol. 23 (2010) 183–192.
[5] U. Jacobi, M. Kaiser, R. Toll, S. Mangelsdorf, H. Audring, N. Otberg, W. Sterry, J. Lademann, Porcine ear skin: an in vitro model for human skin, Skin Res. Technol. 13 (2007) 19–24.
[6] J. Lademann, A. Patzelt, H. Richter, S. Schanzer, W. Sterry, A. Filbry, K. Bohnsack, F. Rippke, M. Meinke, Comparison of two in vitro models for the analysis of follicular penetration and its prevention by barrier emulsions, Eur. J. Pharm. Biopharm. 72 (2009) 600–604.
[7] V. Klang, J.C. Schwarz, A. Hartl, C. Valenta, Facilitating in vitro tape stripping: application of infrared densitometry for quantification of porcine stratum corneum proteins, Skin Pharmacol. Physiol. 24 (2011) 256–268.
[8] N. Sekkat, Y.N. Kalia, R.H. Guy, Biophysical study of porcine ear skin in vitro and its comparison to human skin in vivo, J. Pharm. Sci. 91 (2002) 2376–2381.
[9] C. Herkenne, A. Naik, Y.N. Kalia, J. Hadgraft, R.H. Guy, Pig ear skin ex vivo as a model for in vivo dermatopharmacokinetic studies in man, Pharm. Res. 23 (2006) 1850–1856.
[10] A.P. Popov, J. Lademann, A.V. Priezzhev, R. Myllylä, Reconstruction of stratum corneum profile of porcine ear skin after tape stripping using UV/VIS spectroscopy, in: D. Schweitzer, M. Fitzmaurice (Eds.), Diagnostic Optical Spectroscopy in Biomedicine IV, Proceedings of SPIE-OSA Biomedical Optics, Optical Society of America, vol. 6628, 2007 (Paper 6628_70).
[11] V. Klang, J.C. Schwarz, N. Matsko, E. Rezvani, N. El-Hagin, M. Wirth, C. Valenta, Semi-solid sucrose stearate-based emulsions as dermal drug delivery systems, Pharmaceutics 3 (2011) 275–306.
[12] D.C. Carrer, C. Vermehren, L.A. Bagatolli, Pig skin structure and transdermal delivery of liposomes: a two photon microscopy study, J. Control. Release 132 (2008) 12–20.
[13] S. Hoeller, V. Klang, C. Valenta, Skin-compatible lecithin drug delivery systems for fluconazole: effect of phosphatidylethanolamine and oleic acid on skin permeation, J. Pharm. Pharmacol. 60 (2008) 587–591.
[14] F. Stracke, B. Weiss, C.M. Lehr, K. Konig, U.F. Schaefer, M. Schneider, Multiphoton microscopy for the investigation of dermal penetration of nanoparticle-borne drugs, J. Invest. Dermatol. 126 (2006) 2224–2233.
[15] X. Wu, B. Biatry, C. Cazeneuve, R.H. Guy, Drug delivery to the skin from submicron polymeric particle formulations: influence of particle size and polymer hydrophobicity, Pharm. Res. 26 (2009) 1995–2001.
[16] D. Hildebrandt, K. Ziegler, U. Wollina, Electrical impedance and transepidermal water loss of healthy human skin under different conditions, Skin Res. Technol. 4 (1998) 130–134.
[17] N. Otberg, D. Grone, L. Meyer, S. Schanzer, G. Hoffmann, H. Ackermann, W. Sterry, J. Lademann, Water-filtered infrared-A (wIRA) can act as a penetration enhancer for topically applied substances, Ger. Med. Sci. 6 (2008) 1–14.
[18] M. Vettor, S. Bourgeois, H. Fessi, J. Pelletier, P. Perugini, F. Pavanetto, M.A. Bolzinger, Skin absorption studies of octyl-methoxycinnamate loaded poly(D,L-lactide) nanoparticles: estimation of the UV filter distribution and release behaviour in skin layers, J. Microencapsul. 27 (2010) 253–262.
[19] Y.N. Kalia, I. Alberti, N. Sekkat, C. Curdy, A. Naik, R.H. Guy, Normalization of stratum corneum barrier function and transepidermal water loss in vivo, Pharm. Res. 17 (2000) 1148–1150.
[20] H. Loeffler, F. Dreher, H.I. Maibach, Stratum corneum adhesive tape stripping: influence of anatomical site, application pressure, duration and removal, Br. J. Dermatol. 151 (2004) 746–752.
[21] H. Wagner, K.H. Kostka, C.M. Lehr, U.F. Schaefer, Drug distribution in human skin using two different in vitro test systems: comparison with in vivo data, Pharm. Res. 17 (2000) 1475–1481.
[22] M. Breternitz, M. Flach, J. Prassler, P. Elsner, J.W. Fluhr, Acute barrier disruption by adhesive tapes is influenced by pressure, time and anatomical location: integrity and cohesion assessed by sequential tape stripping. A randomized, controlled study, Br. J. Dermatol. 156 (2007) 231–240.
[23] U. Lindemann, K. Wilken, H.J. Weigmann, H. Schaefer, W. Sterry, J. Lademann, Quantification of the horny layer using tape stripping and microscopic techniques, J. Biomed. Opt. 8 (2003) 601–607.
[24] C. Lin, H. Lin, H. Chenc, M. Yu, M. Lee, Stability and characterisation of phospholipid-based curcumin-encapsulated microemulsions, Food Chem. 116 (2009) 923–928.
[25] N. Sekkat, Y.N. Kalia, R.H. Guy, Porcine ear skin as a model for the assessment of transdermal drug delivery to premature neonates, Pharm. Res. 21 (2004) 1390–1397.
[26] M. Machado, T.M. Salgado, J. Hadgraft, M.E. Lane, The relationship between transepidermal water loss and skin permeability, Int. J. Pharm. 384 (2010) 73–77.
[27] U. Jacobi, H.J. Weigmann, M. Baumann, A.I. Reiche, W. Sterry, J. Lademann, Lateral spreading of topically applied UV filter substances investigated by tape stripping, Skin Pharmacol. Physiol. 17 (2004) 17–22.
[28] U. Jacobi, S. Schanzer, H.J. Weigmann, A. Patzelt, T. Vergou, W. Sterry, J. Lademann, Pathways of lateral spreading, Skin Pharmacol. Physiol. 24 (2011) 231–237.
[29] R. Pelchrzim, H.J. Weigmann, H. Schaefer, T. Hagemeister, M. Linscheid, V.P. Shah, W. Sterry, J. Lademann, Determination of the formation of the stratum corneum reservoir for two different corticosteroid formulations using tape stripping combined with UV/VIS spectroscopy, J. Dtsch. Dermatol. Ges. 2 (2004) 914–919.
[30] U. Jacobi, N. Meykadeh, W. Sterry, J. Lademann, Effect of the vehicle on the amount of stratum corneum removed by tape stripping, J. Dtsch. Dermatol. Ges. 1 (2003) 884–889.
[31] G. Cevc, U. Vierl, Nanotechnology and the transdermal route: a state of the art review and critical appraisal, J. Control. Release 141 (2010) 277–299.
[32] J.J. Escobar-Chavez, V. Merino-Sanjuan, M. Lopez-Cervantes, Z. Urban-Morlan, E. Pinon-Segundo, D. Quintanar-Guerrero, A. Ganem-Quintanar, The tape-stripping technique as a method for drug quantification in skin, J. Pharm. Pharm. Sci. 11 (2008) 104–130.
[33] J. Hadgraft, M.E. Lane, Transepidermal water loss and skin site: a hypothesis, Int. J. Pharm. 373 (2009) 1–3.
[34] U. Jacobi, J. Gautier, W. Sterry, J. Lademann, Gender-related differences in the physiology of the stratum corneum, Dermatology 211 (2005) 312–317.
[35] R. Darlenski, S. Sassning, N. Tsankov, J.W. Fluhr, Non-invasive in vivo methods for investigation of the skin barrier physical properties, Eur. J. Pharm. Biopharm. 72 (2009) 295–303.
[36] T.B. Fitzpatrick, The validity and practicality of sun-reactive skin types I through VI, Arch. Dermatol. 124 (1988) 869–871.
[37] H. Zhai, E. Dika, M. Goldovsky, H.I. Maibach, Tape-stripping method in man: comparison of evaporimetric methods, Skin Res. Technol. 13 (2007) 207–210.
[38] R. Voegeli, A.V. Rawlings, S. Doppler, J. Heiland, T. Schreier, Profiling of serine protease activities in human stratum corneum and detection of a stratum corneum tryptase-like enzyme, Int. J. Cosmet. Sci. 29 (2007) 191–200.
[39] Y.N. Kalia, L.B. Nonato, R.H. Guy, The effect of iontophoresis on skin barrier integrity: non-invasive evaluation by impedance spectroscopy and transepidermal water loss, Pharm. Res. 13 (1996) 957–960.
[40] P.A. Lehman, S.G. Raney, T.J. Franz, Percutaneous absorption in man: in vitro–in vivo correlation, Skin Pharmacol. Physiol. 24 (2011) 224–230.
[41] F. Benech-Kieffer, P. Wegrich, R. Schwarzenbach, G. Klecak, T. Weber, J. Leclaire, H. Schaefer, Percutaneous absorption of sunscreens in vitro: interspecies comparison, skin models and reproducibility aspects, Skin Pharmacol. Appl. Skin Physiol. 13 (2000) 235–324.
[42] A. Patzelt, H. Richter, R. Buettemeyer, H.J. Huber, U. Blume-Peytavi, W. Sterry, J. Lademann, Differential stripping demonstrates a significant reduction of the hair follicle reservoir in vitro compared to in vivo, Eur. J. Pharm. Biopharm. 70 (2008) 234–238.
[43] I. Alberti, Y.N. Kalia, A. Naik, J.D. Bonny, R.H. Guy, In vivo assessment of enhanced topical delivery of terbinafine to human stratum corneum, J. Control. Release 71 (2001) 319–327.
[44] S.B. Calderilla-Fajardo, J. Cazares-Delgadillo, R. Villalobos-Garcia, D. Quintanar-Guerrero, A. Ganem-Quintanar, R. Robles, Influence of sucrose esters on the in vivo percutaneous penetration of octyl methoxycinnamate

Please cite this article in press as: V. Klang et al., In vitro vs. in vivo tape stripping: Validation of the porcine ear model and penetration assessment of novel sucrose stearate emulsions, Eur. J. Pharm. Biopharm. (2011), doi:10.1016/j.ejpb.2011.11.009

ARTICLE IN PRESS

formulated in nanocapsules, nanoemulsion, and emulsion, Drug Dev. Ind. Pharm. 32 (2006) 107–113.
[45] J. Cazares-Delgadillo, A. Naik, Y.N. Kalia, D. Quintanar-Guerrero, A. Ganem-Quintanar, Skin permeation enhancement by sucrose esters: a pH-dependent phenomenon, Int. J. Pharm. 297 (2005) 204–212.
[46] D.I. Friedman, J.S. Schwarz, M. Weisspapir, Submicron emulsion vehicle for enhanced transdermal delivery of steroidal and nonsteroidal antiinflammatory drugs, J. Pharm. Sci. 84 (1995) 324–329.
[47] K. Bouchemal, S. Briancon, E. Perrier, H. Fessi, Nano-emulsion formulation using spontaneous emulsification: solvent, oil and surfactant optimisation, Int. J. Pharm. 280 (2004) 241–251.
[48] T. Tadros, P. Izquierdo, J. Esquena, C. Solans, Formation and stability of nano-emulsions, Adv. Colloid Interf. Sci. 108–109 (2004) 303–318.

Please cite this article in press as: V. Klang et al., In vitro vs. in vivo tape stripping: Validation of the porcine ear model and penetration assessment of novel sucrose stearate emulsions, Eur. J. Pharm. Biopharm. (2011), doi:10.1016/j.ejpb.2011.11.009

G Model
IJP-12264; No. of Pages 8
ARTICLE IN PRESS

International Journal of Pharmaceutics xxx (2011) xxx–xxx

Contents lists available at SciVerse ScienceDirect

International Journal of Pharmaceutics

journal homepage: www.elsevier.com/locate/ijpharm

Pharmaceutical Nanotechnology

Effect of γ-cyclodextrin on the in vitro skin permeation of a steroidal drug from nanoemulsions: Impact of experimental setup

Victoria Klang, Silvia Haberfeld, Andrea Hartl, Claudia Valenta*

University of Vienna, Department of Pharmaceutical Technology and Biopharmaceutics, Faculty of Life Sciences, Althanstraße 14, 1090 Vienna, Austria

ARTICLE INFO

Article history:
Received 2 November 2011
Received in revised form
22 November 2011
Accepted 23 November 2011
Available online xxx

Keywords:
γ-Cyclodextrin
Skin penetration
Skin permeation
Fludrocortisone acetate
Permeation enhancement
Franz-type diffusion cell

ABSTRACT

Numerous reports on the enhancement effect of cyclodextrins (CDs) on the skin permeation of dermally applied drugs exist, the majority of which is based on in vitro diffusion cell studies. The specific experimental setup of such studies may skew the obtained results, which is rarely discussed in the context of CD studies. Thus, the aim of this work was to conduct a systematic in vitro investigation of the permeation enhancement potential of γ-CD on a steroidal drug from a nanoemulsion. The role of critical diffusion cell parameters such as the dose of application, occlusive conditions, the nature of the receptor medium and the skin thickness were investigated. The results showed that significantly enhanced skin permeation rates of fludrocortisone acetate were indeed caused by 1% (w/w) of γ-CD at both finite and infinite dose conditions. At 0.5% (w/w) of γ-CD, significant enhancement was only achieved at infinite dose application. Additional in vitro tape stripping experiments confirmed these tendencies, but the observed effects did not reach statistical significance. It may be concluded that the full permeation enhancement potential of the CD as observed in the franz-cell setup can only be realised at infinite dose conditions while preserving the formulation structure.

© 2011 Elsevier B.V. All rights reserved.

1. Introduction

Cyclodextrins (CDs) are commonly used pharmaceutical excipients which are well known for their ability to complex lipophilic compounds. Both the natural cyclic oligosaccharides α-, β- and γ-CD as well as their derivatives can be employed for the solubilisation or stabilisation of drugs. In dermal drug delivery, CDs are highly useful for the stabilisation of sensitive compounds which are prone to chemical degradation (Lopez et al., 2000; Scalia et al., 2007). In addition, they may serve to stabilise formulations themselves or to influence the skin penetration of active substances by either promoting or decreasing drug penetration (Klang et al., 2010; Loftsson et al., 1991; Montassier et al., 1998; Rajewski and Stella, 1996; Trichard et al., 2007). This effect depends on the affinity of the respective drug to the lipophilic cavity of the employed CD and its solubility within the vehicle. Since CDs can interact with various lipophilic molecule structures, their use in topical formulations has to be carefully evaluated for each new product. Such preliminary investigations frequently consist of in vitro skin permeation experiments using diffusion chambers and excised human skin or suitable substitutes. Numerous reports dealing with the effect of incorporated CDs on the skin permeation of model drugs from different formulations can be found in the literature (Loftsson and Olafsson, 1998; Loftsson and Masson, 2001; Loftsson and Bodor, 2006; Matsuda and Arima, 1999). However, the effect of the experimental setup on the outcome of skin permeation studies involving CDs has not been discussed or systematically investigated so far. Important parameters in this context are the amount of applied dose, the nature of the receptor medium and the effect of occlusion conditions. Since CDs may contribute to enhanced skin permeation rates of lipophilic drugs by simply increasing their solubility in the donor medium, such an effect might be severely overestimated during in vitro diffusion cell studies where an infinite dose of sample is provided in the donor chamber. Under such conditions, the CD might indeed facilitate the diffusion of the drug within the surplus formulation and lead to an increased concentration of drug at the skin surface which is available for permeation. However, such an effect might not be reached under in vivo conditions where a finite dose of a semi-solid sample is rubbed into the skin.

Therefore, the aim of this work was to systematically investigate the permeation enhancement effect of γ-CD on a steroidal model drug and to elucidate the influence of different in vitro setups on the results. To this end, skin permeation experiments were conducted using established nanoemulsion formulations containing the lipophilic drug fludrocortisone acetate (Klang et al., 2011a). For these fluid submicron-sized O/W emulsions, remarkably enhanced skin permeation rates of steroidal drugs had been observed after

Abbreviations: CD, cyclodextrin; DLS, dynamic light scattering; PDI, polydispersity index; ZP, zeta potential; BSA, bovine serum albumin; PEG 400, polyethylene glycol 400; TEWL, transepidermal water loss.

* Corresponding author. Tel.: +43 1 4277 55 410; fax: +43 1 4277 9554.
E-mail address: Claudia.valenta@univie.ac.at (C. Valenta).

0378-5173/$ – see front matter © 2011 Elsevier B.V. All rights reserved.
doi:10.1016/j.ijpharm.2011.11.037

Please cite this article in press as: Klang, V., et al., Effect of γ-cyclodextrin on the in vitro skin permeation of a steroidal drug from nanoemulsions: Impact of experimental setup. Int J Pharmaceut (2011), doi:10.1016/j.ijpharm.2011.11.037

G Model
IJP-12264; No. of Pages 8
ARTICLE IN PRESS
2 V. Klang et al. / International Journal of Pharmaceutics xxx (2011) xxx–xxx

incorporation of γ-CD using franz-type diffusion cells (Klang et al., 2010, 2011a). The validity of these results should be tested in comprehensive in vitro skin permeation studies to address the questions discussed above. It should be clarified whether the observed enhancement effect could be reproduced under different experimental setups. To this end, extensive franz-type diffusion cell studies using porcine abdominal skin were performed with corresponding formulations containing fludrocortisone acetate and different amounts of γ-CD. The comparison of these different formulations containing 0, 0.5 or 1% (w/w) of γ-CD served to elucidate the importance of the amount of incorporated γ-CD for the permeation enhancement effect. Experimental diffusion cell parameters such as the dose of application, occlusion conditions, pre-treatment of the skin, skin thickness and the nature of the receptor medium were systematically modified and optimised for the envisioned studies.

In addition, comparative tape stripping experiments were performed to provide a different in vitro setup using a finite dose application while avoiding the maceration effects of a receptor fluid. Thus, a more realistic estimation of the actual enhancement potential of CDs in topically applied formulations should be gained and the observed trends were compared to those of the diffusion cell experiments.

2. Materials and methods

2.1. Materials

Egg lecithin Lipoid E-80 was kindly donated by Lipoid GmbH (Ludwigshafen, Germany). PCL-liquid (cetearyl ethylhexanoate, isopropyl myristate) was purchased from Dr. Temt Laboratories (Vienna, Austria). Potassium sorbate was obtained from Herba Chemosan Apotheker-AG (Vienna, Austria). Fludrocortisone acetate (CAS: 514-36-3) and bovine serum albumin (CAS: 9048-46-8) were purchased from Sigma Aldrich (St. Louis, USA). Polyethylene glycol 400 (CAS: 25322-68-3) was obtained from Gatt-Koller GmbH, Absam, Austria. Cyclodextrin γ (Cavamax® W8 Pharma) was obtained from Wacker Chemie AG (Munich, Germany). All further chemicals used were of analytical reagent grade and used without further purification. Standard Corneofix® adhesive films with a square area of 4.0 cm^2 were obtained from Courage + Khazaka GmbH (Cologne, Germany).

2.2. Formulations

The model nanoemulsions were prepared as previously described (Klang et al., 2011a). Briefly, the aqueous phase, consisting of freshly distilled water and potassium sorbate, was stirred at 50 °C. Lecithin E-80 was dissolved in PCL-liquid and the lipophilic drug fludrocortisone acetate was incorporated into the resulting oil phase. Additional γ-CD was dissolved in the aqueous phase. The two phases were mixed and pre-homogenised with an ultra-turrax (Omni 500, 4 min, 2500 rpm). Afterwards, the mixture was stirred and heated to 50 °C before further homogenisation with a high-pressure homogeniser (EmulsiFlex C3, Avestin) for 20 homogenisation cycles at 750 bars. The composition of the resulting formulations and the corresponding abbreviations are given in Table 1.

Table 1
Composition of the model nanoemulsion NE with fludrocortisone acetate. For the additional nanoemulsions γ-0.5% NE and γ-1% NE, additional γ-CD was incorporated at either 0.5 or 1.0% (w/w). Abbreviations of the three formulations are detailed below.

Excipients	Composition (%, w/w)
PCL liquid	20.0
Lecithin E-80	2.5
Potassium sorbate	0.1
Fludrocortison acetate	1.0
Distilled water	ad 100

Abbreviations: NE = basic nanoemulsion without additional γ-CD; γ-0.5% NE = nanoemulsion with 0.5% (w/w) of γ-CD; γ-1% NE = nanoemulsion with 1% (w/w) of γ-CD.

2.3. Emulsion characterisation

2.3.1. Particle size, polydispersity index and particle surface charge

The systems were analysed for their particle size and particle size distribution by dynamic light scattering (DLS, photon correlation spectroscopy) using a Zetasizer Nano ZS (Malvern, UK) at 25 °C. Samples were diluted with freshly distilled water 1:100 (v/v) to diminish opalescence. The measured parameters were the hydrodynamic diameter expressed as *z*-average value, i.e. the intensity weighted mean diameter of the bulk population of oil droplets, as well as the polydispersity index (PDI). The latter represents the particle size distribution within the formulations; values below 0.2 indicate a narrow size distribution and thus good long-term stability (Mueller, 1996a). All samples were analysed in triplicate ($n = 3$) and each individual result was automatically calculated as the average of 3 measurements with 20 sub-measurements each.

In addition, the particle surface charge or zeta potential (ZP) of the nanoemulsions was determined by laser Doppler electrophoresis, again using the Zetasizer Nano ZS (Malvern, UK) at 25 °C. The samples were diluted with distilled water (1:100 v/v) containing sodium chloride (0.01 mmol) to ensure constant conductivity below 0.05 mS/cm and thus reproducible measurement conditions (Klang et al., 2011a). The ZP was determined in triplicate for all nanoemulsions ($n = 3$); again each individual result was calculated as the average of 3 measurements with 20 sub-runs each. Overall, the obtained data should ensure the use of representative and intact formulations for all further studies.

2.3.2. Drug content and pH

The drug content of all nanoemulsions was analysed immediately after preparation to ensure appropriate drug incorporation. Briefly, 10 mg of each system were dissolved in 1 ml of methanol, centrifuged for 6 min at 12,000 rpm (Hermle Z323K, MIDSCI, USA) and analysed by HPLC. Samples were taken at least in triplicate ($n \geq 3$). In addition, the pH of the formulations was determined using a pH meter (Orion 420A, Bartelt, Austria) at ambient temperature (25 °C, $n = 3$).

2.4. Preparation of porcine abdominal skin and porcine ear skin

For the diffusion cell studies, porcine abdominal skin was freed from hair and dermatomed (GB 228R, Aesculap, Germany) to a thickness of 1.2 mm. Since full-thickness skin represents an unphysiologically strong barrier for the diffusion of lipophilic drugs (Bosman et al., 1998; Lehman et al., 2011), additional experiments were performed using porcine abdominal skin that was dermatomed to a thickness of 0.5 mm. The dermatomed skin was stored in aluminium foil and polyethylene bags at −20 °C and was thawed prior to the experiments. Under such conditions the skin is stable in regard to SC properties for diffusion studies for up to 6 months (Leveque et al., 2004; Wagner et al., 2000).

2.5. Solubility of the model drug and choice of the receptor medium

The investigated receptor media were pure aqueous phosphate buffer (Pharmacopoea Europea, pH 7.4, 0.012 M) as well as buffer

Please cite this article in press as: Klang, V., et al., Effect of γ-cyclodextrin on the in vitro skin permeation of a steroidal drug from nanoemulsions: Impact of experimental setup. Int J Pharmaceut (2011), doi:10.1016/j.ijpharm.2011.11.037

G Model
IJP-12264; No. of Pages 8
ARTICLE IN PRESS
V. Klang et al. / International Journal of Pharmaceutics xxx (2011) xxx–xxx 3

containing 1.4% or 5% (w/v) of bovine serum albumin (BSA) or 20% (v/v) of either propylene glycol, polyethylene glycol 400 (PEG 400) or ethanol.

The saturation solubility of the fludrocortisone acetate in the designated receptor fluids was determined by HPLC analysis. To this end, an excess of fludrocortisone acetate was dissolved in 1 ml of the respective medium at 25 °C. The dispersion was then shaken for 24 h at room temperature, centrifuged to separate undissolved drug and was filtered (Minisart RC4 0.45 μm, Sartorius stedim Biotech GmbH, Göttingen, Germany) and analysed by HPLC. At least 4 individual experiments were performed for each medium ($n \geq 4$).

2.6. Skin permeation experiments using franz-type diffusion cells

In vitro skin permeation studies were performed using Franz-type diffusion cells (Permegear, USA) (Franz, 1975). Porcine abdominal skin was chosen as model membrane because of its similarity to human skin regarding morphology and permeability (Michniak-Kohn et al., 2005). Appropriately cut skin pieces were clamped between the donor and the receptor chamber of the diffusion cells having a permeation area of 0.95 cm^2. The receptor compartment was filled with 2 ml of the respective receptor medium. Pure phosphate buffer (pH 7.4, 0.012 M) was employed as standard receptor medium. Comparative studies were performed with buffer media containing 1.4% (w/v) of BSA or 20% (v/v) of either propylene glycol, PEG 400 or ethanol to evaluate the benefit of an adapted receptor medium. The diffusion cells were kept at the average skin surface temperature of 32 ± 0.5 °C and were continuously stirred with magnetic bars for 24 h. The accurately weighted formulation was placed on the excised skin in the donor chamber. Samples of 200 μl were removed at defined time intervals for HPLC analysis and were replaced by fresh receptor medium. Permeation profiles of fludrocortisone acetate were constructed by plotting the time (hours) against the cumulative amount of the drug (μg/cm^2) as determined in the receptor solution. The steady state flux (J, μg cm^{-2} h^{-1}) was calculated by linear regression after the respective lag-times.

Different sets of experiments were performed. The influence of the amount of applied formulation was tested. To this end, respectively 5, 50 and 500 mg/cm^2 of each nanoemulsion, corresponding to a finite, semi-infinite and infinite dose application (Henning et al., 2009), were applied onto the skin ($n \geq 8$, respectively). Information about the influence of the incorporated γ-CD at the different amounts of formulation could likewise be obtained in these experiments. Additional experiments served to investigate whether pre-treatment with the CD would affect the skin permeation of the drug from the applied standard nanoemulsion as well. To this end, the skin was pre-macerated within the franz-cell setup using 50 μl of either 1% (w/w) aqueous buffer solution of γ-CD, pure aqueous buffer solution or no additional solute for 16 h. These experiments were carried at all three amounts of applied formulation.

During all experiments, the donor compartment as well as the sampling arm was occluded to prevent evaporation. For selected comparative studies, additional non-occluded conditions with an open donor compartment were employed.

Further experiments to optimise the setup for the standard nanoemulsion involved variation of the model skin thickness as well as the nature of the receptor medium. These experiments served to identify the most suitable working protocol for general studies of nanoemulsions containing highly lipophilic drugs.

2.7. Skin penetration experiments via in vitro tape stripping

In vitro tape stripping was conducted to elucidate whether the enhancement effect of CD incorporation would be reproducible under a different experimental setup. Thus, the penetration behaviour of fludrocortisone acetate into the stratum corneum of porcine ear skin was investigated. Penetration profiles were constructed from the results of at least eight individual tape stripping experiments for each formulation ($n \geq 8$). Fresh porcine ears were kindly donated by the Clinic for Swine, University of Veterinary Medicine, Vienna. The ears were stored at −20 °C, thawed prior to the experiments, cleaned with cold water and blotted dry. The skin was freed from hair with scissors and the skin barrier function of representative areas was confirmed by determination of the transepidermal water loss (TEWL) using the closed-chamber device AquaFlux® (Biox Ltd., London, UK) (Klang et al., 2011b). The formulations were then applied to a marked area at a concentration of 6 mg/cm^2 with a saturated vinyl glove finger for 30 s.

After 1 h of penetration time, Corneofix® tapes were employed to remove the superficial stratum corneum layers of the porcine ear skin (Klang et al., 2011b,c). The outline of the first adhesive film was indicated with a permanent marker. Pressure was applied for 3 s with a rolling movement of the vinyl glove-covered thumb at a constant pressure of 49 N (5 kg). The tape was subsequently removed in a single rapid movement. This procedure was repeated with 25 tapes per experiment. The amount of adherent corneocytes was determined using the infrared densitometer SquameScan™ 850A (Heiland electronic GmbH, Wetzlar, Germany) (Voegeli et al., 2007). The optical pseudo-absorption of the adhesive films at 850 nm (A, in %) was employed to quantify the amount of stratum corneum proteins by employing the equation $m = A/0.41$ (μg/cm^2) (Klang et al., 2011b). The mean cumulative amount of the stratum corneum proteins removed with the tapes was employed to establish the penetration depth of fludrocortisone acetate in relation to the complete horny layer thickness. The latter was determined by continuous stripping of the complete stratum corneum in four of the experiments ($n = 4$) until the detection limit of the IR-densitometer was reached.

2.8. HPLC analysis

The samples were analysed for their drug content by HPLC (Series ISS-200, Perkin Elmer, USA), consisting of an auto sampler, a lc pump and an UV-diode array detector (235 C) using a Nucleosil 100-5 C18 column (250 mm × 4 mm, Macherey-Nagel, USA) plus pre-column (CC8/4, 40 mm × 4 mm). The oven temperature was set at 50 °C and the injection volume was 20 μl for all samples. Data analysis was performed using the TotalChrom Navigator 6.2.0 software. The quantification of fludrocortisone acetate was performed as previously reported (Klang et al., 2011a) at a detection wavelength of 240 nm using acetonitrile/water (40/60, v/v) as the mobile phase. The retention time was around 11 min at a flow rate of 0.8 ml/min. Standard solutions of fludrocortisone acetate in methanol were prepared and a calibration curve was calculated by plotting the analysed drug concentrations against the obtained peak area values. The concentration range of the standard solutions was between 0.018 μg/ml and 35.88 μg/ml with a coefficient of determination of $R^2 = 1$. However, the limit of reasonable quantification was set at 0.06 μg/ml since values below this concentration showed limited reproducibility.

2.9. Statistical data analysis

All results are expressed as means of at least three experiments ± SD. Statistical data analyses were performed using the GraphPadPrism3 program. Student's t-test or ANOVA with $P < 0.05$ as respective minimum level of significance were employed for the analysis of parametric data. Non-parametric data were analysed using the Mann–Whitney test or the Kruskal–Wallis-test with $P < 0.05$ as minimum level of significance, respectively. For the

Please cite this article in press as: Klang, V., et al., Effect of γ-cyclodextrin on the in vitro skin permeation of a steroidal drug from nanoemulsions: Impact of experimental setup. Int J Pharmaceut (2011), doi:10.1016/j.ijpharm.2011.11.037

G Model
IJP-12264; No. of Pages 8
ARTICLE IN PRESS
4 V. Klang et al. / International Journal of Pharmaceutics xxx (2011) xxx–xxx

Table 2
Physicochemical properties of nanoemulsions with fludrocortisone acetate (1%, w/w). All given values are means of at least three experiments ± SD ($n \geq 3$). The parameters shown in Table 2a are the mean hydrodynamic diameter or mean droplet size in nm, the PDI, the ZP values in mV as well as the conductivity of the diluted samples. The parameters given in Table 2b are the mean drug content in % of the originally incorporated drug amount as well as the pH of the investigated formulations.

(2a)

Formulation	Size (*d*, nm)	PDI	ZP (mV)	Cond (mS/cm)
NE	178.40 ± 0.66	0.040 ± 0.029	−31.27 ± 1.55	0.024 ± 0.006
γ-0.5% NE	171.03 ± 0.32	0.098 ± 0.042	−33.17 ± 0.75	0.021 ± 0.001
γ-1% NE	169.73 ± 2.35	0.033 ± 0.049	−31.73 ± 1.52	0.019 ± 0.001

(2b)

Formulation	Drug content (%)	pH
NE	96.17 ± 05.64	6.84 ± 0.02
γ-0.5% NE	91.93 ± 01.73	6.74 ± 0.01
γ-1% NE	93.13 ± 02.11	6.78 ± 0.02

diffusion cell studies, both cumulative amounts permeated and drug fluxes were statistically evaluated in parallel. The results were consistent in all cases.

3. Results and discussion

3.1. Nanoemulsion characterisation

The physicochemical properties of the produced nanoemulsions are given in Table 2. The mean hydrodynamic diameter of the droplets showed only a slight change upon incorporation of the CD (Table 2a). The PDI values after CD incorporation showed slightly increased standard deviations, but largely unaltered absolute values below 0.1, which represents a narrow droplet size distribution (Mueller and Schuhmann, 1996b). The ZP values, which characterise the surface charge of the emulsion droplets in solution, ranged slightly above −30 mV for all formulations, which indicates sufficient electrochemical stability. The low conductivity confirmed the validity of the ZP measurements (Mueller, 1996a). Overall, these results are in good agreement with previous studies (Klang et al., 2011a) and the produced formulations were therefore employed for the subsequent experiments on porcine skin.

As shown in Table 2b, both the mean drug content and the pH values of all formulations were in a satisfying range and confirmed the representative nature of the formulations for the envisioned studies.

3.2. In vitro skin permeation: franz-type diffusion cells

A standard nanoemulsion containing a steroidal model drug was chosen for comprehensive diffusion cell studies in order to systematically identify the most suitable experimental setup to obtain reliable permeation data for this and similar systems. In addition, these basic data served as a basis for comparison with formulations containing additional γ-CD.

3.2.1. Effect of the applied dose: finite vs. infinite dose

The effect of the applied dose on the skin permeation of fludrocortisone acetate into the aqueous buffer solution was investigated. In context of this finite/infinite dose comparison, two additional formulations with different amounts of γ-CD were evaluated in the same manner. The results of these experiments are given in Table 3. Quite expectedly, the skin permeation of fludrocortisone acetate from the standard nanoemulsion could be ranked in the order 5 mg/cm^2 < 50 mg/cm^2 < 500 mg/cm^2. Both the cumulative drug amount after 24 h and the mean drug flux were roughly ten-fold increased for the semi-infinite and infinite dose conditions ($P < 0.05$, respectively). No significant difference, however, was observed between the 50 and 500 mg/cm^2 application ($P > 0.05$). This suggests that infinite dose conditions were already reached at 50 mg/cm^2 although different reports exist (Lehman et al., 2011).

The ten-fold increase in applied dose from 5 to 50 mg/cm^2 was nicely reflected in the respective permeated drug amounts and fluxes. Comparatively large standard deviations were observed in all experiments since the overall permeated drug amounts were very low and biological material was involved as a model membrane.

In case of both systems containing additional γ-CD, the ten-fold increase in applied dose from 5 to 50 and from 50 to 500 mg/cm^2 was clearly reflected in the permeated drug amounts and fluxes ($P < 0.05$, respectively). Apparently, the addition of the CD magnified the increase in permeation with the increasing doses.

The enhancement effects caused by the incorporated γ-CD were clearly related to the amount of CD as well as the experimental setup. When comparing the formulation containing 0.5% (w/w) of γ-CD to the standard nanoemulsion, the permeation behaviour was quite similar at applied doses of 5 and 50 mg/cm^2 ($P > 0.05$, respectively). A significant enhancement effect was only observed at infinite dose conditions (500 mg/cm^2, $P < 0.05$). In case of 1.0% (w/w) of γ-CD, a significant enhancement effect was observed at all applied doses of 5, 50 and 500 mg/cm^2 when compared to the standard nanoemulsion ($P < 0.05$, respectively). This indicates that an enhancement effect can be achieved at both finite and infinite dose conditions if the amount of incorporated CD within the formulation is sufficiently high.

To exclude any direct effect of the CD on the skin, additional experiments were performed using the standard nanoemulsion. The skin was pre-impregnated within the franz-cell setup with 50 μl of either pure aqueous buffer, buffer containing 1% (w/w) of

Table 3
Skin permeation data of fludrocortisone acetate from standard nanoemulsions (NE) and corresponding formulations with 0.5% or 1.0% of additional γ-CD (γ-0.5% NE and γ-1% NE). Given values are means ± SD of at least 8 experiments ($n \geq 8$). Finite, semi-infinite and infinite dose conditions were tested with applied amounts of 5, 50 or 500 mg/cm^2 of formulation. For each setup, statistically significant differences with $P < 0.05$ against the standard nanoemulsion (NE) are marked with a '*'.

Formulation	Applied amount (mg)	Cumulative amount after 24 h ± SD (μg cm^{-2})	Mean drug flux ± SD (*J*, μg cm^{-2} h^{-1})
NE control	5	0.12 ± 0.11	0.008 ± 0.007
γ-0.5% NE	5	0.11 ± 0.09	0.005 ± 0.004
γ-1% NE	5	0.45 ± 0.23 *	0.067 ± 0.047 *
NE control	50	1.31 ± 1.11	0.08 ± 0.07
γ-0.5% NE	50	1.83 ± 0.63	0.08 ± 0.03
γ-1% NE	50	4.68 ± 2.44 *	0.90 ± 0.64 *
NE control	500	1.36 ± 1.10	0.09 ± 0.07
γ-0.5% NE	500	12.99 ± 2.53 *	0.63 ± 0.11 *
γ-1% NE	500	54.23 ± 15.65 *	2.48 ± 0.68 *

Please cite this article in press as: Klang, V., et al., Effect of γ-cyclodextrin on the in vitro skin permeation of a steroidal drug from nanoemulsions: Impact of experimental setup. Int J Pharmaceut (2011), doi:10.1016/j.ijpharm.2011.11.037

G Model
IJP-12264; No. of Pages 8
ARTICLE IN PRESS
V. Klang et al. / International Journal of Pharmaceutics xxx (2011) xxx–xxx 5

dissolved γ-CD or no additional solute. The skin permeation of fludrocortisone acetate in this setup was highly comparable to that observed in the conventional studies with untreated model skin ($n \geq 4$, $P > 0.05$ at all applied doses, data not shown). It may thus be assumed that the CD does not have a direct effect on the skin barrier function, which is in accordante with previous theories (Klang et al., 2011a) and studies where no permeation enhancement was observed after pre-treatment of skin with CDs in vitro (Williams et al., 1998). It likewise confirms that maceration effects, which are known to skew the results of diffusion cell studies after extended experiment times of over 24 h, are mainly a problem when investigating hydrophilic drugs (Otberg et al., 2008).

In conclusion, the assumed mechanism behind the enhanced permeation of fludrocortisone acetate is not related to any direct effects on skin, but most likely to solubility effects within the vehicle. In literature, the most frequently suggested mechanism of action relies on the better dispersion of the drug molecules within the vehicle through complexation with the CD and thus better solubilisation of the drug (Loftsson and Masson, 2001; Loftsson et al., 2007). As a consequence, more drug is available at the skin surface to enter the SC through diffusion. The CD molecules themselves are too large to penetrate into the skin themselves. As previously discussed (Klang et al., 2011a), it remains to be clarified whether this mechanism can be held responsible for the observed strong effects if only small molar amounts of CD are present within the vehicle. CDs may also affect the interfacial films of the emulsion droplets (Klang et al., 2011a). Thus, the modified emulsion structure could also contribute to the altered drug release from the droplets. Since we are dealing with dynamic systems, a combination of both mechanisms is well possible.

In summary, the amount of applied dose was confirmed to be a crucial parameter in the diffusion cell studies of the fluid nanoemulsions. For experiments with semi-solid systems, finite dose conditions are usually recommended although certain applications for infinite doses exist as well (Gillet et al., 2011). For theoretical evaluations, infinite dose conditions offer the advantage of standardised kinetic conditions as the influence of the dose on skin permeation is minimised (Wagner et al., 2002). Thus, the permeation of different drugs might be compared more directly. In our case, we primarily benefited from more accurate drug quantification by HPLC grace to the increased amounts of drug detected in the receptor medium. Likewise, application of the formulation onto the diffusion cells was facilitated due to the larger amount of sample. Thus, errors due to inaccurate weighing are minimised (Wagner et al., 2002). Since the permeation data obtained for the 50 mg/cm^2 dose of the standard nanoemulsion were a very accurate upscale from the finite dose of 5 mg/cm^2, the former dose was chosen for further studies with this system to investigate the effects of other methodological parameters.

3.2.2. Occluded vs. non-occluded conditions

For comparative reasons, additional studies were performed using diffusion cells with non-occluded upper chambers. The skin permeation of fludrocortisone acetate from the standard nanoemulsion was investigated at all three amounts of applied dose (5, 50 and 500 mg/cm^2, Fig. 1). Large standard deviations were observed under non-occluded conditions at all amounts of applied dose. At occluded conditions, this was primarily the case for finite dose application. Apart from this slight trend, no statistically significant differences were observed between the experiments at occluded or non-occluded conditions regarding cumulative amounts drug amounts or drug fluxes at all amounts of applied dose ($P > 0.05$, respectively).

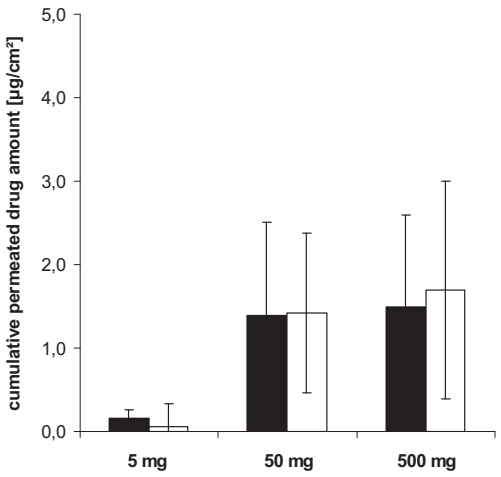

Fig. 1. Cumulative permeated amounts of fludrocortisone acetate after 24 h from standard nanoemulsions (NE) at occluded (black bars) or non-occluded conditions (white bars). Finite (5 mg/cm^2), semi-infinite (50 mg/cm^2) and infinite dose (500 mg/cm^2) application of the formulation were employed. Given values are means ± SD of at least 8 experiments ($n \geq 8$).

3.2.3. Effect of the skin thickness

Since the thickness of the employed model skin plays a major role in diffusion cell experiments, two differently dermatomed skin samples of 1.2 or 0.5 mm thickness were employed for comparative studies. Again, the experiments were performed using the model nanoemulsion at all amounts of applied dose (5, 50 and 500 mg/cm^2, Fig. 2). Quite expectedly, significantly higher cumulative drug amounts and drug fluxes were observed at a skin thickness of 0.5 mm for all applied amounts of standard nanoemulsion ($P < 0.05$, respectively). The use of split-thickness or strongly dermatomed skin is indeed recommended for absorption studies of poorly water soluble drugs (Lehman et al., 2011). However, the drug fluxes for the thin skin samples were rather irregular and

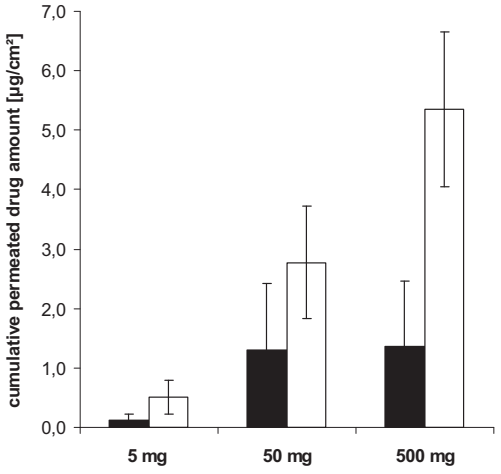

Fig. 2. Cumulative permeated amounts of fludrocortisone acetate from standard nanoemulsions (NE) after 24 h through porcine abdominal skin at a skin thickness of either 1.2 mm (black bars) or 0.5 mm (white bars). Finite (5 mg/cm^2), semi-infinite (50 mg/cm^2) and infinite dose (500 mg/cm^2) application of the formulation were employed. Given values are means ± SD of at least 5 experiments ($n \geq 5$).

Please cite this article in press as: Klang, V., et al., Effect of γ-cyclodextrin on the in vitro skin permeation of a steroidal drug from nanoemulsions: Impact of experimental setup. Int J Pharmaceut (2011), doi:10.1016/j.ijpharm.2011.11.037

G Model
IJP-12264; No. of Pages 8
ARTICLE IN PRESS
6 V. Klang et al. / International Journal of Pharmaceutics xxx (2011) xxx–xxx

Table 4
Solubility of fludrocortisone acetate in different receptor media. All values were determined at least in quadruplicate ($n \geq 4$).

Receptor fluid	Drug solubility (μg/ml) ± SD
Phosphate buffer pH 7.4	15.04 ± 2.43
Phosphate buffer/BSA (1.4%, w/v)	34.69 ± 0.19
Phosphate buffer/BSA (5%, w/v)	63.91 ± 0.16
Phosphate buffer/propylene glycol (80/20, v/v)	57.81 ± 0.66
Phosphate buffer/PEG 400 (80/20, v/v)	72.34 ± 7.65
Phosphate buffer/ethanol (80/20, v/v)	105.09 ± 1.38

hardly showed a consistent increase over time. This might be due to the fact that producing dermatomed skin samples of such small thickness becomes increasingly difficult and already small aberrations in the skin may lead to variable results. Thus, a compromise regarding skin thickness should be found to produce adequately homogeneous skin samples without creating an unphysiologically strong barrier for lipophilic drugs.

3.2.4. Effect of the acceptor medium

The solubility data obtained for the different receptor media are given in Table 4. As expected, the solubility of fludrocortisone acetate was markedly increased in the presence of the different additives. The strongest increase in solubility was caused by the presence of 20% (v/v) of ethanol, followed by the respective amounts of PEG 400, propylene glycol and finally BSA at 1.4% (w/v). The buffer containing 5% (w/v) of BSA was excluded from further studies due to its high foaming tendency, which rendered this medium impractical for the envisioned studies.

Pure phosphate buffer still represents the receptor fluid of choice if undesired interactions with constituents of the skin or the employed formulation are to be avoided. This was particularly important in our case where the specific effect of the CD should be investigated separately and undisturbed by any additional factors. Thus, the phosphate buffer was employed for all basic studies. The different receptor media were compared in additional studies using the standard nanoemulsion at 50 mg/cm^2 application (Table 5). In this setup, semi-infinite dose application was employed to emphasise potential differences in drug permeation. A comparison of the different receptor media revealed that both cumulative drug amounts and drug fluxes were highly comparable for the control buffer and the buffer media containing either BSA, propylene glycol or PEG 400 ($P > 0.05$ in all cases). Merely in case of the ethanol-containing buffer a significantly increased drug permeation was noticeable when compared to the control buffer ($P < 0.05$). This indicates that in case of this steroidal model drug, the increased solubility in the different receptor media caused by BSA, propylene glycol or PEG 400 was apparently not sufficient to promote its skin permeation. Comparative studies employing an application dose of 500 mg/cm^2 revealed the same tendency, at the same time confirming that no significant difference between the two amounts of applied dose are to be expected irrespective of the employed receptor medium ($n \geq 5$, $P > 0.05$ in all cases, data not shown). The remarkably enhanced skin permeation in context with ethanol that was observed for both 50 and 500 mg/cm^2 application is in accordance with the solubility data given in Table 4. It may however be assumed that the impact of ethanol on the skin itself may have contributed to this pronounced effect.

Table 5
Skin permeation of fludrocortisone acetate from standard nanoemulsions (NE) at semi-infinite dose conditions using 50 mg/cm^2 of applied formulation and different acceptor media. Given values are means ± SD of at least 8 experiments ($n \geq 8$).

Investigated receptor medium	Applied dose (mg)	Cumulative amount after 24 h ± SD (μg cm^{-2})	Mean drug flux ± SD (J, μg cm^{-2} h^{-1})
Buffer	50	0.80 ± 0.88	0.29 ± 0.21
Buffer with BSA	50	0.19 ± 0.13	0.17 ± 0.13
Buffer with PG	50	0.57 ± 0.62	0.20 ± 0.17
Bufffer with PEG	50	0.47 ± 0.48	0.21 ± 0.13
Buffer with EtOH	50	5.46 ± 3.43	2.09 ± 0.98

As commonly known, current recommendations such as the OECD guidelines rely on the use of isotonic buffer media for skin permeation studies with franz-type diffusion cells. The receptor fluid should provide adequate solubility of the permeant so as not to hinder its absorption, but at the same time be innocuous to the skin (Gillet et al., 2011). In case of lipophilic drugs, the solubility requirements are usually not met by standard buffer media such as phosphate buffered saline. Thus, additives which increase the solubility of the permeant may be incorporated in the receptor medium, such as surfactants, propylene glycol, bovine serum albumin or even ethanol. However, these additives may affect the skin samples and can alter the apparent skin diffusion rates of applied substances (Gillet et al., 2011; Lehman et al., 2011). This is frequently observed for both propylene glycol and ethanol, which may act as permeation enhancers (Megrab et al., 1995a, b). They supposedly act via increasing drug solubility in the stratum corneum, but may also directly affect stratum corneum components. However, solvent concentrations of over 60% may lead to dehydration of the skin, thus decreasing drug flux. Likewise, a solvent gradient across the membrane may influence the results due to osmotic or solvent drag effects, i.e. the co-transport of water and solvent through the membrane and back-diffusion effects (Megrab et al., 1995a; Sznitowska, 1996). For these reasons, we chose to limit the amounts of additives in the receptor medium to 20% (v/v). If the rate of absorption of a given compound is quite low even isotonic buffer can serve as an adequate receptor for some compounds that are otherwise considered water insoluble (Lehman et al., 2011). In context with the presented experiments, this might explain why the aqueous buffer medium performed equally well when compared to other media containing BSA, propylene glycol or PEG 400.

3.3. In vitro skin penetration: tape stripping

Additional skin penetration studies without the use of buffer media were conducted to exclude any maceration or skin hydration effects on the outcome. Since it is well-known that a strong inter-individual variability in SC thickness exists (Dickel et al., 2010; Jacobi et al., 2007; Kalia et al., 2000; Schwindt et al., 1998), at least 8 individual experiments were performed for each formulation ($n \geq 8$). The experiments served to determine the skin penetration potential of the standard nanoemulsion itself. Furthermore, the effect of additionally incorporated γ-CD should be evaluated in this in vitro setup as well. Fig. 3 shows the skin penetration profile (Lademann et al., 2009) of fludrocortisone acetate from the standard nanoemulsion. The penetration depth of the three formulations was in the order of γ-1% NE > γ-0.5% NE > NE (Fig. 4). However, these differences did not reach statistical significance ($P > 0.05$ in all cases). In case of the nanoemulsion containing 1% of γ-CD, up to 87% of the total SC thickness were reached; the latter was found to be around 8.06 ± 1.22 μm ($n = 4$) for the employed porcine ears. The summarised penetrated drug amounts were in the range of 20–30 μg/cm^2 in all cases.

In additional studies, corresponding formulations with a different oil phase consisting of the commonly used squalene were produced and investigated in identical tape stripping experiments with fludrocortisone acetate (data not shown). Again, a slightly deeper skin penetration of the formulations containing γ-CD was observed. The differences did not reach statistical significance in this case, either, but the same trends were observed.

Please cite this article in press as: Klang, V., et al., Effect of γ-cyclodextrin on the in vitro skin permeation of a steroidal drug from nanoemulsions: Impact of experimental setup. Int J Pharmaceut (2011), doi:10.1016/j.ijpharm.2011.11.037

G Model
IJP-12264; No. of Pages 8
ARTICLE IN PRESS
V. Klang et al. / International Journal of Pharmaceutics xxx (2011) xxx–xxx 7

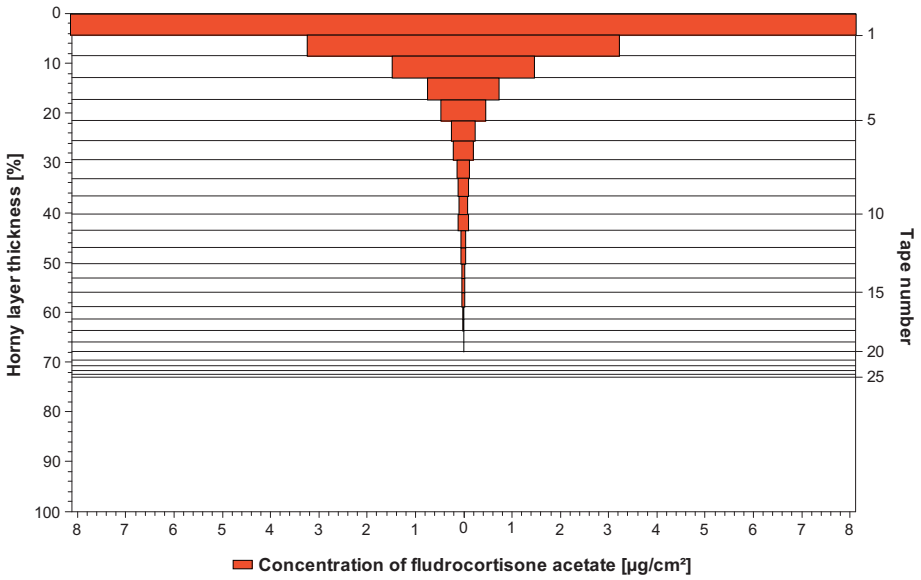

Fig. 3. Skin penetration profile of fludrocortisone acetate from a standard nanoemulsion (NE). The depicted values are means of eight individual experiments ($n = 8$). The distances between the horizontal lines correspond to the respective amounts of removed SC while the coloured areas represent the corresponding amounts of recovered drug on the respective tape strips. The upper line of the profiles corresponds to the skin surface, the lowest line to the boundary of living cells below the SC.

When comparing these findings to the results of the diffusion cell experiments, it may be assumed that the non-destructive manner of formulation application in the franz-cell setup might be associated with the permeation enhancement. In diffusion cell setups, the formulation is not massaged into the skin as during tape stripping and the emulsion structure remains intact. This preservation of the internal formulation structure might be the underlying cause of the disproportionately strong permeation enhancement effect through γ-CD especially at infinite dose conditions. Thus, the discussed solubility effects or changes in formulation structure caused by the incorporation of the CD may take hold.

It may be advisable to conduct additional tape stripping experiments when investigating the permeation enhancement potential of CDs in diffusion cell studies. With a conventional finite-dose in vivo application, the strong enhancement potential of the CD as observed in the franz-cell setup will not be realised to its full extent. The development of infinite-dose vehicles for in vivo application, such as matrix patches, might serve to overcome this limitation.

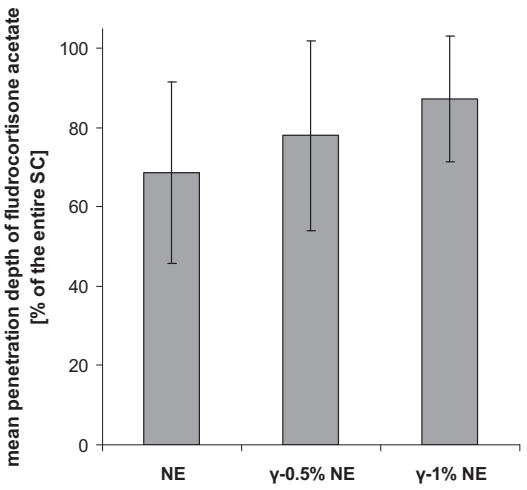

Fig. 4. Skin penetration depth observed after in vitro tape stripping with a standard nanoemulsion containing fludrocortisone acetate (NE) as well as corresponding nanoemulsions containing additional amounts of 0.5 or 1% of γ-CD. The presented values are means ± SD of at least 8 individual experiments ($n \geq 8$).

3.4. Optimisation of the franz-cell technique for nanoemulsion studies with steroidal drugs: conclusive remarks

Overall, we found that the classical franz-cell method consisting of using a skin thickness of 1.2 mm, infinite dose application of the formulation and pure phosphate buffer as acceptor medium led to the most reproducible results and is likewise the most practical working procedure in regard to skin preparation, sampling accuracy and quantification limits. In the case of formulations containing CDs, additional in vitro methods such as tape stripping experiments are recommended to detect potential overestimations caused by the conditions of the franz-cell setup.

4. Conclusion

Remarkably strong permeation enhancement effects for the steroidal model drug were obtained with the franz-cell setup at sufficiently high amounts of γ-CD, especially at infinite dose conditions. These effects were obviously related to the peculiarities of the experimental setup, where large amounts of formulation are applied without massaging them into the skin. The potential of this enhancement strategy cannot be realised to its full extent upon mechanical application of a finite dose on skin, as was shown in tape stripping experiments in vitro. As a next step, in vivo experiments would be of interest. Future research should focus on the development of novel dermal delivery systems such as matrix patches

Please cite this article in press as: Klang, V., et al., Effect of γ-cyclodextrin on the in vitro skin permeation of a steroidal drug from nanoemulsions: Impact of experimental setup. Int J Pharmaceut (2011), doi:10.1016/j.ijpharm.2011.11.037

G Model
IJP-12264; No. of Pages 8
ARTICLE IN PRESS
8 V. Klang et al. / International Journal of Pharmaceutics xxx (2011) xxx–xxx

enforced by CDs where infinite dose application may be employed while maintaining the formulations' original structure.

Conflicts of interest

No conflicts of interest occurred in the context of this study for any of the authors.

Acknowledgements

The authors would like to thank Wolfgang Sipos and the Veterinary University of Vienna for providing fresh porcine ears. The financial support of the research platform "Characterisation of Drug Delivery Systems on Skin and Investigation of Involved Mechanisms" is gratefully acknowledged.

References

Bosman, I.J., Ensing, K., de Zeeuw, R.A., 1998. Standardization procedure for the in vitro skin permeation of anticholinergics. Int. J. Pharm. 169, 65–73.
Dickel, H., Goulioumis, A., Gambichler, T., Fluhr, J.W., Kamphowe, J., Altmeyer, P., Kuss, O., 2010. Standardized tape stripping: a practical and reproducible protocol to uniformly reduce the stratum corneum. Skin Pharmacol. Physiol. 23, 259–265.
Franz, T.J., 1975. Percutaneous absorption. On the relevance of in vitro-data. J. Invest. Dermatol. 64, 190–195.
Gillet, A., Evrard, B., Piel, G., 2011. Liposomes and parameters affecting their skin penetration behaviour. J. Drug. Del. Sci. Tech. 21, 35–42.
Henning, A., Schaefer, U.F., Neumann, D., 2009. Potential pitfalls in skin permeation experiments: influence of experimental factors and subsequent data evaluation. Eur. J. Pharm. Biopharm. 72, 324–331.
Jacobi, U., Kaiser, M., Toll, R., Mangelsdorf, S., Audring, H., Otberg, N., Sterry, W., Lademann, J., 2007. Porcine ear skin: an in vitro model for human skin. Skin Res. Technol. 13, 19–24.
Kalia, Y.N., Alberti, I., Sekkat, N., Curdy, C., Naik, A., Guy, R.H., 2000. Normalization of stratum corneum barrier function and transepidermal water loss in vivo. Pharm. Res. 17, 1148–1150.
Klang, V., Matsko, N., Zimmermann, A.M., Vojnikovic, E., Valenta, C., 2010. Enhancement of stability and skin permeation by sucrose stearate and cyclodextrins in progesterone nanoemulsions. Int. J. Pharm. 393, 152–160.
Klang, V., Matsko, N., Raupach, K., El-Hagin, N., Valenta, C., 2011a. Development of sucrose stearate-based nanoemulsions and optimisation through gamma-cyclodextrin. Eur. J. Pharm. Biopharm. 79, 58–67.
Klang, V., Schwarz, J.C., Hartl, A., Valenta, C., 2011b. Facilitating in vitro tape stripping: application of infrared densitometry for quantification of porcine stratum corneum proteins. Skin Pharmacol. Physiol. 24, 256–268.
Klang, V., Schwarz, J.C., Matsko, N., Rezvani, E., El-Hagin, N., Wirth, M., Valenta, C., 2011c. Semi-solid sucrose stearate-based emulsions as dermal drug delivery systems. Pharmaceutics 3, 275–306.
Lademann, J., Jacobi, U., Surber, C., Weigmann, H.J., Fluhr, J.W., 2009. The tape stripping procedure—evaluation of some critical parameters. Eur. J. Pharm. Biopharm. 72, 317–323.
Lehman, P.A., Raney, S.G., Franz, T.J., 2011. Percutaneous absorption in man: in vitro-in vivo correlation. Skin Pharmacol. Physiol. 24, 224–230.
Leveque, N., Makki, S., Hadgraft, J., Humbert, P., 2004. Comparison of Franz cells and microdialysis for assessing salicylic acid penetration through human skin. Int. J. Pharm. 269, 323–328.
Loftsson, T., Olafsdottir, B.J., Bodor, N., 1991. The effect of cyclodextrins on transdermal delivery of drugs. Eur. J. Pharm. Biopharm. 37, 30–33.
Loftsson, T., Olafsson, J.H., 1998. Cyclodextrins: new drug delivery systems in dermatology. Int. J. Dermatol. 37, 241–246.
Loftsson, T., Masson, M., 2001. Cyclodextrins in topical drug formulations: theory and practice. Int. J. Pharm. 225, 15–30.
Loftsson, T., Bodor, N., 2006. Effect of cyclodextrins on percutaneous transport of drugs. In: Smith, E.W., Maibach, H.I. (Eds.), Percutaneous Penetration Enhancers. C.R.C. Press Inc., New York, pp. 335–342.
Loftsson, T., Vogensen, S.B., Brewster, M.E., Konradsdottir, F., 2007. Effects of cyclodextrins on drug delivery through biological membranes. J. Pharm. Sci. 96, 2532–2546.
Lopez, R.F., Collett, J.H., Bentley, M.V., 2000. Influence of cyclodextrin complexation on the in vitro permeation and skin metabolism of dexamethasone. Int. J. Pharm. 200, 127–132.
Matsuda, H., Arima, H., 1999. Cyclodextrins in transdermal and rectal delivery. Adv. Drug Deliv. Rev. 36, 81–99.
Megrab, N.A., Williams, A.C., Barry, B.W., 1995a. Oestradiol permeation across human skin, silastic and snake skin membranes: the effects of ethanol/water co-solvent systems. Int. J. Pharm. 116, 101–112.
Megrab, N.A., Williams, A.C., Barry, B.W., 1995b. Oestradiol permeation through human skin and silastic membrane: effects of propylene glycol and supersaturation. J. Control. Release 36, 277–294.
Michniak-Kohn, B.B., Wertz, P.W., Al-Khalili, M., Meidan, V.M., 2005. Skin: physiology and penetration pathways. In: Rosen, M.R. (Ed.), Delivery System Handbook for Personal Care and Cosmetic Products. William Andrew Inc., New York, pp. 77–100.
Montassier, P., Duchene, D., Poelman, M.-C., 1998. In vitro release study of tretinoin from tretinoin/cyclodextrin derivative complexes. J. Incl. Phen. Mol. Recogn. Chem. 31, 213–218.
Mueller, R.H., 1996. Zetapotential und Partikelladung in der Laborpraxis, Band 37. Wissenschaftliche Verlagsgesellschaft mbH, Stuttgart.
Mueller, R.H., Schuhmann, R., 1996. Teilchengrößenmessungen in der Laborpraxis. Wissenschafltiche Verlagsgesellschaft mbH, Stuttgart.
Otberg, N., Grone, D., Meyer, L., Schanzer, S., Hoffmann, G., Ackermann, H., Sterry, W., Lademann, J., 2008. Water-filtered infrared-A (wIRA) can act as a penetration enhancer for topically applied substances. Ger. Med. Sci. 6, 1–14.
Rajewski, R.A., Stella, V.J., 1996. Pharmaceutical applications of cyclodextrins. 2. In vivo drug delivery. J. Pharm. Sci. 85, 1142–1169.
Scalia, S., Tursilli, R., Iannuccelli, V., 2007. Complexation of the sunscreen agent, 4-methylbenzylidene camphor with cyclodextrins: effect on photostability and human stratum corneum penetration. J. Pharm. Biomed. Anal. 44, 29–34.
Schwindt, D.A., Wilhelm, K.P., Maibach, H.I., 1998. Water diffusion characteristics of human stratum corneum at different anatomical sites in vivo. J. Invest. Dermatol. 111, 385–389.
Sznitowska, M., 1996. The influence of ethanol on permeation behaviour of the porous pathway in the stratum corneum. Int. J. Pharm. 137, 137–140.
Trichard, L., Fattal, E., Besnard, M., Bochot, A., 2007. Alpha-cyclodextrin/oil beads as a new carrier for improving the oral bioavailability of lipophilic drugs. J. Control. Release 122, 47–53.
Voegeli, R., Heiland, J., Doppler, S., Rawlings, A.V., Schreier, T., 2007. Efficient and simple quantification of stratum corneum proteins on tape strippings by infrared densitometry. Skin Res. Technol. 13, 242–251.
Wagner, H., Kostka, K.H., Lehr, C.M., Schaefer, U.F., 2000. Drug distribution in human skin using two different in vitro test systems: comparison with in vivo data. Pharm. Res. 17, 1475–1481.
Wagner, H., Kostka, K.H., Lehr, C.M., Schaefer, U.F., 2002. Human skin penetration of flufenamic acid: in vivo/in vitro correlation (deeper skin layers) for skin samples from the same subject. J. Invest. Dermatol. 118, 540–544.
Williams, A.C., Shatri, S.R., Barry, B.W., 1998. Transdermal permeation modulation by cyclodextrins: a mechanistic study. Pharm. Dev. Technol. 3, 283–296.

Please cite this article in press as: Klang, V., et al., Effect of γ-cyclodextrin on the in vitro skin permeation of a steroidal drug from nanoemulsions: Impact of experimental setup. Int J Pharmaceut (2011), doi:10.1016/j.ijpharm.2011.11.037

Skin integrity testing and monitoring of in vitro tape stripping by capacitance-based sensor imaging

Victoria Klang[a], Julia C. Schwarz[b], Silvia Haberfeld[a], Perry Xiao[c], Michael Wirth[a], Claudia Valenta[ab*]

[a]University of Vienna, Department of Pharmaceutical Technology and Biopharmaceutics, Faculty of Life Sciences, Althanstraße 14, 1090 Vienna, Austria
[b]University of Vienna, Research Platform "Characterisation of Drug Delivery Systems on Skin and Investigation of Involved Mechanisms", Vienna, Austria
[c]Faculty of ESBE, London South Bank University, 103 Borough Road, London SE1 0AA, United Kingdom
[*]Corresponding Author: Claudia Valenta, Claudia.valenta@univie.ac.at, Tel: +43 1 4277 55 410, Fax: +43 1 4277 9554

Abstract

Background: Despite the frequent use of porcine ear skin for tape stripping experiments the peculiarities of this skin type have not been characterised in detail yet. Thus, different techniques were employed to investigate the skin surface structure of porcine ear skin and the changes in barrier function during in vitro tape stripping. To this end, the potential of capacitance-based skin hydration imaging as means of skin quality control was investigated for the first time.
Methods: The porcine ear model was characterised before and during tape stripping by TEWL measurements, capacitance-based sensor imaging, ATR-FTIR and optical light microscopy.
Results: The capacitance-based sensor was found to deliver precise information about the quality of the employed skin sites before and during tape stripping. The removal of stratum corneum proteins was highly reproducible even for different porcine ear types. The mean greyscale values showed an excellent linear correlation to the corresponding TEWL values and the respective penetration depth. Optical light microscopy confirmed the presence of canyons on the surface of porcine ear skin.
Conclusion: The results suggest that the capacitance-based sensor is a suitable tool for skin integrity testing of porcine ear skin in vitro and for monitoring changes in skin barrier function.
Keywords: stratum corneum, porcine ear skin, capacitance-based sensor imaging, tape stripping, transepidermal water loss, skin surface structure, ATR-FTIR

1 Introduction

The tape stripping procedure is a well-established method to determine the skin penetration behaviour of active substances. Adhesive films are employed to remove the uppermost corneocyte layers of the stratum corneum (SC) and penetration profiles can be obtained by analysing both the amount of drug and the amount of proteins on the individual tapes (1, 2). This technique is most frequently employed for in vivo experiments on human forearm skin (3). In an approach to minimise such in vivo experiments and the associated organisatorial effort, the porcine ear model is increasingly investigated as an in vitro model for tape stripping experiments (4). Apart from a standardised working procedure and reliable methods of protein quantification, a constant high quality of the employed porcine ear skin is of vital importance for such in vitro experiments. However, porcine ears may be of a variable nature depending on the breed and upbringing of the sacrificed animal. The most suitable areas for tape stripping experiments, namely the central part of the dorsal side of the ear (5, 6), may be damaged due to tags or injuries (Figure 1). Small superficial lesions or

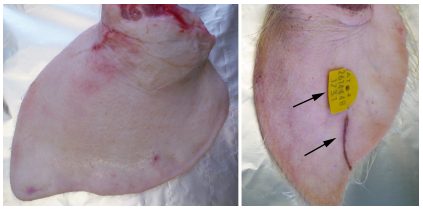

Figure 1: Fresh porcine ears. Care has to be taken to avoid damaged skin areas (indicated by arrows) or regions of excessive hair growth.

diseases of the skin may not be this obvious to the naked eye and require additional techniques for quality control of the employed skin. An established method for this purpose is the assessment of the transepidermal water loss (TEWL), which is related to the skin barrier function. Low TEWL values can be considered as a sign of an intact barrier. However, this technique originates from in vivo applications and does not offer the exact same applicability in vitro. Since excised porcine ears lack an active circulation, the tissue as well as the skin will invariably dehydrate over the course of an experiment. Thus, the obtained TEWL values cannot be considered as absolute values representing the in vivo situation since they are entirely dependent on the state of the ear. Although the TEWL in vitro can be employed to monitor the defrosting process and the hydration state of porcine ears within a set of experiments with satisfying accuracy (4, 7, 8), the discussed limitations represent a source of error. Thus, we decided to investigate the suitability of further methods for the quality assessment of porcine ear skin for tape stripping experiments. Apart from systematic TEWL measurements, a microscopic investigation of the tapes removed from the skin surface was performed. In addition, the properties of the skin surface structure were characterised by capacitance-based measurements with a specifically designed fingerprint sensor. Capacitance-based sensor imaging allows for recording capacitance images of the skin surface and is a convenient tool to describe and quantify skin surface hydration (9). Capacitive skin images also give a high resolution representation of skin topography, in terms of wrinkles and cells. In dermatology and cosmetics, skin topography characterisation is employed to identify lesions, evaluate the effect of topical formulations or evaluate skin ageing (10). Interestingly, this technique has not been employed for skin integrity testing in context with tape stripping experiments on either human or porcine skin. Therefore, the aim of this work was to validate the technique of capacitance-based sensor imaging for quality control of skin samples and monitoring of the changes in skin barrier function dur-

ing tape stripping. Comparative assessment of TEWL values should reveal whether the two techniques deliver comparable results and are equally suitable for an initial control of porcine ear skin and a subsequent in-process control during in vitro tape stripping. The latter represents an important prerequisite to obtain reliable skin penetration data. Irregular protein removal may occur quite suddenly during tape stripping if large skin patches loose cohesion (3). As a consequence, inaccurate skin penetration profiles may be obtained if optical methods of protein quantification are employed (11). Therefore, such biased data should be identified and excluded from further evaluation. In addition, attenuated total reflection fourier transform infrared spectroscopy (ATR-FTIR) measurements were conducted to observe the changes in SC barrier function during tape stripping on porcine ear skin. In respect to the pig ear model, a further aim of this work was to confirm previous observations regarding the skin surface structure of human and porcine skin by microscopic investigation of removed tape strips. Although the structure of porcine ear skin is highly similar to that of human skin, the superficial appearance of porcine and human skin may differ considerably, as was recently observed during NIR-densitometric measurements for the quantification of porcine stratum corneum proteins during tape stripping (4). Since the different protein coverage of the tape strips was only demonstrated in photographs, we hereby provide microscopic images for a more precise visualisation of this phenomenon.

2 Materials and Methods

Materials and preparation of the porcine ears

Standard D-Squame® adhesive tapes with a diameter of 22 mm and an area of 3.8 cm^2 were purchased from CuDerm Corp. (Dallas, TX, USA). Standard Corneofix® adhesive films with a square area of 4.0 cm^2 were obtained from Courage + Khazaka GmbH (Cologne, Germany). Tesa film crystal clear tapes (product number 57859-00000) were obtained from Tesa GmbH (Vienna, Austria). Different types of pig ears were investigated. In order to ensure logistic feasibility and reproducibility of the experiments, all porcine ears were stored at -24°C and thawed prior to the experiments. The porcine ear skin may be variable in thickness and hair growth depending on the pig's age and breed. On the one hand, ears of fattened full grown pigs from a local farmer were tested immediately after slaughtering (aged 6 to 10 months). It may be assumed that most porcine ears employed in studies are obtained from fattened pigs (12). These large ears possessed thick, rough and dry skin exhibiting dense coverage with long hair. On the other hand, small porcine ears were obtained from another pig breed from the Clinic for Swine, University of Veterinary Medicine Vienna. These ears could be obtained at much younger age of the pigs (3 to 4 months) directly after sacrifice. The skin of these small ears was very soft and almost free of hair. Nevertheless, pigs of more than 12 weeks of age are considered adult (13). After defrosting, the ears were cleaned carefully with purified water and blotted dry with soft tissue. The skin remained at the cartilage at all times except in case of the separate ATR-FTIR measurements. In addition, one set of non-invasive in vivo sensor measurements was conducted on pigs aged 3 to 4 months at the Clinic for Swine, University of Veterinary Medicine Vienna, in accordance with the respective regulations.

Characterisation of the porcine skin surface in comparison to human forearm skin in vivo

The skin surface properties of the model ears were established using TEWL measurements, capacitance-based sensor measurements and optical light microscopy for analysis of individually removed tapes. For the latter task, both Corneofix® and DSquame® tapes were tested. The same techniques were applied to human forearm skin of the experimenter for comparison.

In vitro tape stripping

Ten individual tape stripping experiments were performed using Corneofix® tapes (n=10). Two different types of porcine ears were employed for comparison (n=5, respectively). The pig ear skin was carefully freed from hair with scissors. After marking the outline of the respective first adhesive film on the dorsal skin surface, up to 120 tapes were removed from the same area after pressure application with the thumb as previously described (4). The tape stripping procedure was stopped when the detection limit of the NIR-densitometer for protein quantification was reached. Both assessment of the TEWL, capacitance-based sensor measurements and microscopic analyses of the removed tapes were performed in regular intervals during the tape stripping process.

Protein quantification by NIR-densitometry

The amount of corneocytes removed with each tape strip was analysed using the infrared densitometer SquameScanTM 850A (Heiland electronic GmbH, Wetzlar, Germany) (14). Briefly, the optical pseudo-absorption of the adhesive films at a wavelength of 850 nm was determined against a blank reference tape. Using previously determined calibration data for porcine skin (4), the mass of corneocytes on the adhesive films can be calculated by employing the equation m = A / 0.41 (in $\mu g \cdot cm^{-2}$). The mean cumulative amount of removed SC proteins was employed to calculate the removed SC thickness assuming the mean protein density of the tissue to be around 1 g $\cdot$ cm-3 (7).

Correlation of the removed stratum corneum amount with the number of tape strips

The total values of absorbance at 850 nm of all consecutively removed tape strips were obtained by adding up the individual absorption values of these tape strips as determined by NIR-densitometric measurements. This sum absorbance can be regarded as representative for the thickness of the complete SC. Therefore, this value can be set as a standard for 100% of the SC thickness. This relation can be used to transform the relative amount of SC that is removed with each tape strip into a percentage value as demonstrated for human SC (15). Since human and porcine skin is not entirely comparable, we hereby for the first time established this correlation for in vitro tape stripping using porcine ear skin.

The addition of individual absorbances to obtain a sum absorbance of the whole SC was carried out 10 times (n=10). The mean of the obtained sum absorbances was set as 100% of SC thickness. This value was employed to calculate the cumulative relative horny layer thickness that was removed after 1 to a maximum of 120 tape strips, respectively. The exponential correlation between the number of removed tape strips and the relative horny layer thickness as derived from sum absorbance values was calculated using the software program R.

TEWL measurements

The TEWL of the investigated porcine ear skin sites was determined before and during the tape stripping process with the closed-chamber device Aquaflux® (Biox Ltd., London, UK). Determination of the TEWL is a standard procedure for assessing skin integrity before experiments or during wound healing processes (16). The TEWL is expressed in $g/m^2/h$ and represents the quantity of water that is lost via the skin per hour and 1 m^2 of skin area. If larger quantities of water pass through the skin when compared to established standard values, barrier defects may be suspected (16).

Capacitance - based fingerprint sensor imaging

The skin relief, i.e. the surface texture or topography, is an important biophysical feature that cannot be evaluated by the naked eye alone. A method that was found highly useful for in vivo studies due to its simplicity and speed of data acquisition is capacitance mapping of the skin (17, 18). Skin capacitance imaging is a non-invasive and non-optical method that can distinguish different levels of stratum corneum hydration and can thus identify sites of dermal inflammation, lesions or sweat gland disturbances in vivo (19, 20). Skin capacitance is an electrical property of the skin measurable at the level of the SC. The obtained values are related to the moisture content of the tissue (21). Changes in the SC structure may be related to its water holding capacity or alterations of the barrier function which affect the electrical properties of the skin (20). The capacitive pixel-sensing technology is an area-integrating surface texture method that images the capacitance at 50 μm intervals on the skin surface and exposes skin pores, primary and secondary lines and wrinkles (17, 21, 22). The technique is based on silicone image sensor technology, initially developed for the assessment of fingerprints in biometric security procedures (20).

In our case, a specifically designed capacitance-based fingerprint sensor (MBF 200, Fujistu Ltd.) (23) was employed for skin hydration imaging and surface analysis. The employed sensor consisted of 256x300 pixels, a 50x50 μm spatial resolution and an 8-bit greyscale value scale ranging from 0 to 255 to represent low to high skin hydration levels (23). This device is a hand-held probe which is applied onto the skin for rapid assessment of the current skin hydration properties. The skin surface pattern of hydration and topography is then viewed in the form of high-resolution real-time non-optical images: dark pixels represent hydrated areas of high capacitance while bright pixels may represent dry spots on the skin or depressions and lines in the skin's micro relief which impede the contact between the probe and the stratum corneum (20). Areas where skin moisture is lost via the SC, be it via natural routes such as sweat glands or through damaged skin areas, can be detected. The sensor can be used to detect subclinical irritation, acne or psoriatic lesions or sweat gland disturbances in vivo (19) and to monitor the effect of moisturisers and surfactants (24).

So far, the potential of this technique has not been explored for in vitro tape stripping experiments. In this context, the sensor could be employed to assess the intactness of the skin barrier function before experiments. This was performed in the course of in vitro tape stripping experiments to test whether the changes in skin barrier function could be monitored and if an in-process control during the experiment was possible. Sensor measurements were performed every 10 removed tapes at the least. The device was closely applied to the skin surface with slight pressure for a maximum of 2 seconds so as not to interfere with the water

flux and water content inside the SC (20).

ATR-FTIR experiments during tape stripping

Additional tape stripping experiments on porcine ear skin were conducted to monitor changes in skin barrier function by ATR-FTIR spectroscopy. Since preliminary experiments had shown no dependence of the data on the employed ear type, six large porcine ears were chosen for this study (n=6). The dorsal ear skin was removed from the cartilage, carefully freed from hair with scissors and cut into strips of 1.0 x 7.5 cm that were pinned onto pieces of styrofoam (25). Subsequently, consecutive tape stripping was performed with 20 adhesive films, this time chosing a brand suitable for corneocyte removal on a larger piece of skin (Tesa film crystal clear). The amount of corneocytes removed was again determined by NIR-densitometry using the SquameScanTM 850A. ATR-FTIR spectra were recorded before tape stripping as well as after 5, 10, 15 and 20 tape strips, which represent the anticipated major changes in skin barrier function. Infrared spectra of the skin samples were obtained using a FTIR spectrophotometer (Tensor 27, Bio-ATR I tool, Bruker Optics, Germany) thermostatted at 32°C. The skin samples were placed on the ZnSe crystal with the stratum corneum facing down. To achieve reproducible spectra of constant intensity an exact weight of 100.00 g was mounted on the samples during ATR-FTIR analysis.

Microscopic analysis

Microscopic analysis of adhesive films removed from both porcine skin in vitro and human skin in vivo should elucidate potential differences in the skin surface structure and corneocyte coverage of the tapes. As a first step, individual adhesive films of both Corneofix® and DSquame® tapes were taken from representative areas on the centre of the dorsal side of excised pig ears. For comparison, the procedure was applied to human forearm skin in vivo as well. The tapes were removed according to the respective protocols and were analysed by optical light microscopy using a photo microscope (Zeiss Axio Observer.Z1 microscopy system, Carl Zeiss, Oberkochen, Germany). All images were taken at 5-fold magnification in conventional bright field mode. Apart from these tapes for comparative investigation, selected adhesive films removed during a conventional tape stripping procedure were analysed in regular intervals to monitor the changes in protein coverage of the tapes.

Statistical data analysis

Results are expressed as means of three or more experiments ± SD. Statistical data analyses were performed with the program GraphPadPrism3 while using $P<0.05$ as a minimum level of significance. Parametric data were analysed using the Student's t-test or ANOVA. Non-parametric data were analysed using the Mann-Whitney test or the Kruskal-Wallis-Test.

3 Results and Discussion

Characterisation of the skin surface

The skin surface properties were investigated by means of TEWL measurements and capacitance-based sensor measurements. It should be clarified whether both methods served equally well as a means of quality control for skin integrity testing. The TEWL of the intact dorsal porcine ear skin was found to be around $18.36 \pm 3.66\ g/m^2/h$ in 47 individual measurements on 12 porcine ears (n=47). This corresponds well with previous findings and can be seen as an indicator for an undam-

aged skin surface and normal hydration state of the excised tissue (4, 7). The corresponding mean greyscale value as determined with the capacitance-based sensor was 101.41 ± 25.72 on a scale ranging from 0 to 255. No significant differences between the TEWL values of the different ear types were found when evaluated separately (P>0.05, 19.02 ± 3.44 vs. $17.09 \pm 3.84\ g/m^2/h$, 31 measurements on large ears vs. 16 measurements on small ears). This indicates that the skin barrier function of the two different ear types was highly comparable. In contrast, the capacitance-based sensor led to significantly different greyscale values for large and small ears (P<0.0001, 88.02 ± 17.92 vs. 128.20 ± 16.16). Since the greyscale values reflect the water content of the skin, these differences indicate that the skin water content was quite different for the different ear types despite the similar skin barrier function. Since the contact area observed during the measurements was highly comparable for the different ear types before and during the tape stripping procedure (P>0.05 in all cases), it may be assumed that the skin surface texture of the different ear types was nevertheless quite similar. For optimal results of tape stripping studies, model skin of the highest possible similarity should be employed. In this respect, capacitance-based sensor imaging might prove to be a useful tool in the future to study the homogeneity and the level of skin surface hydration.

Another parameter of interest that can be extracted from the grey-level histogram of the images is the skin micro relief in % (9). Interestingly, the differences between the ears as observed in terms of mean greyscale values was not reflected in the corresponding micro relief values. The mean micro relief value of 47 individual measurements conducted on 12 porcine ears was 0.62±0.36 % (n=47) with a mean contact area of 61.01 ± 15.14 %. When evaluated separately, the values remained highly similar for both ear types (P>0.05, respectively). This suggests that the skin surface structure of the ear types is highly similar and the differences in greyscale values, which reflect the different skin water content, might be related to age-induced differences in skin properties of the animals.

For reasons of comparison, the capacitance-based sensor was employed for measuring selected areas of human skin in vivo and porcine ear skin in vivo as well (Figure 2). As can be seen, the human forearm skin exhibits a fine pattern of wrinkles which is only disturbed if sweat glands become active (Figure 2B) or fresh or healed lesions occur (Figure 2C). The criss-cross pattern of primary and secondary lines of the skin micro-topography can be clearly seen (20). These preliminary measurements may already serve to exclude damaged or unsuitable areas from tape stripping experiments in vivo. Areas with increased sweat gland density such as the human fore-

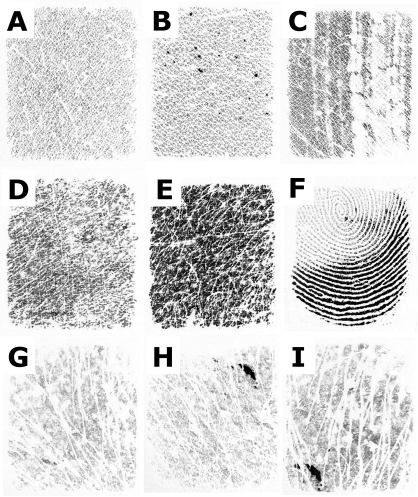

Figure 2: Influence of skin surface properties on the greyscale value as assessed by the fingerprint sensor. (A) Human forearm skin in vivo; (B) Human forearm skin in vivo with active sweat glands; (C) Human forearm skin in vivo damaged by a scar; (D) Human forehead skin in vivo; (E) Human forehead skin in vivo with active sweat glands; (F) Human index finger skin damaged by a blister after thermal damage; (G) Porcine ear skin in vivo; (H) and (I) Porcine ear skin in vivo exhibiting small lesions.

head skin (Figure 2D and 2E) are both unsuitable and impractical for tape stripping experiments. Active sweat pores appear as pin point-sized darker regions of high conductance (20). Whitish areas of low capacitance, such as scars (Figure 2C) and blisters (Figure 2F) can likewise be identified and excluded. Thus, heterogeneities in the quality and physical properties of the SC can be revealed (20).

In case of porcine ear skin in vivo, the larger numbers of hair represent an obstacle to skin hydration measurements by capacitance-based techniques (Figure 2G, H and I). Nevertheless, areas of increased water loss such as small lesions of the stratum corneum can be clearly identified even in static measurements (Figure 2H and I). The same tendencies were observed in the subsequent in vitro experiments using excised porcine ears.

For in vivo studies, further comparative data are necessary to establish a set of control values as performed for the TEWL. Our preliminary in vivo measurements on human and porcine skin in vivo revealed that the mean greyscale values obtained by capacitance-based sensor imaging are highly comparable for human forearm skin and porcine ear skin, namely 69.43 ± 14.99 and 63.30 ± 15.31 (n=3, respectively). In vitro values for the same area appear to be increased in the porcine ear, as is the case for TEWL values. When measuring different areas of human skin in vivo, further analogies to the TEWL are found, such as higher values for the skin of the forehead.

These results indicate that the capacitance-based sensor is an equally suitable tool for investigating the skin surface properties of both human and porcine skin when compared to the classical TEWL measurements with a condenser chamber. In case of in vitro experiments on porcine ears, the sensor might even be superior since the TEWL is only a rough estimate of the hydration state of the excised tissue. The sensor may be employed for occlusive measurements of a longer duration, which have been shown to be more sensitive to barrier defects than measurements with a condenser chamber (26).

Indirect characterisation of the skin surface structure by light microscopy

The surface structure of the employed porcine skin was likewise investigated by microscopic analysis of tape strips removed in individual experiments. Thus, the nature of the removed corneocytes and their tendency to aggregate should be elucidated. In addition, the differences between human and porcine SC surface properties should be visualised by optical light microscopic images. In a first step, only single adhesive films were respectively removed from the skin surface of human forearm skin or porcine ear skin and were analysed with a light microscope (Figure 3). As can be seen,

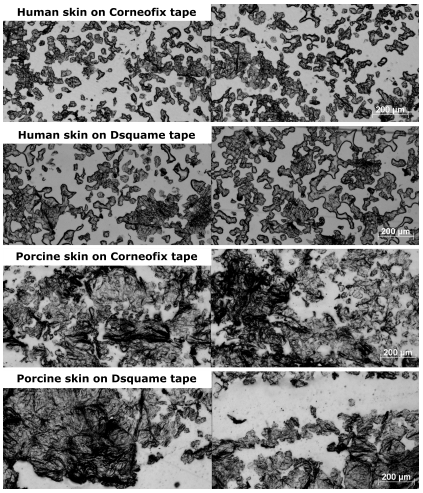

Figure 3: Microscopic analysis of the corneocyte covering of the first adhesive films removed from the skin surface of human and porcine skin during tape stripping. Two representative examples of corresponding adhesive tapes are given per row (left and right-hand side). On the adhesive films removed from human forearm skin in vivo, a certain amount of humidity is noticeable especially with DSquame® tapes. On the adhesive films removed from porcine ear skin in vitro, much larger aggregates as well as "canyons" are present, especially with DSquame® tapes.

the human corneocytes were more equally distributed on the tapes than the porcine corneocytes and rarely formed larger clusters. In contrast, porcine skin was characterised by large cell clusters interrupted by "canyons" (27). This phenomenon, however, was primarily noticeable on the first removed tape strip of every experiment while the subsequently removed tapes exhibited increasingly homogeneous protein coverage. Figure 4 shows microscopic images of adhesive films removed during consecutive tape stripping on porcine ear skin. The looser packing and concomitant ease of removal of the corneocytes at the skin surface have been attributed to the decrease in the number of desmosomes and presumably explain the presence of thicker tissue layers on the initial tape strips (28). When monitoring the entire tape stripping process it becomes clear that the overall removal of porcine corneocytes is sufficiently homogeneous to obtain reproducible and reliable results. As already discussed, overlapping stacks of corneocytes or inhomogeneous protein coverage of the tapes might lead to inaccurate results when employing optical protein quantification methods (11). However, the numerous benefits of the highly efficient, rapid and practical methods of optical protein quantification tend to justify the potential slight inaccuracy for the first removed tape. As previously observed, Corneofix® tapes appear to be less prone to the stack effect due to their decreased adhesive power (4). Thus, they were used for the presented tape stripping experiments. Overall, the obtained images confirm our previous observations and indicate that the different surface structure of human and porcine skin should be taken into consideration during in vitro tape stripping especially when performing optical methods of skin analysis.

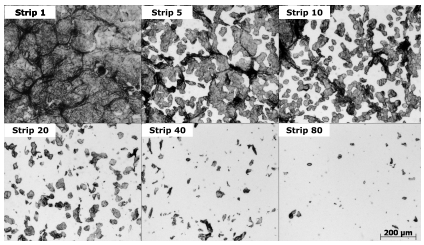

Figure 4: Monitoring of the tape stripping process performed on excised porcine ears of fattened pigs (age 6-10 months) with Corneofix® adhesive films. The removed tapes were analysed by optical light microscopy (bright field mode, 5-fold magnification). For average to low corneocyte coverages, optical methods of analysis give results with satisfying accuracy.

In vitro tape stripping: estimation of the relative stratum corneum depth

The SC of the tested porcine ears was removed completely during consecutive tape stripping experiments. The entire SC thickness was determined by summarising the individually determined values of pseudo-absorption at 850 nm and employing the appropriate calibration data and protein density for calculation. The mean SC thickness was found to be $7.28 \pm 1.49 \mu$m for all experiments (n=10). When evaluated separately, the large and small porcine ears showed a significantly different SC thickness of 8.83 ± 0.82 μm and 6.50 ± 1.07 μm ($P<0.05$, n=5, respectively). The summarised mean pseudo-absorption values correspond to the entire SC thickness removed in the experiments. The experiments were only stopped when the detection limit of the NIR-densitometer was reached. The cumulative relative horny layer thickness that was removed after 1 to a maximum of 120 tape strips was calculated in percentages for every experiment. These data were employed to establish a general correlation between the number of removed tape strips (n) and the relative thickness of the removed SC (y). The resulting exponential equation is shown below (Equation 1). In conclusion, the relative thickness of the SC removed after a given number of tape strips can be calculated as a percentage of the

absolute SC thickness.

$$y = 98.858 - 99.589e^{-n*0.0727} \text{ (in \%)} \quad (1)$$

It was thus possible to correlate the amount of removed SC with each consecutively removed adhesive film with satisfying accuracy. For instance, after 10 adhesive tapes a relative amount of 50.39 ± 6.59 % of the SC was removed while 87.40 ± 3.54 % were removed after 30 tapes. This corresponds quite well with the values observed for human SC (15), confirming that the majority of the porcine SC is likewise removed after comparatively few adhesive tapes. In contrast, the removal of the following cell layers processes quite slowly due to the increased cohesion. The number of tapes required for removal of the entire SC may vary, in the present case between 80 to 120 for the large ears and 60 to 80 for the small ears. However, these last adhesive films only contribute a very small percentage of the entire SC thickness. Irrespective of the type of ear used, the removal of the SC can thus be characterised by the presented non-linear equation (Figure 5). This confirms that despite the differences in skin surface structure between human and porcine skin and the expected inter-individual differences, reliable and reproducible results can be obtained in tape stripping experiments on porcine ears. The presented general relationship can be employed to estimate the relative amount of SC removed from pig ear skin by any number of tape strips. Thus, complete removal of the SC, which is time- and cost-intensive, can be avoided in future experiments (15).

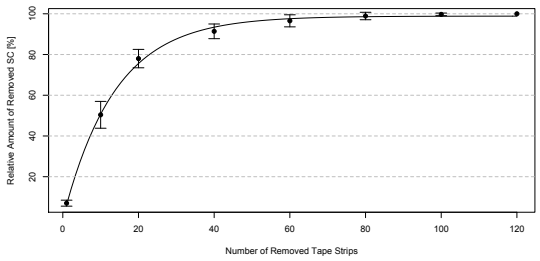

Figure 5: Correlation of the relative amounts of SC removed with increasing numbers of adhesive tapes according to Equation 1 ($R^2 = 0.9999$).

Changes in skin barrier function as observed with ATR-FTIR spectroscopy

The changes in skin barrier function during tape stripping experiments were additionally analysed by ATR-FTIR. Table 1 shows an overview of typical skin bands that were observed: CH_2 asymmetric and symmetric stretching vibrations describing the conformational order of the SC lipid acyl chains, amid I (C=O) and amid II (C–N) vibrations elucidating changes in SC protein conformation as well as CH_2 scissoring mode 1 and 2 characterising the lateral packing of the SC lipid alkyl chains (25, 29-31). For most bands, no qualitative change in the SC composition was detected by analysis of the skin during tape stripping. Minor if statistically significant shifts of the symmetric CH_2 stretching band and the amide 1 vibration were recorded. After the removal of twenty tape strips the frequency of the symmetric CH_2 stretching mode was shifted to a higher wavenumber, namely to 2850.59 ± 0.08 cm^{-1} (Table 1). This shift may indicate a transition from the hexagonal to the liquid phase resulting in a higher degree of disorder (29, 32). This is in good agreement with the observed process of SC removal (Figure 5). After removal of 20 tapes, roughly 80% of the horny layer is generally already removed and thus the barrier function is impaired to quite some extent. Moreover, after five tape strips a statistically significant shift to a higher frequency was observed for the amide 1 band (Table 1). This shift could indicate a change in the secondary structure of keratin (33). As

	asymm.CH_2	symm. CH_2	Amide 1	Amide 2	CH_2 sciss. 1	CH_2 sciss. 2
skin before tape stripping	2918.23 ± 0.42	2850.35 ± 0.24	1637.10 ± 2.27	1541.80 ± 2.00	1466.24 ± 0.27	1454.98 ± 0.59
skin after 5 removed tapes	2918.01 ± 0.22	2850.16 ± 0.00	1640.88 ± 1.89 *	1541.93 ± 0.88	1466.34 ± 0.07	1455.03 ± 0.48
skin after 10 removed tapes	2917.96 ± 0.35	2850.24 ± 0.13	1639.43 ± 2.06	1542.14 ± 1.32	1466.34 ± 0.07	1454.92 ± 0.66
skin after 15 removed tapes	2918.31 ± 0.25	2850.43 ± 0.24	1639.25 ± 1.50	1542.76 ± 0.70	1466.05 ± 0.25	1455.30 ± 0.58
skin after 20 removed tapes	2918.60 ± 0.40	2850.59 ± 0.08 *	1639.44 ± 2.33	1543.72 ± 0.88	1466.18 ± 0.31	1455.06 ± 0.37

Table 1: Wavenumbers [cm^{-1}] of characteristic skin bands before and during tape stripping experiments on porcine ear skin (n=6). Given values are means ± SD. Significant differences between the tape stripped skin versus the control skin before tape stripping are marked with *.

expected, the change in keratin structure was most apparent in the uppermost layers of the SC. Likewise, the subsequently recorded spectra during the tape stripping procedure showed a similar, if not statistically significant shift. In short, the ATR-FTIR analysis of the skin before and during tape stripping confirmed the damage in skin barrier function caused by the tape stripping procedure while the qualitative composition of the SC remained unchanged up to 80% of its entire thickness.

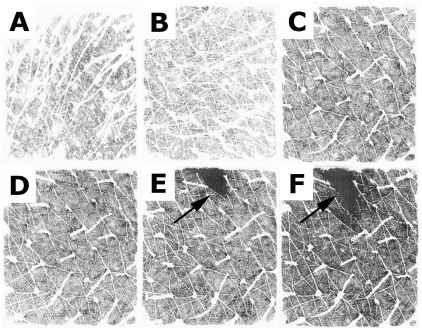

Figure 6: Monitoring of the tape stripping process on porcine ear skin. Image (A) shows porcine ear skin in vivo (young domestic pig of approximately 3-4 months of age). Remnants of dirt and moisture as well as numerous hairs cause a slightly blurred appearance. Image (B) is a corresponding image in vitro with trimmed hair. Image (B) to (F) show the skin surface structure before and during the tape stripping process on an excised porcine ear in vitro: the furrows become more accurately visible while the greyscale value of the images changes after the removal of 5 (Image C), 10 (Image D), 15 (Image E) and 20 (Image F) adhesive films. The occurrence of dark regions (as marked by the arrows) indicates a major disturbance of the skin barrier, which was confirmed by visual observation: a single large patch of skin was removed in one piece. Subsequently, the tape stripping data gained after this occurrence will become increasingly inaccurate.

In-process control of in vitro tape stripping via capacitance-based sensor imaging

The skin surface properties of porcine ear skin in vitro as observed by capacitance-based sensor imaging may not only serve as a quality control of the skin, but can likewise be employed to monitor the tape stripping process. Figure 6 shows the skin hydration profile of porcine ear skin before (A in vivo, B in vitro) and during removal of an increasing number of tapes on the excised porcine ear in vitro. Irregularities in protein removal as seen in Fig. 6E and 6F can thus be detected and the experiment can be aborted since the optical corneocyte quantification, which relies on homogeneous cell distribution, would produce inaccurate results. Apart from these visual aspects, the mean greyscale values obtained from a larger set of experiments on intact skin can serve as standardised control values. Thus, intact representative skin areas can be identified and the tape stripping process can be monitored (Figure 7). As can be seen in Figure 7A, the mean greyscale value shows a fairly regular increase with the first removed tapes and reaches a plateau after 30 removed tapes. This increase in greyscale value corresponds to an increase in the detected skin water content and a concomitant decrease in skin barrier function as confirmed by increasing TEWL values.

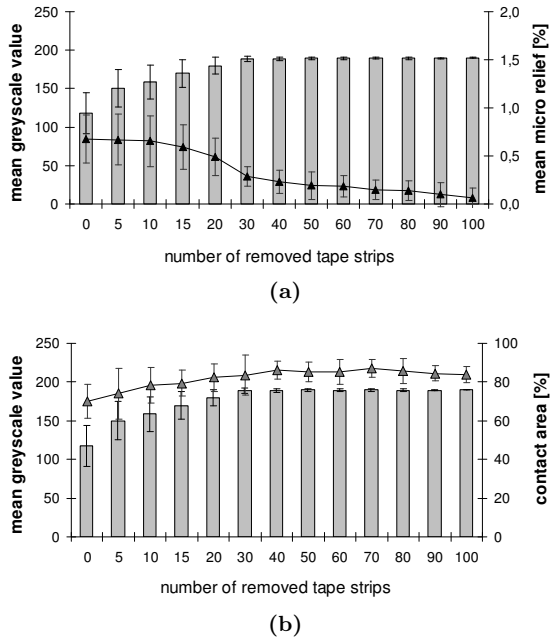

Figure 7: Fingerprint sensor measurements on porcine ear skin before and during tape stripping with Corneofix® tapes (n=10). In Figure 7(A), the mean greyscale values (grey bars) determined during tape stripping are plotted on the left-hand side scale while the mean micro relief values in % (black line) are given on the right hand-side scale. In Figure 7(B), the right-hand side scale characterises the mean contact area in % (grey line), again in relation to the mean greyscale values (grey bars).

Since most of the barrier was removed after 30 tapes, no further changes of the greyscale value were observed. The skin micro relief appeared to be inversely correlated to the greyscale value and decreased with increasing numbers of removed tapes, which indicates that the skin surface achieved increasing uniformity. It may be assumed that irregularities within the uppermost corneocyte layers, including loose cell stacks or wrinkles, were removed with the first few adhesive tapes and thus no more changes were observed after the first 30 removed tapes. The contact area recorded during the measurements increased in analogy to the increasing greyscale values, which supports this theory (Figure 7B). As already noticed during characterisation of the ear skin, the mean greyscale values differed significantly for the different ear types when evaluated separately ($P<0.05$). The greyscale values of large porcine ears were noticeably lower than those observed for the smaller ears. These differences were observed during the tape stripping process until most of the SC had been removed with approximately 30 tapes. However, the observed micro relief values did not reflect these differences at any stage of the tape stripping process and were highly similar for both ear types ($P>0.05$, Figure 7A). When regarding the corresponding TEWL values determined in parallel to the sensor measurements, the exact same tendencies as for the greyscale values were observed (Figure 8). After 30 removed adhesive

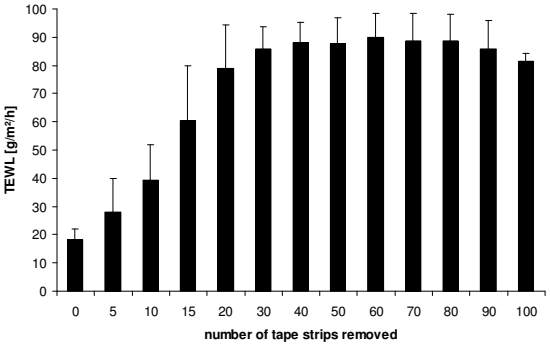

Figure 8: Measurement of the TEWL on porcine ear skin before and during tape stripping with Corneofix® tapes (n=10). Given values are means ± SD.

tapes, further tape stripping resulted in little or no change of the TEWL. Due to the prolonged experiment times, the recorded values even started to decrease after more than 100 removed tapes due to irreversible dehydration of the tissue.

Correlation of mean greyscale values and the TEWL

The mean greyscale values and the corresponding TEWL values as determined before and in regular intervals during the tape stripping ex-

periments were employed for a linear regression analysis (Figure 9). When plotting the mean greyscale values against the mean TEWL values measured at the same skin sites during the consecutive removal of 100 tapes, a highly linear correlation was obtained with $R^2 = 0.9249$ (Figure 9A). This indicates that the two methods lead to highly comparable conclusions about the state of the skin barrier function and the TEWL. The same conclusions were reached when correlating either the mean greyscale values (Figure 9B) or the TEWL values (Figure 9C) to the respectively reached SC depth. Highly satisfying coefficients of determination were obtained in both cases.

4 Conclusion

Capacitance-based sensor imaging was shown to be a suitable tool for skin integrity testing as means of quality control for porcine ear skin for in vitro tape stripping. Likewise, it can be employed for in-process control during the tape stripping process since inhomogeneous damages within the SC through irregular corneocyte removal can be visualised. The mean greyscale values obtained during tape stripping were found to be highly reproducible for a larger number of experiments. Excellent linear correlations between the mean greyscale values and corresponding TEWL values and the associated skin penetration depths were observed. This technique might represent an important contribution towards the standardisation of in vitro tape stripping and the involved porcine ear skin.

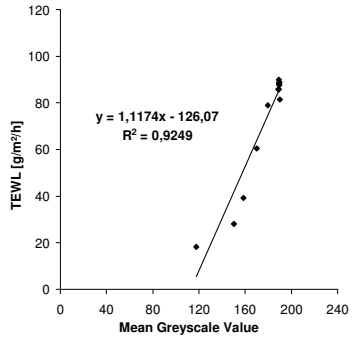

(a)

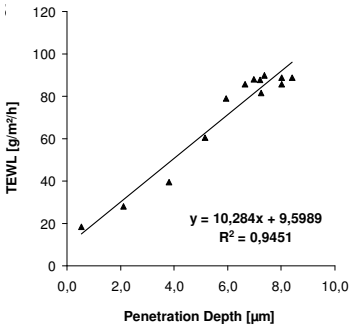

(b)

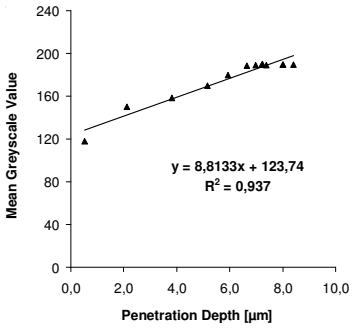

(c)

Figure 9: (A) Correlation of the mean greyscale value as obtained via capacitance-based sensor measurements and the mean TEWL values as determined with the Aquaflux® device during continuous tape stripping of the entire SC. Data points were taken before the procedure as well as after 5, 10, 15, 20 and subsequently every 10 tapes until 100 adhesive films were removed. The correlated values are means of 10 experiments (n=10). Images B and C show the correlation of the mean penetration depth achieved in these experiments to the corresponding mean TEWL values (B) and the corresponding mean greyscale values (C).

Acknowledgements

The authors would like to thank Susanne Drechsler and Wolfgang Sipos from the University of Veterinary Medicine Vienna for providing fresh porcine ears and recording the in vivo images of porcine ears. We would like to express our gratitude to Jürgen Lademann and his group of the Charité Berlin for technical assistance and Arvid Staub of the Technical University Vienna for valuable discussion. The financial support of the research platform "Characterisation of Drug Delivery Systems on Skin and Investigation of Involved Mechanisms" is gratefully acknowledged.

References

1. Weigmann HJ, Jacobi U, Antoniou C, Tsikrikas GN, Wendel V, Rapp C, Gers-Barlag H, Sterry W, Lademann J. Determination of penetration profiles of topically applied substances by means of tape stripping and optical spectroscopy: UV filter substance in sunscreens. J Biomed Opt 2005;10:14009-1 - 14009-7.

2. Weigmann H, Lademann J, Meffert H, Schaefer H, Sterry W. Determination of the horny layer profile by tape stripping in combination with optical spectroscopy in the visible range as a prerequisite to quantify percutaneous absorption. Skin Pharmacol Appl Skin Physiol 1999;12:34-45.

3. Lademann J, Jacobi U, Surber C, Weigmann HJ, Fluhr JW. The tape stripping procedure–evaluation of some critical parameters. Eur J Pharm Biopharm 2009;72:317-323.

4. Klang V, Schwarz JC, Hartl A, Valenta C. Facilitating in vitro tape stripping: application of infrared densitometry for quantification of porcine stratum corneum proteins. Skin Pharmacol Physiol 2011;24: 256-268.

5. Meyer W, Zschemisch NH. Skin layer thickness at the ear of the domesticated pig , with special reference to the use of the ear integument for human dermatological research. Berl Muench Tierarztl Wochenschr 2002;115:401-406.

6. Meyer W. Bemerkungen zur Eignung der Schweinehaut als biologisches Modell für die Haut des Menschen. Der Hautarzt 1996;47:178-182.

7. Sekkat N, Kalia YN, Guy RH. Biophysical study of porcine ear skin in vitro and its comparison to human skin in vivo. J Pharm Sci 2002;91:2376-2381.

8. Sekkat N, Kalia YN, Guy RH. Porcine ear skin as a model for the assessment of transdermal drug delivery to premature neonates. Pharm Res 2004;21:1390-1397.

9. Batisse D, Giron F, Leveque JL. Capacitance imaging of the skin surface. Skin Res Technol 2006;12:99-104.

10. Bevilacqua A, Gherardi A. Age-related Skin Analysis by Capacitance Images. Proceedings of the 17th International Conference on Pattern Recognition 2004 (ICPR2004), Cambridge, United Kingdom, Aug. 23-26.

11. Weigmann HJ, Lindemann U, Antoniou C, Tsikrikas GN, Stratigos AI, Katsambas A, Sterry W, Lademann J. UV/VIS absorbance allows rapid, accurate, and reproducible mass determination of corneocytes removed by tape stripping. Skin Pharmacol Appl Skin Physiol 2003;16:217-227.

12. Jacobi U, Kaiser M, Toll R, Mangelsdorf S, Audring H, Otberg N, Sterry W, Lademann J. Porcine ear skin: an in vitro model for human skin. Skin Res Technol 2007;13:19-24.

13. Raney SG, Hope MJ. The effect of bilayer and hexagonal H(II) phase lipid films on transepidermal water loss. Exp Dermatol 2006;15:493-500.

14. Voegeli R, Heiland J, Doppler S, Rawlings AV, Schreier T. Efficient and simple quantification of stratum corneum proteins on tape strippings by infrared densitometry. Skin Res Technol 2007;13:242-251.

15. Jacobi U, Weigmann HJ, Ulrich J, Sterry W, Lademann J. Estimation of the relative stratum corneum amount removed by tape stripping. Skin Res Technol 2005;11:91-96.

16. Czaika V, Alborova A, Richter H, Sterry W, Vergou T, Antoniou C, Lademann J, Kocha S. Comparison of Transepidermal Water Loss and Laser Scanning Microscopy Measurements to Assess Their Value in the Characterization of Cutaneous Barrier Defects. Skin Pharmacol Physiol 2012;25:39-46.

17. Tchvialeva L, Zeng H, Markhvida I, McLean DI, Lui H, Lee TK. Skin Roughness Assessment. In: Campolo D. New Developments in Biomedical Engineering 2010, InTech, OpenAccessPublisher Online.

18. Leveque JL, Xhauflaire-Uhoda E, Pierard GE. Skin capacitance imaging, a new technique for investigating the skin surface. Eur J Dermatol 2006;16:500-506.

19. Pierard GE, Leveque JL. What is SkinChip? From silicon image sensor technology to SkinChip. Dermatology 2004;208:291-292.

20. Xhauflaire-Uhoda E, Pierard-Franchimont C, Pierard GE. Skin capacitance mapping of psoriasis. J Eur Acad Dermatol Venereol 2006;20:1261-1265.

21. Xhauflaire-Uhoda E, Pierard GE, Quatresooz P. The skin landscape following nonoptical capacitance imaging. Am J Clin Dermatol 2010;11:89-94.

22. Leveque JL, Querleux B. SkinChip, a new tool for investigating the skin surface in vivo. Skin Res Technol 2003;9:343-347.

23. Xiao P, Singh H, Ou X, Caparnagiuc AR, Ciortea LI, Berg EP, Imhof RE. In-vivo Trans-Dermal Drug Delivery Study by Using Capacitive Fingerprint Sensors. Skin Forum 2011, Frankfurt, Germany, March 28th-29th.

24. Xhauflaire-Uhoda E, Paquet P, Quatresooz P, Pierard GE. Characterization of the skin using capacitance imaging. Expert Review of Dermatology 2010;5:149-158.

25. Hasanovic A, Winkler R, Resch GP, Valenta C. Modification of the conformational skin structure by treatment with liposomal formulations and its correlation to the penetration depth of aciclovir. Eur J Pharm Biopharm 2011;79:76-81.

26. Xiao P, Ciortea LI, Singh H, Zheng X, Berg EP, Imhof RE. Stratum Corneum Barrier Function Measurement using Fingerprint Sensor and Condenser-TEWL Methods. OEESC Conference 2009, Edinburgh, Scotland.

27. Carrer DC, Vermehren C, Bagatolli LA. Pig skin structure and transdermal delivery of liposomes: a two photon microscopy study. J Control Release 2008;132:12-20.

28. Kalia YN, Pirot F, Guy RH. Homogeneous transport in a heterogeneous membrane: water diffusion across human stratum corneum in vivo. Biophys J 1996;71:2692-2700.

29. Rodriguez G, Rubio L, Cocera M, Estelrich J, Pons R, de la Maza A, Lopez O. Application of Bicellar Systems on Skin: Diffusion and Molecular Organization Effects. Langmuir 2011;26:10578-10584.

30. Babita K, Kumar V, Rana V, Jain S, Tiwary AK. Thermotropic and spectroscopic behavior of skin: relationship with percutaneous permeation enhancement. Curr Drug Deliv 2006;3:95-113.

31. Boncheva M, Damien F, Normand V. Molecular organization of the lipid matrix in intact Stratum corneum using ATR-FTIR spectroscopy. Biochim Biophys Acta 2008;1778:1344-1355.

32. Moore DJ, Rerek ME, Mendelsohn R. FTIR spectroscopy studies of the conformational order and phase behaviour of ceramides. J Phys Chem B 1997;101:8933-8940.

33. He W, Guo X, Xiao L, Feng M. Study on the mechanisms of chitosan and its derivatives used as transdermal penetration enhancers. Int J Pharm 2009;382:234-243.

Semi-solid O/W emulsions based on sucrose stearates: influence of oil and surfactant type on morphology and rheological properties

Victoria Klang[a], Anna Novak[a], Michael Wirth[a], Claudia Valenta[a*]

[a]University of Vienna, Department of Pharmaceutical Technology and Biopharmaceutics, Faculty of Life Sciences, Althanstraße 14, 1090 Vienna, Austria
[*]Corresponding Author: Claudia Valenta, Claudia.valenta@univie.ac.at, Tel: +43 1 4277 55 410, Fax: +43 1 4277 9554

Abstract

Sucrose stearate blends of intermediate lipophilicity are mild surfactants with thermosensitive gelling behaviour. Binary systems and emulsions with sucrose stearate S-970 or S-1170 were developed and investigated by thermoanalytical and rheological measurements. The presence of an oil phase promoted the gelling potential of the esters especially at higher production temperatures. Semi-solid emulsions with viscoelastic properties comparable to weak gels were obtained with different dermatologically acceptable oils. The complex internal structure as visualised by fluorescence microscopy exhibited changes during storage in dependence of oil and surfactant type. A combination of S-970 with cetearyl ethylhexanoate-based oil phases led to superior physical stability.
Keywords: sucrose stearate, semi-solid, fluorescence microscopy

1 Introduction

Sucrose ester mixtures are commonly employed surfactants in the food industry, but have likewise been investigated as compounds of drug delivery systems to enhance drug solubility and to increase absorption of topically applied actives [1-4]. Since sucrose esters are non-ionic biodegradable surfactants of low toxicity they are ideal compounds to create alternative matrices for lipid-based drug delivery systems for dermal application [5]. Unlike the more frequently investigated carbohydrate-based alkylpolyglucoside surfactants [6-8], the behaviour of sucrose ester surfactants in multiphase systems has not been thoroughly investigated yet. In recent investigations we found that the sucrose stearate blend S-970 can be employed to create highly viscous O/W emulsions [9]. Although the peculiar rheological behaviour of certain sucrose esters in water has been reported in early literature [10, 11], few studies have attempted to employ this feature in specific formulations for dermal application. The majority of reports deal with binary systems of the surfactant mixture in water [5, 12, 13] and it is evident that the exact processing conditions may lead to significant changes in the macroviscosity of the binary systems. So far, no such investigations on the effect of processing conditions on the physical properties of sucrose ester-stabilised emulsions have been reported. The presence of an oil phase permits the incorporation of lipophilic drugs [9], but may likewise affect the gelling properties of the employed sucrose ester. There is a significant need for a systematic investigation dealing with the effect of production conditions and composition on the developed emulsion systems. Thus, the aim of the present work was to elucidate the influence of the processing temperature, the type and amount of sucrose ester and the incorporated oil on the physical properties of the produced emulsions. A detailed characterisation of the systems was conducted to understand the internal emulsion structure and to optimise formulation properties. Important physical parameters were determined by optical light microscopy and fluorescence microscopy as well as thermoanalytical and rheological investigations. To obtain an overview of the gelling behaviour of different sucrose ester blends and their suitability to form semi-solid binary systems or emulsions, thorough preliminary studies were conducted. A range of different ester blends was tested and only two sucrose stearate blends, namely S-970 and S-1170 which are characterised by different ester compositions, were selected for further studies. As a first step, a concentration range from 2.5% up to 20% of the esters was employed to form binary systems at different production temperatures. Having selected an appropriate surfactant concentration, we moved on towards the development of O/W emulsions. The choice of excipients was guided by the aim of achieving optimal skin-friendliness. The production parameters were optimised using a model emulsion and five different eudermic oils were then investigated in a comparative study. The rheological properties of a system are of particular importance for the stability, the processing and the application of the final product. Thus, the rheological properties of fresh and stored emulsions were compared to investigate potential changes in the macroviscosity of the formulations. It should be clarified whether all tested oil types would produce systems of satisfying shelf-life for practical application despite the lack of additional gelling agents.

2 Materials and Methods

2.1 Materials

Sucrose stearate S-970 and S-1170 (Ryoto Sugar Esters® S-970 and S-1170) were kindly donated by Mitsubishi-Kagaku Food Corpora-

tion (Tokyo, Japan). The exact composition of these sucrose stearate blends as well as their melting ranges and HLB values according to the manufacturer are given in Table 1. Corn oil, soybean oil, isopropyl myristate (IPM, 1-Methylethyl-tetradecanoat) and PCL® liquid (cetearyl ethylhexanoate, isopropyl myristate) were purchased from Dr.Temt Laboratories (Vienna, Austria). Tegosoft® liquid (cetearyl octanoate) was provided by Evonik Industries (Essen, Germany). Potassium sorbate was obtained from Herba Chemosan Apotheker-AG (Vienna, Austria). Bodipy® 493/503 (4,4-difluoro-1,3,5,7,8-pentamethyl-4-bora-3a,4a-diaza-s-indacene) was purchased from Invitrogen (Eugene, USA) while Atto 594 and fluorescein sodium salt were purchased from Sigma Aldrich (St. Louis, USA).

2.2 Investigation of the gelling potential of different esters

Selection of sucrose ester blends

The gelling ability of different commercially available sucrose ester blends in distilled water was examined. The HLB value of the tested compounds (L-195, S-270, L-595, S-970, S-1170, OWA 1570, S-1670, P-1670 and L-1695) ranged from 1 to 16. Each sucrose ester blend was dissolved in distilled water at 5 % w/w, was stirred for 30 minutes at room temperature and homogenised with an ultra-turrax (2500 rpm, 3 minutes). Sucrose esters of HLB 1 - 5 were insoluble in water. Sucrose esters with intermediate HLB value from 9 to 11 formed highly viscous dispersions. Sucrose esters with high HLB value from 15 to 16 gave highly fluid and slightly turbid dispersions except for L-1695 which gave a clear solution. The sucrose esters for which a successful gelling was observed, namely sucrose stearate S-970 and S-1170, were chosen for further investigations.

Effect of production temperature

As a next step, the gelling potential of the chosen ester blends was investigated in binary systems and model emulsions with PCL® liquid to elucidate the effect of different production temperatures. A concentration range of respectively 2.5%, 5%, 10% and 20% w/w of S-970 as well as S-1170 in distilled water was prepared to investigate the influence of increasing ester concentrations on the resulting aqueous dispersions. The concentration ranges were prepared at 25°C, 40°C and 60°C. All samples were produced in triplicate (n=3). The mixtures were characterised by optical light microscopy as well as thermoanalytical and rheological measurements. In addition, representative model emulsions with PCL® liquid as the oil phase (A S-970 and A S-1170, Table 2) were chosen to investigate the effect of the production temperature on emulsions in general. Emulsions were prepared in triplicate by incorporating the respective sucrose ester into the oil and stirring of the resulting mixture for 30 minutes at different temperatures (25°, 40°, 50° and 60°C) until the water phase was added. After further stirring for 5 minutes, homogenisation with an ultra-turrax (2500 rpm, 3 minutes) was performed. These emulsions were additionally produced with small amounts of fluorescent dyes (section 2.4).

2.3 Final emulsions

Different emulsions were produced to investigate the effect of the oil phase. Their composition and abbreviations are given in Table 1. After testing a large number of dermatologically acceptable oils, the following were chosen: tegosoft® liquid, PCL® liquid, corn oil, soybean oil and isopropyl myristate (IPM). The final emulsions were prepared according to an optimised protocol based on the preliminary studies. The respective sucrose ester/oil

S-970	% w/w	S-1170	% w/w
sucrose monostearate	31 - 33	sucrose monostearate	37 - 39
sucrose distearate	20 - 22	sucrose distearate	20 - 22
sucrose monopalmitate	11 - 13	sucrose monopalmitate	14 - 15
sucrose tristearate	9 - 10	sucrose dipalmitat	7 - 8
other sucrose alkylates	18 - 25	other sucrose alkylates	13 - 19
ash, moisture, residual			
fatty acids, free sucrose	< 10	ash, moisture	< 3
melting point (DSC)	49℃ - 56℃		49℃ - 55℃
HLB	9		11

Table 1: Composition of the employed sucrose stearate blends.

mixture was stirred and only briefly heated to 40°C. Then the aqueous phase was added, the resulting emulsion was further stirred for 5 minutes and homogenised with an ultra-turrax (2500 rpm, 3 minutes). The final emulsions were stored in sealed glass containers at 8°C until a follow-up investigation after 3 months. The pH value of the emulsions was likewise monitored at 25°C using a pH meter (Orion 420A, Bartelt, Austria).

2.4 Optical light and fluorescence microscopy

The microscopic analyses were performed using a photo and fluorescence microscope (Zeiss Axio Observer.Z1 microscopy system, Carl Zeiss, Oberkochen, Germany) equipped with phase contrast and LD Plan-Neofluar objectives. A small amount of sample was placed on an object slide, covered and analysed immediately. Images of binary systems and emulsions were taken in conventional bright field mode and with phase contrast at 10- and 20-fold magnifications. In addition, polarisation microscopy (Optiphot 2, Nikon GmbH, Austria) was employed to detect the presence of lyotropic liquid crystalline phases. Both binary systems and emulsions were investigated by optical light microscopy. In addition, representative model emulsions with PCL® liquid as the oil phase (A S-970 and A S-1170, Table 2) were investigated by fluorescence microscopy after incorporation of different fluorescent dyes to visualise the lipophilic and hydrophilic domains. The coloured reagents were chosen according to their excitation and emission maxima as well as their aqueous solubility. The hydrophilic Atto 594 (590 nm / $\geq$ 615 nm) and fluorescein sodium (470 nm / 525 nm) were respectively incorporated into the aqueous bulk phase. The lipophilic Bodipy® (470 nm / 525 nm) was employed to stain the oil phase. These emulsions were prepared at both 40°C and 60°C and with or without treatment with an ultra-turrax to reveal whether the energy input had any impact on the distribution of the fluorescent dyes. It should be clarified whether structures other than oil droplets were present in the systems. In particular, the presence of aqueous network structures which might account for the increased emulsion viscosity should be investigated.

(2a) Composition	% w/w
oil	20
sucrose stearate blend	5
potassium sorbate	0.1
distilled water to	100

(2b) Oil type	Abbreviations
PCL® liquid	A S-970
	A S-1170
tegosoft® liquid	B S-970
	B S-1170
corn oil	C S-970
	C S-1170
soybean oil	D S-970
	D S-1170
isopropyl myristate	E S-970
	E S-1170

Table 2: Basic composition of all investigated emulsions (a) and abbreviations of the different formulations according to the employed oil type (b).

2.5 Thermoanalytical Measurements

Thermoanalytical measurements were performed with the pure emulsifier, the aqueous binary system and the emulsions. The sucrose ester blends in powder form were analysed by differential scanning calorimetry (DSC) using a DSC-7 (Perkin Elmer, Austria) working with a continuous flow of dry nitrogen and an indium calibration. About 5 mg of sample were sealed within aluminium pans and heated from 25 to 80°C. For analysis of the recrystallisation process, the samples were subsequently cooled down again to 25°C and reheated to 80°C. The heating and cooling rate was 1°C/min in all cases. For the thermal analysis of the sucrose ester dispersions and emulsions, microcalorimetry (micro differential scanning calorimetry, microDSC) was employed using a Setaram III microcalorimeter (Setaram, Mainz, Germany). About 500 mg of each sample containing 25 mg of sucrose ester were sealed in batch cells and scanned against a reference sample of distilled water. The samples were heated from 25 to 80°C at a constant heating rate of 1°C/min. Again, subsequent cooling back to 25°C and another heating cycle to 80°C were additionally performed at 1°C/min to gain information about re-crystallisation phenomena and potentially irreversible changes in the formulation structure. Thermal transitions were calculated using Setsoft 2000 Setaram software. The obtained thermograms were analysed in terms of linear onset, transition or peak maximum temperature and total enthalpy.

2.6 Rheological experiments

Continuous and oscillatory measurements were performed in triplicate on a Bohlin CVO Rheometer (Malvern Instruments, UK) with a thermostatic control system (Bohlin KTB30, Malvern, UK). A cone and plate tool with 40 mm in diameter and a 4° angle (CP 4°/40 mm, 2 g of applied sample) was employed for all viscous systems. A coaxial cylinder system with 25 mm in diameter (cup and bob C25, 15 g of applied sample) was employed only for dispersions prepared at 60°C that were too fluid for the cone/plate tool. The temperature was maintained at 21 ± 0.5 °C with a gap size of 0.15 mm. Additional experiments were performed for the final emulsions at 32 ± 0.5°C, thus simulating the skin surface temperature in vivo. Flow curves were established for all systems. The flow properties of both dispersions and emulsions were investigated by measuring the dynamic viscosity η (in Pas) under shear stress. Rheological experiments in a controlled-rate mode were performed. A con-

trolled shear rate γ was employed at a constant temperature to determine the viscosity of the samples as a function of the shear rate ranging from 0.1 s^{-1} to 100 s^{-1} and back from 100 s^{-1} to 0.1 s^{-1}. Moreover, oscillatory shear experiments were performed for all systems, i.e. a sinusoidal stress was applied to the sample and the induced strain was measured [14, 15]. Beforehand, the linear viscoelastic region of all samples was determined by performing an amplitude sweep at a frequency of 1 Hz (stress ramp from 0.1 to 20 Pa or higher if necessary). Subsequently, a frequency sweep test was performed over a frequency range of 1 – 40 Hz at a constant shear stress of 2 Pa. Thus, important formulation parameters such as the elastic modulus G', the viscous modulus G'', the complex modulus G* and the dynamic viscosity η' were determined as a function of the oscillatory frequency (v, in Hz). The elastic modulus (storage modulus) G' is defined as $G' = G^* \cos(\delta)$ and describes the recoverable energy that is stored within an elastic system. The viscous modulus (loss modulus) G'' is calculated by $G'' = G^* \sin(\delta)$ and represents the energy that is dissipated in the viscous flow and transformed into heat. These moduli represent the parts of the complex dynamic shear modulus G* [14-16].

2.7 Statistical data analysis

Results are expressed as means of at least three experiments ± SD unless stated otherwise. Statistical data analyses were performed using the software program GraphPadPrism3. Parametric data were analyzed using the Student's t-test while non-parametric data were analyzed using the Mann-Whitney test or the Wilcoxon signed rank test with $P<0.05$ as a general minimum level of significance.

3 Results and Discussion

3.1 Optical light and fluorescence microscopy

Morphology of binary systems and effect of production temperature

The effect of increasing sucrose stearate concentrations of 2.5%, 5%, 10% and 20% w/w in aqueous dispersions prepared at different temperatures was visualised by optical light microscopy. In general, air bubbles were observed after preparation at 25°C (Figure 1a and 1c). At 60°C, the mixtures became more fluid and less prone to foaming. In case of S-970, increasing amounts of undissolved surfactant were observed for all concentrations after preparation at 25°C. In contrast, preparation at 60°C led to complete dissolution of S-970 at all concentrations except for 20% w/w. This phenomenon is demonstrated in Figure 1a and 1b on dispersions with 5% w/w of S-970. Sucrose stearate S-1170 exhibited a completely different behaviour (Figure 1c and 1d). A dense internal structure was observed for all concentrations after preparation at 25°C. After preparation at 60°C, a similar structure was observed for all concentrations except for 2.5% w/w. These observations suggest that the gelling-behaviour of S-970 is more temperature-sensitive than that of S-1170 and that S-1170 forms specific structures irrespective of the temperature.

Morphology of emulsions and effect of production temperature

Conventional microscopic analysis confirmed a crowded interior emulsion structure [9]. The fluorescence microscopic investigations of model emulsions with PCL® liquid (A S-970 and A S-1170) with additional fluorescent dyes provided more accurate information. The visual observations were complemented by calculations with the software program ImageJ®

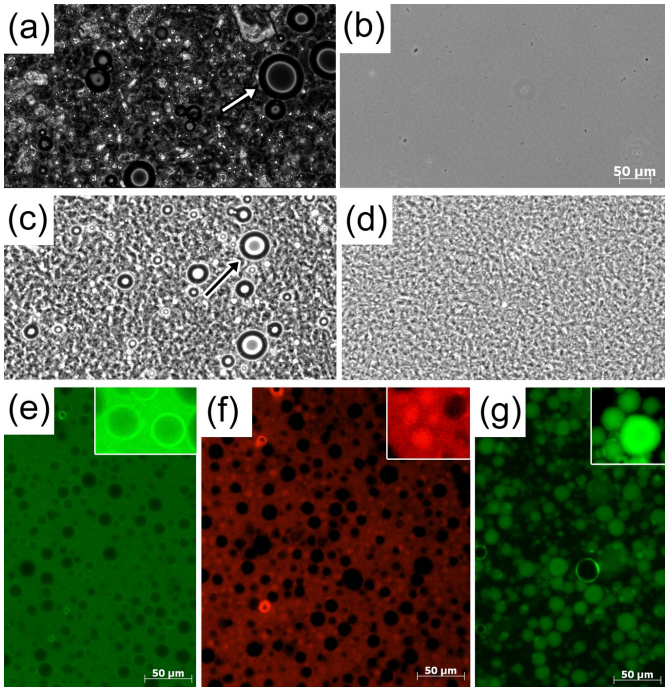

Figure 1: Morphology of binary systems: Light microscopic images of aqueous dispersions of 5% w/w of sucrose ester. The binary systems were produced with sucrose stearate S-970 at **(a)** 25°C and **(b)** 60°C and with sucrose stearate S-1170 at **(c)** 25°C and **(d)** 60°C. The large spherical structures marked by arrows are air bubbles. Images were obtained using phase contrast mode at 10-fold magnification. **(e-g)** Morphology of emulsions: Fluorescence microscopic images at 20-fold magnification of model emulsion A S-970 after incorporation of **(e)** fluorescein sodium (bright bulk phase), **(f)** Atto 594 (bright bulk phase) or **(g)** Bodipy® (bright droplets). The respective small image parts have been enhanced in contrast to emphasise the structural details.

(open source) using the automatic particle count and size determination functions. After incorporation of fluorescein sodium salt into the aqueous phase, dark oil droplets were observed in front of a bright green fluorescent background (Figure 1e). Within this fluorescent aqueous bulk phase, numerous fluorescent vesicles could be distinguished which were apparently of hydrophilic nature. Oil droplets, vesicles or air bubbles were frequently encircled by a brighter fluorescent ring. This might either represent an artefact caused by the illumination or the accumulation of the hydrophilic dye on interfacial surfactant films. Fluorescein sodium might be incorporated into or adsorbed onto the interfacial films through an interaction with surfactant molecules. The ImageJ® analysis of the dark oil droplets indicated a mean droplet size of 28.43 ± 11.65 µm while the analysed droplet area corresponded exactly to the incorporated oil phase volume (19.38 ± 1.30 %, n=5). After incorporation of Atto 594 into the aqueous phase (Figure 1f), dark oil droplets could be distinguished in front of a bright red fluorescent background. In this case, it was even more apparent that the fluorescent aqueous bulk phase consisted of numerous small aqueous vesicles. The incorporated air bubbles again showed strong fluorescent rings at the interface, caused either by illumination artefacts at the air/water interface or adsorption of the dye to the in-

terfacial film. Incorporation of Bodipy® into the oil phase led to bright green fluorescent oil droplets in front of a dark aqueous bulk phase (Image 1g). However, the amount of fluorescent spherical structures appeared too high for the incorporated oil volume of 20% w/w. ImageJ® calculations confirmed this assumption. The calculated area fraction of fluorescent structures amounted to 40%, which represents an overestimation of the amount of oil droplets. This indicates that not only oil droplets were affected by the fluorescence dye and thus included in the calculations. Presumably, spherical vesicular structures composed of surfactant aggregates or bilayers were associated with Bodipy® as well, e.g. due to solubilisation of the lipophilic dye within the fatty acid chains of the surfactant molecules. To clearly distinguish between the oil and aqueous phase and to detect overlapping regions, both Bodipy® and Atto 594 were incorporated into a model emulsion A. Preparation at 40°C led to numerous air bubbles due to foaming for both sucrose stearate blends (Figure 2a, b). The bright green fluorescent oil droplets in S-970 emulsions were homogeneously distributed while a network-like aggregation was observed for S-1170 emulsions. An ImageJ® analysis revealed a mean droplet size of 26.22 ± 19.52 µm with an accurately analysed area of 20.66 ± 3.68 % (n=7). These data are in agreement with the fluorescein sodium data. The analysis of the oil droplets containing Bodipy® was apparently facilitated due to the overlapping fluorescent regions of the aqueous vesicles; better contrast between strongly and slightly green fluorescent structures was obtained. Omitting the homogenisation step with the ultra-turrax did not affect the distribution of the fluorescent dyes within the emulsions, but led to a decrease in air bubbles and an increase in droplet size. Increasing the preparation temperature from 40°C to 60°C led to an overall fluidisation during preparation and also an increase in droplet size (Figure 2c, d). At 60°C, the systems were mostly free of air irrespective of the homogenisation step. Additional fluorescence microscopic tests on modified emulsions A with a decreased surfactant content of 2.5% w/w revealed a much less crowded structure. Mainly oil droplets were formed while no surplus surfactant was available to form additional vesicular structures. These systems with 2.5% w/w of surfactant were much more fluid than their counterparts with 5% w/w of sucrose ester. It may thus be concluded that the internal vesicular structure is indeed responsible for the increased viscosity of the emulsions.

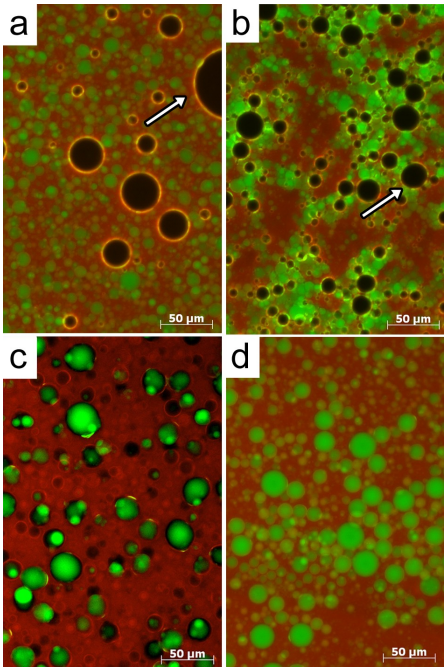

Figure 2: Influence of production temperature on emulsion morphology: Fluorescence microscopic images at 20-fold magnification of model emulsion A prepared at 40°C **(a, b)** or 60°C **(c,d)** including homogenisation with an ultra-turrax. The employed surfactants were S-970 (on the left, a and c) or S-1170 (on the right, b and d). The aqueous phase was coloured red (Atto 594), the lipophilic phase was coloured green (Bodipy®). The large dark fields encircled by a brightly fluorescent film are air bubbles (arrows).

Morphology and stability of the final emulsions

The microscopic investigation of the final emulsions A to E (Table 2) was focused on the effect of the oil phase. The microscopic appearance of the final emulsions was highly similar for all oils except in case of IPM. Numerous air bubbles and a dense network of small vesicles were generally observed [9]. In case of emulsions E S-970 and E S-1170 with IPM the structure was denser and darkened by even larger numbers of small air bubbles. Undissolved surfactant appeared to be present in all fresh and stored systems irrespective of the ester blend, suggesting a certain re-crystallisation of the sucrose esters after preparation. Light microscopic investigation after 3 months of storage revealed that most of the air bubbles were gone from the systems. The stored systems showed a less crowded internal structure than the fresh ones. The spherical aqueous structures forming the gel network appeared to have increased in size, indicating slow separation of the aqueous phase. These phenomena appeared to have the strongest impact on the physical properties of emulsions E with IPM, especially in case of E S-1170. Interestingly, the mean oil droplet size showed only a slight increase after the storage period. Comparison of fluorescent microscopic images of fresh and stored model emulsions A containing Atto 594 and Bodipy® confirmed that the incorporated air bubbles had mostly vanished and the average droplet size had only increased slightly (Figure 3). The pH value of the final emulsions was quite comparable around 6.48 (S-970) and 6.45 (S-1170) for all oil phases except for IPM. For the latter, slightly higher values around 6.70 were observed for both esters. After 3 months of storage, all emulsions showed a decrease in pH to values around 6.41 (S-970) and 6.38 (S-1170). In case of IPM, a decrease to values around 6.57 was observed. This can be considered as the normal ageing process due to chemical degradation [17]. The overall pH was suitable for dermal application and indicated a mild surfactant nature [6].

3.2 Thermoanalytical characterisation

Melting behaviour of pure ester blends

Investigation of the two ester blends in powder form led to similar thermograms. Upon heating, an endothermic transition was observed with positive enthalpy values, which represents physical changes induced by melting or softening of the esters when reaching their glass transition temperature [12]. The obtained heating thermograms did not show a single sharp peak corresponding to a specific melting point since the ester blends are composed of mono-, di- and poly-esters of sucrose and fatty acids [18]. Thus, a melting range was observed that consisted of a smaller and a larger peak. This first peak occurred around 40°C for S-970 and around 35°C for S-1170. The maximum peak temperatures T_m of the main peak were highly comparable for the two ester blends and were located at 44.66 ± 0.08 °C and 44.79 ± 0.09 °C (n=3, respectively, $P>0.05$). The observed melting enthalpy (ΔH, J/g) was significantly larger for S-1170 than for S-970 ($P<0.05$) due to the different composition of the ester mixtures. It may be assumed that the observed transition represents the transformation of an amorphous phase into a liquid crystalline mesophase [12]. This transition may be explained by the intermolecular hydrogen bonding network between the hydroxyl groups of the sucrose molecules, which is the driving force for the thermotropic self-organisation of the sucrose ester [12].

A subsequent cooling and second heating of the samples was performed. After the first melting and solidification process, the struc-

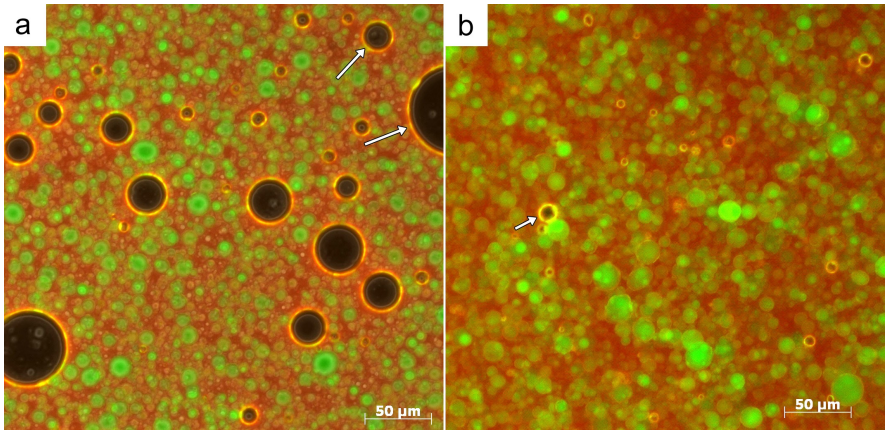

Figure 3: Effect of storage on emulsion morphology: Fluorescence microscopic images at 20-fold magnification of model emulsion A S-970 **(a)** directly after preparation and **(b)** after 3 months of storage. The aqueous phase is coloured red (Atto 594), the lipophilic phase is coloured bright green (Bodipy®). The dark spheres encircled by a brightly fluorescent film are air bubbles (arrows).

tures of the sucrose esters were rebuilt to varying extents. During the second heating of both esters, the shape of the transition changed to a sharper single peak, i.e. only the large endothermic peaks were respectively observed while the preceding smaller peaks had vanished. The T_0 and T_m of the main peaks remained largely unchanged. However, the overall enthalpy values were respectively smaller than during the first heating process ($P<0.05$), indicating that irreversible changes had been induced. Re-crystallisation during cooling was possible to a certain extent for both esters of intermediate HLB values [19], indicating better physical stability of the material than reported for esters of higher HLB value [18].

Melting behaviour of binary systems: effect of production temperature

In the microDSC heating thermograms of aqueous dispersions of 5% w/w of the two sucrose stearate blends, endothermic transitions were observed as a result of the melting process of the dispersed ester molecules. Unlike for the pure ester mixtures, single melting peaks were observed during the first heating process irrespective of the preparation temperature of the dispersions. For systems prepared at 25°C, the obtained thermograms were quite similar for the two sucrose stearate blends showing a single sharp melting peak with T_0 around 45°C and 46°C, T_m at 48°C and comparable enthalpy values ($P>0.05$). Compared to the crystalline ester powders, the T_0 and T_m of these dispersions were located at higher temperatures, which could be ascribed to the hydration of the surfactant molecules [7]. These findings are in good agreement with previous reports; the exact transition temperatures are dependent on the ester concentrations within the binary systems as well as the heating rate [5, 12]. In case of dispersions prepared at 50°C, the single peaks had a slightly broader shape especially in case of S-1170. The T_0 and T_m of S-970 dispersions were located at slightly lower values than S-1170 dispersions ($P<0.05$). In case of S-970, the elevated preparation temperature led to a shift of T_0 from 45°C to 43°C and of T_m from 48°C to 47°C when compared to the dispersions prepared at 25°C. In case of S-1170, only a slight shift of T_0 from 46°C

to 45°C was observed. For both ester blends, the enthalpy values were significantly smaller for the pre-heated dispersions than for those prepared at room temperature ($P<0.05$). This indicates that the sucrose ester mixtures only re-crystallised to a certain extent after heating and cooling of the produced binary systems. Hydrophilic monoesters might remain dissolved after preparation [5]. In summary, heating induced irreversible changes within the sucrose ester dispersions although their structure has been reported to be restored with time [18]. The exact composition of the employed ester blends has an immense impact on the structure of the dispersions and thus the observed phase transitions [12, 18]. At low sucrose ester concentrations, both micellar systems [10] and bilayer formation have been reported [12]. In our study, as reported by Sadtler et al., the employed sucrose ester blends were not able to form micellar structures due to their comparatively low aqueous solubility [12]. Likewise, no liquid crystalline structures such as lamellar phases were observed in the polarisation microscope. It may be assumed that the formation of bilayers or liposomal vesicles is the most likely explanation for the increased viscosity.

Melting behaviour of emulsions: effect of production temperature

MicroDSC measurements of the model emulsions A prepared at different temperatures were performed. When comparing the melting behaviour of S-970 and S-1170 emulsions prepared at 25°C to the melting behaviour of the pure esters, T_0 and T_m of the ester blends within the emulsions were located at slightly higher values around 42°C and 47°C, respectively. The shift to higher temperatures was not as pronounced as for the binary systems, suggesting that the ester is not present in a purely hydrated state, but associated with the oil phase as well. As the production temperature was increased, the observed transition was shifted to lower temperatures and the enthalpy values became progressively smaller. The comparatively broad transition peak observed for emulsion A S-970 prepared at 25°C also became more inhomogeneous with increasing preparation temperature. A smaller shoulder peak preceding the large main peak was observed which became more pronounced with increasing preparation temperatures. In case of emulsion A S-1170, the same tendencies were observed. The thermograms generally showed higher enthalpy values and smaller shoulder peaks. As observed for the binary systems, a second heating cycle mostly led to a minor peak shift to higher temperatures while enthalpy values were generally lower than in the first heating cycle.

Melting behaviour of the final emulsions: influence of oil type

The microDSC measurements of the final emulsions revealed that the nature of the oil phase had a definite impact on the endothermic transitions observed during heating (Figure 4). Overall, the mean T_0 and T_m increased in the order E<A<B<C<D for emulsions with both ester blends while the opposite trend was observed for the corresponding enthalpy values. The shape of the endothermic peaks changed with the different oil phases. For emulsions with PCL® liquid and tegosoft® liquid, a smaller shoulder peak preceding the main peak was observed with both ester blends. For emulsions with corn oil and soybean oil, a comparatively sharp single peak was respectively observed. The heating thermograms of emulsions with IPM exhibited a very early onset and a broad irregular transition. A second heating cycle after cooling back to room temperature only induced minor changes of the transitions, mostly to

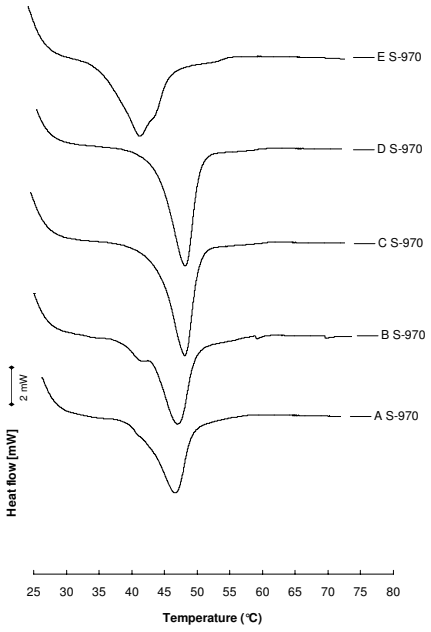

(a) S-970

Figure 4: Heating curves of the emulsions

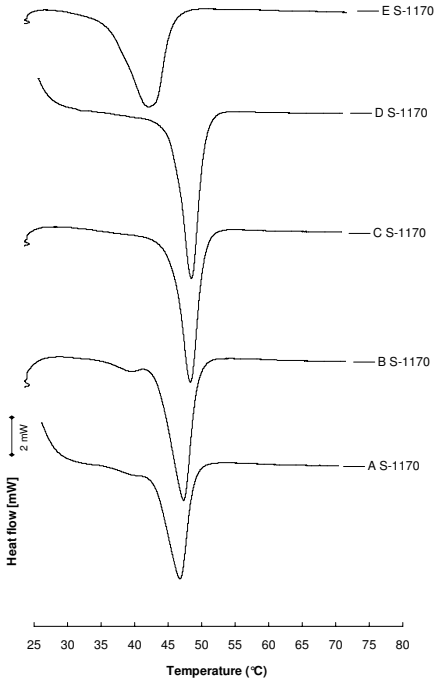

(b) S-1170

Figure 4: Heating curves of the emulsions: Endothermic transitions of the final emulsions A, B, C, D and E with **(a)** S-970 or **(b)** S-1170. The influence of the preparation temperature of 25°, 40°, 50° or 60°C can be derived from the changes in peak onset temperature, peak maximum temperature, peak shape and heat flow.

higher values. The enthalpy values were significantly lower for all emulsions during the second heating cycle ($P<0.05$), confirming irreversible structural changes induced by heating.

3.3 Rheological studies

Rheological behaviour of binary systems

Aqueous sucrose ester dispersions exhibited a power-law decrease in dynamic viscosity with increasing shear rate, i.e. shear-thinning flow behaviour. The dynamic viscosity of the systems increased with increasing sucrose ester concentrations (Table 3). As expected, a certain viscoelasticity was observed which likewise increased with increasing sucrose ester concentrations (data not shown). This concentration-dependence of the gelling potential of sucrose esters is in agreement with literature [13]. Likewise, the preparation temperature had a marked influence on the rheological properties of the aqueous dispersions. Both esters exhibited a strong gelling ability both at room temperature and after heating [19]. For systems prepared at 25°C, sucrose ester S-1170 exhibited a significantly stronger gelling ability than S-970 at all tested concentrations ($P<0.05$, Table 3). At a preparation temperature of 40°C, these differences in gelling potential between the two esters became negligible ($P>0.05$). After a preparation at 60°C, the gelling efficiencies of the esters were reversed with significantly stronger gel networks formed by S-970 than by S-1170 ($P<0.05$). It is noteworthy to emphasize that small differences in production may strongly influence the physical properties

Dynamic viscosity (Pas)			
Sample	**25 °C**	**40 °C**	**60 °C**
2.5% S-970	0.19 ± 0.03	0.40 ± 0.08	0.011 ± 0.001
5% S-970	1.30 ± 0.12	1.05 ± 0.42	0.06 ± 0.01
10% S-970	3.38 ± 0.42	3.89 ± 1.29	1.76 ± 0.28
20% S-970	12.18 ± 0.74	18.57 ± 1.16	21.00 ± 1.66
2.5% S-1170	0.47 ± 0.09	0.27 ± 0.09	0.008 ± 0.0003
5% S-1170	1.77 ± 0.31	0.80 ± 0.21	0.01 ± 0.001
10% S-1170	6.36 ± 0.73	3.39 ± 0.42	0.28 ± 0.03
20% S-1170	24.18 ± 1.86	15.43 ± 0.97	13.27 ± 0.58

Table 3: Influence of sucrose ester concentration and production temperature on the dynamic viscosity of binary systems. The aqueous sucrose ester dispersions of either S-970 or S-1170 were prepared at 25°, 40° or 60°C and their dynamic viscosity was compared at a shear rate of 50 s^{-1}. Values are given as means ± SD of at least three experiments ($n \geq 3$).

of the produced systems when sucrose esters are employed [5]. The underlying cause for the changes in viscoelastic properties with surfactant concentration and temperature might be related to different aspects. On the one hand, micelle formation has been reported to play a role in this context [13]. However, the type of surfactant association depends on the molecular geometry and the packing parameter and micelle formation has not been observed for sucrose esters of intermediate HLB value [12]. It may be assumed that the gel network is rather formed by H-bonds between ester and water molecules which form an aqueous gel network at ambient temperatures due to steric hindrances [7]. A temperature rise may progressively break down these H-bonds, finally leading to fluidisation. For sucrose esters of higher HLB, a temperature rise may lead to hydratisation of the polar head groups and favour the growing of micelles, which may in turn increase the viscosity of the systems [13]. Overall, S-1170 exhibited a far more linear gelling behaviour than S-970. The dynamic viscosity decreased with increasing temperature at all investigated concentrations of S-1170 (Table 3). In case of S-970, the dynamic viscosity remained largely constant or increased slightly at 40°C at all tested concentrations. At 60°C, the viscosity decreased strongly at all concentrations except at 20% w/w, which clearly represents an exception in terms of physical properties due to the high content of undissolved sucrose ester. In summary, a concentration of 5 % w/w of sucrose ester was confirmed to be sufficient for the formation of semi-solid systems. Thus, this concentration was employed for the development of emulsions.

Rheological behaviour of emulsions: influence of production temperature

The effect of different production temperatures on the dynamic viscosity of the model emulsions A S-970 and A S-1170 at a shear rate of 50 s^{-1} is depicted in Figure 5. The gelling ability of S-1170 at 25°C was significantly stronger than that of S-970 ($P<0.05$). These differences decreased upon an increase in temperature during production. At 40°C, 50°C and 60°C, no significant differences between the dynamic viscosity of the different

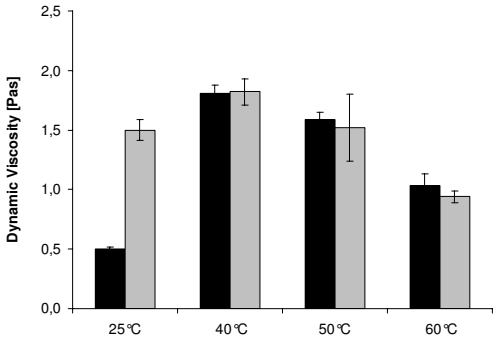

Figure 5: Influence of production temperature on emulsion viscosity: Influence of the production temperature on the dynamic viscosity of the model emulsions A S-970 (black bars) or A S-1170 (grey bars). The dynamic viscosity values were compared at 21°C and a shear rate of 50 s^{-1}. The depicted values are means ± SD of at least three experiments ($n \geq 3$).

esters was observed (P>0.05). At 40°C, both sucrose ester blends appeared to reach a maximum in terms of gelling ability. A stronger increase in production temperature led to a decrease of the dynamic viscosity for both esters. The model emulsions exhibited shear-thinning flow behaviour and viscoelasticity, i.e. a semi-solid appearance, irrespective of the preparation temperature. This might be ascribed to the formation of a weak gel-like network. As indicated by the microscopic images, the surplus sucrose ester appears to form a continuous matrix interdispersed with oil droplets [20]. Upon application of shear, this matrix is disrupted. After sufficiently long shear times, the sucrose ester might even separate into cluster domains that disturb the microstructure of the emulsions, thus decreasing the overall viscosity [20]. Thus, the mixtures should not be subjected to mechanical shearing during productions for prolonged periods of time. When comparing the dynamic viscosity of these emulsions with corresponding binary systems after preparation at 25°C, the dispersions exhibited slightly higher dynamic viscosity values. At increasing production temperatures of 60°C, the presence of the oil phase apparently reinforced the gelling potential of the sucrose esters, leading to systems of higher viscosity than observed for the aqueous dispersions (P<0.05, respectively). This aspect renders the sucrose esters highly useful for the formation of semi-solid multicomponent emulsion systems, since many compounds require elevated production temperatures. In addition, oscillatory frequency sweep tests were conducted for the model emulsions. Oscillation tests are dynamic methods for determining the viscoelastic properties of the investigated material in its rheological basic state. Unlike continuous shear techniques, oscillatory techniques do not disrupt static structures [21]. For both esters, the model emulsions exhibited gel characteristics at all tested preparation temperatures, i.e. the elastic moduli were significantly higher than the viscous moduli at all frequencies (P<0.05). When comparing the elastic and viscous moduli at a frequency of 1 Hz, the highest values for both parameters were reached at 40°C for S-970 and at 50°C for S-1170. When directly comparing the gelling potential of the different sucrose esters at 25°C, S-1170 exhibited significantly higher values of both the elastic and the viscous modulus than S-970 (P<0.05, respectively). At 40°C, no differences between the elastic and the viscous moduli of S-970 and S-1170 were observed (P<0.05, respectively). At 50 and 60°C, S-1170 exhibited higher values for the elastic and viscous moduli than S-970. Overall, the investigated emulsions exhibited properties of a weak gel, i.e. the viscous and elastic modulus were slightly dependent on the oscillatory frequency and the elastic modulus G' was larger than the viscous modulus G'' at all times [13]. A slight increase in elastic behaviour with increasing frequencies was observed, as is common for viscoelastic substances [5]. Under strong deformation or continuous flow conditions, the weak gel network breaks down into smaller flow units and may flow homogeneously [13]. This might explain

why the elastic and viscous moduli of S-1170 model emulsions at 50°C and 60°C were higher than that of S-970 emulsions although the dynamic viscosity data indicated otherwise. If a system is more structured in the gel state, it is also more sensitive to shear that induces an alteration of the microstructure [12]. In case of S-1170 emulsions prepared at higher temperatures, the gel network apparently broke down earlier during the continuous shear experiments.

Rheological behaviour of the final emulsions: influence of the oil type

The dynamic viscosity of the final emulsions at a shear rate of 50 s^{-1} at 21°C is given in Figure 6. Values are given for both fresh and stored emulsions with S-970 (Figure 6a) and S-1170 (Figure 6b). As can be seen, S-1170 led to higher viscosity values than S-970 with all employed oil phases ($P<0.05$) except for IPM ($P>0.05$). Regarding the influence of the oil type, different trends were observed for the two ester blends. In case of the fresh S-970 emulsions, the viscosity was ranked in the order E > C > A / B / D. In case of fresh S-1170 emulsions, the ranking was D > A / B / C > E. The only oil phase that showed the strongest dependency on the employed ester type was IPM. When regarding the changes in the dynamic viscosity of the formulations after storage, interesting trends were revealed (Figure 6). In case of A S-970 and B S-970 emulsions, the dynamic viscosity showed a significant increase after 3 months of storage ($P<0.05$, respectively). In case of the other three oils, a more or less strong decrease of the dynamic viscosity was observed. In case of S-1170 emulsions, all systems showed a pronounced decrease of the dynamic viscosity after 3 months. This suggests that only the combination of sucrose stearate S-970 with oil phases based on cetearyl ethylhexanoate, as is the case for PCL® liquid and tegosoft® liquid, leads to systems that exhibit thickening during storage. This thickening effect presumably occurs as air bubbles leave the system, as confirmed by the microscopic images. In case of the other oil phases, however, fluidisation of the emulsions occurs especially in case of IPM, indicating slow destabilisation. In case of S-1170, no thickening effects were observed, indicating that the exact composition of the surfactant blend plays an important role in this context. Additional oscillatory measurements confirmed the observed trends. For the determined elastic modulus G' and viscous modulus G'', the same orders of ranking for the differ-

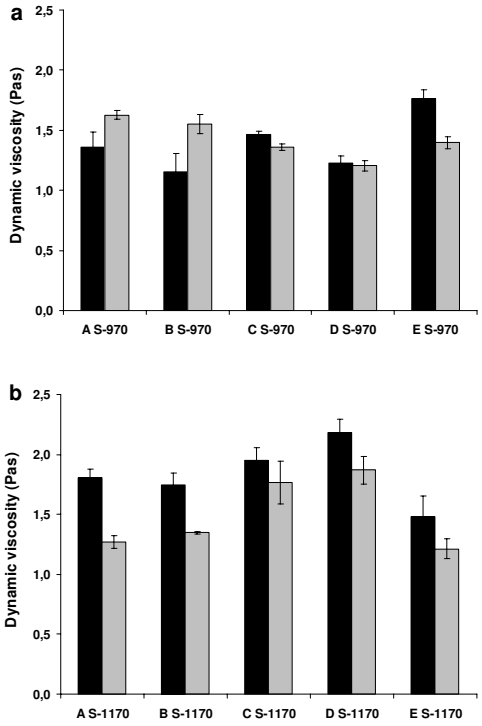

Figure 6: Effect of storage on emulsion viscosity: Comparison of the dynamic viscosity of emulsions A, B, C, D and E stabilised by (a) S-970 or (b) S-1170 at a shear rate of 50 s^{-1} at 21°C. Values were determined on fresh emulsions (black bars) and after 3 months of storage (grey bars). The depicted values are means ± SD of at least three experiments ($n \geq 3$).

ent emulsions were observed as for the viscosity values, thus confirming the effect of the different oil phases (Figure 7). The elastic modulus

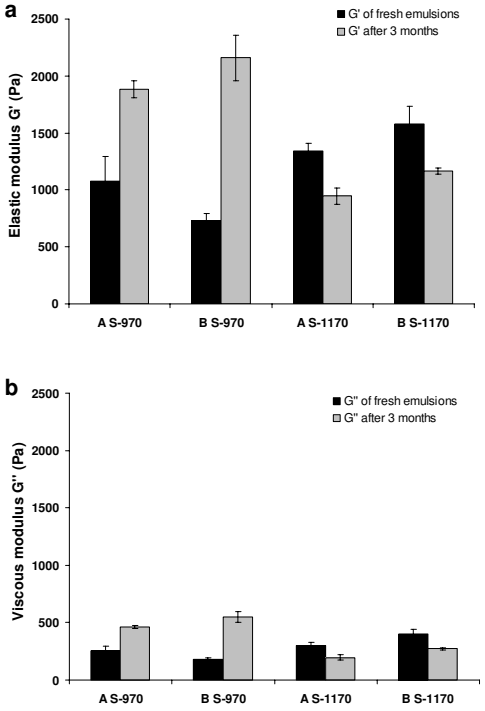

Figure 7: Effect of storage on emulsion viscoelasticity: Comparison of the elastic modulus G' (a) and the viscous modulus G" (b) at a frequency of 1 Hz at 21°C of the model emulsions A and B stabilised by S-970 or S-1170. Values were determined on fresh emulsions (black bars) and after 3 months of storage (grey bars). The depicted values are means ± SD of at least three experiments ($n \geq 3$).

was significantly higher than the viscous modulus for all formulations (P<0.05, respectively), i.e. all semi-solid emulsions exhibited a gel-like structure with a prevailing elastic component similar to standard dermal preparations [21]. The orders of magnitude of the elastic and viscous moduli were respectively comparable for all emulsions. When comparing the different ester blends, higher values of the elastic modulus G' and the viscous modulus G'' were generally obtained with S-1170 except in case of IPM-emulsions. Figure 7 shows the elastic and viscous moduli of representative emulsions and the changes observed after 3 months of storage. As observed for the viscosity values, both the elastic and the viscous moduli of A S-970 and B S-970 emulsions show a significant increase after storage (P<0.05, respectively). In case of C S-970 and D S-970, the parameters remained largely constant or showed a slight decrease. The strongest decrease in the elastic and the viscous modulus was observed for E S-970 with IPM. In case of S-1170, all formulations showed a more or less pronounced decrease in both the viscous and elastic moduli after 3 months of storage; no thickening effects were observed. As another aspect of interest, the effect of different measurement temperatures on the rheological properties of the fresh systems was investigated by performing additional measurements at the skin surface temperature of 32°C. At this temperature, all emulsions exhibited noticeably decreased dynamic viscosity values. In case of S-970 emulsions, the determined values at 32°C were highly comparable for all emulsions irrespective of the oil type (P>0.05), ranging around 1 Pas at 50 s^{-1}. In case of S-1170 emulsions, the dynamic viscosity values at 32°C were in the same ranking order as at 21°C, but were likewise reduced to values only slightly above 1 Pas at 50 s^{-1}. This indicates that the rheological differences in emulsion properties observed at 21°C might play a role during processing and storage, but might be minimised upon application in vivo. At a measurement temperature of 32°C the gel strength of the emulsions based on the different sucrose ester blends becomes largely comparable. Slightly higher viscosity values for S-1170 emulsions were merely observed in case of tegosoft® liquid and soybean oil (P<0.05, respectively). The corresponding oscillatory frequency sweep tests confirmed these tendencies. Both the elastic and viscous moduli were decreased for all emulsions at a measurement temperature of 32°C. In general, the elastic

modulus G' showed a more pronounced decrease than the viscous modulus G''. The elastic moduli were reduced by up to 50% of their initial values. The strongest decrease of both G' and G'' was observed for IPM-emulsions. Overall, all emulsions exhibited shear-thinning flow behaviour with slightly to moderately pronounced thixotropy, which is desirable for cosmetic and pharmaceutical emulsions [7]. The observed gel-like structure of the model emulsions might be related to the hydrogen bonding of water molecules to the sucrose hydroxyl moieties, causing specific conformation and the formation of an aqueous gel network due to steric hindrances [7].

4 Conclusion

Both sucrose stearate S-970 and S-1170 are excellent surfactants for the formation of skin-friendly semi-solid emulsions with a complex aqueous bulk phase. The temperature-dependent gelling potential of the ester blends within multiphase systems was higher than in aqueous binary systems especially at elevated preparation temperatures, rendering them interesting additives for emulsion preparation. The nature of the oil phase played a major role in terms of emulsion stability. Interestingly, formulations with sucrose stearate S-970 and oil phases containing cetearyl ethylhexanoate showed an increase in viscoelasticity with storage time. These findings indicate a remarkable potential of these conveniently applicable dermal formulations. The exact nature of the interactions responsible for the beneficial physical properties remains to be clarified.

Acknowledgements

The authors would like to thank Elham Rezvani and Gerhard Schleining of the University of Natural Resources and Life Sciences Vienna and Xueyan Wang of the University of Vienna for technical assistance. The financial support of the research platform "Characterisation of Drug Delivery Systems on Skin and Investigation of Involved Mechanisms" is gratefully acknowledged.

References

Journals:

[1] M. Otsuka, Y. Matsuda, Effect of cogrinding with various kinds of surfactants on the dissolution behavior of phenytoin, J. Pharm. Sci. 84 (1995) 1434-1437.

[2] S.B. Calderilla-Fajardo, J. Cazares-Delgadillo, R. Villalobos-Garcia, D. Quintanar-Guerrero, A. Ganem-Quintanar, R. Robles, Influence of sucrose esters on the in vivo percutaneous penetration of octyl methoxycinnamate formulated in nanocapsules, nanoemulsion, and emulsion, Drug Dev. Ind. Pharm. 32 (2006) 107-113.

[3] J. Cazares-Delgadillo, A. Naik, Y.N. Kalia, D. Quintanar-Guerrero, A. Ganem-Quintanar, Skin permeation enhancement by sucrose esters: a pH-dependent phenomenon, Int. J. Pharm. 297 (2005) 204-212.

[4] V. Klang, N. Matsko, K. Raupach, N. El-Hagin, C. Valenta, Development of sucrose stearate-based nanoemulsions and optimisation through gamma-cyclodextrin, Eur. J. Pharm. Biopharm. 79 (2011) 58-67.

[5] S. Ullrich, H. Metz, K. Maeder, Sucrose ester nanodispersions: microviscosity and viscoelastic properties, Eur. J. Pharm. Biopharm. 70 (2008) 550-555.

[6] S. Savic, M. Savic, S. Tamburic, G. Vuleta, S. Vesic, C.C Mueller-Goymann, An alkylpolyglucoside surfactant as a prospective pharmaceutical excipient for topical formulations: the influence of oil polarity on the colloidal structure and hydrocortisone in vitro/in vivo permeation, Eur. J. Pharm. Sci. 30 (2007) 441-450.

[7] S. Savic, M. Lukic, I. Jaksic, S. Reichl, S. Tamburic, C. Mueller-Goymann, An alkyl polyglucoside-mixed emulsifier as stabilizer of emulsion systems: the influence of colloidal structure on emulsions skin hydration potential, J. Colloid. Interface Sci. 358 (2011) 182-191.

[8] S.D. Savic, M.M. Savic, S.A. Vesic, G.M. Vuleta, C.C. Mueller-Goymann, Vehicles based on a sugar surfactant: Colloidal structure and its impact on in vitro/in vivo hydrocortisone permeation, Int J Pharm. 320 (2006) 86-95.

[9] V. Klang, J.C. Schwarz, N. Matsko, E. Rezvani, N. El-Hagin, M. Wirth, C. Valenta, Semi-Solid Sucrose Stearate-Based Emulsions as Dermal Drug Delivery Systems, Pharmaceutics. 3 (2011) 275-306.

[10] C. Calahorro, J. Munoz, M. Berjano, A. Guerrero, C. Gallegos, Flow behavior of sucrose stearate/water systems, J. Am. Oil Chem. Soc. 69 (1992) 660-666.

[11] C. Gallegos, C. Calahorro, J. Munoz, M. Berjano, A. Guerrero, High-HLB sucrose esters: a peculiar viscous behaviour, Comunicaciones presentadas a la Jornadas del Comite Espanol de la Detergencia 22 (1991) 283-295.

[12] V.M. Sadtler, M. Guely, P. Marchal, L. Choplin, Shear-induced phase transitions in sucrose ester surfactant, J. Colloid. Interface Sci. 270 (2004) 270-275.

[13] A. Szuts, M. Budai-Szucs, I. Eros, N. Otomo, P. Szabo-Revesz, Study of gel-forming properties of sucrose esters for thermosensitive drug delivery systems, Int. J. Pharm. 383 (2010) 132-137.

[14] C. Valenta, C.E. Kast, I. Harich, A. Bernkop-Schnuerch, Development and in vitro evaluation of a mucoadhesive vaginal delivery system for progesterone, J. Control. Release. 77 (2001) 323-332.

[15] C. Valenta, K. Schultz, Influence of carrageenan on the rheology and skin permeation of microemulsion formulations, J. Control. Release. 95 (2004) 257-265.

[16] S.H. Klang, A. Baszkinb, S. Benita, The stability of piroxicam incorporated in a positively-charged submicron emulsion for ocular administration, Int. J. Pharm. 132 (1996) 33-44

[18] A. Szuts, E. Pallagi, G. Jr. Regdon, Z. Aigner, P. Szabo-Revesz, Study of thermal behaviour of sugar esters, Int. J. Pharm. 336 (2007) 199-207.

[19] A. Szuts, Z. Makai, R. Rajko, P. Szabo-Revesz, Study of the effects of drugs on the structures of sucrose esters and the effects of solid-state interactions on drug release, J. Pharm. Biomed. Anal. 48 (2008) 1136-1142.

[20] P. Partal, A. Guerrero, M. Berjano, C. Gallegos, Transient flow of O/W sucrose palmitate emulsions, J. Food Eng. 41 (1999) 33-41.

[21] A. Lippacher, R.H. Mueller, K. Maeder, Semisolid SLN dispersions for topical application: influence of formulation and production parameters on viscoelastic properties, Eur. J. Pharm. Biopharm. 53 (2002) 155-160.

PhD Thesis:

[17] C. Wabel, Influence of Lecithin on Structure and Stability of Parenteral Fat Emulsions, PhD Thesis, Friedrich-Alexander-Universität Erlangen-Nürnberg, Germany (1998).

CHAPTER 4

Conclusions

Colloidal carrier systems offer useful properties for dermal drug delivery. Continuous research has promoted the development of formulations with optimised long-term stability which can nevertheless be produced with the help of skin-friendly biodegradable compounds. The focus of this work was placed on formulation development as well as on methodological approaches to characterise the novel formulations regarding their skin penetration potential.

As a first step, lecithin-based nanoemulsions for the delivery of lipophilic drugs were successfully optimised by introducing skin-friendly natural co-stabilisers instead of polyethoxylated surfactants. Sucrose stearate mixtures of intermediate HLB value proved to be useful co-surfactants to improve nanoemulsion stability and morphology. The incorporation of natural CDs contributed to an improved physical stability of selected formulations, but was mostly found to improve the skin permeation rates of lipophilic steroidal drugs. This effect was particularly pronounced in case of γ-CD. A comparative study investigating lecithin and sucrose stearate mixtures as sole surfactants in nanoemulsions indicated that sucrose stearate mixtures are more suitable to form curved surfaces and thus homogeneous nanoemulsion droplets. In addition, better electrochemical stabilisation was observed for sucrose stearate nanoemulsions. In terms of skin permeation potential, both emulsifiers performed equally well. The incorporation of additional γ-CD again led to higher skin permeation rates in combination with a steroidal model drug. This effect was more pronounced for lecithin-based nanoemulsions than for sucrose stearate-based nanoemulsions, which indicates that synergistic mechanisms are involved. Cryo TEM studies revealed improved nanoemulsion homogeneity and more spherical droplet structures of lecithin-based systems after addition of γ-CD. The permeation enhancement effect of γ-CD on steroidal model drugs under infinite dose conditions was confirmed separately in a follow-up study using diffusion

cell techniques. The effect can most likely be attributed to solubility effects within the vehicle that come into play under infinite dose application. Under finite dose conditions during in vitro tape stripping, only a slight tendency towards higher skin penetration was observed.

During the development of sucrose stearate-based nanoemulsions a temperature-dependent gelling effect was observed. The peculiar rheological properties of sucrose stearate blends of intermediate HLB value were thus employed to create semi-solid sucrose stearate-based o/w emulsions of identical composition as the nanoemulsions. Comparative diffusion cell studies as well as tape stripping experiments revealed that despite the differences in mean droplet size and viscosity the systems exhibited comparable skin permeation and penetration rates for different model drugs. Further studies revealed that the exact composition of the sucrose stearate blend as well as the employed oil phase had a noticeable influence on the physical properties and stability of the resulting semi-solid emulsions. The complex internal structure of the emulsions could be visualised by fluorescence microscopy. Oil droplets suspended within a dense matrix of aqueous structures were revealed. This matrix was presumably composed of excess surfactant and water, causing temperature-dependent gelling upon preparation of the emulsions.

As a second major aspect of this work, the tape stripping technique was adapted and optimised for in vitro experiments using porcine ear skin. Important parameters such as tape brand as well as duration, mode and intensity of pressure application were optimised for the porcine ear model. The technique of NIR-densitometry was calibrated for the quantification of porcine SC proteins using an established protein assay for conducting a linear correlation analysis. Determination of the TEWL was found useful as a means of skin integrity testing. Likewise, skin hydration mapping with a capacitance-based sensor was found to be a useful tool to identify intact porcine skin areas or to visualise irregularities during the tape stripping process. Finally, comparative tape stripping experiments using model formulations such as microemulsions and hydrogels revealed that the porcine ear is indeed an appropriate model for preliminary in vitro tape stripping experiments.

In conclusion, the presented consecutive publications served to develop, characterise and optimise novel nanoemulsion and emulsion systems stabilised by eudermic biodegradable raw materials. The observed strong permeation enhancement effect of CDs could be attributed to solubility effects due to infinite dose experimental setups; different approaches in formulation development are required to exploit this enhancement potential under in vivo conditions. The tape stripping technique was successfully adapted for in vitro experiments on porcine ear skin and was further employed for the characterisation of the skin penetration potential of the different developed systems.

CHAPTER 5

References

[1] B.B. Michniak-Kohn, P.W. Wertz, M. Al-Khalili, V.M. Meidan, Skin: Physiology and Penetration Pathways, in: Delivery System Handbook for Personal Care and Cosmetic Products, M.R. Rosen (Ed.), William Andrew, New York (2005) p. 77-100.

[2] K. Wolff, Die Epidermis als Abwehrorgan, in: Die Haut als Abwehrorgan, O. Braun-Falco, G. Geiler, St. Jablonska (Eds.), Wissenschaftliche Verlagsgesellschaft mbH, Stuttgart (1991) p. 21-32.

[3] J. Hadgraft, R.H. Guy, Feasibility Assessment in Topical and Transdermal Drug Delivery: Mathematical Models and in Vitro Studies, in: Transdermal Drug Delivery, R.H. Guy, J. Hadgraft (Eds.), Marcel Dekker, New York (2003) p. 1-23.

[4] M.S. Roberts, K.A. Walters, Dermal Absorption and Toxicity Assessment, Marcel Dekker, New York (1998).

[5] G.L. Flynn, Topical Drug Absorption and Topical Pharmaceutical Systems, in: Modern Pharmaceutics, G.S. Banker, C.T. Rhodes (Eds.), Marcel Dekker, New York (1990) p. 265.

[6] J.A. Bouwstra, P.L. Honeywell-Nguyen, G.S. Gooris, M. Ponec, Structure of the skin barrier and its modulation by vesicular formulations, Prog. Lipid Res. 42 (2003) 1-36.

[7] Skin Care Forum 35, www.scf-online.com, BASF Personal Care and Nutrition GmbH (January 2012).

[8] K. Moser, K. Kriwet, A. Naik, Y.N. Kalia, R.H. Guy, Passive skin penetration enhancement and its quantification in vitro, Eur. J. Pharm. Biopharm. 52 (2001) 103-112.

[9] J. Hadgraft, Skin, the final frontier, Int. J. Pharm. 224 (2001) 1-18.

[10] J. Hadgraft, M.E. Lane, Skin: the ultimate interface, Phys. Chem. Chem. Phys. 13 (2011) 5215-5222.

[11] P.M. Elias, Epidermal lipids, barrier function and desquamation, J. Invest. Dermatol. 80 (1983) 44s-49s.

[12] J. Hadgraft, M.E. Lane, Skin permeation: the years of enlightenment, Int. J. Pharm. 305 (2005) 2-12.

[13] B.W. Barry, Mode of action of penetration enhancers in human skin, J. Control. Release 6 (1987) 85-97.

[14] A. Patzelt, H. Richter, R. Buettemeyer, H.J. Huber, U. Blume-Peytavi, W. Sterry, J. Lademann, Differential stripping demonstrates a significant reduction of the hair follicle reservoir in vitro compared to in vivo, Eur. J. Pharm. Biopharm. 70 (2008) 234-238.

[15] J. Lademann, H. Richter, A. Teichmann, N. Otberg, U. Blume-Peytavi, J. Luengo, B. Weiss, U.F. Schaefer, C.M. Lehr, R. Wepf, and W. Sterry, Nanoparticles–an efficient carrier for drug delivery into the hair follicles, Eur. J. Pharm. Biopharm. 66 (2007) 159-64.

[16] J. Lademann, A. Patzelt, H. Richter, S. Schanzer, W. Sterry, A. Filbry, K. Bohnsack, F. Rippke, M. Meinke, Comparison of two in vitro models for the analysis of follicular penetration and its prevention by barrier emulsions, Eur. J. Pharm. Biopharm. 72 (2009) 600-604.

[17] B.W. Barry, Novel mechanisms and devices to enable successful transdermal drug delivery, Eur. J. Pharm. Sci. 14 (2001) 101-114.

[18] H.A. Benson, Transdermal drug delivery: penetration enhancement techniques, Curr. Drug Deliv. 2 (2005) 23-33.

[19] S. Savic, G. Vuleta, R. Daniels, C.C. Mueller-Goymann, Colloidal microstructure of binary systems and model creams stabilized with an alkylpolyglucoside nonionic emulsifier, Colloid Polym. Sci. 283 (2005) 439-451.

[20] A.C. Williams, B.W. Barry, Penetration enhancers, Adv. Drug Deliv. Rev. 56 (2004) 603-618.

[21] I. Jaksic, M. Lukic, A. Malenovic, S. Reichl, C. Hoffmann, C. Mueller-Goymann, R. Daniels, S. Savic, Compounding of a topical drug with prospective natural surfactant-stabilized pharmaceutical bases: Physicochemical and in vitro/in vivo characterization - A ketoprofen case study, Eur. J. Pharm. Biopharm. 80 (2012) 164-175.

[22] S. Savic, M. Savic, S. Tamburic, G. Vuleta, S. Vesic, C.C. Mueller-Goymann, An alkylpolyglucoside surfactant as a prospective pharmaceutical excipient for topical formulations: the influence of oil polarity on the colloidal structure and hydrocortisone in vitro/in vivo permeation, Eur. J. Pharm. Sci. 30 (2007) 441-450.

[23] S. Savic, M. Lukic, I. Jaksic, S. Reichl, S. Tamburic, C. Mueller-Goymann, An alkyl polyglucoside-mixed emulsifier as stabilizer of emulsion systems: the influence of colloidal structure on emulsions skin hydration potential, J. Colloid. Interface Sci. 358 (2011) 182-191.

[24] S.D. Savic, M.M. Savic, S.A. Vesic, G.M. Vuleta, C.C. Muller-Goymann, Vehicles based on a sugar surfactant: Colloidal structure and its impact on in vitro/in vivo hydrocortisone permeation, Int. J. Pharm. 320 (2006) 86-95.

[25] V. Klang, N. Matsko, A.M. Zimmermann, E. Vojnikovic, C. Valenta, Enhancement of stability and skin permeation by sucrose stearate and cyclodextrins in progesterone nanoemulsions, Int. J. Pharm. 393 (2010) 152-160.

[26] V. Klang, N. Matsko, K. Raupach, N. El-Hagin, C. Valenta, Development of sucrose stearate-based nanoemulsions and optimisation through gamma-cyclodextrin, Eur. J. Pharm. Biopharm. (2011).

[27] V. Klang, J.C. Schwarz, N. Matsko, E. Rezvani, N. El-Hagin, M. Wirth, C. Valenta, Semi-Solid Sucrose Stearate-Based Emulsions as Dermal Drug Delivery Systems, Pharmaceutics 3 (2011) 275-306

[28] C.B. Fox, Squalene emulsions for parenteral vaccine and drug delivery, Molecules 14 (2009) 3286-3312.

[29] T.G. Mason, J.N. Wilking, K. Meleson, C.B. Chang, S.M. Graves, Nanoemulsions: formation, structure, and physical properties, J. Phys.: Condens. Matter 18 (2006) R635-R666.

[30] M.T. Baker, M. Naguib, Propofol: the challenges of formulation, Anesthesiology 103 (2005) 860-876.

[31] K. Welin-Berger, B. Bergenstahl, Inhibition of Ostwald ripening in local anesthetic emulsions by using hydrophobic excipients in the disperse phase, Int. J. Pharm. 200 (2000) 249-260.

[32] W. van Nieuwenhuyzen, B.F. Szuhaj, Effects of lecithins and proteins on the stability of emulsions, Fett/Lipid. 100 (1998) 282-291.

[33] C. Solans, P. Izquierdo, J. Nolla, N. Azemar, M.J. Garcia-Celma, Nano-emulsions, Curr. Opin. Coll. Int. Sci. 10 (2005) 102-110.

[34] R. Daniels, Galenic principles of modern skin care products, Skin Care Forum (2001), Society for Dermopharmacy,
http://www.scf-online.com/english/25_e/galenic_25_e.htm, (January 2012)

[35] V. Klang, C. Valenta, Lecithin-based nanoemulsions, J. Drug Del. Sci. Tech. 21 (2011) 55-76.

[36] W. van Nieuwenhuyzen, M.C. Tomás, Update on vegetable lecithin and phospholipid technologies, Eur. J. Lipid Sci. Technol. 110 (2008) 472-486.

[37] Y.A. Shchipunov, Self-organising structures of lecithin, Russ. Chem. Rev. 66 (1997) 301-322.

[38] A. Szuts, Z. Makai, R. Rajko, P. Szabo-Revesz, Study of the effects of drugs on the structures of sucrose esters and the effects of solid-state interactions on drug release, J. Pharm. Biomed. Anal. 48 (2008) 1136-1142.

[39] A. Szuts, M. Budai-Szucs, I. Eros, R. Ambrus, N. Otomo, P. Szabo-Revesz, Study of thermo-sensitive gel-forming properties of sucrose stearates, J. Excipients and Food Chem. 1 (2010) 13-20.

[40] S. Takegami, K. Kitamura, H. Kawada, Y. Matsumoto, T. Kitade, H. Ishida, C. Nagata, Preparation and characterization of a new lipid nano-emulsion containing two cosurfactants, sodium palmitate for droplet size reduction and sucrose palmitate for stability enhancement, Chem. Pharm. Bull. (Tokyo) 56 (2008) 1097-1102.

[41] S.B. Calderilla-Fajardo, J. Cazares-Delgadillo, R. Villalobos-Garcia, D. Quintanar-Guerrero, A. Ganem-Quintanar, R. Robles, Influence of sucrose esters on the in vivo percutaneous penetration of octyl methoxycinnamate formulated in nanocapsules, nanoemulsion, and emulsion, Drug Dev. Ind. Pharm. 32 (2006) 107-113.

[42] J. Cazares-Delgadillo, A. Naik, Y.N. Kalia, D. Quintanar-Guerrero, A. Ganem-Quintanar, Skin permeation enhancement by sucrose esters: a pH-dependent phenomenon, Int. J. Pharm. 297 (2005) 204-212.

[43] R.H. Mueller, R. Schuhmann, Teilchengrößenmessungen in der Laborpraxis, Wissenschaftliche Verlagsgesellschaft mbH, Stuttgart (1996).

[44] S. Benita, M.Y. Levy, Submicron emulsions as colloidal drug carriers for intravenous administration: comprehensive physicochemical characterization, J. Pharm. Sci. 82 (1993) 1069-1079.

[45] V. Klang, N.B. Matsko, C. Valenta, F. Hofer, Electron microscopy of nanoemulsions: An essential tool for characterisation and stability assessment, Micron 43 (2012), 85-103.

[46] J. Kuntsche, J.C. Horst, H. Bunjes, Cryogenic transmission electron microscopy (cryo-TEM) for studying the morphology of colloidal drug delivery systems, Int. J. Pharm. (2011).

[47] R.H. Mueller, Zetapotential und Partikelladung in der Laborpraxis, Band 37, Paperback APV, Wissenschaftliche Verlagsgesellschaft mbH, Stuttgart (1996).

[48] D.J. McClements, Food Emulsions: Principles, Practices, and Techniques, CRC Press, Boca Raton, Florida (2005).

[49] T. Loftsson, D. Duchene, Cyclodextrins and their pharmaceutical applications, Int. J. Pharm. 329 (2007) 1-11.

[50] P. Jansook, T. Loftsson, CDs as solubilizers: effects of excipients and competing drugs, Int. J. Pharm. 379 (2009) 32-40.

[51] R.A. Rajewski, V.J. Stella, Pharmaceutical applications of cyclodextrins. 2. In vivo drug delivery, J. Pharm. Sci. 85 (1996) 1142-1169.

[52] D. Duchene, A. Bochot, S.C. Yu, C. Pepin, M. Seiller, Cyclodextrins and emulsions, Int. J. Pharm. 266 (2003) 85-90.

[53] A. Bochot, L. Trichard, G. Le Bas, H. Alphandary, J.L. Grossiord, D. Duchene, E. Fattal, Alpha-Cyclodextrin/oil beads: an innovative self-assembling system, Int. J. Pharm. 339 (2007) 121-129.

[54] M. Inoue, K. Hashizaki, H. Taguchi, Y. Saito, Emulsion preparation using beta-cyclodextrin and its derivatives acting as an emulsifier, Chem. Pharm. Bull. (Tokyo) 56 (2008) 1335-1337.

[55] P. Rother, Influence of cyclodextrins on oil-in-water emulsions containing hypromellose (HPMC) as a polymeric emulsifier, PhD Thesis, Faculty of Chemistry and Pharmacy, Eberhard-Karls-Universität Tübingen, Germany (2009).

[56] T. Loftsson, M. Masson, Cyclodextrins in topical drug formulations: theory and practice, Int. J. Pharm. 225 (2001) 15-30.

[57] K. Shimada, Y. Ohe, T. Ohguni, K. Kawano, J. Ishii, T. Nakamura, Emulsifying properties of a-, ß- and γ-cyclodextrins, Nipp. Shok. Kogyo Gakkaishi 38 (1991) 16-20.

[58] K. Shimada, K. Kawano, J. Ishii, T. Nakamura, Structure of inclusion complexes of cyclodextrins with triglyceride at vegetable oil / water interface, J. Food Sci. 57 (1992) 655-656.

[59] M. Inoue, K. Hashizaki, H. Taguchi, Y. Saito, Formation and characterization of emulsions using beta-cyclodextrin as an emulsifier, Chem. Pharm. Bull (Tokyo) 56 (2008) 668-671.

[60] S.C. Yu, A. Bochot, G.L. Bas, M. Cheron, J. Mahuteau, J.L. Grossiord, M. Seiller, and D. Duchene, Effect of camphor/cyclodextrin complexation on the stability of O/W/O multiple emulsions, Int J Pharm. 261 (2003) 1-8.

[61] K. Hashizaki, Kageyama, T., Inoue, M., Taguchi, H., Ueda, H., Saito, Y., Study on preparation and formation mechanism of n-alkanol/water emulsion using alpha-cyclodextrin, Chem. Pharm. Bull. (Tokyo) 55 (2007) 1620-1625.

[62] T.J. Franz, Percutaneous absorption. On the relevance of in vitro-data, J. Invest. Dermatol. 64 (1975) 190-195.

[63] M. Kietzmann, W. Loscher, D. Arens, P. Maass, D. Lubach, The isolated perfused bovine udder as an in vitro model of percutaneous drug absorption. Skin viability and percutaneous absorption of dexamethasone, benzoyl peroxide, and etofenamate, J. Pharmacol. Toxicol. Methods 30 (1993) 75-84.

[64] H. Wagner, K.H. Kostka, C.M. Lehr, U.F. Schaefer, Drug distribution in human skin using two different in vitro test systems: comparison with in vivo data, Pharm. Res. 17 (2000) 1475-1481.

[65] H. Wagner, K.H. Kostka, C.M. Lehr, U.F. Schaefer, Interrelation of permeation and penetration parameters obtained from in vitro experiments with human skin and skin equivalents, J. Control. Release 75 (2001) 283-295.

[66] H. Weigmann, J. Lademann, H. Meffert, H. Schaefer, W. Sterry, Determination of the horny layer profile by tape stripping in combination with optical spectroscopy in the visible range as a prerequisite to quantify percutaneous absorption, Skin Pharmacol. Appl. Skin Physiol. 12 (1999) 34-45.

[67] H. Weigmann, J. Lademann, R. Pelchrzim, W. Sterry, T. Hagemeister, R. Molzahn, M. Schaefer, M. Lindscheid, H. Schaefer, V.P. Shah, Bioavailability of clobetasol propionate-quantification of drug concentrations in the stratum corneum by dermatopharmacokinetics using tape stripping, Skin Pharmacol. Appl. Skin Physiol. 12 (1999) 46-53.

[68] T. Hahn, S. Hansen, D. Neumann, K.H. Kostka, C.M. Lehr, L. Muys, U.F. Schaefer, Infrared densitometry: a fast and non-destructive method for exact stratum corneum depth calculation for in vitro tape-stripping, Skin Pharmacol. Physiol. 23 (2010) 183-192.

[69] J. Lademann, U. Jacobi, C. Surber, H.J. Weigmann, J.W. Fluhr, The tape stripping procedure–evaluation of some critical parameters, Eur. J. Pharm. Biopharm. 72 (2009) 317-323.

[70] H.J. Weigmann, U. Jacobi, C. Antoniou, G.N. Tsikrikas, V. Wendel, C. Rapp, H. Gers-Barlag, W. Sterry, J. Lademann, Determination of penetration profiles of topically applied substances by means of tape stripping and optical spectroscopy: UV filter substance in sunscreens, J. Biomed. Opt. 10 (2005) 14009.

[71] F. Dreher, A. Arens, J.J. Hostynek, S. Mudumba, J. Ademola, H.I. Maibach, Colorimetric method for quantifying human Stratum corneum removed by adhesive-tape stripping, Acta Derm. Venereol. 78 (1998) 186-189.

[72] F. Dreher, B.S. Modjtahedi, S.P. Modjtahedi, H.I. Maibach, Quantification of stratum corneum removal by adhesive tape stripping by total protein assay in 96-well microplates, Skin Res. Technol. 11 (2005) 97-101.

[73] C. Herkenne, A. Naik, Y.N. Kalia, J. Hadgraft, R.H. Guy, Pig ear skin ex vivo as a model for in vivo dermatopharmacokinetic studies in man, Pharm. Res. 23 (2006) 1850-1856.

[74] I. Bommannan, R.O. Potts, R.H. Guy, Examination of stratum corneum barrier function in vivo by infrared spectroscopy J. Invest. Dermatol. 95 (1996) 403-408.

[75] U. Lindemann, K. Wilken, H.J. Weigmann, H. Schaefer, W. Sterry, J. Lademann, Quantification of the horny layer using tape stripping and microscopic techniques, J. Biomed. Opt. 8 (2003) 601-607.

[76] H.J. Weigmann, U. Lindemann, C. Antoniou, G.N. Tsikrikas, A.I. Stratigos, A. Katsambas, W. Sterry, J. Lademann, UV/VIS absorbance allows rapid, accurate, and reproducible mass determination of corneocytes removed by tape stripping, Skin Pharmacol. Appl. Skin Physiol. 16 (2003) 217-27.

[77] U. Lindemann, H.J. Weigmann, H. Schaefer, W. Sterry, J. Lademann, Evaluation of the pseudo-absorption method to quantify human stratum corneum removed by tape stripping using protein absorption, Skin Pharmacol. Appl. Skin Physiol. 16 (2003) 228-236.

[78] R. Voegeli, J. Heiland, S. Doppler, A.V. Rawlings, T. Schreier, Efficient and simple quantification of stratum corneum proteins on tape strippings by infrared densitometry, Skin Res. Technol. 13 (2007) 242-251.

[79] W. Meyer, Bemerkungen zur Eignung der Schweinehaut als biologisches Modell für die Haut des Menschen, Der Hautarzt 47 (1996) 178-182.

[80] W. Meyer, N.H. Zschemisch, Skin layer thickness at the ear of the domesticated pig, with special reference to the use of the ear integument for human dermatological research, Berl. Muench. Tierarztl. Wochenschr. 115 (2002) 401-406.

[81] Y.N. Kalia, I. Alberti, N. Sekkat, C. Curdy, A. Naik, R.H. Guy, Normalization of stratum corneum barrier function and transepidermal water loss in vivo, Pharm. Res. 17 (2000) 1148-1150.

[82] M. Machado, T.M. Salgado, J. Hadgraft, M.E. Lane, The relationship between transepidermal water loss and skin permeability, Int. J. Pharm. 384 (2010) 73-77.

[83] D. Hildebrandt, K. Ziegler, U. Wollina, Electrical impedance and transepidermal water loss of healthy human skin under different conditions, Skin Res. Technol. 4 (1998) 130-134.

[84] Y.N. Kalia, F. Pirot, R.H. Guy, Homogeneous transport in a heterogeneous membrane: water diffusion across human stratum corneum in vivo, Biophys. J. 71 (1996) 2692-2700.

[85] G.E. Nilsson, Measurement of water exchange through skin, Med. Biol. Eng. Comput. 15 (1977) 209-218.

[86] D.L. Miller, A.M. Brown, E.J. Artz, Indirect measures of transepidermal water loss, in: Bioengineering and the Skin, P. Marks, P.A. Payne (Eds.), MTP Press, Lancaster (1981) p. 161-171.

[87] R.E. Imhof, M.E. De Jesus, P. Xiao, L.I. Ciortea, E.P. Berg, Closed-chamber transepidermal water loss measurement: microclimate, calibration and performance, Int. J. Cosmet. Sci. 31 (2009) 97-118.

[88] S. Farahmand, L. Tien, X. Hui, H.I. Maibach, Measuring transepidermal water loss: a comparative in vivo study of condenser-chamber, unventilated-chamber and open-chamber systems, Skin Res. Technol. 15 (2009) 392-398.

[89] F. Netzlaff, K.H. Kostka, C.M. Lehr, U.F. Schaefer, TEWL measurements as a routine method for evaluating the integrity of epidermis sheets in static Franz type diffusion cells in vitro. Limitations shown by transport data testing, Eur. J. Pharm. Biopharm. 63 (2006) 44-50.

[90] R.E. Imhof, E.P. Berg, R.P. Chilcott, L.I. Ciortea, F.C. Pascut, P. Xiao, New Instrument for Measuring Water Vapour Flux Density from Arbitrary Surfaces, IFSCC Magazine 5 (2002) 297-301.

[91] R.E. Imhof, P. Xiao, E.P. Berg, L.I. Ciortea, Rapid measurement of TEWL with a condenser-chamber instrument, 15th Int. Meeting of the ISBS, Philadelphia (2005).

[92] N. Sekkat, Y.N. Kalia, R.H. Guy, Biophysical study of porcine ear skin in vitro and its comparison to human skin in vivo, J. Pharm. Sci. 91 (2002) 2376-2381.

[93] N. Sekkat, Y.N. Kalia, R.H. Guy, Porcine ear skin as a model for the assessment of transdermal drug delivery to premature neonates, Pharm. Res. 21 (2004) 1390-1397.

[94] E. Xhauflaire-Uhoda, G.E. Pierard, P. Quatresooz, The skin landscape following nonoptical capacitance imaging, Am. J. Clin. Dermatol. 11 (2010) 89-94.

[95] G.E. Pierard, J.L. Leveque, What is SkinChip? From silicon image sensor technology to SkinChip, Dermatology 208 (2004) 291-292.

[96] E. Xhauflaire-Uhoda, C. Pierard-Franchimont, G.E. Pierard, Skin capacitance mapping of psoriasis, J. Eur. Acad. Dermatol. Venereol. 20 (2006) 1261-1265.

[97] D. Batisse, F. Giron, J.L. Leveque, Capacitance imaging of the skin surface, Skin Res. Technol. 12 (2006) 99-104.

[98] L. Tchvialeva, H. Zeng, I. Markhvida, D.I. McLean, H. Lui, T.K. Lee, Skin Roughness Assessment, in: New Developments in Biomedical Engineering, D. Campolo (Ed.), InTech, OpenAccessPublisher Online (2010).

[99] J.L. Leveque, E. Xhauflaire-Uhoda, G.E. Pierard, Skin capacitance imaging, a new technique for investigating the skin surface, Eur. J. Dermatol. 16 (2006) 500-506.

[100] J.L. Leveque, B. Querleux, SkinChip, a new tool for investigating the skin surface in vivo, Skin. Res. Technol. 9 (2003) 343-347.

[101] A. Bevilacqua, A. Gherardi, Age-related Skin Analysis by Capacitance Images, Proceedings of the 17th Int. Conference on Pattern Recognition (ICPR2004), I.C.S. Press, Cambridge, UK, Aug. 23rd - 26th (2004).

[102] E. Xhauflaire-Uhoda, P. Paquet, P. Quatresooz, G.E. Pierard, Characterization of the skin using capacitance imaging, Exp. Rev. Dermatol. 5 (2010) 149-158.

[103] P. Xiao, H. Singh, X. Ou, A.R. Caparnagiuc, L.I. Ciortea, E.P. Berg, R.E. Imhof, In-vivo Trans-Dermal Drug Delivery Study by Using Capacitive Fingerprint Sensors, Skin Forum, Frankfurt, Germany, March 28th - 29th (2011).

All reprinted images were included with the permission of the respective copyright holders to the best of the author's knowledge. Should any uncertainties arise, please contact the author.

CHAPTER 6

Abstracts

6.1 Abstract

Lecithin-based nanoemulsions are skin-friendly and efficient vehicles for the delivery of lipophilic drugs. Since lecithin alone is a comparatively poor stabiliser, a primary aim of this work was to improve the physical stability of o/w nanoemulsions with eudermic additives such as natural cyclodextrins and sucrose ester surfactants. The nanoemulsions were characterised by dynamic light scattering, laser Doppler electrophoresis, cryo transmission electron microscopy and thermoanalytical measurements. The skin permeation rates of incorporated drugs were investigated with the help of in vitro skin diffusion studies. In this context, cyclodextrins were found to exert a certain positive influence on nanoemulsion stability. Moreover, they strongly enhanced the skin permeation of steroidal drugs under infinite dose application. Solubilisation effects as well as interactions at the o/w interface may be held responsible for this enhancement. The investigated sucrose stearate mixtures were found to be valuable co-surfactants, but also superior main surfactants. The peculiar rheological behaviour of the employed sucrose ester mixtures was additionally employed to create appealing semi-solid o/w emulsions without the use of gelling agents or polymers. Interestingly, the droplet size of these emulsions had no impact on the skin permeation of model drugs when compared to nanoemulsions of identical composition. Extensive rheological, thermoanalytical and fluorescence microscopic investigations revealed that the composition of the employed sucrose stearate blend and the nature of the oil phase strongly influenced the physical properties of these novel emulsions.

To further investigate the skin penetration potential of all developed vehicles, the tape stripping method was adapted for in vitro experiments on porcine ear skin. As a second major aim of this work, near infrared-densitometry was vali-

dated for quantification of the removed corneocytes. A condenser chamber and a capacitance-based sensor were successfully introduced for skin quality testing in vitro. Conclusive comparative in vivo experiments confirmed the suitability of the porcine ear model for skin penetration studies.

6.2 Zusammenfassung

Nanoemulsionen auf Lezithinbasis sind hautfreundliche und effiziente Vehikel für lipophile Arzneistoffe. Die Verwendung von Lezithin als alleiniges Tensid führt jedoch meist zu unbefriedigender Stabilität der Formulierungen. Daher war es ein Hauptziel dieser Arbeit, die physikalische Stabilität von O/W-Nanoemulsionen mit hautverträglichen Additiva wie natürlichen Cyclodextrinen und Sacharoseester-Tensiden zu optimieren. Die Formulierungen wurden mittels verschiedener Techniken wie Dynamischer Lichtstreuungsmessung, Laser Doppler-Elektrophorese, Kryo-Transmissionselektronenmikroskopie und thermoanalytischer Untersuchungen charakterisiert. Die Freisetzung eingearbeiteter Modellarzneistoffe wurde mittels in vitro-Hautdiffusionsstudien untersucht. Cyclodextrine konnten in der Tat zu einer Verbesserung der Nanoemulsions-Stabilität beitragen; wesentlich ausgeprägter und spezifischer war jedoch ihr permeationsfördernder Effekt auf steroidale Arzneistoffe unter infinite dose - Bedingungen. Hierfür könnten sowohl Löslichkeitseffekte als auch eine Beteiligung der Cyclodextrine am O/W-Grenzflächenfilm der Öltröpfchen verantwortlich sein. Die untersuchten Saccharosestearat-Mischungen erwiesen sich sowohl in Kombination mit Lezithin als auch alleine als höchst vorteilhafte Stabilisatoren für Nanoemulsionen. Das beobachtete starke Quellvermögen dieser Tenside wurde zusätzlich genutzt, um durch geringfügige Modifikationen im Herstellungsprozess halbfeste O/W-Emulsionen von ansprechender Konsistenz und guter Stabilität ohne Verwendung zusätzlicher Gelbildner herzustellen. In vergleichenden Hautpermeationsstudien mit Modellarzneistoffen erzielten diese Emulsionen interessanterweise ebenso hohe Permeationsraten wie die entsprechenden Nanoemulsionen mit identischer Zusammensetzung. Ausführlichere rheologische, thermoanalytische und licht- sowie fluoreszenzmikroskopische Untersuchungen zeigten, dass die Zusammensetzung der Saccharoseester-Mischungen sowie die Art der Ölphase eine bedeutende Rolle für die physikalischen Eigenschaften dieser neuartigen Emulsionen spielten.

Um die Hautpenetration aller entwickelten Formulierungen genauer zu untersuchen wurde als zweiter Hauptpunkt dieser Arbeit die Methodik des Tape Stripping für in vitro - Experimente an porziner Ohrenhaut adaptiert. Für die Quantifizerung der abgezogenen porzinen Korneozyten wurde die Methode der NIR-Densitometrie erstmals validiert. Eine Kondensor-Kammer-Methode sowie ein kapazitanzbasierter Sensor wurden erfolgreich für die Qualitätskontrolle der Haut eingesetzt. Abschließend bestätigten vergleichende in vivo-Studien, dass das porzine Ohrenmodell ein geeignetes in vitro-Ersatzmodell für aufwändige in vivo-Studien darstellt.

CHAPTER 7

List of Scientific Contributions within this Work

Publications

- **V. Klang**, N. Matsko, A.-M. Zimmermann, E. Vojnikovic, C. Valenta, Enhancement of stability and skin permeation by sucrose stearate and cyclodextrins in progesterone nanoemulsions, Int. J. Pharm. 393 (2010), 152-160.
- **V. Klang**, N. Matsko, K. Raupach, N. El-Hagin, C. Valenta, Development of sucrose stearate-based nanoemulsions and optimisation through γ-cyclodextrin, Eur. J. Pharm. Biopharm. 79 (2011), 58-67
- **V. Klang**, J.C. Schwarz, A. Hartl, C. Valenta, Facilitating in vitro tape stripping: application of infrared densitometry for quantification of porcine stratum corneum proteins, Skin Pharmacol. Physiol. 24 (2011), 256-268
- **V. Klang**, J.C. Schwarz, N. Matsko, E. Rezvani, N. El-Hagin, M. Wirth, C. Valenta, Semi-solid Sucrose Stearate-Based Emulsions as Dermal Drug Delivery Systems, Pharmaceutics 3 (2011), 275-306
- **V. Klang**, J.C. Schwarz, B. Lenobel, M. Nadj, J. Auböck, M. Wolzt, C. Valenta, In Vitro vs in Vivo Tape Stripping: Validation of the Porcine Ear Model and Penetration Assessment of Novel Sucrose Stearate Emulsions, Eur. J. Pharm. Biopharm., *in press*
- **V. Klang**, S. Haberfeld, A. Hartl, C. Valenta, Effect of γ-cyclodextrin on the in vitro skin permeation of a steroidal drug from nanoemulsions: Impact of experimental setup, Int. J. Pharm., *in press*

- **V. Klang**, J.C. Schwarz, S. Haberfeld, P. Xiao, M. Wirth, C. Valenta, Skin integrity testing and monitoring of in vitro tape stripping by capacitance-based sensor imaging, Skin Res. Techn., *submitted Nov 18th 2011 - under review*

- **V. Klang**, A. Novak, M. Wirth, C. Valenta, Semi-solid O/W emulsions based on sucrose stearates: influence of oil and surfactant type on morphology and rheological properties, J. Disp. Sci. Technol., *accepted for publicaton*

Poster Presentations

- **V. Klang**, C. Valenta, Cyclodextrins as natural co-stabilising agents in submicron emulsions. Skin and Formulation, 3rd Symposium and Skin Forum, 10th Annual Meeting, Versailles, France, March 9th - 10th, 2009.

- **V. Klang**, A.-M. Zimmermann, C. Valenta, Natural cyclodextrins as stabilising additives in lecithin-based nanoemulsions. 15th International Cyclodextrin Symposium, Vienna, Austria, May 9th - 12th, 2010.

- **V. Klang**, E. Vojnikovic, C. Valenta, Cyclodextrins as permeation enhancers for progesterone in lecithin-based nanoemulsions. 15th International Cyclodextrin Symposium, Vienna, Austria, May 9th - 12th, 2010.

- **V. Klang**, K. Raupach, C. Valenta, Comparative evaluation of natural emulsifiers in nanoemulsions: lecithin versus sucrose stearate. Skin Forum, 11th Annual Meeting, Edinburgh, Scotland, July 6th - 7th, 2010.

- **V. Klang**, J.C. Schwarz, A. Hartl, C. Valenta, Infrared Densitometry for Quantification of Porcine Stratum Corneum Proteins. Skin Forum, 12th Annual Meeting, Frankfurt, Germany, March 28th - 29th, 2011.

- **V. Klang**, J.C. Schwarz, N. Matsko, N. El-Hagin, C. Valenta, Semi-Solid Sucrose Stearate-Based Emulsions as Dermal Drug Delivery Systems. Skin Forum, 12th Annual Meeting, Frankfurt, Germany, March 28th - 29th, 2011.

- **V. Klang**, S. Haberfeld, A. Hartl, C. Valenta, Effect of γ-Cyclodextrin on In Vitro Skin Permeation of Steroidal Drugs from Nanoemulsions: Impact of Experimental Setup. Joint Meeting of the Austrian and German Pharmaceutical Societies (ÖPHG/DPHG), Innsbruck, Austria, September 20th - 23rd, 2011.

- **V. Klang**, J.C. Schwarz, B. Lenobel, M. Nadj, A. Hartl, J. Auböck, M. Wolzt, C. Valenta, In vitro vs in vivo tape stripping: validation of the porcine

ear model. 8th World Meeting on Pharmaceutics, Biopharmaceutics and Pharmaceutical Technology, Istanbul, Turkey, March 19th - 22nd, 2012.

- **V. Klang**, A. Novak, M. Wirth, C. Valenta, Novel semi-solid O/W emulsions stabilised by sugar surfactants: influence of oil and surfactant type on morphological and rheological properties. 8th World Meeting on Pharmaceutics, Biopharmaceutics and Pharmaceutical Technology, Istanbul, Turkey, March 19th - 22nd, 2012.
- **V. Klang**, S. Haberfeld, M. Wirth, C. Valenta, Visualisation of the skin surface structure of porcine and human skin by fingerprint sensor imaging and implications for in vitro tape stripping. 8th World Meeting on Pharmaceutics, Biopharmaceutics and Pharmaceutical Technology, Istanbul, Turkey, March 19th - 22nd, 2012.

Oral Presentations

- **V. Klang**, C. Valenta, Cyclodextrins as natural co-stabilising agents in submicron emulsions. 21st Scientific Conference of the ÖPHG (Austrian Pharmaceutical Society), Vienna, Austria, April 16th - 18th, 2009.
- **V. Klang**, C. Valenta, Skin penetration of lecithin-based nanoemulsions - influence of sugar surfactants, cyclodextrins and the cationic phytosphingosine. 14th Scientific Conference of the GD (Society for Dermopharmacy) Berlin-Dahlem, Germany, March 22nd - 24th, 2010.
- **V. Klang**, J.C. Schwarz, C. Valenta, In vitro skin penetration studies on the porcine ear model for investigation of novel dermal and cosmetic formulations. Awarding of the P.B. Czedik-Eysenberg prize, Lebensmittelchemiktage, Linz, Austria, scheduled April 25th - 27th, 2012.

CHAPTER 8

List of Scientific Contributions beyond this Work

Publications

- S. Hoeller, **V. Klang**, C. Valenta, Skin-compatible lecithin drug delivery systems for fluconazole: effect of phosphatidylethanolamine and oleic acid on skin permeation, J. Pharm. Pharmacol. 60 (2008), 587-591

- **V. Klang**, C. Valenta, Lecithin-based nanoemulsions, J. Drug Delivery Sci. Technol. 21 (2011), 55-76

- **V. Klang**, N.B. Matsko, C. Valenta, F. Hofer, Electron microscopy of nanoemulsions: An essential tool for characterisation and stability assessment, Micron 43 (2012), 85-103

- J.C. Schwarz, **V. Klang**, S. Karall, D. Mahrhauser, G.P. Resch, C. Valenta, Optimisation of multiple W/O/W nanoemulsions for dermal delivery of acyclovir, Int. J. Pharm., *in press*

- J.C. Schwarz$^{\Delta}$, **V. Klang**$^{\Delta}$, M. Hoppel, M. Wolzt, C. Valenta, Corneocyte quantification by NIR densitometry and UV/Vis spectroscopy for human and porcine skin and the role of skin cleaning procedures, Skin Pharm. Physiol., *in press*

- J.C. Schwarz, **V. Klang**, M. Hoppel, D. Mahrhauser, C. Valenta, Natural microemulsions: formulation design and skin interaction, Eur. J. Pharm. Biopharm., *under review*

- **V. Klang**, C. Valenta, N. B. Matsko, Electron Microscopy of Pharmaceutical Systems, Micron, invited review, *in preparation*

Poster Presentations

- J.C. Schwarz, **V. Klang**, C. Valenta, Development of Eudermic W/O/W Nanoemulsions for Delivery of Hydrophilic Drugs. Skin Forum, 12$^{\text{th}}$ Annual Meeting, Frankfurt, Germany, March 28$^{\text{th}}$ - 29$^{\text{th}}$, 2011.
- J.C. Schwarz$^{\Delta}$, **V. Klang**$^{\Delta}$, D. Mahrhauser, T.M. Wrodnigg, C. Valenta, Influence of novel sugar-amino acid conjugates on skin structure and penetration of flufenamic acid. 8$^{\text{th}}$ World Meeting on Pharmaceutics, Biopharmaceutics and Pharmaceutical Technology, Istanbul, Turkey, March 19$^{\text{th}}$ - 22$^{\text{nd}}$, 2012.
- C. Nagelreiter, S. Krepcik, **V. Klang**, C. Valenta, Skin penetration of basic industrial dermal vehicles and assessment of lateral spreading in vitro. 8$^{\text{th}}$ World Meeting on Pharmaceutics, Biopharmaceutics and Pharmaceutical Technology, Istanbul, Turkey, March 19$^{\text{th}}$ - 22$^{\text{nd}}$, 2012.

The symbol $^{\Delta}$ denotes shared first authorship.

CHAPTER 9

Curriculum Vitae

Personal Information

Name	Victoria Klang
Academic Degree	Master of Pharmacy (Magistra)
Date of Birth	January 6th, 1984
Address	Aichholzgasse 18/7, 1120 Vienna
Telephone	+43 (0) 680 1184706
E-Mail	victoria.klang@univie.ac.at

Education and Professional Experience

04/2012	Thesis Defense (Department of Pharmaceutical Technology and Biopharmaceutics, University of Vienna, Austria), *scheduled*
04/2012	Awarding of the Peter B. Czedik-Eysenberg Prize 2012, *scheduled*
09/2011 - 02/2012	Lector for the practical courses in cosmetics (Department of Pharmaceutical Technology and Biopharmaceutics, University of Vienna, Austria)
10/2009	Scientific training session at the Charité Berlin (Dermatologische Universitätsklinik)
05/2008 - 04/2012	Lector for the practical courses on *Magistral Formulae* (Department of Pharmaceutical Technology and Biopharmaceutics, University of Vienna, Austria)
05/2008 - 04/2012	Lector for the practical courses *Introduction to Pharmaceutical Technology* (Department of Pharmaceutical Technology and Biopharmaceutics, University of Vienna, Austria)
05/2008 - 04/2012	Postgraduate education at the Department of Pharmaceutical Technology and Biopharmaceutics at the University of Vienna, Austria
02/2008	Master's Degree of Pharmacy at the University of Vienna, Austria. Diploma thesis *Einfluss von Öl- und Tensidgehalt auf das Diffusionsverhalten von Fluconazol in ausgewählten Mikroemulsionen*
02/2007 - 03/2007	Pharmaceutical trainee, Apotheke zum Weinberg, Vienna, Austria
10/2006 - 06/2007	Teaching assistant in the practical courses on *Magistral Formulae* (Department of Pharmaceutical Technology and Biopharmaceutics, University of Vienna, Austria)
02/2005 - 06/2005	Student exchange semester at the University of Nantes, France, supported by the ERASMUS program

10/2002 - 02/2008	Undergraduate/graduate studies in pharmacy at the University of Vienna, Austria
09/1994 - 06/2002	Secondary School (BRG & RG Erlgasse and Rosasgasse, Vienna, Austria)
09/1990 - 06/1994	Primary School (Bischofgasse, Vienna, Austria)

Skills

Languages	German as mother tongue
	English on a professional level in written and verbal form
	French on an advanced level in written and verbal form
Word Processing	Microsoft Office
	LaTeX